It is good to have an end to journey toward,
but it is the journey that matters in the end.

Ursula K. LeGuin

Physiological constraints on the latitudinal distribution of the mangrove *Avicennia marina* (Forsk.) Vierh subsp. *australasica* (Walp.) J. Everett in New Zealand

A thesis

submitted in partial fulfilment

of the requirements for the Degree

of

Doctor of Philosophy in Biological Sciences

at the

University of Waikato

by

Catherine M. Beard

THE UNIVERSITY OF WAIKATO
Te Whare Wānanga o Waikato

The University of Waikato

2006

Abstract

New Zealand's only mangrove species, *Avicennia marina* (Forsk.) Vierh. subsp. *australasica* (Walp) Everett (Avicenniaceae), has a clearly defined southern natural limit around latitude 38° S. Historically, this has been attributed to the lethal effects of winter frosts (Chapman & Ronaldson, 1958) and, more recently to poor species dispersal and lack of suitable habitat south of the present species boundary (de Lange & de Lange, 1994).

A series of investigations of frost tolerance, leaf gas exchange, stomatal conductance, chlorophyll *a* fluorescence, water relations and stable carbon isotope analyses of New Zealand *Avicennia* were undertaken in the laboratory and field in order to characterise frost tolerance limits and photosynthetic performance under normal and stressed conditions. By so doing, the relative importance of winter frosts and low air temperatures in defining the range of *Avicennia* in New Zealand could then be determined.

It was found that photosynthetic performance in *Avicennia* was increasingly depressed near its southern limits. Photosynthetic responses were consistent with those typical for cold-sensitive species after exposure to low temperatures. Large decreases in photosynthetic production, photoinhibition and chlorophyll loss were evident following exposure to night temperatures lower than 4°C, suggesting that critical damage occurred even at temperatures well above freezing.

Frosts probably still play an important, additional and episodic role in defining the range of mangrove in New Zealand. The physiological stress effects of low temperatures were compounded by sub-zero temperatures and productivity in frost-prone areas was significantly reduced by physical damage to leaves, branches and reproductive tissue. Freeze-injury of this form also reduced the likelihood of successful seedling establishment and long-term survival of saplings.

These findings indicate that latitude 38° S acts as a physiological barrier for mangrove in New Zealand. *Avicennia* might persist further south than its present natural range if dispersal to suitable microclimates occurred. However, the probability of this occurring naturally is small, given the species poor dispersal abilities, and the reduced likelihood of survival in the face of damage and physiological stresses brought about by cold winter temperatures.

Acknowledgements

Although written acknowledgments can only be brief, I want to share my gratitude here for all those who helped me through this Ph.D.....my thanks to the following in particular:

To my supervisors Prof. Allan Green, Prof. Warwick Silvester and Dr. Chrissen Gemmill for giving me this opportunity to expand my horizons. Many thanks to you, (both collectively and individually), for showing me the path – I really appreciate your patience over the last few years, but also all the knowledge, encouragement, guidance and enthusiasm that you shared with me.

Additional thanks to Allan for giving so much of your time to work in the mangroves and the mud (although falling through the jetty was well beyond the call of duty). Also for your unerringly excellent sense of timing with chocklit.

To my family (especially my parents and A.A.Aunty Anne), whose love, support, and help kept the engine running.

To Cathy Jones, for patiently cradling my sanity, and for continuing to listen all those times when the record got stuck.

To Prof. Terry Healy, for generously sharing your expertise and resources, and for those words of advice and encouragement that made a real difference, thank you.

To Sue McCurdy, for taking great care of my two furry boys and my house so many times when I've been out playing in the mud. Also for reading my caffeine requirements so accurately!

To Katrin Walbert, for all those great crazy days in the field, and being an excellent collaborator on the mangrove front.

To Gavin Reynolds and Margaret Auger, for your willingness to plod around in (and occasionally become stuck in) the mud while helping me with my field work.

To Tracey Jones, for helping me to understand the mysteries of genetic analysis software.

To those friends and colleagues I haven't mentioned here by name (hopefully you all know who you are), for helping out, for cutting me some slack, and for helping me keep it all in perspective.

To Sam and Max, because cat cuddles go a long way.

To Margaret Tuite and Daphne Rae for allowing access from their properties to our research sites.

Very special thanks to the late Emma Sammes, for giving me far more than all the fabulous meals and a wonderful place to stay during my field work. You were one out of the box and are very much missed.

Finally, my thanks to the Royal Society Marsden Fund and the University of Waikato (in particular, the Department of Biological Sciences) for supporting this research project.

Physiological constraints on the latitudinal distribution of the mangrove *Avicennia marina* (Forsk.) Vierh subsp. *australasica* (Walp.) J. Everett in New Zealand

Table of Contents

Chapter Five

Figures, Tables, Plates

List of Tables

List of Figures

List of Plates

List of symbols and abbreviations

°C	degrees Celsius
A	rate of CO_2 assimilation
A_{max}	Maximal rate of CO_2 assimilation
c_e	mole fractions of CO_2 in the gas streams entering the cuvette
Chl	chlorophyll
c_i	Leaf internal CO_2 concentration
c_o	mole fractions of CO_2 in the gas streams leaving the cuvette
C_{out}	CO_2 concentration of cuvette air
d	day
E	transpiration rate
e_{leaf}	saturated vapour pressure at leaf temperature
EM	predicted extreme minimum temperature (°C)
e_{out}	water vapour pressure of the air leaving the cuvette
ETR	rate of linear electron transport through PSII
F	steady state fluorescence
F_0	minimum fluorescence yield
F_0'	minimum fluorescence in the light adapted state,
F_m	minimum fluorescence
F_m'	maximum fluorescence under illumination
F_v	variable fluorescence maximum
F_v/F_m	maximal quantum efficiency of PSII primary photochemistry
g_s	stomatal conductance (mol m^{-2} s^{-1})
h	hour
It	index of injury
LAI	Leaf area index
Lk	final conductivity measurement ()
Lt	conductivity of the bathing solution
m	metre
MAT	mean annual temperature (°C)
MHWN	mean high water at neap tide
MHWS	mean high water at spring tide
MPa	mega pascals

MTCM	minimum temperature (°C) of the coldest month year
MTWM	maximum temperature (°C) of the warmest month
°C	degrees Celsius
PAR	photosynthetically active radiation
P	measured xylem pressure,
P	atmospheric pressure
PFD	photon flux density
ppm	parts per mille
PSI	photosystem I
PSII	photosystem II
qE	energy dependant quenching
qI	photoinhibitory quenching,
qT	state-1 state-2 transition quenching
r_b	boundary layer resistance to water vapour.
RB	boundary layer resistance
Ro	fractional release of electrolytes from an unfrozen sample
r_s	stomatal resistance to water vapour
Rt	fractional release of electrolytes from a sample exposed to a particular treatment temperature
SD	standard deviation
SE	standard error
u_e	molar flow of air entering the cuvette chamber
u_o	molar flow of air leaving the cuvette chamber
w_e	mole fraction of water vapour in the gas streams entering the cuvette
w_o	mole fraction of water vapour in the gas streams leaving the cuvette
Ψ_s	osmotic potential of xylem fluid.
Ψ_w	water potential of leaf cells

Chapter One

Chapter One

Physiological constraints on the latitudinal distribution of the mangrove *Avicennia marina* (Forsk.) Vierh. subsp. *australasica* (Walp.) J. Everett (Avicenniaceae) in New Zealand

1.1 Introduction to thesis

Mangroves are a taxonomically diverse group of halophytic (salt-tolerant) plants comprising approximately 70 species within some 19 families. They are typically woody trees or shrubs taller than 0.5 m, and inhabit the intertidal margins of low-energy marine coastal and estuarine environments over a wide range of latitude, centered on the tropics (Duke, 1998, Tomlinson, 1986). They normally occupy the zone between mean sea level and high tide, growing on a variety of substrates including volcanic rock, coral, fine sands and muddy sediments.

Although many species of mangrove are taxonomically unrelated, they all share a number of important traits that allow them to live successfully under environmental conditions that exclude other species. Morphological, physiological and reproductive specializations, such as aerial breathing roots, support structures (buttresses or above-ground roots), the ability to excrete or exclude salts; salt tolerance, vivipary, and habitat specificity within estuaries, enable mangroves to successfully adapt to and thrive within their environments, and so to form some of the richest and most productive ecosystems on earth (Tomlinson 1986).

Mangroves are most commonly associated with tropical and subtropical coastlines and only a small number of species extend their range into the cooler warm-temperate climates typical of parts of New Zealand, Australia, Japan, South America and South Africa (Chapman, 1977, McNae, 1966). A latitudinal pattern of species richness is evident, with diversity and extent both greatest at the equator and diminished towards the north and south (Ellison, 2002). Communities near the northern geographic boundaries maintain some diversity with up to six mangrove species present (Miyawaki, 1980), whilst those near the southern limits are mangrove-poor, supporting between one and three species.

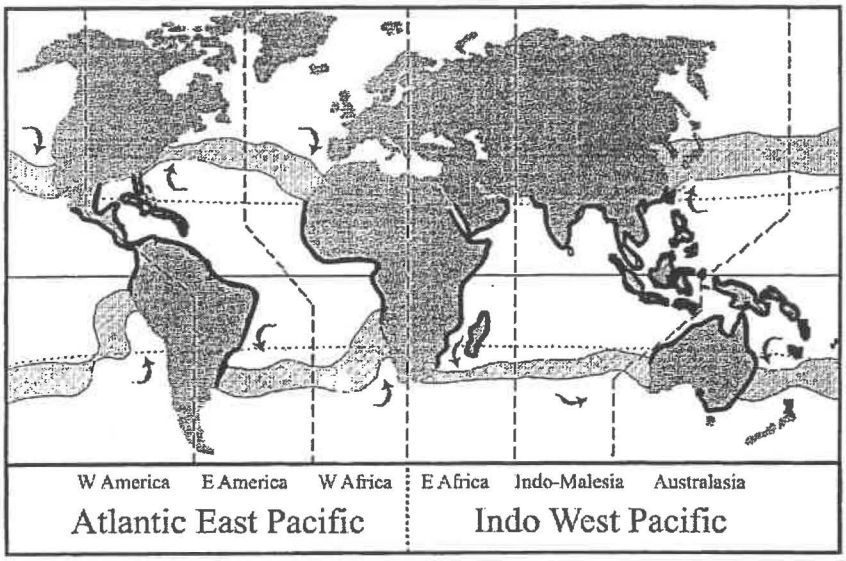

Figure 1.1 Global distribution of mangrove (indicated by bold coastline) showing extent within six biogeographic regions. Grey ocean shading shows the range of summer and winter positions of the 20°C isotherm which is influenced by ocean currents (arrows). Figure modified from Duke, 1998.

The present limits of global mangrove growth occur in the southern hemisphere within Corner Inlet, Westernport Bay in Victoria, Australia, at latitude 38°54.8′ S (de Lange & de Lange, 1994) and, in the northern hemisphere, in Japan around latitude 31°23' N (Sun *et al.*, 1998). As the mangrove approach their geographical limits, they become increasingly restricted to particular microhabitats, giving rise to disjunct or fragmented distribution patterns that are typical of some regions in the North Island of New Zealand.

Temperature, either of air or water, plays one of the most significant roles in determining plant distributions (Woodward, 1987). Mangroves are generally restricted to tropical climates where mean air temperatures of the coldest months are warmer than 20°C and where the seasonal range does not exceed 10°C (Chapman, 1976, Chapman, 1977, Duke, 1998). The actual geographic limits of mangrove growth are coincident with ground frost occurrence and, in addition, their global distribution appears closely linked with the 20°C winter isotherm for seawater (Duke, 1998) (Figure 1.1). Notable exceptions to this pattern include New Zealand, parts of Australia, and the coastlines of eastern South America. Duke (1998) suggests that these outlying distributions either coincide with extensions of irregular warm oceanic currents or that they are refugia for relict populations established during periods of greater poleward distributions.

In addition, species in these outlying areas show a broader tolerance of environmental extremes; certainly, *Avicennia* in Australia exist in colder environments than those stated above, growing south to where mean daily mid-winter temperatures (July) fall between 4°C and 7°C and where minimum temperatures are lower than 0°C (Hutchings & Saenger, 1987). Some populations of *Avicennia* in New Zealand occur in areas where mild winter frosts (-4°C < 0°C) occur regularly (C.Beard *personal observation*).

It is widely recognized that mangrove presence relies not only on favourable environmental or climatic conditions that allow the physiological growth of the various species, but also on successful reproduction and subsequent successful establishment of propagules (the young plantlets arising from viviparous reproduction). Climatic factors, such as air temperature, frost, water temperature, rainfall and wind have a significant influence on the composition and quality of mangrove vegetation (Chapman, 1976, de Lange & de Lange, 1994, Duke, 1998, Kao *et al.*, 2004, Sherrod, 1986). The influences of geography, soils, salinity, tides, ocean currents and the transportation of propagules created by geographical conditions are also important in defining mangrove distribution patterns (de Lange & de Lange, 1994, Dodd *et al.*, 2002, Duke, 1992, 1995, 1998)

New Zealand supports only a single species of mangrove; *Avicennia marina* (Forsk.) Vierh. subsp. *australasica* (Walp.) J. Everett (grey mangrove or Manawa as it is commonly known). Naturally occurring in the North Island to latitude 38°03′ S (Figure 2.2), New Zealand populations of *Avicennia* have occasionally been referred to as the southernmost in the world. Although this distinction actually belongs to populations of *Avicennia* in southern Australia, favourable microclimates have allowed transplanted individuals in New Zealand to survive latitudes much further south than their natural limit, such as at the Hutt River at 41°13′ S and Golden Bay in the South Island at 40°43′ S (de Lange & de Lange, 1994, Walsby, 1992).

1.2 Thesis aims

The aims of this study were to investigate some of the physical and physiological consequences of mangrove growing in a cold climate, and to assess the importance of low winter temperatures and frost in defining the southern distribution limits of *A. marina* subsp. *australasica* in New Zealand. To answer these questions, two main possibilities were considered:

1. Lethal conditions (e.g., temperature) may limit a species distribution and may need only to occur occasionally (i.e., the rare, but severe, event)
2. Species distributions are limited more often by conditions that are regularly sub-optimal (rather than lethal) leading to reductions in growth or reproduction or an increased chance of mortality (i.e., continual stress leading to sub-optimal performance).

Until recently, the southern spread of mangrove in New Zealand was thought to be constrained solely by extreme, low winter temperatures. Chapman and Ronaldson (1958), based on their observations of damaged and dying mangroves in Henderson Creek, Waitemata harbour, Auckland (Figure 2.2, location 31) following a period of frosts June 28 – July 4, 1951, first suggested that mangroves would either not survive or persist further south of a point where coastal frosts exceeded -2.2°C. Later frost tolerance studies of New Zealand *Avicennia* by Sakai and Wardle (1978) set an ultimate tolerance limit of -3°C to winter freezing. However, doubt has since been cast on whether mangroves had actually experienced lethal conditions and whether climate (frost) was truly the determining factor for the southern boundaries of mangrove in New Zealand (de Lange & de Lange, 1994). There is some confusion over the severity and frequency of frost experienced by the Henderson creek plants, as some supposedly frost-killed plants recovered, viable populations are known well south of Auckland (Crisp *et al.*, 1990), and transplanted specimens have survived much further south than the natural limit (Daniel, 1986). In addition, information from outside New Zealand has also shown that mangrove show a latitude dependent response to chilling (Markley *et al.*, 1982, McMillan, 1974),

Consequently, one aim of the present study was to define frost tolerance and critical temperature limits in *Avicennia*. The electrical conductivity method was used to measure cell damage in relation to depth of freezing (Flint, 1967) and damage to the PSII photosystem was assessed using chlorophyll *a* fluorescence techniques (Schreiber & Berry, 1977). Microclimate parameters (air and substrate temperatures, photon flux density and relative humidity) were also monitored on-site in the field. The following questions were addressed (results and conclusions are presented in Chapter three):

- what temperatures are critical or lethal for New Zealand *Avicennia*?

- do lethal conditions occur within the present natural range of mangrove in New Zealand; and if so, how frequently do they occur?
- does *Avicennia* have the ability to acclimatise to cold temperatures?

Prior to the present study, relatively little was known about photosynthetic function of mangrove plants in the New Zealand environment. A number of overseas studies provided useful comparative data (Andrews *et al.*, 1984, Cheeseman *et al.*, 1991, Lin & Sternberg, 1992, Moore *et al.*, 1972, Naidoo *et al.*, 1998) but, without a detailed investigation in New Zealand mangrove, it was still not possible to determine the photosynthetic capacity or to assess if the plants were limited at their southern distribution boundaries by poor photosynthetic performance. Consequently a series of investigations of photosynthetic performance in New Zealand *Avicennia* were undertaken as described below.

The first of the investigations was designed to determine some physiological baselines for New Zealand *Avicennia*. Leaf gas exchange, chlorophyll *a* fluorescence and water relations were measured seasonally in three mangrove populations that spanned the species natural range in New Zealand. The following questions were addressed (results and conclusions are presented in Chapter 4).

- Does photosynthetic performance of *Avicennia* vary across the latitudinal range of this species in New Zealand (do southern populations perform poorly)?
- To what extent are photosynthesis and water relations in *Avicennia* constrained by microclimate?
- Is there evidence of seasonal variation in photosynthetic performance?

Avicennia shows inhibition of photosynthesis following overnight chilling or freezing in a manner similar to many cold-sensitive woody trees such as mango (Nir *et al.*, 1997) and *Eucalyptus* (Davidson *et al.*, 2004, King & Ball, 1998). It is widely recognised that such responses result from complex interactions between several physical factors and processes rather than a single critical factor (e.g., frost), but these are difficult to reproduce in a laboratory setting. To overcome this limitation, two further studies were undertaken to investigate photosynthetic performance in *Avicennia* in relation to low temperature stress (chilling and frost) under natural field conditions. One was designed to track the performance of

plants through an entire winter season in their natural state, taking into account different parts of the canopy (i.e., exposed and shaded leaves) (see Chapter 5), while the other was a short-term detailed study in which temperature conditions were manipulated (artificially engineered frosts) to assess the photosynthetic consequences of frost/chill intensity and frequency (see Chapter 6).

Ohiwa harbour in the Eastern Bay of Plenty was considered an ideal site for these studies, given that it is one of the southernmost locations of natural mangrove growth in New Zealand, and frost- and chilling-nights are known to occur amongst the mangrove stands from late autumn through to early spring. Microclimate parameters, leaf chlorophyll, gas exchange, and chlorophyll *a* fluorescence were measured with a view to answering the following questions (results and conclusions are presented in Chapters 5 and 6):

- What patterns of photosynthetic activity are evident in *Avicennia* during winter at the natural southern limit of mangrove in New Zealand?
- Do frost and chilling nights alter photosynthetic performance? If so, how significant is the frequency and intensity of the chill or freeze events?
- To what extent is photosynthetic performance in exposed- and shaded-leaves affected by photoinhibition and photodamage?

Field measurements of leaf gas exchange, fluorescence and water relations can only provide a picture of how a plant is functioning at a specific point in time, or over a relatively short time period. Given that all plant processes are subject to variation according to a number of interacting factors, it is often more desirable to obtain an integrated measure of performance over a longer time-span. Analysis of stable carbon isotope abundance in plant tissue is one method by which this can be assessed (O'Leary, 1988). Hence, a fourth study was undertaken to investigate long-term photosynthetic performance of *Avicennia* in its natural environment by determining stable carbon isotope abundance in leaf, stem and propagule tissue sampled from the entire natural range of this species in New Zealand. Comparisons were also made with examples in published literature.

The following questions were addressed (results and conclusions are presented in Chapter 7):

- Do carbon stable isotope ratios indicate changes in photosynthetic performance in New Zealand mangrove? If so, does this vary with

latitude? Are the southernmost plants the poorest performers and/or under the greatest photosynthetic stress?

- How does long-term photosynthetic performance of New Zealand mangrove compare with that of mangrove growing in tropical locations?

The thesis concludes at Chapter 8 with an overview of the factors that influence the distribution of *A. marina* subsp. *australasica*, and final conclusions on what factors define the southern geographic boundary of this species in New Zealand.

Chapter Two

Chapter Two

Materials and Methods

2.1 Introduction

Central to the work in this thesis is the mangrove *Avicennia marina* (Forsk.) Vierh. subsp. *australasica* (Walp.) J. Everett. This chapter presents a broad overview of the taxon; its distribution, general structure, habit and history in New Zealand. Also included are detailed descriptions and the locations of three field sites, where a large proportion of the work discussed in the following chapters was undertaken, or from which plant material was sourced for the investigations.

The chapter does not include descriptions of all the materials, methods and protocols used in the entire study. Those relating to stand-alone investigations such the determination of frost tolerance, stable isotope analysis and those protocols specific to a single experiment are described fully in their relevant chapters. However, since a number of the investigations (particularly those with an ecophysiological focus) involved the use of similar methodology and equipment, much of the general background theories, materials and protocols are presented together in this chapter to avoid later repetition. The theory and operation of the CIRAS-1 system measuring gas-exchange in leaves is described in addition to PAM chlorophyll fluorometry, measurement of water potential, chlorophyll content and the monitoring of environmental parameters.

2.2 Genus *Avicennia*

2.2.1 Taxonomy

The New Zealand mangrove belongs to one of several taxa in the pantropical genus *Avicennia* L. This genus is named in tribute to Abu Ali Husain Ibu Abd Allah, "Avicenna" (980 – 1037 AD); a celebrated Persian philosopher, physician, mathematician and naturalist (Lear & Turner, 1977). In many treatments *Avicennia* is placed within or near the family Verbenaceae Jaume Saint-Hilaire (Green, 1994), or as the sole genus within family Avicenniaceae Endlicher, (Duke, 1991). More recently molecular evidence indicates it may have closer affinities to the Acanthaceae s.l. (Schwarzbach & McDade, 2002).

2.2.2 Distribution

The ranges of individual taxa within *Avicennia* remain uncertain due to the troublesome systematics of the group. However, in the broad sense, and based on the species recognised in recent accounts of the genus by Duke (1991) and Tomlinson (1986) (Table 2.1), *Avicennia* occurs in two widely separated biogeographical regions: the "New World" regions of the Atlantic, Caribbean and Eastern Pacific and the "Old World" regions of the Indo-western Pacific (including Australia, New Zealand, New Guinea and other islands in the south-western Pacific) and East Africa.

Table 2.1 Recognized taxa (excluding varieties and subspecies) within the genus *Avicennia* based on recent treatments of the group by Duke (1991) and Tomlinson (1986)

Avicennia africana P. Beauv.
Avicennia alba Blume
Avicennia bicolor Standley
Avicennia germinans (L.) Stearn
Avicennia integra N C Duke
Avicennia marina (Forsk.) Vierh.
Avicennia officinalis L.
Avicennia rumphiana Hallier f.
Avicennia schaueriana Stapf & Leechman ex Moldenke

A. marina (Forsk.)Vierh. *sensu lato* has the broadest geographical range of all mangrove species. It dominates mangrove systems from the southernmost assemblages in Australia and New Zealand, northwards through the western Pacific islands, the Philippines, eastern Africa, the Persian Gulf, Indo-Malesia, India, south-east Asia, China and Japan. It also tolerates wide ranges of salinity, temperature and substrate and, in so doing, occupies a diverse variety of littoral habitats from around mean sea level to high spring level (Duke, 1991).

Duke's treatment (1991) recognises three varieties of *Avicennia marina* in Australasia:

- *A. marina* (Forsk.) Vierh var. *australasica* (Walp.) Moldenke (Now *A. marina* subsp. *australasica* (Walp.) J. Everett, 1994). This taxon is

- restricted to temperate and subtropical latitudes, occurring in New Zealand, Lord Howe Island, New Caledonia and the south-eastern coast of mainland Australia. It forms the southernmost mangrove populations at Corner Inlet, Wilson's Promontory, Victoria Australia at latitude 38°54' S
- *A. marina* (Forsk.) Vierh var. *eucalyptifolia* (Zipp. ex Moldenke) J. Everett: distribution uncertain, but suggested to range from the Philippines, Indonesia to the northern tropical coast of Australia.
- *A.marina* (Forsk.) Vierh var. *marina*: East Africa, Indo-Malaya, New Caledonia and the western coast of Australia (Tomlinson, 1986).

2.3 *Avicennia marina* subsp. *australasica* in New Zealand

2.3.1 Taxonomy

New Zealand mangroves are accepted to comprise just one taxon. Duke's (1991) revision placed the New Zealand mangrove as a variant of *A. marina*, and subsequently it was given sub-specific status by Everett (1994). The currently accepted name in New Zealand is *Avicennia marina* subsp. *australasica* (Walp.) J. Everett. (Allan Herbarium, 2000). Historically this taxon has been known by the combinations *A. resinifera* G. Forst. (Allan, 1982), and *A. marina* (Forsk.) Vierh var. *resinifera* (Forst.f.) Bakh. (in *Bull. Jard. Bot. Buitenz* 1921). The epithet *resinifera* refers to lumps of kauri resin that were found amongst the mangrove and mistakenly attributed to it by botanists on Captain James Cook's initial voyage of discovery to New Zealand. In vernacular terms it is known variously as manawa, mangrove or grey mangrove.

2.3.2 Description and Ecology

2.3.2.1 Habit

A. marina subsp. *australasica* in New Zealand is a small evergreen tree or shrub to 10 m tall (Duke, 1991) displaying considerable variability in size and growth form, both within populations and over a range of latitude (Plate 2.1).

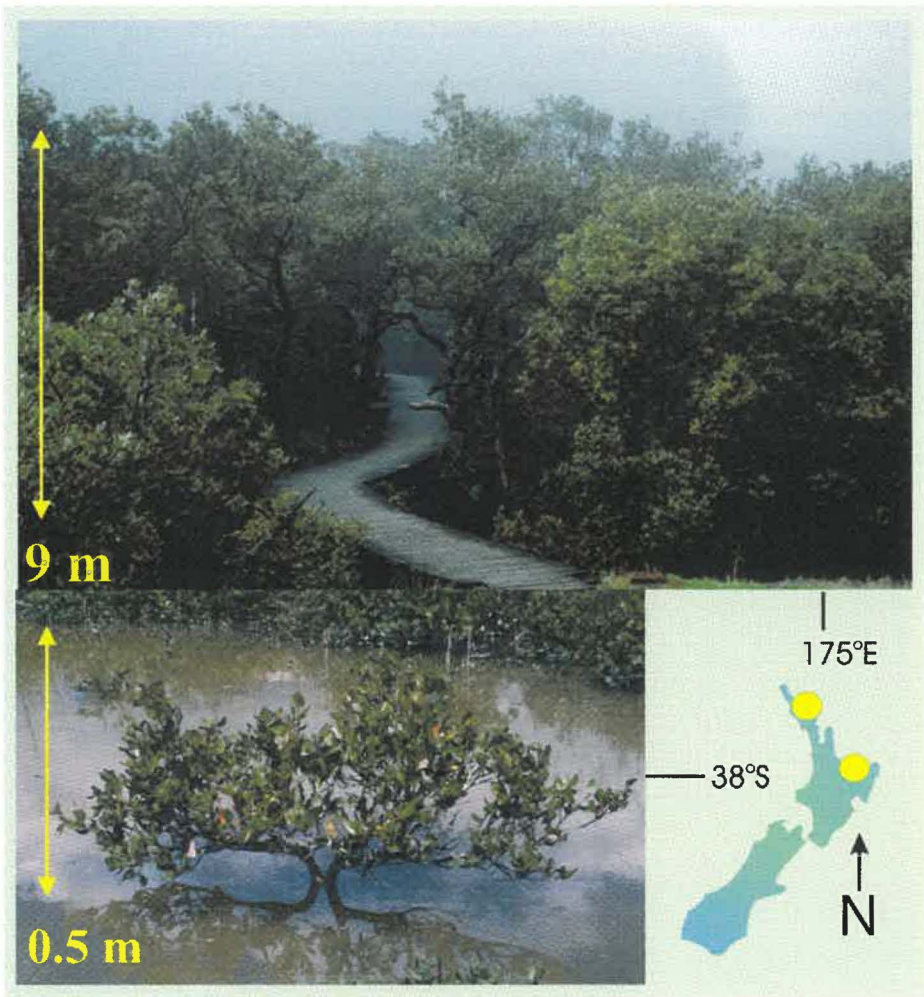

Plate 2.1 Growth forms of *Avicennia marina* subsp. *australasica* in New Zealand. Above: typical tall form at Paihia, Bay of Islands (Latitude 35°12′ S). Below left: dwarf form at Ohiwa Harbour, Bay of Plenty, (Latitude 38°03′ S). Below right: Locations (East Coast, North Island, New Zealand) of the growth forms illustrated in the photographs. (Photos C. Beard, 2001)

A trend of decreasing maximal height with increasing latitude has often been reported in the literature (e.g., Burns, 1982, Walsby 1992), but is not widely accepted as fact except in the broadest sense (Crisp *et al.*, 1990, Dingwall, 1984). DeLange and deLange (1994) compared growth forms over the full latitudinal range and found no systematic trends in maximal size. However, they did distinguish three growth forms:

- *Stunted forms* – those with a well developed trunk, restricted height and a low spreading canopy. This form, growing typically to heights between 30 and 100 cm, is common in, but not unique to, mangrove populations around the southern latitudinal limits of mangrove growth (C. Beard

personal observation). Various explanations have been offered for the stunted forms, including response to climate, high salinities, drainage, substrate characteristics, and a lack of interspecific competition allowing survival of stressed individuals (Burns, 1982)

- *Tall forms* – 'those significantly taller than the average mangroves in any given region and forming an incomplete canopy cover'. This form, growing typically to heights of around 10 m, is generally restricted to northern populations (C. Beard *pers. obs.*)
- *Normal forms* – 'those not specifically identified as either stunted or tall'. Larger trees are also more common on the outer margins of mangrove systems and on the borders of streams where drainage is favourable (Dingwall, 1984).

2.3.2.2 Leaves

Leaves are arranged in opposite pairs on the stems and measure up to 40 – 70 mm long by 18 – 36 mm wide (Plate 2.2). They are simple, ovate-elliptical in shape with a pointed tip, shiny green and hairless on the upper surface with a pale whitish-grey and finely hairy underside (Allan, 1961). Salt glands occur over the entire leaf surface, but are more abundant on the lower surface (Tomlinson, 1986)

Plate 2.2 Leaf form and arrangement in *Avicennia marina* subsp. *australasica*. Left: sun exposed leaves at Ohiwa Harbour. Right: Protected (shaded) leaves at Whitianga Harbour. (Photo: C. Beard, 2002).

2.3.2.3 Roots

Root architecture of *Avicennia* conforms to that of specialised mangroves. Following Tomlinson (1986), three components of the root system can be recognised (Figure 2.1). The aerating component consists of numerous vertical breathing roots or pneumatophores, which are exposed at least part of the time to the atmosphere and facilitate gas exchange via lenticels in the corky outer layers (Plate 2.3).

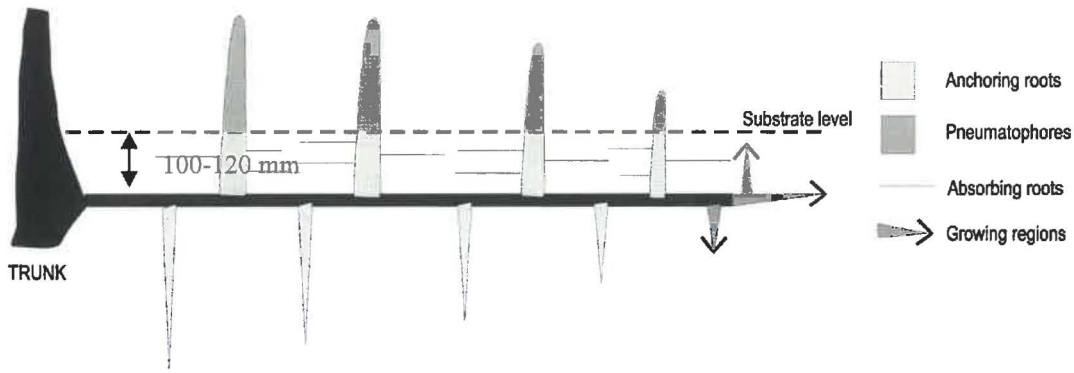

Figure 2.1 Schematic diagram of root architecture in *Avicennia* showing aerating, anchoring and cable components. (After Tomlinson, 1986)

Plate 2.3 Various forms of aerial roots in *Avicennia*: Left: developing prop roots. Right: Pneumatophores Scale bar = 1 cm. (Photos: C. Beard, Whitianga Harbour 2003)

The absorbing and anchoring component consists of downward-pointing roots that are the basis of anchorage for the system and the site of absorption. The cable component consists of horizontally spreading roots that connect the aerial and anchoring portions of the system, and help to secure the plant in unstable substrates such as soft mud. In *Avicennia* the cable portion is subterranean and extends the root system far wider than the tree canopy (Plate 2.4). Prop roots are not uncommon where trees are exposed, or are growing in very soft substrates (Plate 2.3).

Plate 2.4 *Avicennia marina* subsp. *australasica* spreading root system, indicated by lines of emerging pneumatophores. (Photo: C. Beard, Whitianga Harbour, 2003)

2.3.2.4 Flowers

The inflorescence, produced during summer and autumn on the tips of pubescent branches, is cymose and typically comprises four to eight hermaphrodite flowers. The flowers (Plate 2.5) are small, each only approximately 6-7 mm in diameter with 4 to 5 broad, leathery yellow-orange coloured petals, and 4 stamens inserted at the corolla throat (Allan, 1961). They are strongly scented and attract a variety of insect pollinators including bees, flies, butterflies and beetles (Walsby, 1992).

Flowering of *Avicennia* in New Zealand is reported to occur from February to June (Salmon, 1980), but has been observed to continue into September at Ohiwa Harbour (C. Beard *pers. obs.*). The onset of flowering varies considerably with latitude, occurring much later in the season at higher latitudes. For example, at latitude 38°S, flowering occurs May to June, approximately six months later than it does at latitude 25°S (Duke, 1991).

Some literature implies that mangrove plants growing at their southern geographical limits do not flower, or are unable to survive to a stage where flowers are produced (Chapman & Ronaldson, 1958, Mildenhall, 2001). This is not supported by observation in New Zealand where mangrove plants produce an abundance of flowers at the southern natural limits on both coasts as do those in the naturalised population at Tolaga Bay, south of the natural range of mangrove (C. Beard *pers. obs.*). Full anthesis may not always occur at the latitudinal limits (Crisp *et al.*, 1990), however it may be incomplete in only a portion of the plants. Viable flowers and propagules were observed at all of the southernmost populations over the years 2000 to 2004 (C. Beard *personal observation*).

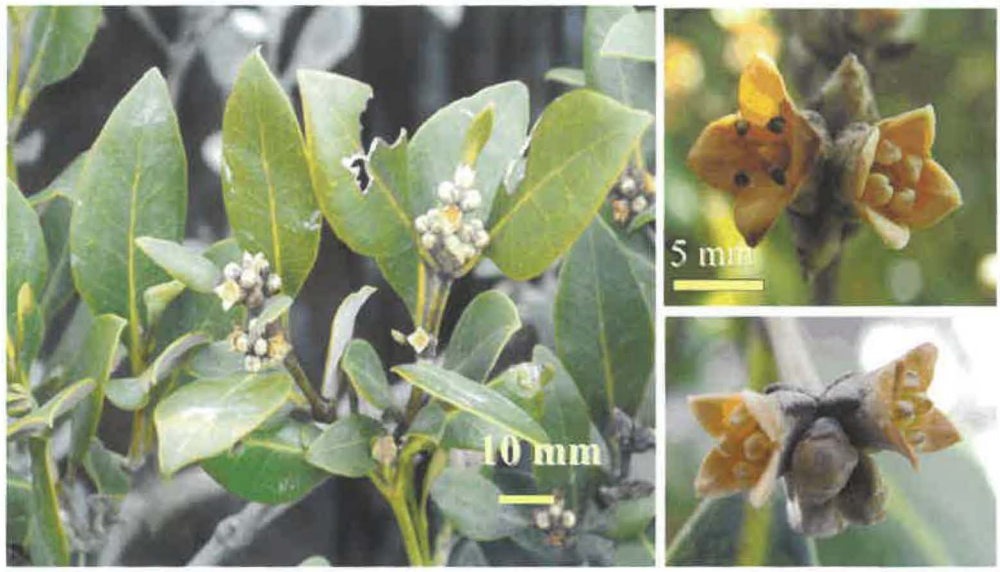

Plate 2.5 Left: The cymose inflorescence of *Avicennia marina* subsp. *australasica*, Ohiwa Harbour, June 2002. Above right: an older flower with spent anthers (left) and a recently opened bloom (right). Below right: developing buds and recently opened blooms, Matapouri, May 2004. Photos: C. Beard.

2.2.3.5 Reproduction

Approximately one third of mangrove species employ the reproductive strategy of vivipary whereby the embryo shows no dormancy, it germinates in the seed while still attached to the parent tree, and penetrates through the fruit pericarp before dispersal. Vivipary allows for rapid establishment of seedlings in unstable environments (Dawes, 1998), is a potential strategy to overcoming toxic chloride effects on seed germination (Bhosale, 1983), and may contribute to reducing the salt concentration in viviparous embryos (Farnsworth, 2000). *Avicennia* employs the strategy of cryptovivipary, where in a similar fashion to vivipary the embryo grows out of the seed while still attached to the parent plant, but it does not enlarge sufficiently to rupture the fruit pericarp.

The fruit of *Avicennia* is a 2-valved, 1-seeded capsule (Plate 2.6), and germination is well advanced before fruit fall (Allan, 1961). The developing embryo, rudimentary root structures and two fleshy cotyledons are enclosed by a protective pericarp, forming what is in effect a young growing plant (Plate 2.7). This unit, known as the propagule, is buoyant and is dispersed by flotation (Dawes, 1998).

Plate 2.6 Developing fruit of *Avicennia marina* subsp. *australasica*. Left: at maturity, the seed has germinated and the mature propagule is ready to drop from the parent plant. Right: at fruit set. Scale bar = 10 mm. Photo: C. Beard, Ohiwa Harbour July 2003, November 2003.

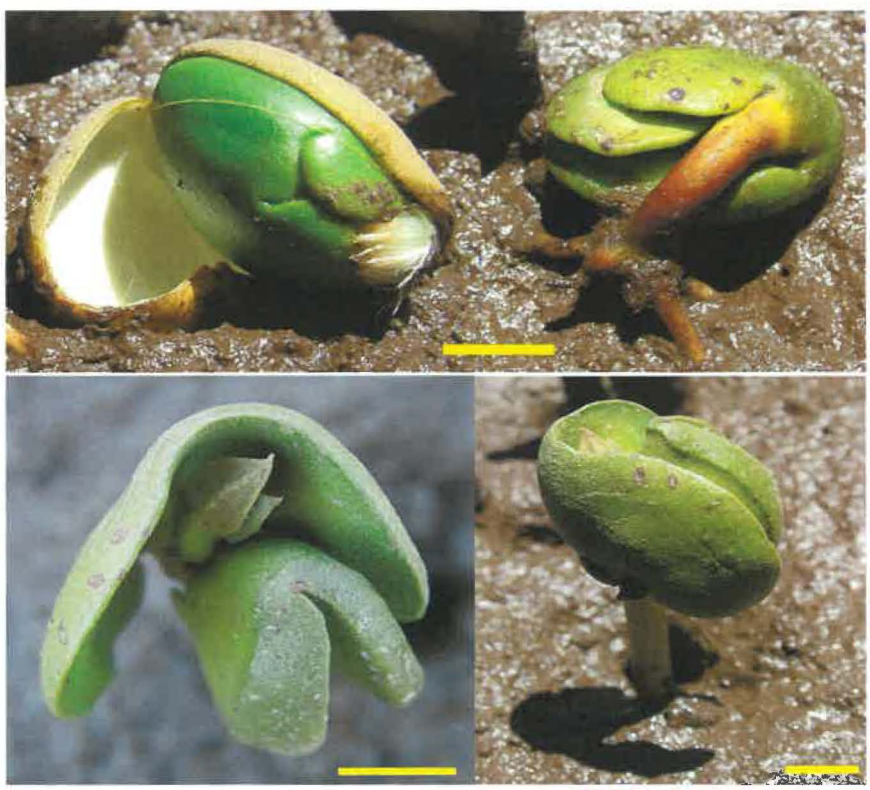

Plate 2.7 *Avicennia marina* subsp. *australasica* propagule establishment. Clockwise from left: The pericarp splits away from the propagule on contact with a moist substrate; developing roots anchoring the seedling in the mud; top view of first emerging leaf pair; side view of upright established seedling . Scale bars = 10 mm. Photo: C. Beard, Tauranga Harbour, January 2004.

Avicennia propagules in New Zealand mature during October and November and vary greatly in size within and between populations. Fresh propagule weights range from approximately 1 g to 10 g, their size apparently decreasing with a corresponding increase in latitude (Burns, 1982).

Timing between pollination, fruit development and propagule release is variable. Burns (1982) reported that propagule release in *Avicennia* from tropical northern Queensland occurred within two months of flowering, whereas in the temperate climates of New Zealand and Melbourne Australia, it occurred approximately five months after flowering. His suggestion was that the delay might either be simply a response of an essentially tropical species to the New Zealand winter, or else be a result of some genetic mechanism that allows propagules to be shed immediately prior to the best time of the year for seedling establishment.

2.4 Present and Recent Past Distribution: New Zealand

The source and timing of *Avicennia* arrival in New Zealand is not certain; although it is probable that some populations have Australian origins (McNae, 1968). The earliest confirmed evidence of mangrove in New Zealand lies in sediments from the Firth of Thames (North Island) dated at approximately 11 000 years BP (Pocknall, 1989). While this location lies well within the present range of *Avicennia* in New Zealand, historically this taxon extended much further south. Mildenhall (2001) reported *Avicennia* pollen from middle Holocene sediments (between 9000 and 7000 years BP) in Te Puroa Lagoon, northern Hawke Bay on the east coast, a location approximately 140 km south of the southernmost modern natural occurrences of mangrove in New Zealand. Pollen has also been recorded in Holocene sediments from Sponge Bay, and Awapuni, both locations on the east coast of the North Island in Poverty Bay (Mildenhall & Brown, 1987, Mildenhall, 1994). Radiocarbon dates indicate that *Avicennia* became locally extinct in this region approximately 6500-6000 years ago, at the time that post-glacial sea levels receded or when tectonics lifted the coastlines (Mildenhall, 2001)

The present range of *A. marina* subsp. *australasica* in New Zealand is restricted to coastal regions of the upper North Island with a southern limit that is approximately coincident with the 14°C isotherm. It forms dense stands along the sheltered littoral margins of most major estuaries, shallow harbours, lagoons and tidal creeks or rivers north of about latitude 38°S (Figure 2.2).

The southern natural limit occurs at almost identical latitudes on both east (Kutarere, Ohiwa Harbour, latitude 38°03'S) and west (Kawhia Harbour, latitude 38°05'S) coasts of North Island (de Lange & de Lange, 1994), (herbarium specimen WAIK 9299, collected in 1988, P. J. deLange). Recent investigations of both Aotea and Kawhia Harbours revealed that viable populations of mangrove are present but are very scattered, with fewer than 25 individuals seen at both locations (Meg Graeme, *pers. com.*, 2005)

Mangroves, when transplanted, are known to grow south of their natural limits in New Zealand. The southernmost occur on the east coast of the North Island at latitude 38°23' S, where a small population in the Uawa estuary, Tolaga Bay, has established successfully over the last 20 years from specimens transplanted out of Ohiwa Harbour (Crisp *et al.*, 1990, Daniel, 1986). Transplanted mangroves have also been previously documented, but are longer present further south between latitude on the west coast of New Zealand at the Awakino, Mohakatino and Urenui river mouths (Crisp *et al.*, 1990, de Lange & de Lange, 1994) and alongside the Hutt River at latitude 41°13' S in the North Island (de Lange & de Lange, 1994). Isolated plants survived at Parapara Inlet, Golden Bay, at latitude 40°43' S in the South Island of New Zealand (Walsby, 1992) for a number of years; one being removed from that location by the Department of Conservation as recently as March 2005 (C. Jones *personal communication*).

Mangrove propagules are occasionally washed ashore outside their natural range, to around latitude 38°40' S in Poverty Bay on the East Coast of the North Island (J.Quirk *personal communication*), and to Waikanae at latitude 40°52' S on the West Coast (M.Buchler *personal communication*). However, mangroves have not established successfully in these areas.

2.5 General climate of the mangrove zone in New Zealand

Mangrove occurrence in New Zealand is restricted to the warm temperate coastlines north of latitude 38°S (Crisp *et al.*, 1990) where the mean annual temperature ranges from about 16°C in the north to around 14°C in the eastern Bay of Plenty and Raglan Harbour. The coldest periods occur in July, and the warmest in January and February. In coastal regions there is relatively little variation between summer and winter temperatures, although further inland and to

the east of the ranges the variation can be up to 14°C. Winter frosts occur in estuarine areas south of around latitude 36°30'S.

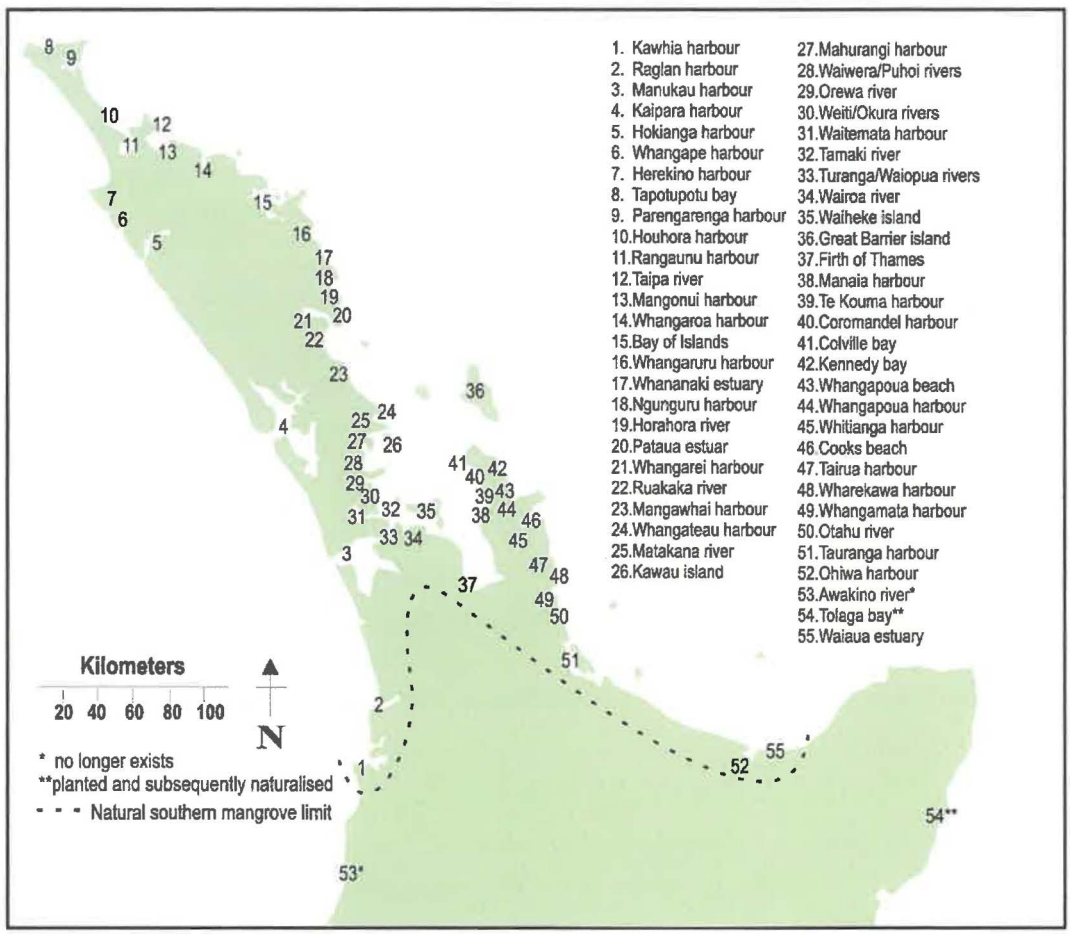

Figure 2.2 Present range, distribution and southern limits of *Avicennia marina* subsp. *australasica* in the upper North Island, New Zealand (after Crisp *et al.*, 1990).

Rainfall and sunshine-hours also vary throughout the range of mangrove in New Zealand with between 600 and 1600 mm of rain falling annually in most regions. The northern and central regions receive more rain in winter than in summer, and as a general rule, the driest periods occur over summer. Most places receive around 2000 hours of sunshine annually, but areas that are sheltered from the south and the west, such as the Bay of Plenty, generally receive more. The Whakatane region for example, including Ohiwa Harbour, receives more than 2350 hours of sunshine per year (McKensie, 1995, NIWA, 2003b).

2.6 Mangrove population structure at the study sites

All mangrove populations used in these studies were considered to be of mixed age based on the presence of seedlings and individuals ranging in size from small to large, relative to the largest plant present. Mature individuals were considered to be those producing flowers and fruit. The experimental work was generally undertaken on individuals that were considered to be of a similar age, based on their size and reproductive status. However, it must be noted that age estimations based on size alone were merely speculative given that growth rings in the wood of *Avicennia* are formed by anomalous cambial activity and the relationship between age and the number of growth rings is variable (Burns, 1982).

2.7 Study site descriptions

2.7.1 Ohiwa Harbour

Ohiwa Harbour (Figure 2.3), extending south to latitude 38°S, marks the southernmost natural limit for mangrove on the east coast of New Zealand. It is a barrier-enclosed estuarine lagoon (Healy & Kirk, 1982) located within the eastern Bay of Plenty of New Zealand's North Island and is regarded as somewhat unusual for its small catchment size and relatively insignificant river input (Healy, 2002).

Mangrove is widespread within the harbour, occupying fine mud sediments of the upper intertidal regions. In many places new mangrove colonies are continuing to establish on open areas of mudflat.

Throughout the harbour, the mangroves are typically short in stature with broadly spreading crowns. Many individuals, particularly those around Motuotu Island (top panel, Figure 2.3), are around 50 cm in height with spreading crowns up to 3 or 4 meters in diameter. On average however, most specimens grow to heights of between 1 and 1.8 metres.

Two sites within Ohiwa Harbour were chosen for research activities; one next to the main road east ("Wainui Road" site), and the other accessed from the property of Margaret Tuite ("Tuite" site) (Figure 2.3).

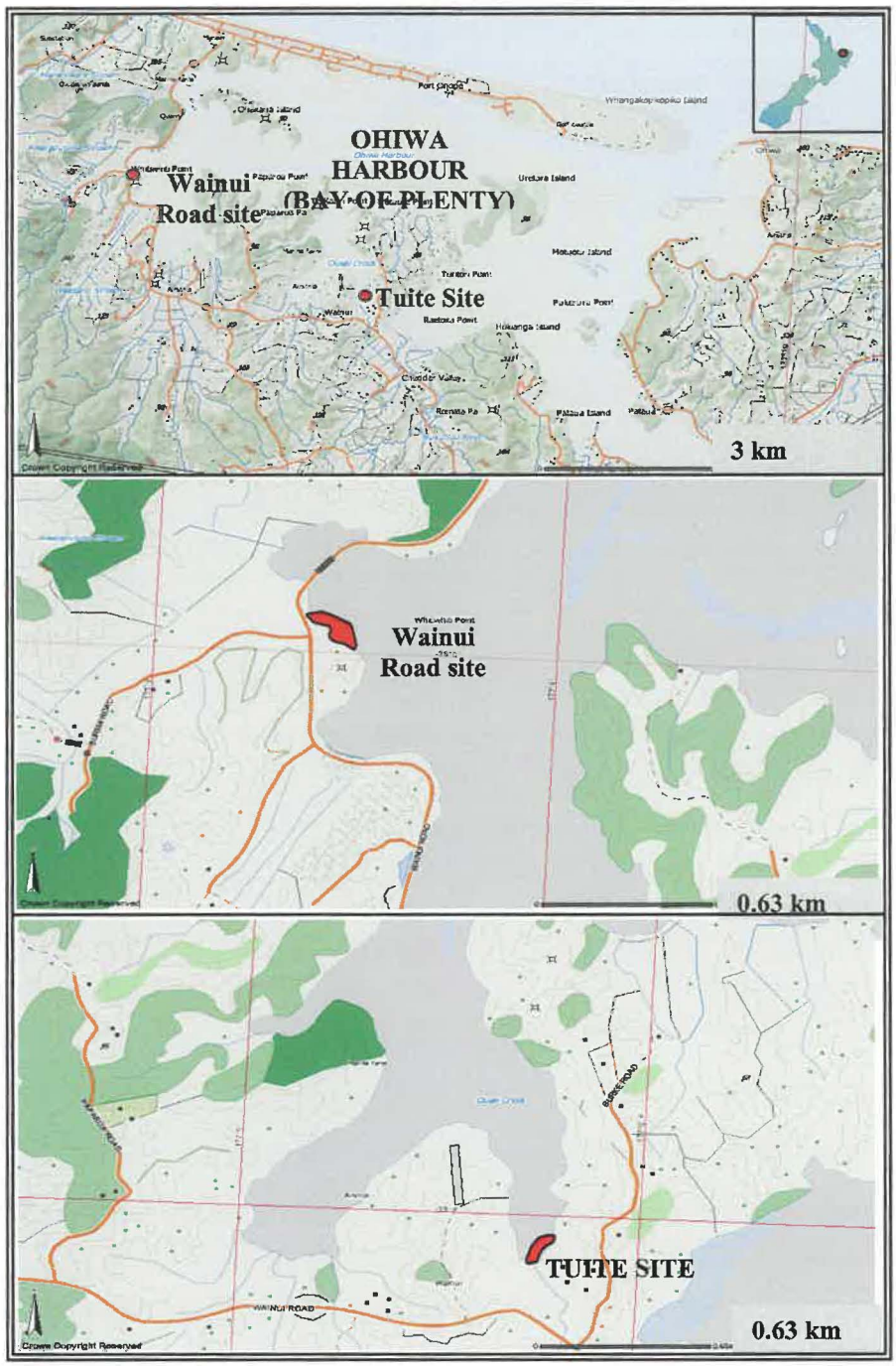

Figure 2.3 Locations of the Wainui Road and Tuite research sites, Ohiwa Harbour, Bay of Plenty, North Island, New Zealand. Above: Ohiwa Harbour. Middle: Position of the Wainui Road research site (delineated by red shading on the map) located at latitude 37°59'S, longitude 177°03'E. Below: Position of the Tuite mangrove site (delineated by red shading on the map) in the Ouaki Creek arm of Ohiwa Harbour Latitude 38°01'S, Longitude 177°05'E. (Maps: nztopoonline.linz.govt.nz).

2.7.1.1 Wainui Road Research Site

The Wainui Road research site is located on the western edge of Ohiwa Harbour near Ohakaua Island at latitude 37°59' S, longitude 177°03' E (Figure 2.3).

It occupies a northerly aspect on the harbour side of a causeway on Wainui Road, and comprises approximately one hectare of dwarf *A. marina* subsp. *australasica* forest interspersed with patches of sea rush salt marsh, *Juncus krausii* Hochst. subsp. *australiensis* (Buchenau) Snogerup (Plate 2.8). The mangrove population is of mixed-age and the tallest individuals are around 1.5 metres in height. Seedlings are abundant in the open patches of salt marsh and around the perimeters of larger specimens.

At mean high water of spring tide (MHWS), the site is inundated to depths of approximately 40 mm, but at mean high water of neap tide (MHWN) the site is seldom fully flooded. During each tidal cycle, water recedes fully from the area across a gently sloping mudflat. There are no major drainage channels in close proximity to the mangroves.

Plate 2.8 The author (1.78m) amongst *Avicennia* at the Wainui Road mangrove research site, Ohiwa Harbour, Bay of Plenty New Zealand. August, 2004. (Photo: T.G.A.Green).

Several studies were based at the Wainui Road site over the course of this project. In the winter and summer of 2001, and the spring and autumn of 2002, diurnal investigations of gas exchange, chlorophyll *a* fluorescence, water relations and chlorophyll content in the leaves of up to five mangrove plants were undertaken to establish baseline information about mangrove performance in the

area (refer to Chapter 4). Over the autumn and winter of 2003, monthly measurements of leaf gas exchange, chlorophyll *a* fluorescence and chlorophyll content were made on two plants to investigate the physiological effects of winter frosts on the mangrove.

Leaf samples were also collected for stable isotope and genetic analyses. Climate parameters, including air and substrate temperatures, relative humidity and light levels were monitored continuously on site until equipment failure in 2002. Subsequently through 2003, only air temperatures within and above the mangrove canopy were recorded.

2.7.1.2 Tuite Research Site

The Tuite research site is situated at latitude 38°01' S, longitude 177°05' E in the narrow estuarine mouth of Ouaki Creek towards the south-western margin of Ohiwa Harbour (Figure 2.3). The site is flanked by steep farmed hill-slope on its eastern boundary, leaving the mangrove plants fully shaded for up to one-and-a-half hours after sunrise.

Plate 2.9 View of the Tuite mangrove site, looking north, Ohiwa Harbour, Bay of Plenty New Zealand. (Photo: C.Beard, 2003).

Tidal waters flood the site on a diurnal basis, although at MHWN seldom exceeds a depth of 50 mm around the study plants. The area is inundated to approximately 700 mm depth at MHWS. Tidal waters recede fully from the site along a shallow channel that is situated in bare mudflat approximately 10 m

distant from the mangrove fringe and which runs parallel to the shoreline in the centre of the estuary arm.

The eastern shoreline of this part of the estuary is bordered by a 10 - 15 m margin of *Juncus* spp. and *Bolboschoenus* salt marsh and a dense fringe of low-growing *A. marina* subsp. *australasica* (Plate 2.9). The mangroves grow to a maximum height of approximately 1.5 m and are rooted in substrate that grades from fine firm mud near the salt marsh boundary to sandy mud near the main drainage channel.

The Tuite site was utilised in December 2002, January and March 2003 for the development and implementation of experiments investigating the response of mangrove to artificial frost nights (refer: Chapter 5).

2.7.2 Bay of Islands

Mangroves are widespread throughout the Bay of Islands, forming extensive forests in most estuaries, and dense fringes along the banks of most estuarine rivers, streams and creeks in the area. They grow on a wide variety of substrates ranging from sandy and silty muds to solid basalt rock. Stunted or dwarf mangroves, such as are common further south in the Bay of Plenty, are atypical of northland populations; instead the majority of individuals grow to heights of 8 or 9 metres with trunk diameters up to 30 cm.

2.7.2.1 Paihia A and B research sites

Paihia site A is located at latitude 35°17'S, longitude 174°04'E on the southern shore of what is essentially the estuarine mouth of the Waitangi River, but is also where the Kaipatiki Stream and Hutia Creek exit into the estuary (Figure 2.4). The mangroves are of mixed age, and the oldest specimens are approximately 6 m tall (Plate 2.10). In the upper intertidal zone they are growing on coarse shelly mud. Those in the lower zones are rooted in fine silty mud sediments. Paihia site A was abandoned after August 2001 due to security concerns, and the experiments were transferred approximately 3 km south to Paihia site B. This site adjoins the edge of causeway north of Te Haumi in the estuarine mouth of the Haumi River, and faces east to the Veronica channel (Figure 2.4). The trees are of a similar age and size to those at site A, and grow in firm fine mud (Plate 2.11).

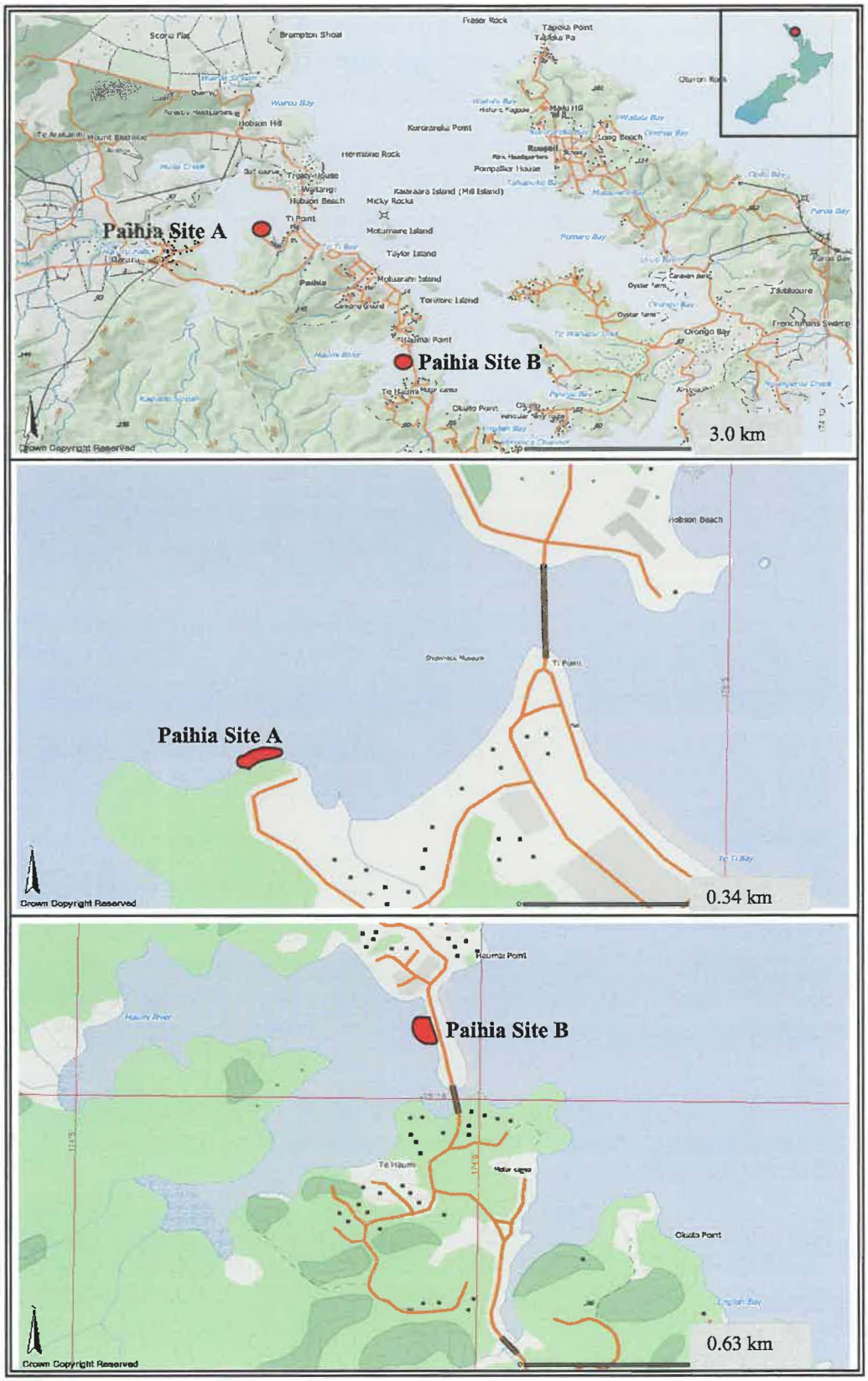

Figure 2.4: Above: Locations of the Paihia research sites at latitudes (A) 35°17' S and (B) 35°18'S, longitude 174°04'E, Bay of Islands, North Island, New Zealand. Middle: Site A (red shaded area), in the estuary where the Kaipatiki Stream Waitangi River and Hutia Creek converge south of the Waitangi Marae. Bottom: Site B (red shaded area), in the mouth of the Haumi River on the western edge of the causeway north of Te Haumi settlement. (Maps: nztopoonline.linz.govt.nz)

Plate 2.10 The Paihia A research site in the estuarine mouth of the Waitangi river, Kaipatiki Stream and Hutia Creek, south of the Waitangi Marae: Bay of Islands, North Island, New Zealand. (Photo: C. Beard, August 2001).

Plate 2.11 The Paihia B research site adjoining the edge of causeway north of Te Haumi in the estuarine mouth of the Haumi River, facing east to the Veronica channel. (Photo: T.G.A. Green, December 2003).

Investigations of leaf gas exchange, chlorophyll *a* fluorescence and water relations were undertaken in August and December 2001 at two sites near Paihia Township (refer Chapter 4). Leaf samples were also collected from the sites for chlorophyll content, stable isotope and genetic analyses. Microclimate parameters including air and substrate temperatures, relative humidity and light were also recorded on-site during 2001 and 2002

2.7.3 Coromandel Peninsula

2.7.3.1 Whitianga Harbour

Whitianga Harbour, on the North Island's Coromandel Peninsula, is a bayhead barrier-enclosed inlet that faces east to Mercury Bay and the Pacific Ocean (Plate 2.12). The harbour is fed by a number of tributaries, but its main source of fresh water is the extended catchment area of four rivers; the Whangamaroro, Waiwawa, Whenuakite, and Ounuora. The harbour supports an abundance of mangroves, and has done so for quite some time. In 1769 when the explorer Captain James Cook was in the vicinity to observe the transit of Mercury, he named the harbour waters "The River of Mangroves" (Beaglehole, 1955).

Plate 2.12 Aerial view of mangrove in the Whangamaroro River, Whitianga Harbour. White arrow indicates research site. (Photo: T. R. Healy, June 1997).

The Whitianga research site is situated at latitude 36°51' S longitude 175°42' E on the northern edge of the estuary where the Whangamaroro river enters Whitianga Harbour (Figure 2.5, Plate 2.12). The mangroves here are a mixed-age population and form a 60 to 80 m fringe between residential properties

and the estuary. They grow in a soft substrate of fine mud sediment and reach a maximum height of approximately 5 metres. Most of the research at this site was undertaken from a small jetty that extended about 30 metres into the mangrove fringe (Plate 2.13).

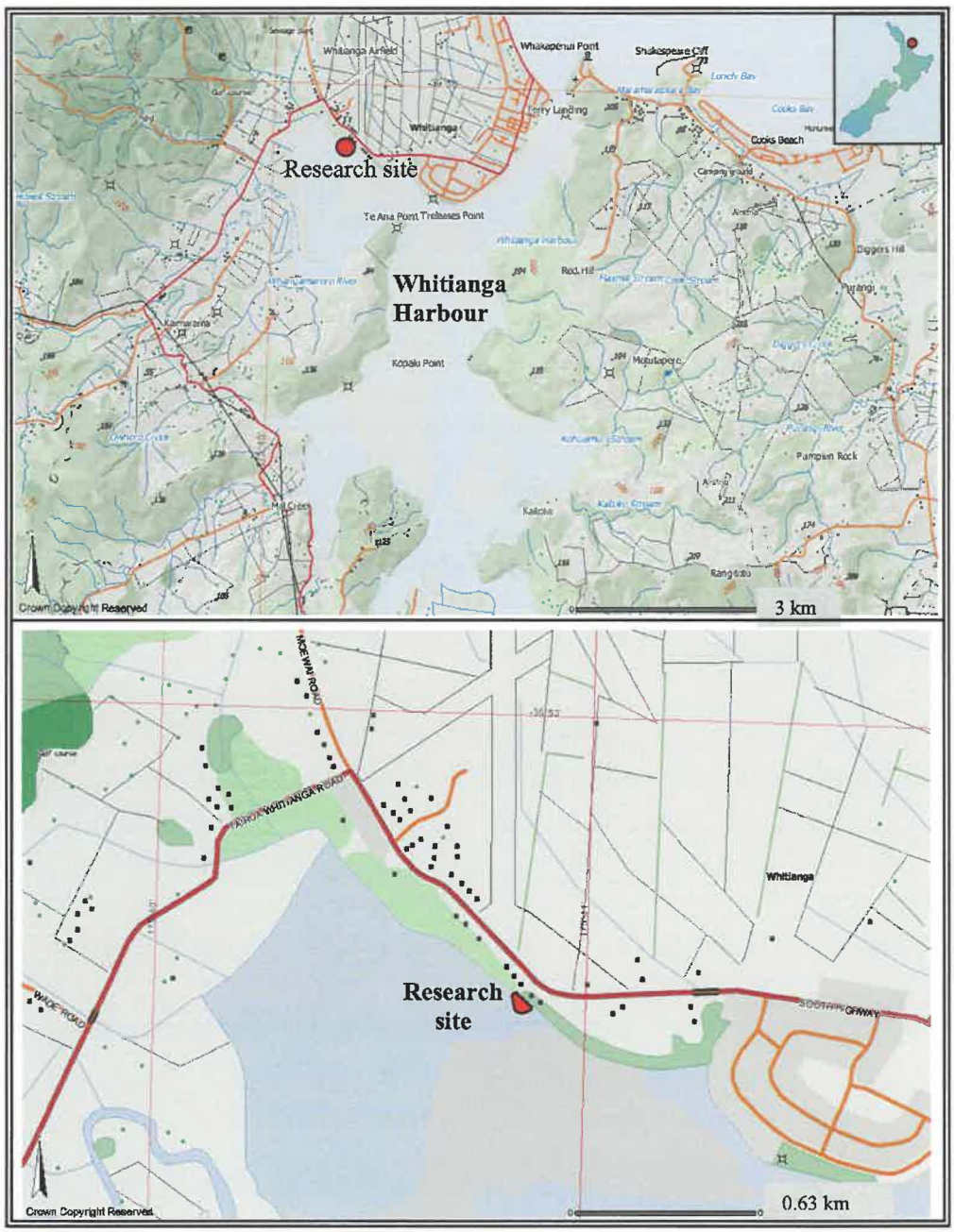

Figure 2.5 Location of Whitianga Harbour on the east coast of the Coromandel Peninsula, North Island New Zealand, and the research site (red dot on upper map and red shaded area on lower map) at latitude 36°51'S longitude 175°42'E (Maps: nztopoonline.linz.govt.nz).

Plate 2.13 The Whitianga research site, Whitianga Harbour, Coromandel Peninsula, North Island New Zealand. (Photo: C. Beard, August 2001).

The Whitianga site was utilised for diurnal investigations of leaf gas exchange, chlorophyll fluorescence and water relations in July and November of 2001 and March 2002, and development of equipment and protocols for a series of experiments on artificial frost in 2003. Leaves were sampled from the site for chlorophyll content, stable isotope and genetic analyses. Microclimate parameters of light, relative humidity, air and substrate temperatures were also monitored on-site.

2.8 Microclimate

On-site climate parameters were recorded with several types of data-logging devices, including Campbell, Hobo and I-button loggers.

2.8.1 Campbell data-loggers

An array of sensors connected to CR10 and CR10X Campbell data-loggers (Campbell Scientific Inc, Utah, U.S.A.) were used to record temperatures (degrees Celsius), light levels (photon flux density, PFD, 400 to 700 nm in μmol m^{-2} s^{-1}) and relative humidity at three study sites at Paihia (Bay of Islands), Whitianga and

Ohiwa Harbours over various periods during the years 2001 – 2003 (refer Chapters 4-6).

Ambient air temperature and percent relative humidity were monitored with Campbell 207 temperature/RH probes attached to either a sturdy branch or a wooden pole within the mangrove canopy or in nearby trees at a height of approximately 2m. Campbell 107 temperature probes were used to measure substrate temperatures at a depth of 2cm and ambient air temperature at selected heights within the mangrove canopy. The temperature and humidity sensors tracking conditions outside the mangrove canopy were mounted in screens to prevent heating by incident radiation.

PFD was measured inside and above the canopy with either Hom-me (Landcare Research, Hamilton, New Zealand) or LI-190SA Li-Cor Quantum sensors (Li-Cor Biosciences, Nebraska, U.S.A.). All light sensors were calibrated to manufacturer's standards using a Li-Cor LF- 1800-02 calibrator.

The Campbell data-logger set-up described above was also used in the field to monitor the environment during artificial cooling experiments. During these events, additional sensors (Campbell Type-T copper-constantan thermocouples) were used to measure the surface temperature of cold-treated leaves during the experimental freeze/thaw cycles and the ambient temperatures inside the artificial cooling chambers (refer to Chapter 6).

The CR10 and CR10X data-loggers were programmed using PC208W Data-logger Support Software vs.3.0 (Campbell Scientific Inc, Utah, U.S.A.), with recording intervals set at 10, 15 or 20 minutes. The data were downloaded in the field to a Toshiba Satellite laptop computer, and later manipulated using the spreadsheet programme Excel 2000 (Microsoft, U.S.A). The PC208 operating programmes designed to monitor both study site and artificial cooling chamber microclimate are appended in Appendix I.

2.8.2 Hobo data-loggers (Onset Computer Corporation, U.S.A.)

Air temperature in degrees Celsius was also monitored at three sites in Ohiwa Harbour with small portable StowAway TidbiT loggers (Plate 2.16). According to the manufacturer's specifications, the Hobo loggers are accurate to ± 0.2°C, with resolution at ±0.16°C, and response time varying from 50 minutes in still air to 18 minutes in air moving at approximately 1 metre per second (typical to 90%) (Onset Computer Corporation, 2004).

The data-loggers were positioned in a vertical profile in relation to a single mangrove specimen; one logger approximately 2 cm above the substrate, one within the bulk of the canopy at a height of approximately 60 cm, and one level with the tip of the canopy approximately 150 cm above the substrate. The loggers were attached with plastic cable-ties to sturdy branches or to wooden poles tied to the mangrove plants (Plate 2.14).

Plate 2.14 An unscreened Hobo StowAway TidbiT temperature logger attached in the upper canopy (approximately 1.5 m above the substrate) of *Avicennia marina* subsp. *australasica* plants, Ohiwa Harbour, Bay of Plenty. (Photo: C.Beard, July 2002)

With their fully waterproof, resin-enclosed design, the Hobo StowAway TidbiT temperature sensors proved to be the most robust of the three types of data-logger used during this project, and remained undamaged by the salty maritime environment. Unfortunately, being unscreened, they proved less than ideal for measuring maximal temperatures in fully exposed positions above the mangrove canopy. The main drawback was that they returned falsely high maximum readings on clear sunny days due to the heating effects of direct sunlight on the probe casing. However, since the primary purpose of these sensors was to track night temperatures when radiative warming was obviously not important, the daytime measurements were largely excluded from analyses.

Data were downloaded in the field using Boxcar vs. 3.6 software, either directly to a Toshiba Satellite laptop computer, or to a Hobo Optic Base Station and later transferred to computer via an Optic Shuttle (Onset Computer Corporation, U.S.A.). The data were manipulated with the spreadsheet programme Excel 2000 (Microsoft, U.S.A), and subsequent graphs were produced using Sigmaplot 2002 for Windows vs. 8.0 (SPSS, United Kingdom).

2.8.3 Climate Stations

Additional climate data was sourced from the National Institute of Water and Atmospheric Research (NIWA) for Paihia, Ohiwa and Whitianga Harbours.

2.9 Water relations and leaf water potential

One of the most widely used techniques for measuring plant water status is the estimation of xylem pressure in harvested tissue with a pressure chamber. The technique is based on the principles of the Cohesion-Tension theory proposed by Dixon and Joly in 1894, summarised recently in Tyree (1997). Its main assumptions are that water in the xylem ascends under negative pressure or tension due to the transpiration pull generated by evaporation of water from the leaf surfaces to the atmosphere. The tension is transmitted from the leaves through a continuous water column to all parts of the plant. If the water column is broken, for example, by the action of excising a leaf, the negative pressure or tension in all the severed vessels is temporarily relieved (i.e., the equilibrium xylem pressure becomes zero), and water recedes from the point at which the cut was first made, moving by osmosis into the surrounding dehydrated cells until equilibrium is established. The equilibrium xylem pressure may be more or less negative than the xylem pressure at the time of cutting depending on pre-existing pressure-gradients within the stem or leaf, and the hydration status of the cells (Tyree, 1997). If the leaf is subsequently enclosed within a sealed chamber with the cut end protruding to the surrounding air, and pressure applied gradually, the water can be forced back into the xylem vessels to the level of the original cut. The lowest pressure required to bring the water back to the cut surface is termed the balance pressure and is assumed to be a direct measure of the tension (negative pressure) that existed within the xylem prior to excision (Slavik, 1974).

In the situation where a leaf has been previously transpiring prior to excision, time must first be allowed for equilibrium of water potential gradients to be reached before the measurement is made, as the pressure chamber is capable only of measuring equilibrium values of negative pressure (Wei *et al.*, 2000).
Water potential of the leaf is calculated indirectly from pressure measurements by the relationship:

$$P = \Psi_w - \Psi_s$$

where P is the measured xylem pressure,

Ψ_w is the water potential of the leaf cells,

Ψ_s is the osmotic potential of the xylem fluid. (As Ψ_s is usually close to zero, in relation to typical midday tensions in the xylem, insignificant, the correction is frequently omitted).

Despite some controversy over the reliability of using a pressure chamber to determine xylem tension (Melcher *et al.*, 1998), this technique was chosen for its convenience and portability in the field to investigate water relations in *A. marina* subsp. *australasica* at Ohiwa Harbour, Whitianga Harbour and Paihia, Bay of Islands over four seasons during years 2001 and 2002. Leaf water potential (Ψ_w) was estimated indirectly using a pressure chamber based on the design of Scholander et. al. (1965) (Figure 2.6).

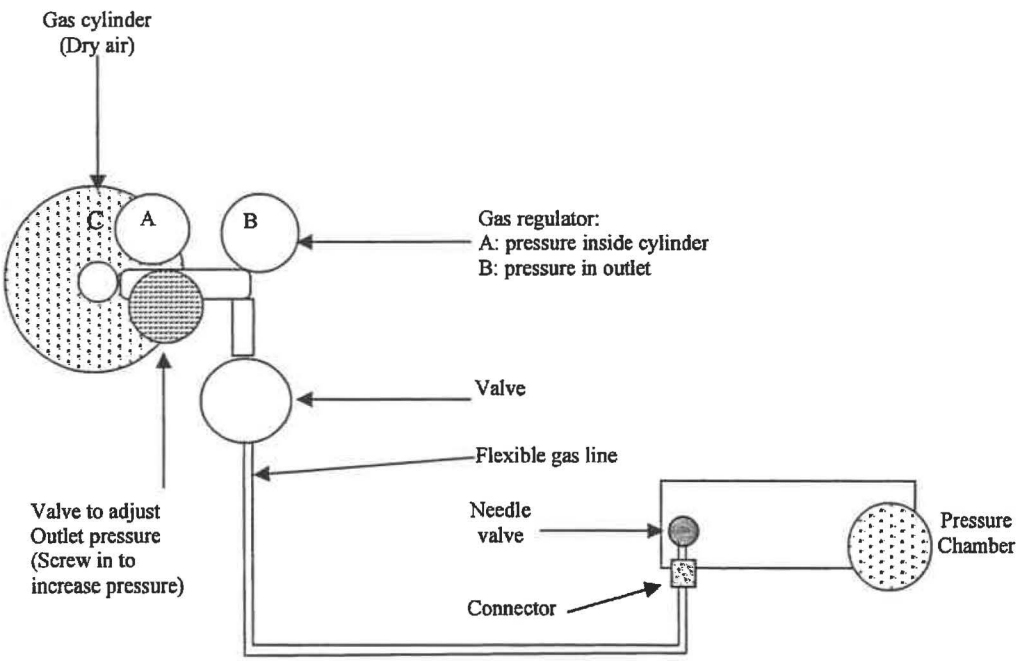

Figure 2.6 Schematic diagram of the Scholander-type pressure bomb used to determine leaf water potential in *Avicennia marina* subsp. *australasica*. During use, the apparatus was connected to a cylinder of pressurised dry air (C).

2.9.1 Sampling procedure: Pressure Bomb

Diurnal patterns of leaf water potential were established by measuring xylem pressure in two leaves from each plant at two-hourly intervals, starting at dawn and finishing at dusk. Leaves were removed from the plant using a sharp razor blade to make a single cut across the petiole, after which they were placed immediately into sealed plastic bags to reduce further water loss. Each leaf was

then sealed inside the pressure chamber with the cut end protruding through a rubber gasket into the open air. The internal chamber pressure was then increased slowly with a controlled needle valve, while simultaneously observing the leaf petiole with a hand-lens. As soon as water was seen to return to the cut surface of the petiole, the balance pressure value was locked on the digital readout and recorded.

Given that leaf water potential can be significantly altered according to the position of the leaf in the canopy (Mwangi Theuri *et al.*, 1999), sampled leaves were removed from approximately the same height on all the trees at each site in order to minimize sampling variability.

2.10 Determination of leaf chlorophyll content

2.10.1 Direct method: Absorbance of extracted pigments

The standard methodology for determining leaf chlorophyll content involves the measurement of the absorbance of extracted pigments. In the present study, chlorophyll pigments were extracted from *Avicennia* leaves from Ohiwa Harbour following the method described by Porra *et. al* (1989).

A 10 mm diameter leaf disc of healthy tissue was first punched from the leaf blade with a cork-borer, avoiding main veins and discoloured areas. The disc was then crushed in liquid nitrogen using a mortar and pestle, and the ground sample transferred to 10 mL of extraction solution comprising 80% acetone and 20% 0.05M aqueous Tris Buffer (Jensen, 1980). Following an extraction time of 12 hours at 4°C in the dark, the extract was centrifuged at 3900 rpm for 10 minutes in a Centaur 2 centrifuge (Fisons, England). The supernatant was decanted, made up to 10 mL with extraction solution, thoroughly mixed and a 5 mL sub-sample transferred to a rectangular quartz spectrophotometer cuvette (optical path of 10 mm).

Chlorophyll absorbance was measured at wavelengths of 663.6 nm, 646.6 nm (the absorption peaks of chlorophyll *a* and *b*), and at 750 nm with a Shimadzu UV-VIS spectrophotometer UV 160 (Shimadzu Corporation, Kyoto, Japan). Calibration to zero absorbance was set using the extraction solution as a blank. Absorption at 750 nm was measured to check the clarity of the extracts, and its value was subtracted from the absorbances at 663.6 nm, 646.6 nm prior to the final calculations. If the absorbance at 750 nm was greater than 5% of absorbance at 663.6 nm the samples were centrifuged a second time and re-measured.

Chlorophyll concentrations (μg Chl ml^{-1}) were calculated after (Porra *et al.*, 1989);

chl a $= 12.25\ A^{663.6} - 2.55\ A^{646.6}$

chl b $= 20.31\ A^{646.6} - 4.91\ A^{663.6}$

chl a+b $= 17.76\ A^{646.6} + 7.34\ A^{663.6}$

where $A^{646.6}$ and $A^{663.6}$ are the absorbances at the corresponding wavelengths less the absorbance at 750 nm.

The fresh weight of the leaf was determined before (FW_{total}) and after removal of the 10mm disc (FW_{rem}). The dry weight of the leaf less the 10mm disc (DW_{rem}) was determined after 24h drying at 100°C. Chlorophyll concentration on a dry weight basis (μg Chl mg^{-1} DW tissue) was then calculated as:

Chlorophyll content = (calculated μg Chl ml^{-1}* 10)/ DW_{total}

Where $DW_{total} = DW_{rem} * (FW_{total})/ FW_{rem})$

and DW_{total} = dry weight of entire leaf

FW_{total} = fresh weight of entire leaf

FW_{rem} = fresh weight of leaf remainder (not used in chlorophyll analysis)

DW_{rem} = dry weight of leaf remainder (after drying at 100°C for 24 h)

2.10.2 Indirect method: SPAD-502 chlorophyll meter

The SPAD-502 meter (Minolta Camera Co., Osaka, Japan) is a field-portable unit that calculates chlorophyll content from the optical density measurements of two light beams passed through a leaf sample. When the measurement head is closed on a leaf, two LEDs in the SPAD illuminating system are turned on, thereby delivering a reference beam with an infrared peak wavelength at approximately 940 nm, and an absorbance beam set to a peak of chlorophyll absorbance at a wavelength of approximately 650 nm. The transmittances of both beams through the leaf are measured by a silicon photodiode receptor in a sensor head measuring 2mm x 3mm. Chlorophyll content is then calculated from the ratio (at calibration and at measurement), of the absorbance beam to the reference beam, and is expressed in terms of SPAD-units (Spectrum, 2002).

In normal use, ten non-overlapping measurements were made on each leaf, ensuring that the sensor head was positioned over healthy tissue and that any major leaf veins were also avoided. Mean SPAD-unit values were calculated for each leaf and were used in all subsequent statistical analyses. Calibration curves were produced by determining the SPAD values for 10mm leaf discs which then had their chlorophyll content determined by the standard extraction procedure.

The advantages of using a chlorophyll meter to estimate foliar chlorophyll content as opposed to more traditional methods of measuring absorbance of extracted pigments are two-fold: firstly, measurements can be made *in-situ,* and secondly, all leaf tissues and pigments are left unharmed by the sampling process. This means relative changes in chlorophyll content can easily be followed over time in the same sample. There are disadvantages associated with this technique mainly related to the accuracy of the calibration and these are fully discussed in relation to results in Chapter 5.

2.11 Porometric gas exchange measurement of leaves

2.11.1 CIRAS-1

A CIRAS-1 Portable Photosynthesis System (PP Systems, UK) was used in the field to measure leaf photosynthesis and transpiration. The CIRAS-1 employs a differential, open-flow system of measurement based on the combination of four absolute infra-red gas analyzers (two CO_2 and two H_2O), an integral air supply unit and a Parkinson leaf cuvette (PLC) (Plate 2.15).

Plate 2.15 Left: The Parkinson Leaf Cuvette and measurement of leaf photosynthesis and transpiration in *Avicennia marina* subsp. *australasica*. (Photo: T.G.A. Green, 2002), Right: The CIRAS-1 Differential CO_2/H_2O Infra-Red Gas Analyser and Parkinson Leaf Cuvette. (Photo: PP-Systems, UK).

Operation of the CIRAS-1 is described simply by the flow diagram below (Figure 2.7). Ambient air entering the system is first scrubbed and dried through a series of columns containing soda-lime, drierite and molecular sieve (A). An automatic air supply unit (B) then controls the addition of pure CO_2 from an internal cartridge, and delivers a regulated flow of air at set partial pressures of CO_2 and (if required) water vapour, to both surfaces of part of a leaf sealed between the upper and lower halves of the leaf cuvette (sample area = 2.5 cm^2) (Plate 2.14).

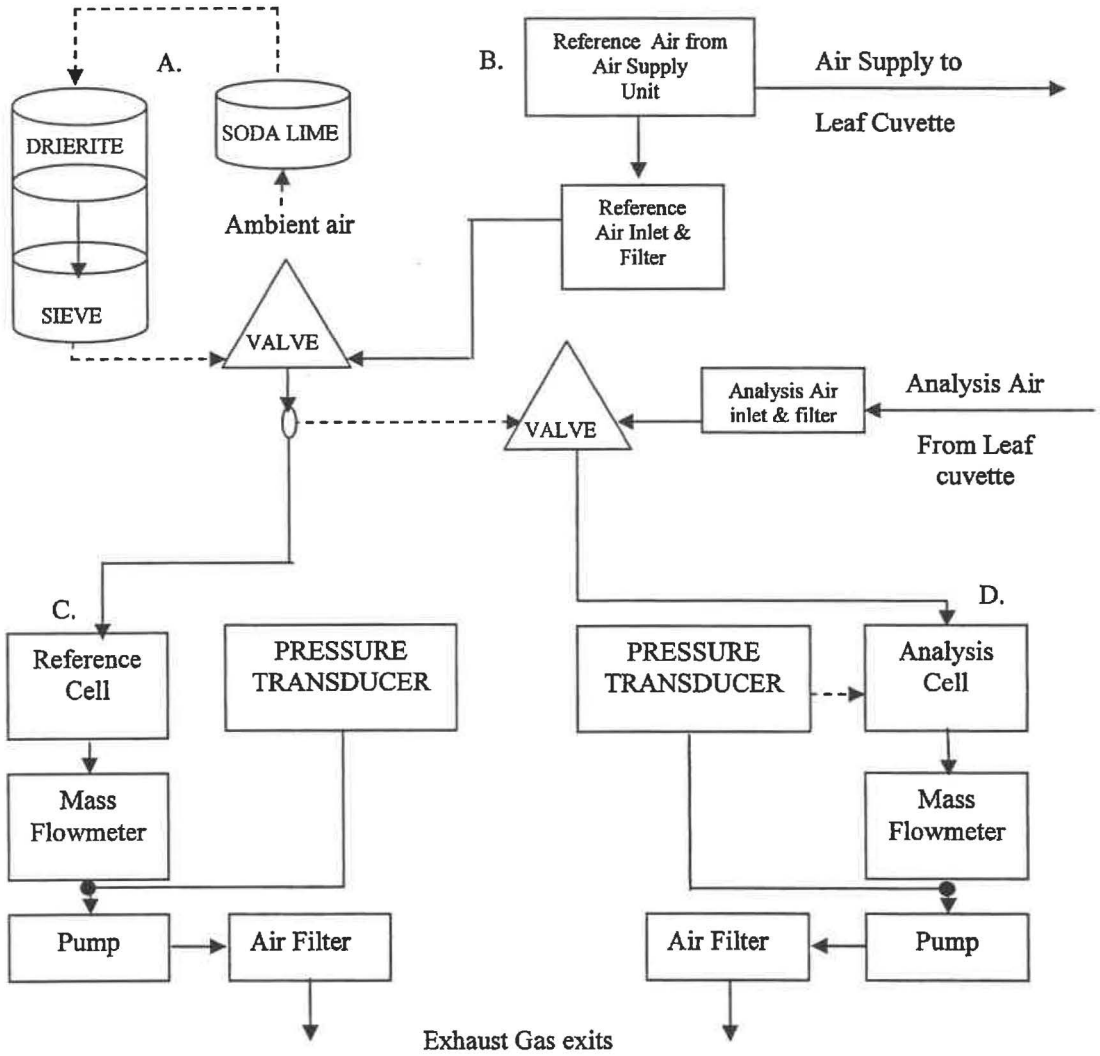

Figure 2.7 Flow diagram of the CIRAS-1 analyser gas circuit. Adapted from the CIRAS-1 Combined Infrared Gas Analyser System Operator's Manual Version 2.4 (PP-systems, United Kingdom)

Uptake or loss of CO_2 and loss of water by a leaf in the cuvette is determined by two pairs of IRGAs that measure the partial pressures (ppm – parts per million) of CO_2 and water vapour in the air streams entering and exiting the

leaf cuvette. One pair of reference IRGAs (C) measure the partial pressures of CO_2 and water vapour in a proportion of the air-stream that is drawn off before it enters the leaf cuvette, and the measurements are then repeated by a second pair of analysis IRGAs (D) on an equivalent sample of air after it has passed through the cuvette.

The system is automatically zeroed by passing CO_2-free dry air at regular intervals through all analysis and reference cells. Differential balance of the IRGAs is also maintained at similar intervals by passing the reference air-stream through all cells. A differential factor is then calculated that equalises the readings. Temperature corrections are not required as the air is equilibrated to a standard temperature before it enters the cells of the IRGAs. Pressure changes in the cells are automatically compensated for by built-in pressure transducers.and H_2O concentrations.

2.11.2 Gas exchange parameters

The absolute values of CO_2 and H_2O measured in the air streams entering and leaving the leaf cuvette were used to calculate a series of parameters for each leaf sample including photosynthetic rate (A, net rate of CO_2 exchange in the cuvette), transpiration rate (E), stomatal conductance to water vapour (gS), and sub-stomatal cavity CO_2 concentration (C_i).

The Parkinson leaf cuvette chamber temperature and photon flux density (PFD, μmol m^{-2} s^{-1}, 400 to 700nm) incident on the leaf chamber were also measured by way of a silicone photodiode sensor mounted adjacent to the leaf cuvette window and a Precision thermistor mounted within the chamber. Temperatures within the leaf chamber were maintained close to ambient with a cooling fan, and the thermal load on the leaf within the cuvette was lessened by design of the cuvette window which filtered out much of the infra-red radiation above 700 nm.

2.11.3 Calculations

The following calculations pertaining to photosynthesis and gas exchange of leaves were derived by von Caemmerer and Farquhar (1981) and are fully explained in their manuscript. The calculations have been summarised here to illustrate the parameters calculated by the CIRAS-1.

The rate of CO_2 assimilation per unit leaf area (A), measured in an open system, can be derived as follows:

Transpiration rate (E) in mol m^{-2} s^{-1} of a leaf with area $s(m^2)$ is

$$sE = u_o w_o - u_e w_e \qquad (1)$$

where u_e and u_o are the molar flows of air entering and leaving the cuvette chamber and w_e, w_o are the mole fractions of water vapour in the gas streams entering and leaving the cuvette.

CO_2 assimilation rate (A) in mol m^{-2} s^{-1} per unit leaf area is

$$sA = u_e c_e - u_o c_o \qquad (2)$$

where c_e and c_o are the mole fractions of CO_2 in the gas streams entering and leaving the cuvette and u_e, u_o are as above. CO_2 uptake within the cuvette is balanced by an efflux of oxygen, but there is no such compensation for water vapour, which increases out-flow from the cuvette by an amount equal to the quantity of water vapour transpired by the leaf. This must be compensated for by further calculation. Therefore, from equation *(1)*:

$$u_o = u_e + (u_o w_o - u_e w_e) \qquad (3)$$

so

$$u_o = \frac{u_e(1 - w_e)}{1 - w_o} \qquad (4)$$

CO_2 assimilation rate (A) is calculated by combining equations *(2)* and *(3)*:

$$A = \frac{u_e}{s}\left\{ c_e - c_o\left(\frac{1 - w_e}{1 - w_o}\right)\right\}$$

Stomatal conductance to water vapour (g_s) in mol m^{-2} s^{-1} is calculated as

$$g_s = 1/r_s$$

where r_s is stomatal resistance to water vapour, derived from the equation

$$r_s = [(e_{leaf} - e_{out}) / (E \times P)] - r_b$$

and e_{leaf} is the saturated vapour pressure at leaf temperature, e_{out} is the water vapour pressure of the air leaving the cuvette, E is the transpiration rate, P is atmospheric pressure and r_b is the boundary layer resistance to water vapour.

Stomatal conductance to CO_2 is calculated as:

$$g_c = 1/ (1.6\, r_s + 1.37\, r_b)$$

where 1.6 is the ratio of diffusivities of CO_2 and water in air, and 1.37 is the ration of diffusivities of CO_2 and water vapour in the boundary layer

Sub-stomatal cavity CO_2 concentration (C_i) is calculated using the equation

$$C_i = \frac{\left[g_c - \frac{E}{2}\right] C_{out} - A}{\left[g_c + \frac{E}{2}\right]}$$

Where g_c is total conductance to CO_2 transfer in mol m^{-2} s^{-1}, E is transpiration rate, and C_{out} is the CO_2 concentration of cuvette air.

Boundary layer resistance (RB) for the cuvette required for the above calculations was obtained using the manufacturer's standard procedure as follows:

A 1 cm^2 piece of wet filter paper with both sides exposed, providing a total area of 2 cm^2, was inserted into the leaf cuvette. Leaf area was entered at the appropriate menu point for use in the automatic RB calculation, and the flow-rate setting increased to 400 mL min^{-1}. The cuvette was then covered with a cloth to reduce incident radiation to zero and the measurement procedure allowed to continue until the humidity difference reaches a steady state (approximately 10 seconds at the same value). At this point, "0" was entered and the CIRAS calculated the value of RB.

2.11.4 Sampling procedures

Measurements were typically undertaken in ambient conditions, meaning that light and leaf temperatures were subject to natural variations according to the environmental conditions present at sampling. On the occasions where measurements were conducted under controlled PFD, a fan-cooled white light

halogen lamp powered by a 12 V car battery was attached to the cuvette window and PFD was varied using a series of neutral density detachable filters.

A normal sampling consisted of a single measurement on each leaf, ensuring that a portion of the blade was fully sealed within the cuvette chamber and that the light sensor and cuvette were receiving the same amount of light (except where an artificial light source or filters were used). Measurements were not documented until the CO_2 assimilation rate and stomatal conductance values had reached steady state values.

2.12 Chlorophyll Fluorescence

The origins of chlorophyll fluorescence measurement and analysis owe much to the work of Kautsky and Hirsch (1931) who first reported the dark/light induction phenomenon in a dark-adapted leaf following illumination, and to Schreiber (Schreiber *et al.*, 1987) whose development of the modulated fluorometer and the saturation pulse technique extended its use, especially into the field. Since these original studies, chlorophyll fluorescence kinetics has developed to become an important and widely used in-vivo probe of the organisation and function of the photosynthetic apparatus, particularly in relation to stress.

2.12.1 Origins and definition of Chlorophyll *a* fluorescence

Photosynthesis is driven by the excitation energy produced when chlorophyll *a* (Chl a) pigments are transformed from the ground state to singlet-state excitation (^{1}Chl*) on absorption of sunlight. This excitation energy is dissipated by way of several processes (Figure 2.8);

a. photochemical energy conversion by charge separation
   (i.e.: the primary photochemical step of photosynthesis where excitation energy funnelled into reaction centres is transferred from the chlorophyll molecules P680 and P700 to acceptor molecules).
b. Radiative decay of the excited state by fluorescence.
c. Non-radiative decay into the ground state resulting in heat formation.
d. Decay via the triplet state (^{3}Chl*).

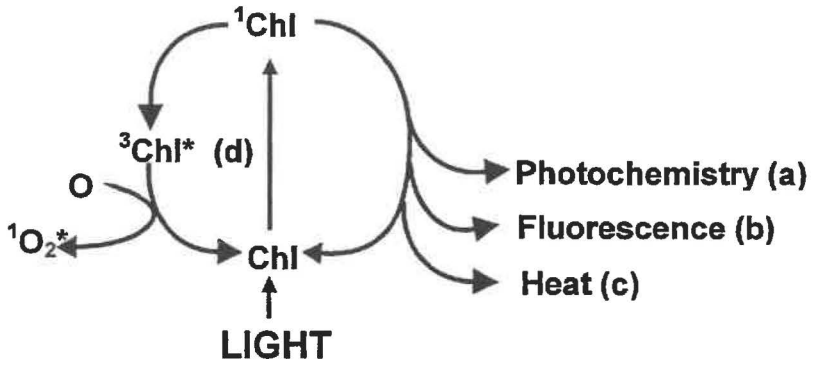

Figure 2.8 Possible fates of excited chlorophyll: redrawn from (Mueller *et al.*, 2001)

Although the total amount of chlorophyll fluorescence is very small (only 1 to 2% of total light absorbed), it is a useful indicator of the reactions and processes of photosynthesis at a number of functional levels (Schreiber, 1997). Its value as such lies in the fact that the above pathways of energy de-excitation are competitive, and any increase in the efficiency of one generally results in decreased yield of the others. Fluorescence changes are primarily indicative of the state of PSII given that chlorophyll of PSI is essentially non-fluorescent and emits either none, or only a weak fluorescence that does not change significantly when the PSI acceptor is reduced and does not affect the ratios calculated (Laisk & Oja, 1998).

2.12.2 Interpreting changes in fluorescence yield:

2.12.2.1 Saturation Pulse Method

One of the most extensively used chlorophyll fluorescence techniques is the quenching analysis of modulated fluorescence by the saturation pulse method. It allows precise fluorescence detection in the presence of background illumination, including full sunlight, and is therefore an extremely useful method for assessing the photosynthetic performance of plants under natural conditions.

An account of chlorophyll fluorescence parameters is illustrated by the typical experimental trace of fluorescence yield in Figure 2.9. Nomenclature follows that of van Kooten and Snel (1990).

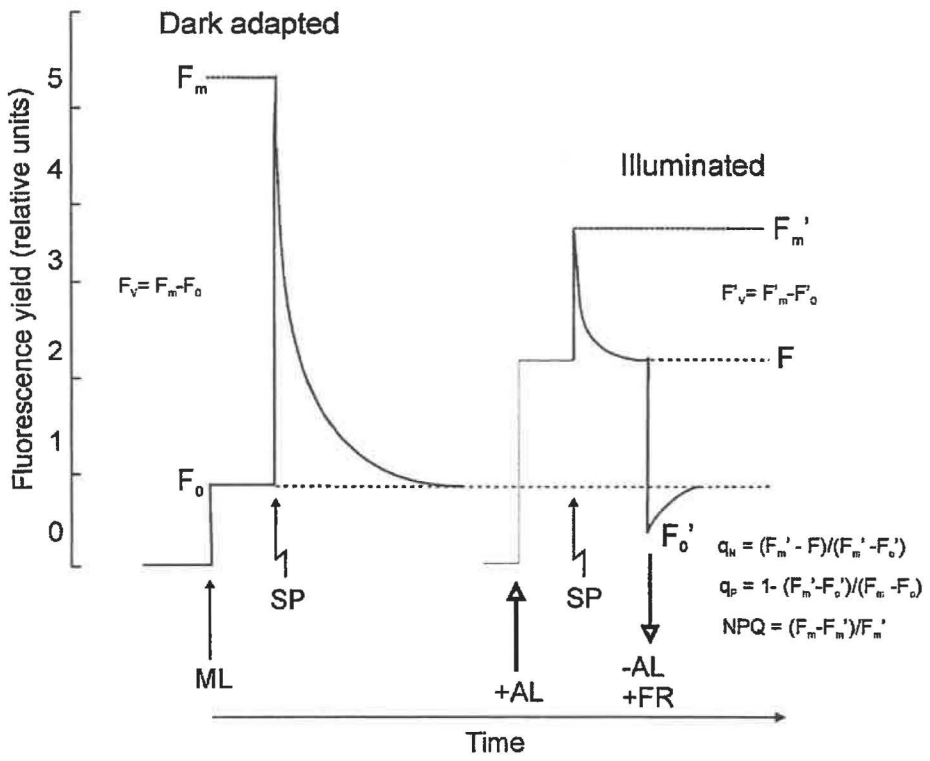

Figure 2.9 Chlorophyll *a* fluorescence induction kinetics of dark-adapted (left) and illuminated (right) photosystems, quenching coefficients and derived fluorescence parameters using the saturation pulse method (see text for explanation of terms). After Schreiber *et al.* (1987)

Minimum fluorescence yield, F_0, is observed when a dark-adapted photosynthetic apparatus is excited with a low intensity light that is too weak to initiate electron transfer. F_0 characterises losses of excitation energy prior to photochemistry at the point where the first stable acceptor of the electron transport chain (Q_A) is fully oxidised and all the reaction centres are open for energy conversion. Subsequent application of a strong light pulse (SP) at an intensity of approximately 8000 μmol m^{-2} s^{-1} and duration of about 1 s, closes all PSII reaction centres, and fluorescence rises to a maximum value, F_m. After fluorescence has reached a maximum level at F_m, it decreases slowly to a steady state. When actinic (continuous) light is then switched on (AL), and a second saturating light pulse is applied (SP), fluorescence rises to its maximum under illumination, F_m' which is generally lower than the dark value, F_m. From this point, fluorescence declines to a steady state denoted by F'. When actinic light is

then removed and far-red light is applied (-AL +FR), minimum fluorescence in the light adapted state (F_0') is reached.

The decline in fluorescence yield observed following the saturating light pulse is termed fluorescence "quenching" and is indicative of excitation energy dissipation by photochemical and non-photochemical processes rather than via the fluorescence pathway. The fluorescence changes are explained in terms of either photochemical or non-photochemical quenching coefficients. An increase in photochemical "quenching", q_P signifies increased photochemical efficiency, or an increase in the rate at which electrons are transported away from PSII. Non-photochemical quenching in-vivo may be caused by three mechanisms; ΔpH- or energy dependant quenching, qE; state-1 state-2 transition quenching, qT; and photoinhibitory quenching, qI (Krause & Weis, 1991).

2.12.2.2 Fluorescence parameters

Fluorescence measurements provide the basis for the calculation of a number of useful parameters used to probe photosynthetic function in plant tissues. These parameters include variable fluorescence F_v, the difference between maximum (F_m) and minimum fluorescence (F_0) which, when divided by the maximum fluorescence, indicates the proportion of the maximum fluorescence that is used in photosynthesis i.e., F_v/F_m (the maximal quantum efficiency of PSII primary photochemistry). In healthy, unstressed terrestrial plant tissue, PSII efficiency is usually in the order of 83 % (i.e., F_v/F_m ratio of 0.83) (Björkman, 1987). Lower values are generally indicative of stress to the photosynthetic system.

ETR, the rate of linear electron transport through PSII (Genty *et al.*, 1989) is derived from the relationship:

$$ETR = \Phi PSII \times PFDa \times 0.5$$

where PFDa is absorbed light (μmol m^{-2} s^{-1}) and 0.5 is a factor that accounts for partitioning of energy between the two photosystems (Maxwell & Johnson, 2000). ΦPSII is derived from the ratio

$$\Delta F/F_m' = (F_m' - F)/F_m'$$

where F_m' is the maximal fluorescence obtained during a saturating flash of light (when all the PSII traps are closed), and F is the steady state value of fluorescence. The correlation between CO_2 fixation and PSII electron transport for C3 plants is significant under laboratory conditions (Genty *et al.*, 1989), but

does not always hold under field conditions where environmental stresses may alter the relationship (Fryer *et al.*, 1998).

2.12.2.3 Fluorescence as an indicator of stress

In addition to providing a useful measure of the photosynthetic performance in plants, numerous studies prove fluorescence measurements to be a highly sensitive indicator of the extent to which the photosynthetic apparatus may be stressed or damaged. There are many examples where fluorescence measurements have successfully been used to investigate the effects of stresses such as temperature extremes (Welander *et al.*, 1994), light (Eggert *et al.*, 2003, Lichtenthaler & Burkart, 1999), salinity, water (Flexas *et al.*, 2002) and nutrients (Parkhill *et al.*, 2001). In general, the stress response produces a decline in F_v/F_m values; a consequence of increasing F_0 or decreasing F_m or a combination of the two. The response can be attributed to any effects that are inhibiting or protecting the PSII reaction centres.

2.12.3 Experimental procedures: PAM-2000 and MINIPAM

Chlorophyll *a* fluorescence was measured in the field with either a PAM-2000 with Poqet PC notebook computer and data acquisition software (DA-2000, Heinz, Walz), or a MINIPAM chlorophyll fluorometer (Walz, Effeltrich, Germany). Fluorescence yield, photosynthetic photon flux density (PPFD) incident on the leaf, and leaf temperature were measured in dark- and light-adapted states, allowing the calculation of the quantum efficiency of PSII, apparent electron transport rates and quenching parameters.

Light-adapted samples were measured with the PAM fibre-optic (directing the measuring light and saturating light pulses), positioned in a leaf clip holder (model 2030-B, Walz) at ring-mark IV and an angle of 60° to the leaf surface (Bilger *et al.*, 1995). Care was taken during measurement to avoid shading of the sample area and the micro quantum sensor attached to the leaf clip. Dark-adapted samples were prepared by placing Walz darkening clips (Plate 2.16) on the leaves at least 15 minutes prior to measurement, essentially reducing electron flow in the photosystems to zero. During measurement the PAM fibre-optic was positioned in the dark-clip barrel (slider open) at an angle of 90° to, and approximately 6 mm from, the sample surface.

Plate 2.16 Dark-adaptation of an *Avicennia marina* subsp. *australasica* leaf in the field using a Walz darkening clip.

When selecting the measuring spot on each leaf, care was taken to keep clear of damaged tissue, leaf margins and, where possible, main veins. However, unavoidable inconsistencies arose where measurements were made on the same leaf over the course of a day, several days or months, even though attempts were made to position the fibre-optic as close to the same measuring spot on the leaf each time. Sampling fluorescence at different points on light-adapted leaf samples is known to contribute variability to the data, however this may be less of a problem in dark-adapted samples where F_m values remain fairly uniform over the whole leaf (Bilger *et al.*, 1995).

Chapter Three

Chapter three

Frost damage and tolerance in *Avicennia marina* subsp. *australasica* over a latitudinal gradient in New Zealand

3.1 Introduction

The hypothesis that northern and southern geographical limits of mangrove are largely defined by low winter temperatures, incidence of frost and the susceptibility of these plants to damage or death on exposure to freezing is long established in literature (Blasco, 1984, Chapman & Ronaldson, 1958, Chapman, 1977, Dingwall, 1984, Tomlinson, 1986). Several studies have also reported a strong relationship between the gross morphology and habit of mangroves and the occurrence of low temperatures (Lugo & Zucca, 1977). A reduction in tree size and tree density is reported from all colder areas together with a decline in species richness of the community. There have, however, been relatively few studies to clarify the relative importance, if any, of these factors.

The effect of chilling (low, non-freezing) temperatures on mangroves was investigated in the Caribbean (McMillan, 1974), (Markley *et al.*, 1982). Seedlings, grown in laboratory conditions for about one year, and 5.5 year old plants grown from seed, and were treated for up to 144 hours at a temperature of 2-4°C. The resulting damage depended on the species, the time of the year and the latitude of the site from which the plant material was originally collected. Leaves of *Avicennia* germinans (L.)L. from Belize, 17° 31' N, were more extensively damaged than those of the same species from Harbor Island, Texas, 27° 50' N, and whilst plants from all the northern sites survived the treatment, only 30% of those from southern sites did. There also appeared to be a seasonal effect with much more damage occurring when the plants were chilled in February than in December. However, the mangroves showed limited ability to acclimate and the plants retained the characteristics of the site from which collected. A similar cline in chilling sensitivity with latitude was also found for *A. marina* in Australia (Markley *et al.*, 1982).

There appear to have been no structured studies on frost resistance of mangroves but in New Zealand several local observations suggest that *A. marina* subsp. *australasica* has a limited tolerance to freezing temperatures.

Chapman and Ronaldson (1958), after observing 50% mortality of mangroves in Henderson Creek Auckland (latitude 36°52' S) following frosts, concluded that the plants could not survive a temperature of –2.2°C. However, the actual temperatures to which the plants were exposed is not known and some of the plants presumed to have been killed were later seen to have recovered (Chapman & Ronaldson, 1958). Sakai and Wardle (1978) demonstrated that *Avicennia* leaf tissues could not survive 4 hours exposure to –3.0°C and, although this temperature has since been accepted as the frost tolerance limit for *A. marina* subsp. *australasica*, (Duke, 1990, Mildenhall & Brown, 1987, Wardle, 1985, Zhang *et al.*, 2001), the result was based on measurements of leaves from a single plant in Auckland. The critical frost tolerance limits of *A. marina* subsp. *australasica* are unlikely to have been adequately defined by either of these studies (de Lange & de Lange, 1994). It is not known whether there are changes in frost sensitivity with latitude and season as have been found for chilling for *A. marina* in Australia and the closely related *A. germinans* (L.) L. from the Gulf of Mexico (Markley *et al.*, 1982, McMillan, 1974).

Given its range in New Zealand from relatively frost-free regions of Northland to areas of frequent winter frosts such as Ohiwa Harbour (for locations refer to Figure 1.), *A. marina* subsp. *australasica* provides an ideal subject for the study of climate factors limiting mangrove distribution. This chapter addresses the hypothesis that the distributional range of the mangrove *A. marina* subsp. *australasica* in New Zealand is determined by the species' limited resistance to winter frosts (Chapman & Ronaldson, 1958). Concepts of low temperature stress, freezing injury and freezing tolerance are discussed in relation to two studies (presented separately in this chapter) that were undertaken to establish frost resistance and critical temperature limits of New Zealand mangrove.

3.1.1 Plants and temperature stress

All aspects of plant life are influenced by the physical factors of their surrounding environment. Temperature, light, humidity, wind, precipitation, and nutrients collectively determine the rate and efficiency of cellular reactions and ultimately the success with which a plant may grow or reproduce. If any of these factors are present outside a certain critical range, then they may eventually limit its growth and survival.

Levitt (1980b) defines biological stress as "any environmental factor capable of inducing a potentially injurious strain in living organisms". The strain or injury resulting from such stress may be reversible, i.e., reparable by an active expenditure of metabolic energy; or it may be permanent and ultimately result in death of the plant because its capacity for metabolic repair has been exceeded. In plants, symptoms of reduced or suppressed growth, leaf chlorosis, tissue necrosis and alterations to reproduction are common stress responses (Treshow, 1970). However, exposure to biological stress is not necessarily lethal since most plants have at least some mechanism or strategy by which they can either tolerate or avoid the stress.

Plants are essentially ectothermic organisms. Although some are able to partly regulate tissue temperatures by means of thermogenic mechanisms (generation of metabolic heat), e.g., flower parts of the aroid *Philodendron* (Seymour & Schultze-Motel, 1997) or by way of morphological adaptations, e.g., insulating hairs of alpine herbs (Körner, 1999), their internal temperatures are largely dictated by the ambient environment. All plants differ in their tolerances to maximum and minimum temperature extremes, and all have an optimal range of temperature within which their growth and developmental processes and their competitive abilities are maximised. When temperatures beyond this range are experienced plants become vulnerable and, in extreme cases, their continued survival may be threatened.

Given that plant function and survival are strongly dependent on ambient air temperature, the close relationship that exists between temperature and the natural geographical distribution of species (as seen in the clearly defined vegetation types associated with particular climate zones) is not unexpected. Climate temperature is strongly correlated to both latitude and altitude; decreasing towards the poles due to the angle of the sun, decreasing with increasing distance from the equator and decreasing with altitude due to the expansion and cooling of rising warm air (Sutcliffe, 1977). Only those species able to tolerate the extremes of maximum and minimum temperature that occur in any one place are able to endure. At higher latitudes, such as the temperate regions of New Zealand, low, rather than high temperatures are limiting and the distribution of species may be dictated by the severity of winter frosts.

3.1.2 Low temperature injury

If plants are exposed to low temperatures (below a critical minimum) two types of injury may result. Chilling injury, as the term suggests, is normally associated with temperatures that are cold enough to cause damage, but not cold enough to freeze the tissue (i.e., above 0°C). It is normally only seen in plants of tropical and subtropical origin and in sensitive species can be initiated at temperatures between 10 - 12°C (Sutcliffe, 1977). In contrast, freezing injury can occur in any plant exposed to sub-zero temperatures. Sensitive species are generally affected by freezing injury at temperatures between -2°C and -5°C.

Low temperature injuries manifest as a range of symptoms including tissue or whole plant death, alteration of physiological functions, or diseases such as canker (Treshow, 1970). The severity of injury is conditional on a number of factors including the rate of cooling and thawing, the minimum temperature reached, the developmental stage of the plant and the duration and history of exposure (Levitt, 1980b, Sakai *et al.*, 1981). New leaves, buds, reproductive organs and other rapidly differentiating tissues are more sensitive to low temperature and incur more severe injuries than older tissues such as mature leaves and stems (Inouye, 2000, Sakai *et al.*, 1981). Chilling or freezing may impact more significantly if the plants have no ability to acclimate, or if the cold temperature exposure occurs early or late in the season when normal protective mechanisms are not operating. Even sub-lethal exposure has wide reaching consequences, reducing growth and development, fruit and seed production success and the potential for sexual reproduction (Inouye, 2000).

Freeze-damaged plant tissue is recognised by its flaccid, discoloured and water-soaked appearance, as if the cells had disintegrated under pressure. Historically, these symptoms supported the theory that the plant cells expanded to a point of rupture due to an increase of internal mass as water turned to ice (Levitt, 1980b). However, most current research now recognises that freezing injury is not so much a symptom of burst cells, but is rather caused by mechanical or chemical disruption to the cell plasma membranes (Steponkus, 1984).

Levitt (1980b) proposed two main types of freezing injury, both involving the cell membrane; one due directly to intracellular ice formation and the other to freeze dehydration and the extracellular formation of ice. He suggested that the membrane lipids of cells with no freezing tolerance undergo a phase transition at

freezing temperature, changing from liquid crystalline to a solid gel state (on rewarming, this process is reversible, but permanent damage may be sustained while the cells are in their frozen state). If the freezing process is rapid, intracellular ice may form as a consequence of decreased membrane permeability. This is always lethal to the cells because the ice crystals physically puncture the membrane, leading to an irreversible loss of cell contents. However, formation of intracellular ice is relatively rare in nature because the process requires very rapid cooling and temperatures well below the tissue freezing point. On the other hand, if the freezing process is gradual (as is more commonly the situation in nature), extracellular as opposed to intracellular ice forms in the tissues. Ice crystals develop initially where sap solute concentrations are most dilute (and therefore have the highest freezing point), such as in the xylem vessels and sub-stomatal cavities.

Following ice nucleation, crystals spread throughout the extracellular spaces in the plant tissue, giving rise to a water potential gradient such that a general efflux of water from the cells occurs. Eventually, the cells collapse and the now solidified membranes fracture. On thawing, essential solutes leak through the fractures and cell death occurs. Levitt (1980b) also hypothesised that low temperatures cause weakening of the hydrophobic bonds in the lipid bilayer of the cell membranes. Subsequent freeze dehydration is thought to initiate structural changes in the membrane lipids and protein bonds, eventually leading to damage to the membrane ion pump, increased permeability, loss of turgor and leakage of electrolytes.

3.1.3 Low temperature tolerance

Low temperature tolerance in plants is a variable parameter determined by a range of physiological and morphological adaptations that reduce sensitivity to low temperature. Adaptations may be seen at the gross morphological level e.g., the rosette growth form and sunken meristem of alpine herbs (Beck *et al.*, 1982); at the cellular level e.g., smaller vacuoles; or as biochemical e.g., low lipid membrane phase transition temperature (Levitt, 1980b), accumulation of sugars or other solutes lowering freezing point (Steponkus, 1984).

Some plant species have the ability to acclimate (harden) over a period of exposure to non-lethal chilling temperatures, thus eliminating or reducing the possibility of low temperature injury. These changes are usually related to the

seasonal change in environmental temperature and normally result in higher tolerances during the winter months. Tolerance also varies according to life form (e.g., seedlings may be more or less tolerant than mature plants) and often differs between parts of the same plant (e.g., young growing tissue, for example a new leaf, is more vulnerable to injury than mature tissue)(Crawford, 1989, Steponkus, 1984).

Plants can be grouped by their tolerances to low temperatures into five categories (Levitt, 1980b). Those growing in the tropical and subtropical regions of the world are poorly adapted to withstand the stresses imposed by low temperatures and are therefore classified as tender (generally killed by the first touch of frost) or slightly hardy (able to survive freezing to no lower than about -5°C). Moderately hardy species, more widespread in the temperate zones, tolerate temperatures between -5°C and -10°C with the help of low temperature avoidance mechanisms such as the development of higher concentrations of cell sap. Very hardy species have well developed tolerances to freeze-dehydration and are able to survive temperatures as low as -20°C. Lastly, extremely hardy species have the ability to tolerate temperatures lower than -196°C due to specialised adaptations of the cell membranes.

3.1.4 Measurement of low temperature injury and resistance

Low temperature injury resistance may be determined using a variety of techniques, ranging from a simple visual assessment of colour change signifying tissue necrosis, to rather more complex techniques involving measurement of conductivity (electrolyte leakage into a bathing solution), chlorophyll a fluorescence, and vital staining of palisade mesophyll cells. (Boorse *et al.*, 1998). Artificial freezing tests of this type are generally accepted to give an accurate estimation of the winter survival ability of plants in the field, but to gain a complete picture of a plant's freezing tolerance, measurements must be made at intervals during the year (to allow for seasonal changes in hardiness) and of different parts of the plant (since there is large variability between frost tolerance of different tissues) (Levitt, 1980b).

The electrical conductivity method for the determination of frost tolerance has been used extensively for investigations of crop hardiness and freezing resistance in a wide variety of plants since its development by Dexter and co-workers in 1932 (Boorse *et al.*, 1998, Read, 1989, Zhang & Willison, 1987). The

freezing or frost tolerance of the species in question is calculated on the basis of electrolyte efflux from the cells immediately after thawing. The greater the amount of damage to the cells, the greater the loss of electrolytes from the tissue and therefore the higher the conductivity of the tissue extract. The standard measure of tolerance is the frost- or freeze- killing point (Lt_{50}), the temperature required to kill 50% of the plant.

Recently, the reliability of the electrical conductivity technique for estimating cell damage or death has been questioned (Boorse *et al.*, 1998). An underestimate of frost tolerance is suggested because uncharged solutes leaked from cells are not detected (Zhang & Willison, 1987) whilst an overestimate would occur if membranes are repaired after initial damage (Palta et al 1977). Despite some evidence disputing the usefulness of this technique, a decision was made to employ it for the present study because large numbers of samples could be processed with limited equipment in a relatively short time after sample collection. In addition, results from preliminary trials using mangrove tissue indicated close agreement with findings from the few known studies of frost tolerance in New Zealand mangrove.

Relative cold and heat sensitivities may also be determined by measuring the rise in F_0, minimum fluorescence yield (see section 2.12) in response to changes in temperature (Schreiber & Berry, 1977). The technique was employed in this study to determine the upper and lower temperature limits of PSII function in *A. marina* subsp. *australasica* (see section 3.6).

3.1.5 Frost damage

In the field, frost damage in *Avicennia* normally manifests itself as necrotic water-soaked and flaccid tissue (leaves, branches, buds and developing fruit) on the day following the freeze event. During the weeks following exposure, the tissue dries out, turns black and is eventually discarded from the affected plants by the action of wind and other disturbances. In some cases the freezing damage may be severe or widespread enough to cause whole plant death, for which there is some documented evidence (Chapman & Ronaldson, 1958). Frequently however, the mangroves sustain only partial damage after freezing, particularly in areas such as the Bay of Plenty (North Island, New Zealand, spanning latitudes 37°S to 38°S) where *Avicennia* is mostly dense-crowned and short in stature (C. Beard *pers. obs.*). Frost damage in these mangroves is most often seen confined

to the upper and outer 200 mm of the squat canopies, the lower and inner leaves remaining unaffected (Plate 3.1).

Plate 3.1. Typical frost damage observed in *Avicennia marina* subsp. *australasica* at Ohiwa harbour, July 2003. Damage in this instance is confined to the upper leaves, branches (left) and developing propagules (right). Photo: C.Beard

3.2 Experiment I: Frost damage and tolerance in *Avicennia marina* subsp. *australasica* over a latitudinal gradient in New Zealand

3.2.1 Research sites

Leaf samples were collected from eight sites within the natural range of mangroves on east and west coasts of the North Island of New Zealand, chosen primarily on the basis of latitude with accessibility as a secondary consideration (Table 3.1, Figure 3.1). The furthest north site at Tapotupotu Bay is the smallest population and closest to open ocean waters (within 1 km). All others are on harbour coastlines up to 8 km inland, with the exception of the Herekino site, situated on a salt marsh flat at the head of Herekino Harbour.

Campbell and Hobo temperature loggers (refer Chapter 2) were installed at the Wainui Road study site at Ohiwa harbour, collecting air and substrate temperature data over several years at intervals of 15, 20 or 30 minutes. The data were used to establish the frequency, duration and severity of frosts over the winter of 2002 in the mangrove area.

Table 3.1 *Avicennia marina* subsp. *australasica* populations sampled for foliar frost tolerance study: location, map reference (New Zealand topographical metric map series 260: scale 1:50 000), latitude, temperature normals. MAT = mean annual temperature (°C); MTWM = highest maximum temperature (°C) of the warmest month; MTCM = lowest minimum temperature (°C) of the coldest month; Frost = average number of frost days per year; EM= predicted extreme minimum temperature (°C)

Location	Map reference	Latitude (°'S)	MAT (°C)	MTWM (°C)	MTCM (°C)	Frost days	EM (°C)
Tapotupotu Bay, East Coast	M02 851 514	34°26'	16.19	23.8	8.7	0.16	2.0
Paihia, Bay of Islands, East Coast	Q05 110 542	35°12'	15.69	24.9	6.7	0.76	0.1
Herekino Harbour, West Coast	O05 303 607	35°15'	15.76	24.6	7.6	0.22	1.1
Mangawhai Harbour, East Coast	RO8 525 644	36°07'	15.54	23.8	7.9	0.68	0.6
Kaipara Harbour, West Coast	Q08 182 635	36°07'	15.04	24.0	6.9	0.86	-0.9
Tauranga Harbour, East Coast	U14 879 868	37°40'	14.43	23.6	5.6	2.82	-1.0
Raglan Harbour, West Coast	R14 747 760	37°48'	14.50	24.0	5.7	2.46	-1.8
Ohiwa Harbour, East Coast	W15 743 426	38°03'	14.15	24.0	3.7	2.98	-2.6

3.2.2 Sample treatment

Single branchlets supporting up to 15 leaves were removed from ten randomly selected mature plants at each study site in November 2000 and May 2001. A plant was determined as mature if it had flowered or was of a comparable height with plants that had flowered. At the same time, five or more seedlings were also collected, each being typically 150 - 200 mm in height with at least two pairs of fully expanded leaves. Seedlings were selected from open areas outside the shelter of the mangrove canopy. All collections were placed in sealed plastic bags with a little fresh water to prevent desiccation then, within two days of collection, returned to the laboratory in an insulated container and kept at 10°C to minimise tissue deterioration until analyses could be conducted. All analyses were completed within five days after collection.

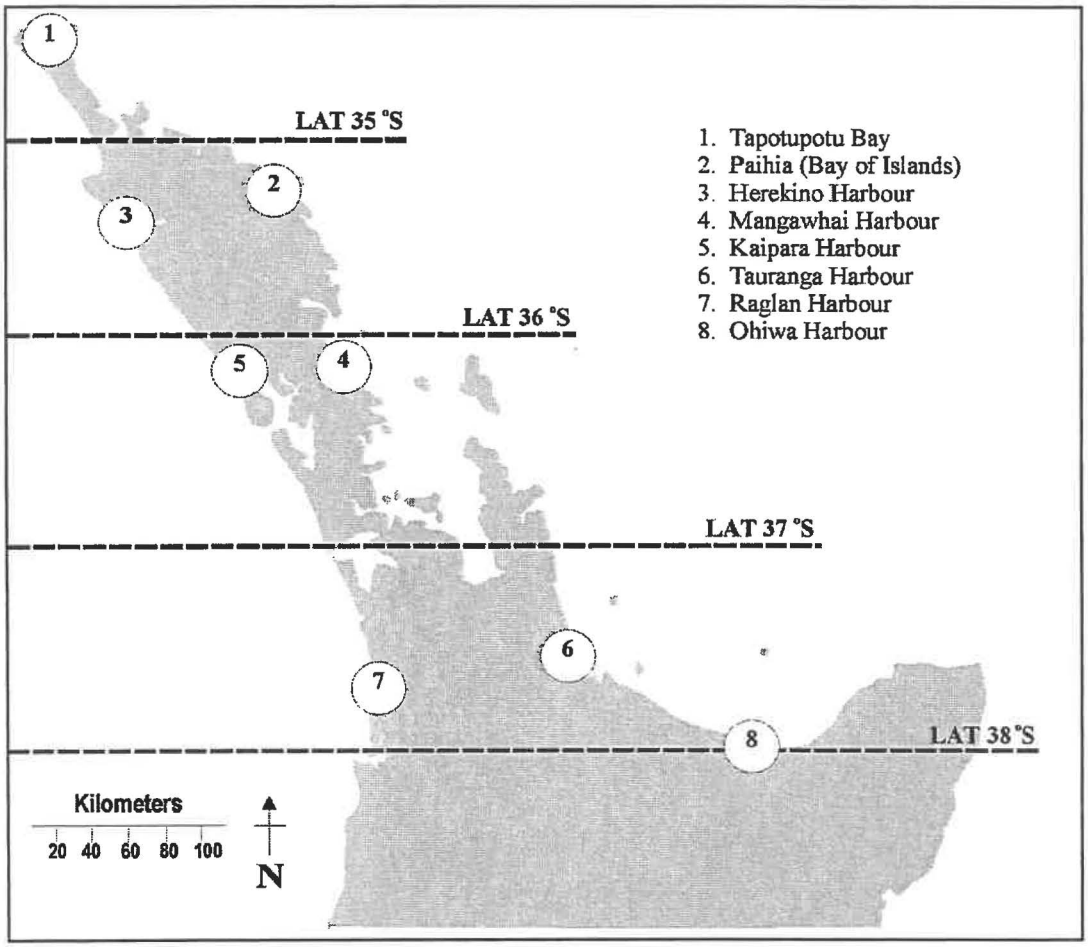

Figure 3.1 Schematic diagram of the upper North Island of New Zealand showing locations of the *Avicennia marina* subsp. *australasica* populations sampled for a foliar frost tolerance study:

3.2.3 Frost tolerance determinations

3.2.3.1 Conductivity Method

The procedure used in this study was adapted from that described in Read and Hope (1989). Fully expanded and undamaged leaves were selected, washed to remove mud and other deposits, and then rinsed in distilled water. 10 mm diameter discs were then punched from the leaves to give a total per site of 300 discs from mature leaf tissue and 150 discs from seedling leaf tissue. After being rinsed again in distilled water, leaf discs were allocated at random on the basis of mature or seedling tissue into sets of six. Each set was placed into sealed 14 ml screw-top glass vials with 0.1 ml distilled water to keep the discs moist and a couple of grains of silver iodide added to prevent super-cooling. A total of ten vials of mature leaf tissue and five of seedling tissue per sample site were used in each temperature treatment.

Vials were floated in an antifreeze solution of 70% glycerol + 30% water in cooling water baths (Julabo F20, Julabo F10 and Heto DX). Sample temperatures during the freezing treatments were monitored using a Campbell CR10 data logger connected to a thermocouples placed within one of the vials. From a starting temperature of 10°C, samples were cooled at a rate of 0.15°C min^{-1} to temperatures of 0, -2, -4, and -6°C. Samples were held at each target temperature for 90 min then warmed at a rate of 0.15°C min^{-1} to 5°C, after which they were removed from the water baths and allowed to return to ambient (c. 20°C) temperature. One set of samples was kept at ambient temperature as a control.

After completion of the freeze-thaw cycle, 8 mL distilled water was added as a bathing solution to each sample of leaf discs and the vials were gently rocked at room temperature (approximately 20°C) for 24 h. Conductivity of the bathing solution (***Lt***) was then measured with an EDT RE387 TX Microprocessor Conductivity Meter and 100 µS – 200 mS glass dip cell with platinum plates (EDT Instruments Ltd, United Kingdom). Samples were then heat-killed by placing the vials in a 75°C water bath for 15 min and, after a further 24 h gentle rocking at 20°C, a final conductivity measurement (***Lk***) was taken.

Mature leaves sampled in November 2000 from Kaipara harbour were not analysed due to equipment failure. Ohiwa harbour populations were not sampled in November 2000.

3.2.3.2 Visual assessment of tissue necrosis

One additional set of samples from Tauranga Harbour was prepared and freeze-treated to compare the conductivity method with visual damage assessment. The samples were subjected to freezing temperatures following the same procedure as used for the electrical conductivity method, after which they were placed on moist paper towels in covered trays at room temperature. Freezing damage was calculated over the following five days from the proportion of each leaf showing visual damage (blackened or discoloured leaf tissue).

3.2.4 Calculation of frost tolerance (Lt_{50})

The method outlined in Read and Hope (1989) was used to calculate frost tolerance Lt_{50}, the temperature producing 50% of maximal damage. First, ***Rt***, the fractional release of electrolytes from a sample exposed to a particular treatment temperature, was calculated as $Rt = Lt/Lk$, where ***Lt*** was the specific conductance of leachate from a sample frozen at temperature (*t*), and ***Lk*** the specific

conductance of leachate from a sample frozen at the same temperature (*t*) but then heat killed. Next, in order to eliminate the variability caused by differences in sample tissue mass, an index of injury (***It***) was calculated where the fractional release of electrolytes (***Rt***) was converted to a percentage scale on which the unfrozen control is counted as 0% and the heat-killed sample as 100%. ***It*** = ***100(Rt-Ro)/(1-Ro)***, where ***Rt*** is the fractional release of total electrolytes from a sample exposed to temperature (*t*) and ***Ro*** is the fractional release of electrolytes from an unfrozen sample (the ambient control).

Finally, Lt_{50} (frost tolerance, or the sub-zero temperature producing 50% injury) was calculated for each sample from the linear regression between ***It*** and temperature for values of ***It*** over the range of temperatures where injury was increasing (Boorse *et al.*, 1998). As appropriate, Lt_{50} was also calculated using visual damage assessed as the proportion of the leaf showing black or discoloured tissue.

3.2.5 Statistical Analyses

Air and substrate temperature data were analysed using Microsoft Excel (Microsoft Corporation, USA) and Statistica vs.6.1 (Statsoft Inc. USA). All statistical analyses were conducted using Statistica vs.6.1, Systat vs.8 and SigmaPlot vs. 8.0 (SPSS Inc, United Kingdom). A Chi-square test of association was conducted for Lt_{50} values vs. latitude. Analysis of covariance was undertaken to test the significance of latitude, sampling period and coastal location on Lt_{50} values. Adjusted least square means for Lt_{50} were calculated from the covariance analysis and used in the comparisons.

3.3 Results

Treatments at ambient temperature (20°C), 0°C and -2°C caused no detectable damaged leaf parts. However, below -2°C there was a sharp increase in injury levels, and at -6°C conductivities reached almost 100% of heat killed values. Frost tolerance (Lt_{50}) of mature leaf tissue changed with site latitude in both November (austral spring) and May (austral autumn) (Table 3.2.). Lt_{50} in November 2000 ranged from -3.50°C at Tapotupotu Bay, the most northerly study site, to –4.99°C at Tauranga harbour, east coast, and –4.68°C at Raglan, west coast. On the east coast the change in frost tolerance over the sampling range was 1.49°C ,equating to 0.46°C per degree latitude, and on the west coast it was 1.18°C , equating to 0.35°C per degree latitude. Plants sampled the following

autumn in May 2001 produced lower Lt_{50} values ranging from -2.74°C at Tapotupotu Bay to -4.76°C at Ohiwa Harbour, the most southerly population sampled in this study. The lapse rates in frost tolerance at this time of the year were greater but differences between the coasts had disappeared (0.56°C per degree latitude, east coast and 0.57°C per degree latitude, west coast). The results for seedlings were very different to those for mature leaves and showed no pattern with latitude at either sampling time. Lt_{50} in November 2000 were nearly constant ranging from -4.59°C to -4.93°C whilst, in May 2001, the range was greater, -3.02°C to –4.67°C, but with the least tolerance shown by seedlings at the southernmost site.

Table 3.2. Mean Lt_{50} (frost hardiness, the sub-zero temperature causing 50% cell injury) calculated for mature and seedling leaf material of *Avicennia marina* subsp. *australasica* in November 2000 and May 2001 using the electrical conductivity method. Figures are shown ± standard error of the mean. (ND=Lt_{50} not determined).

LOCATION (North Island, New Zealand)	LATITUDE (°S)	Lt_{50} (°C) Mature Plants Nov 2000	Lt_{50}(°C) Mature Plants May 2001	Lt_{50} (°C) Seedlings Nov 2000	Lt_{50} (°C) Seedlings May 2001
Tapotupotu Bay, East Coast	34°26'	-3.50±0.18	-2.74±0.06	-4.71±0.10	-4.14±0.28
Paihia, Bay of Islands, East Coast	35°12'	-3.73±0.15	-3.18±0.15	-4.47±0.40	-3.84±0.15
Herekino Harbour, West Coast	35°15'	-4.51±0.15	-3.98±0.07	-4.82±0.08	-4.67±0.08
Mangawhai Harbour, East Coast	36°07'	-4.75±0.07	-4.03±0.06	-4.93±0.09	-4.16±0.09
Kaipara Harbour, West Coast	36°07'	ND	-3.38±0.04	-4.86±0.05	-3.53±0.10
Tauranga Harbour, East Coast	37°40'	-4.99±0.05	-4.69±0.06	-4.90±0.07	-4.29±0.04
Raglan Harbour, West Coast	37°48'	-4.68±0.07	-4.66±0.03	-4.59±0.10	-4.26±0.06
Ohiwa Harbour, East Coast	38°03'	ND	-4.76±0.18	ND	-3.02±0.05

The association between Lt_{50} and latitude for mature leaves was highly significant in both in May and November (χ^2 = 96.387, P<0.0001 and χ^2 = 38.923, P<0.0001) but it was not significant for seedlings. The lapse rate in frost tolerance for mature leaves was almost identical at both samplings being 0.40°C per degree latitude, November 2000, and 0.37°C per degree latitude, May 2001. However, Lt_{50} values were slightly, but significantly, more negative for November 2000 than for May 2001, suggesting the possibility of seasonal variation in tolerance levels.

A significant difference in frost tolerance levels between the two sampling times was evident from the covariance analysis after taking into account the effect of latitude. Adjusted least squares means for frost tolerance were for May and November respectively; -4.18°C and -4.74°C for mature leaves, and -4.16°C and -4.74°C for seedlings (Table 3.3.). The differences between the means were very similar being 0.56°C and 0.58°C for mature leaves and seedlings, respectively.

Table 3.3. Adjusted least squares means ± SE of Lt_{50} (frost hardiness, the sub-zero temperature causing 50% cell injury) for mature and seedling leaves of *Avicennia marina* subsp. *australasica*.

	MAY 2001		NOV 2000	
life form	mean	n	mean	n
Mature	-4.176 ± 0.080	40	-4.741 ± 0.092	30
Seedling	-4.156 ± 0.082	40	-4.737 ± 0.095	30

A small difference in the frost tolerance of mature plants relative to coastal origin was also evident from the analysis of covariance. Plants from populations on the east coast were less frost tolerant than those from the west coast. However the difference was very small and probably biologically insignificant; adjusted least squares means differing by only 0.10°C in May 2001, and 0.22°C in November (Table 3.3). This trend was not statistically significant for seedlings.

3.3.1 Comparison of frost tolerance assessment methods

The Lt_{50} values of mature leaf samples from Tauranga in November were calculated using two techniques. Using the visible damage assessment method Lt_{50} was -5.20°C and using the conductivity method it was -4.99°C (Table 3.2). The slight difference between the results of 0.21°C, suggests that both methods might be suitable for determining frost tolerance for mangroves. However, for this investigation the conductivity method was deemed to be the most efficient technique as it allowed for the assessment of a greater number of samples over a comparably shorter time period.

3.4 Discussion

This study confirms that *A. marina* subsp. *australasica* shows some tolerance to freezing temperatures at the limits of its distribution. The range of frost tolerance found spans the previously reported values for this species which were either estimates from field observations (Chapman & Ronaldson, 1958) or

measurements of an individual plant (Sakai & Wardle, 1978). The level of tolerance found was not great, the lowest Lt_{50} being around -5°C. This value places *A. marina* subsp. *australasica* as a subtropical plant in the summary by Larcher (1995) but with even less tolerance than the -8 to -15°C quoted for evergreen woody plants. This mangrove species does appear to be out of place in a temperate zone, however, Lt_{50} are still in excess of the lowest environmental temperatures to which it is likely to be exposed to over its range (Table 3.2) given its coastal habitat. New Zealand has a temperate climate with mean temperatures at sea level being about 15°C in the far north with a mean annual temperature range of around 8°C and 9°C on the west and east coasts, respectively (NZ Met Service data). Many coastal areas in Northland (approximately latitude 34°20'S to latitude 36°S) are free of frosts, although frequent light frosts occur further inland during the winter months (NZ Met service data).

The paucity of previous results has meant that frost tolerance of the New Zealand mangrove has tended to have been defined by a single value, typically the -3.0°C of Sakai and Wardle (1978). From the results of this study, it would appear that it might be better defined as a variable parameter, subject to change by factors such as latitude, season, and developmental stage of the plant.

Even though *A. marina* subsp. *australasica* has only a slight tolerance to frost, the results of the present study clearly show a statistically significant (χ^2<0.0001) change with latitude. Mature leaves at southern sites are more frost tolerant than those in the north with a maximal difference of about 1.5°C. A similar correlation between latitudinal origin and degree of plant and leaf damage sustained on exposure to chilling temperatures has been reported for the same species elsewhere and *A. germinans* (L.) Lamk. (Markley *et al.*, 1982, McMillan, 1974). The presence of acclimation to both chilling at positive temperatures and to frosts suggests a common mechanism, probably through membrane alteration (Markley *et al.*, 1982).

In both studies on chilling damage in mangroves (Markley *et al.*, 1982, McMillan, 1974), the plants retained their relative sensitivities even after being transplanted and grown for some time under controlled conditions. In the face of this lack of acclimation it is, perhaps, a surprise to find that the Lt_{50} values obtained in this investigation were statistically different at the two sampling times. However, the difference of around 0.6°C was small, and is likely insignificant on a biological level.

Frost tolerance in plants generally follows a pattern of a winter maximum and a summer minimum (Bannister, 1976). Assuming a similar pattern for *A. marina* subsp. *australasica* in New Zealand, the data (Table 3.2) may be indicative of such a cycle; Lt_{50} being slightly higher on average for plants post-winter (November 2000) than pre-winter (May 2001) but further study is needed to confirm this.

Cold tolerance levels often depend on the developmental stage of a plant and can also differ between its component parts (Sutcliffe, 1977, Treshow, 1970). Seedlings and juvenile plants are generally considered to be less cold tolerant than mature plants and young, rapidly growing tissue is usually found to be less resistant than older material (Bannister 1976). In contrast, the mangrove seedlings studied in this investigation not only had greater frost tolerance than the mature leaves but also showed little to no change with latitude. Bannister *et al.* (1995) suggest that is not uncommon for some Southern Hemisphere species because there is a greater incidence of frosts near ground level at higher latitudes with a higher risk to seedlings growing outside the protection of a vegetation canopy. It is unlikely that this explanation applies to the mangrove because of the protection afforded by the warm water and sediments. Seedlings were also abundant at all sites.

In this investigation, leaves from both mature and seedling plants were chosen on the basis that the leaf tissue was fully developed (i.e., not very young leaf tissue), so the results may not necessarily indicate the frost level at which sensitive parts of *A. marina* subsp. *australasica* plants could be damaged in the field. To more accurately address the question of ultimate frost tolerance levels, different parts of the plants, such as new growth, buds and twigs would have to be tested. Freezing tolerance of seedlings may play a role in determining the distribution of the mature plants if they are unable to establish in areas where they are subject to greater extremes of temperature.

Frost tolerance values measured in this study using the electrical conductivity method seem to be in reasonable agreement with the few previous studies in New Zealand. Also, visual assessments of freezing damage in mature leaf tissue from Tauranga produced an Lt_{50} of $-5.2^{\circ}C$ as opposed to $-4.8^{\circ}C$ using the conductivity method suggesting that both methods give similar results but gives no answer as to which is the better. A recent study on Satsuma oranges also

supports electrolyte leakage as a good indicator of leaf damage (Monte *et al.*, 2002).

Temperature profiles measured in *Avicennia* stands over several winters at Ohiwa Harbour may help explain the observed patterns of frost damage. During all frost events, the coldest temperatures were recorded amongst the uppermost exposed leaves. Temperatures below and within the canopy were buffered by surrounding leaves and water or sediments during the coldest periods remained on average 1-2°C warmer. On further analysis of the temperature data it was clear that the upper exposed plant parts also experienced up to three times the frequency of frost nights than inner and lower parts (refer to Chapter 5).

A simple explanation for the pattern of damage is that during many frost events, only the plant parts positioned in the upper canopy (where radiative heat losses are greater), gain exposure to their critical freezing temperatures and are irreversibly damaged. In addition, the architecture of *Avicennia* at its southern limits is such that the more sensitive tissues, (reproductive organs and rapidly differentiating parts such as buds, developing propagules and new leaves), are placed in the zone of lowest temperature. The subsequent loss of apical dominance through bud mortality ("frost nipping") may be one reason why mangroves in frost-prone regions retain their dwarf stature.

3.5 Summary

This study has shown that the New Zealand mangrove, even at its southern limit, shows only limited ability to tolerate frosts. It is possible, therefore, that the southern limit is actually set by the depth of the frosts. Frosts severe enough to overcome the buffering effect of the warm water and sediments would certainly kill the plants. The interaction between tide height, tide timing and a severe frost would make such an event a rare occurrence. The alternative possibility exists that the plants exhibit only the necessary level of tolerance to survive the normal frosts. This is supported by the level of tolerance measured which does appear to be sufficient to protect the plants whilst also being less in comparison to other subtropical plants listed in Larcher (1995). If this possibility is correct then another factor might be limiting or, at the very least, complicating the situation. One such possibility is lowered photosynthetic capacity or productivity due to low temperatures which would affect the plants ability to tolerate any stress.

3.6 Experiment II: Determination of the critical temperature for freeze and heat injury in *Avicennia marina* subsp. *australasica* by the chlorophyll fluorescence method

3.6.1 Introduction

An increase in the intensity of minimal chlorophyll fluorescence (F_0) is generally indicative of stress-induced functional changes within the photosynthetic apparatus. As such, F_0 measurements have been used extensively to determine heat tolerance limits in leaf tissue (Bilger *et al.*, 1984, Schreiber & Berry, 1977, Smillie & Nott, 1979). Recently Pospisil *et al.* (1998), demonstrated that F_0 can also be used to assess cold (freezing) stress in plant tissue. In both cases, when a critical temperature (T_c) is reached, F_0 rises sharply from a relatively steady state and continues to increase until a maximum is attained at a more extreme temperature (peak temperature T_p) (Figure 3.3.).

3.6.2 Methods

Cold and heat tolerances of PSII in *Avicennia* were investigated by monitoring changes in F_0 (the minimal fluorescence of a dark-adapted sample) to gradual decreases or gradual increases in temperature. Four leaves were assessed; two from Raglan harbour at latitude 37°48'S and two from Whitianga harbour at latitude 36°51'S. The samples were all fully expanded leaves from the previous summer flush and were tested within two days of collection.

3.6.2.1 Cooling

Whole leaves were cooled on an aluminium cooling plate through which a solution of 70% glycerol + 30% dH_2O was circulated from a water bath. The cooling plate was insulated above and below with polystyrene sheets and tinfoil, reducing variation in leaf temperature and minimising heat exchange with the ambient environment. Leaf samples were placed adaxial surface upwards on the cooling plate on a layer of damp paper towel. An opaque plastic guide plate was placed on top of the leaf to eliminate incident light on the sample and to accommodate a MiniPAM (Walz, Germany) fibre-optic light at a vertical distance of 4 mm from the leaf surface. Leaf temperature was manipulated manually using the water bath controls to reduce the temperature of the circulating cooling fluid stepwise over 2 hours and 10 minutes from 10.0°C to -11.3°C. Actual leaf

temperature was monitored with a MiniPAM miniature temperature sensor attached to the abaxial leaf surface. Measurements of F_0 were taken at one-minute intervals.

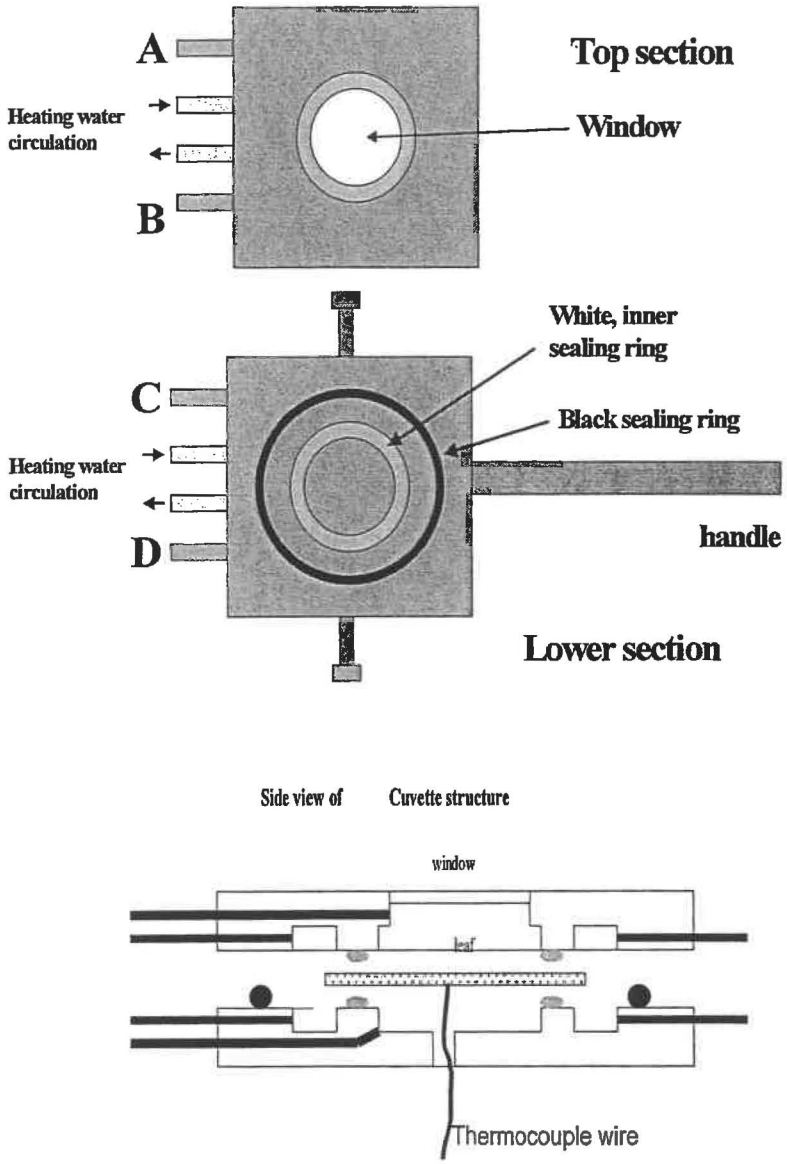

Figure 3.2. Schematic diagram of the leaf cuvette used for the determination of leaf heat resistance. Above: top view of the two cuvette halves. Bottom: side view of assembled leaf cuvette and sample. (Figure by T.G.A.Green)

3.6.2.2 Heating

A leaf disc of approximately 40 mm diameter was sealed within an aluminium cuvette, adaxial surface facing upwards beneath a glass window in the cuvette (Figure 3.2). A MiniPAM fibre-optic light was positioned over the sample (avoiding main veins and damaged tissue) and the entire setup was covered with a dark cloth to eliminate incident ambient light. Leaf temperature

was increased stepwise over 3 hours from 25°C to 74°C by circulating heated water from a thermostat controlled water bath through the two halves of the cuvette. Actual leaf temperatures were measured with a Mini PAM temperature sensor attached to the underside of the leaf sample. F_0 was recorded at 10-minute intervals.

A MiniPAM fluorometer (Walz, Germany) was used to measure minimal fluorescence (F_0) in both cooled and heated samples. The fibre-optic was positioned approximately 4 mm vertical distance from the leaf sample, avoiding main veins and damaged tissue. After 15 minutes dark adaptation, a very low intensity modulated light beam (2 mW m^{-2}) was used to excite fluorescence so as to prevent a light–induced fluorescence increase occurring due to electron accumulation at PSII (Bilger *et al.*, 1984).

3.6.2.3 Calculation of critical (Tc) and peak (Tp) temperature

Relative cold and heat sensitivities were determined from F_0-T curves (Figure 3.3) according to a technique described by Schreiber and Berry (1977). The criteria used were T_c, the critical temperature for the heat/cold induced fluorescence rise, and T_p, the temperature of peak fluorescence.

3.6.3 Results and Discussion

3.6.3.1 Cooling

A three-step rise in minimal chlorophyll fluorescence (F_0) was observed in response to gradually decreasing temperatures below 10°C. At tissue temperatures above 6°C, F_0 remained relatively steady, but as temperatures continued to decrease, fluorescence rose and maintained a steady rate of increase until tissue temperatures reached -6°C. After this point, F_0 increased sharply with decreasing temperature until maximum fluorescence was measured at around -11°C (peak temperature, Tp) (Figure 3.3). F_0 declined rapidly after fluorescence had peaked. The point on the curve where F_0 changed significantly, in this case -6°C (Table 3.4), indicated the critical temperature (T_c) at which irreversible damage to PSII occurred.

3.6.3.2 Heating

In response to gradual heating, minimal chlorophyll fluorescence emissions in the leaf tissue *Avicennia* followed a similar pattern of change as that observed in leaf tissue exposed to decreasing temperatures. F_0 remained steady

until the tissue temperature reached approximately 37°C. From this point, F_0 rose gradually with increasing temperature to approximately 51°C (T_c, critical temperature). Beyond critical temperature, F_0 emissions rose sharply until the leaf was at approximately 58°C (T_p, peak temperature), then declined rapidly.

Table 3.4. Critical and peak temperatures in heated and cooled leaf tissue of *Avicennia marina* subsp. *australasica* as determined from minimal chlorophyll fluorescence (F_0)-temperature curves.

	N	Tc, Critical Temperature (°C)	Tp, Peak Temperature (°C)
Heating	2	51	58
Cooling	2	-6	-11

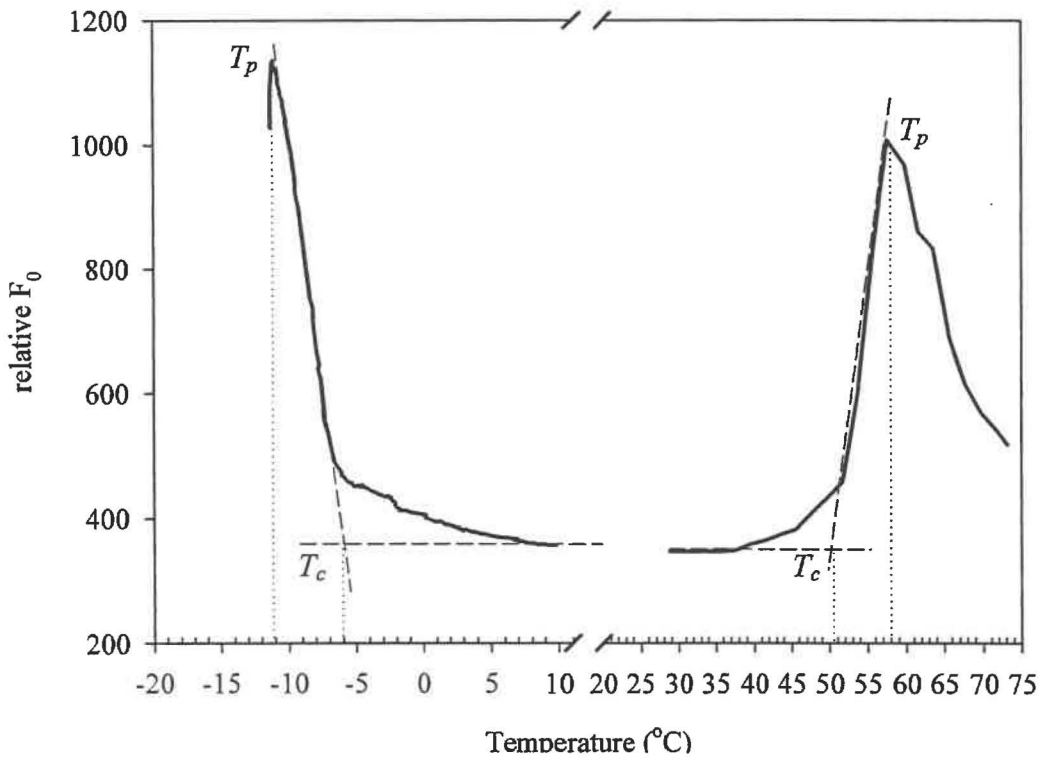

Figure 3.3 Increase in relative fluorescence yield of chlorophyll in leaf sections of *Avicennia marina* subsp. *australasica*; Left: cooled at a rate of approximately 0.16°C per minute Right: heated at a rate of approximately 0.27°C per minute. Temperature values T_c and T_p *(see dotted lines)* are described in the text and actual values are presented in Table 3.4.

3.6.4 Summary

Both heat- and freeze-induced increases in F_0 are understood to result from inhibition of $Q_A - Q_B$ electron transport, blocking of RCII and redistribution of excitation energy (Pospisil *et al.*, 1998). Analysis of F_0 fluorescence in *Avicennia* suggests that the critical temperature limits at which this occurs are around -6°C and 51°C. Given the small sample size and the variable nature of cold tolerance within *Avicennia* these results may not be conclusive for freezing limits, but they indicate that PSII freezing tolerance is slightly lower (more negative) than that estimated for 50% injury, Lt_{50} (as calculated by cell solute leakage and tissue necrosis; see earlier). The results also indicate that although PSII is still operative to temperatures as low as -6°C, the photosystem may be stressed at much warmer temperatures (as evident in an increase of F_0 emissions at chilling temperatures between 5°C and 0°C).

Ultimately, it is the integrity of the cell membrane that determines survival and continued function of plant cells. Therefore, even though the photosystem may remain functional at temperatures as low as -6°C, this is unlikely to be much of an advantage to mangroves during severe frosts because the membrane structures are compromised at temperatures approximately 2°C warmer (see Experiment I, this chapter).

Chapter Four

Chapter four

Characteristics of photosynthesis and water relations in the mangrove *Avicennia marina* subsp. *australasica* in its natural environment in New Zealand

4.1 Introduction

Investigating the photosynthetic processes of a plant species is an important start to understanding the adaptive mechanisms that allow it to cope with the particular environment in which it lives. The principal aims of this part of the study were to investigate temporal (diurnal/seasonal) and spatial (latitudinal) variations in photosynthesis of *Avicennia* plants at, and distant from, their southern limit in New Zealand, and so to learn whether there is any relationship between the geographic boundary of this species, around latitude 38°S, and photosynthetic performance.

Few specifics are known about the photosynthetic and gas exchange characteristics of New Zealand *Avicennia*, but much is understood from overseas studies of this and other mangrove species both in the laboratory (Ball & Critchley, 1982, Ball & Farquhar, 1984a, 1984b) and the natural field setting (Andrews *et al.*, 1984, Cheeseman *et al.*, 1991, Lin & Sternberg, 1992, Moore *et al.*, 1972, Naidoo *et al.*, 1998). Although most of these studies focus on the physiological functions of mangrove in tropical or sub-tropical environments, they provide a useful basis of comparison for mangrove in the comparatively cooler, temperate climate of New Zealand.

Mangrove photosynthetic biochemistry is typical for C_3 plants (Ball, 1986, Cheeseman, 1994, Clough *et al.*, 1982), however some aspects of their photosynthesis are less typical, in particular their water-use efficiency (WUE); the ratio of photosynthesis (A) to water loss in transpiration (E). Ball (1988b) suggests that mangroves cannot afford high losses of water like other C_3 plants because of the high energy costs incurred in salt exclusion during water uptake so that maintaining a high WUE is essential for survival.

There is some controversy as to whether mangroves maintain high or low rates of transpiration. At high salinity, mangroves have low stomatal conductance and transpiration rates (Ball, 1996), a characteristic that may have adaptive significance to survival in the saline environment, and which allows

the plants to maintain a physiologically acceptable salt/carbon balance within the leaves (Ball, 1986, 1995, Hutchings & Saenger, 1987, Naidoo *et al.*, 1998). Salt tolerant species are able to maintain higher rates of transpiration with greater WUE at high salinity and lower humidity compared to non-tolerant species (Ball & Sobrado, 1999). However, conservative WUE is not always the case in mangrove; some studies report stomatal conductance and transpiration in these plants to be comparable to other tropical forest trees (Becker *et al.*, 1997), particularly when growing in low salinity (Sobrado, 1999).

Net rates of photosynthesis in mangrove are comparable to most trees, but are lower than typical for herbaceous plants (Clough *et al.*, 1982). Although net photosynthetic rates of up to 22 μmol CO_2 m^{-2} s^{-1} have been reported in some mangrove species under conditions of favourable light and temperature (Clough & Sim, 1989) or in association with high stomatal conductances (above 200 mmol H_2O m^{-2} s^{-1}) , rates between 5 and 10 μmol CO_2 m^{-2} s^{-1} are more common in most species (Cheeseman, 1994).

The photosynthetic processes of a number of mangrove species usually operate at maximum when leaf temperatures are between 25 - 30°C, and photon flux density is between 30 and 50% of full sunlight; approximately 600 to 1000 μmol quanta m^{-2} s^{-1} (Tuffers *et al.*, 2001). At temperatures above 35°C (Andrews *et al.*, 1984, Ball *et al.*, 1988) and below 15°C (Kao *et al.*, 2004) photosynthetic rates decrease significantly.

Mangrove photosynthesis is also strongly affected by substrate salinity. Decreased CO_2 uptake, stomatal conductance and reduced rates of transpiration are associated with high salinities (Clough & Sim, 1989, Sobrado, 2000, Tuffers *et al.*, 2001). Lower rates of maximal CO_2 uptake of are also associated with low salinity as is a higher incidence of photoinhibition and photoprotection (Tuffers *et al.*, 2001).

The majority of mangrove species, including *Avicennia marina*, have stomata only on the abaxial leaf surfaces and conductances are generally low (Cheeseman, 1994, Iyengar & Reddy, 1996). Healthy leaves of mangroves are reported to operate with leaf internal CO_2 concentration (c_i) values around 170 μl l^{-1}(Ball, 1986), but values between 250-260 μl l^{-1} have also been reported for the mangroves *A. marina* and *B. gymnorrhiza* (Naidoo *et al.*, 1998) and are comparable to those reported for crop plants (Farquhar & Sharkey, 1982).

Water relations in mangrove resemble those of conifers and xerophytic trees with much lower leaf water potentials than well-watered mesophytes (Scholander *et al.*, 1965). Water potentials (Ψ) in mangrove are usually below that of seawater and generally lie between –2.5 MPa and –4.0 MPa (Clough *et al.*, 1982). However, some higher and some much lower values occur, usually in association with unusually low or high salinities. Naidoo *et al.* (1997) reported leaf Ψ of between -1.0 and -2.6 MPa in *A. marina* in waterlogged mangrove in South Africa), and midday leaf Ψ of –8.3 MPa for *Avicennia germinans* during the dry season in northern Venezuela with extreme scarcity of water and hypersaline conditions.

Water potentials in salt excreting species such as *Avicennia* spp. are reported to vary between -2.5 MPa (predawn) and -6 MPa (midday) (Scholander *et al.* 1964, Scholander 1968, Ball & Passioura 1995). In salt-excluding species, lower water potentials must be achieved to maintain the hydrostatic gradient along which water moves into the plant, because salt levels may be much higher in the immediate rhizosphere than in the bulk soil solution due to accumulation of excluded salt around the roots during uptake of water (Clough *et al.*, 1979, Passioura *et al.*, 1992).

Theoretically, to achieve maximum possible carbon gain during a growing season, a plant needs an environment where all requirements for growth are available in quantities that allow the physiological processes to operate without limitation. However this is rarely, if ever the case, particularly in high-stress environments such as the mangrove forest. Salt, high light, water and nutrient stress are important factors in mangrove development and survival, and as such have been the focus of much research. However, low temperature (of great importance in defining the geographical distribution of many plant species), has largely been ignored in relation to mangrove because the majority of those studied have been located in tropical or sub-tropical environments.

Low temperatures may cause physical cell damage (see Chapter 3), and adversely affect many aspects of photosynthesis including causing inhibition of Rubsico activity, stomatal closure, and increasing the potential for photodamage of PSII by decreasing the rate of photosynthesis (Nir *et al.*, 1997). Chill-shock and physical cold-temperature damage have been studied in other *Avicennia* species (Markley *et al.*, 1982, Maxwell, 2001) but, apart from transplant experiments with seedlings (Kao *et al.*, 2004), the present study appears to be one

of very few where photosynthetic responses of mangrove to low winter air temperatures (<5°C) have been measured in their natural environment.

In winter, many coastal locations around northern New Zealand experience low night temperatures followed by relatively warm sunny days. Frosts are frequent around latitude 38°S (the southern limit of mangrove) and, although temperatures rarely drop below 0°C further north around latitude 34°S, chilling nights may be numerous during the winter months. The present study provided an opportunity to investigate not only diurnal variability in mangrove photosynthesis over a range of latitude during the optimal summer growing season, but also to examine the photosynthetic consequences of low chilling- and freezing-temperatures during winter.

4.2 Methods

Making sensible comparisons of ecophysiological data collected under field conditions from a number of locations can be difficult, given that the physical environment offers little constancy in terms of factors influencing plant function. When spatial (e.g., latitude) or temporal (e.g., day, season) variables, plus equipment limitations, are added to the equation comparisons may become even more complex. In this study, within-site variation introduced by minor changes in environmental conditions was accounted for by pooling data collected over several consecutive days. Between-site differences were also investigated, but these comparisons should be interpreted bearing in mind that climate, nutrient status and other physical variables were different at each site and also that measurements were made at different times of the year.

In the winter and summer of 2001 and the spring and summer of 2002, diurnal patterns of gas exchange (namely CO_2 assimilation rates, stomatal conductance and transpiration; refer to section 2.10), water use efficiency, water relations (refer to section 2.8) and chlorophyll *a* fluorescence (refer to section 2.11) were investigated in three mangrove populations at the field sites described in section 2.6 (i.e., Paihia, Whitianga harbour and the Wainui Road research site at Ohiwa harbour). All sampling times are NZST unless otherwise stated.

At all sites the measurements were carried out on a total of ten or twelve healthy, fully-expanded leaves, positioned between 1 and 3 m above substrate level on three or four mature mangrove plants.

4.2.1 Salinity

The study sites were chosen on the basis of similar substrate salinities in order to eliminate the contribution of this factor to inter-site variability in photosynthetic performance. Salinity at the study sites was determined according to the procedures outlined in section 7.5.1.1.

4.2.2 Gas exchange and chlorophyll *a* fluorescence (F_v/F_m)

Up to seven *in-situ* measurements of net CO_2 and H_2O gas exchange were obtained at intervals from each leaf during a complete photoperiod using a CIRAS-1 combined infrared gas analysis system (PP-systems, United Kingdom). During measurements the leaves were oriented towards the sun to ensure they received maximum incident light within the leaf cuvette chamber or leaf clip. Where possible (dependent upon weather conditions), diurnal measurements were continued on the same set of leaves over two to four consecutive days at each site. Chlorophyll *a* fluorescence of the same leaves was measured with a PAM fluorometer (Walz, Germany) following gas exchange measurements and 15 minutes of pre-darkening treatment.

4.2.3 Water potential and microclimate

Two additional leaves were removed from each tree at approximate two-hour sampling intervals for the measurement of leaf water potential in a pressure chamber (refer to section 2.8).

Measurements of irradiance (PFD, μmol m^{-2} s^{-1}), humidity (%RH), and ambient air and substrate temperatures (^{o}C) were also recorded at all sites during, prior to, and after each sampling period using an array of sensors connected to a Campbell CR10X data logger (Campbell Scientific Inc, Utah, U.S.A.; refer to section 2.8.1).

4.2.4 Calculation of net daily photosynthetic income

Net daily photosynthetic income per unit of plant leaf surface (mmol m^{-2} d^{-1}) was calculated for each sample following the method explained by Francey *et al.* (1985), using net photosynthetic rates obtained at regular intervals throughout a sampling day, from samples with a leaf surface area of 25mm^2. As outlined in the example in Figure 4.1, calculations were made assuming that CO_2 assimilation started at a designated time (S) at the rate measured at A (the first sample point of the day), and continued at that rate until a time half-way between the first (A) and

second (B) measurements. From then, until a time half-way between the second and third measurement, net photosynthesis was assumed to continue at the rate obtained at (B), the second measurement of the day, and so on for each interval of the remaining photoperiod until the finish-point (F). Start- and finish-points were designated to be 0700 hr and 1800 hr for sampling periods between October and March and 0730 hr and 1700 hr for sampling periods between April and September.

Net photosynthetic income for each interval was calculated by multiplying interval duration (seconds) by the respective rate of CO_2 assimilation (i.e., the total represented by each hatched block in Figure 4.1). An estimate of net *daily* photosynthetic income for each leaf sample was then obtained by adding the values for all intervals.

Net photosynthesis data were analysed by multiple regression with STATISTICA version 6 (StatSoft, Inc.) using as predictors the minimum ambient air temperature recorded during the night before measurement of photosynthesis, the percentage time during the photoperiod that irradiance was greater than or equal to 500 μmol m^{-2} s^{-1} (saturating irradiance (see Walbert, 2002)), and the latitudinal origin of the plants.

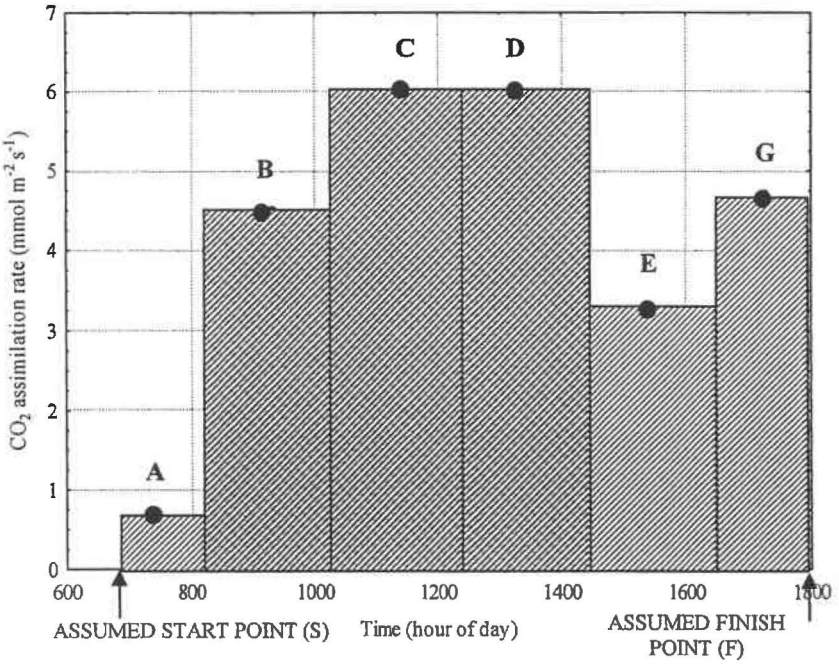

Figure 4.1 Single photoperiod variation in net photosynthesis (25mm^2 sample surface area) of a *A. marina* subsp. *australasica* leaf. Hatching represents total net daily photosynthetic income which is the sum of the individual totals calculated for each measurement. The example is typical of CO_2 assimilation measured on a single leaf at Paihia, Bay of Islands, New Zealand (lat 35°17̃ S) in August (austral winter). Actual measurement points are indicated by the labelled solid dots.

4.3 Results

4.3.1 New Zealand general climate 2001

Diurnal measurements at the three study sites were made within the period May 2001 to December 2002. During this time a number of notable climate events and trends influenced the regional climate at each study site. Data in the following sections (4.3.1 – 4.3.2) were extracted from the National Institute of Water and Atmosphere (NIWA) climate summaries for 2001 and 2002 (NIWA, 2003b)

At 12.8°C, the 2001 national average air temperature for New Zealand was approximately 0.3°C above normal. Higher than average mean temperatures occurred throughout much of the North Island during the months of May, August, September, October and December. Although the beginning of winter (May) was approximately 4°C warmer than average, the end of this month marked the beginning of a period of unusually cold temperatures through June and July with severe frosts in many places. December was characterised by extremely warm overnight minima (between 15.5 and 16.5°C).

During the summer of 2001 much of the North Island recorded near average sunshine hours but these were well below average in the Bay of Plenty (Ohiwa harbour) at approximately 88%, and the lowest recorded since 1957. Rainfall was above average in the Bay of Plenty during this time. Rainfall was also higher than average for the year in Northland (Paihia).

4.3.2 New Zealand general climate 2002

During 2002, sunshine hours were higher than normal in the Bay of Plenty and parts of Northland, with totals up to 105 and 110% of average. There were some heavy rainfall periods during mid-June in Northland and the Coromandel peninsula (Whitianga Harbour), but annual rainfall was actually well below average in many places including the Bay of Plenty (less than 70% of average) and eastern Northland.

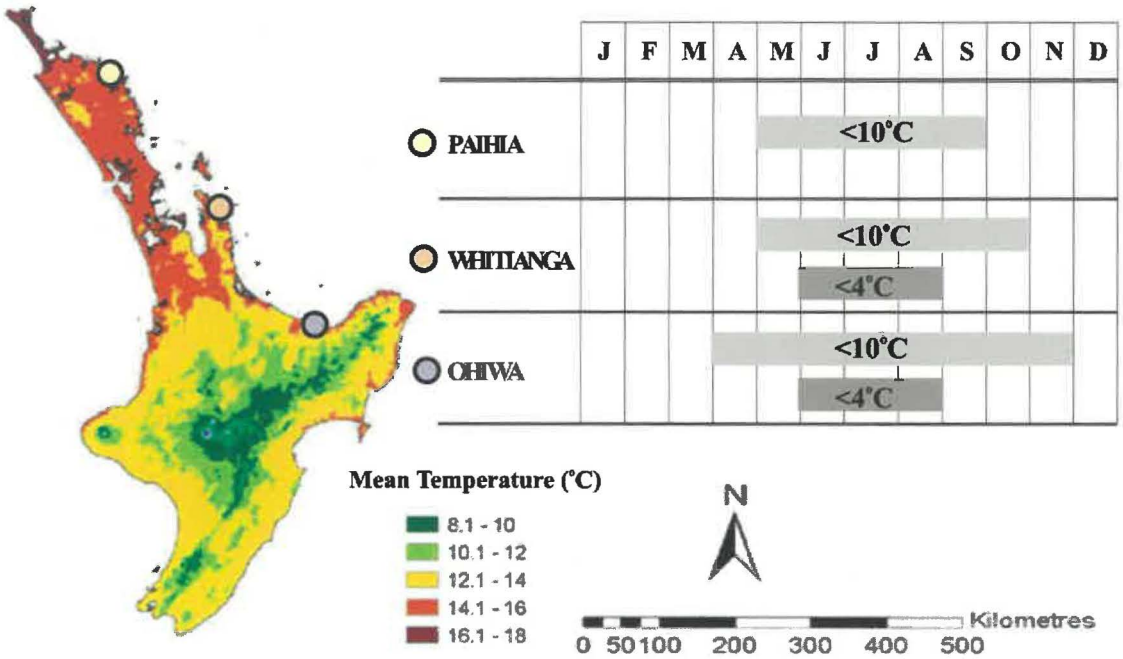

Figure 4.2 Left: New Zealand mean annual temperature (°C) 1971 – 2000. Right: Bars indicate months of the year when mean daily minimum air temperatures fall below 10°C and 4°C at Ohiwa Harbour, Whitianga Harbour and Paihia, Bay of Islands. Map and data sourced from http://www.niwa.co.nz/edu/resources/climate/overview and Summaries of Climatological Observations to 1980, New Zealand Meteorological Service (1983).

Winter 2002 was stormy and unsettled with high incidence of rain and wind. Fewer frosts were evident in most areas due to the lack of clear calm nights. June was the warmest on record with the national mean temperature of 9.8°C above normal by 1.5°C. At Whakatane in the Bay of Plenty the June (winter) temperature average was 2°C above normal. In October the usual spring warming was absent due to frequent southwesterly winds and clear cold nights. Consequently frosts were more frequent during this time.

4.3.3 Study-sites: general climate characteristics

Of the three study sites, the northernmost at Paihia in the Bay of Islands (Figure 2.4) had the warmest mean annual air temperature (15.6°C). Frosts were uncommon in this region and mean daily minimum temperatures below 10°C occurred during only five months of the year (May through to September) (Figure 4.2). Mean air temperatures became progressively cooler with increasing latitude and the frequency of chilling/frost nights escalated. The southernmost study site at Ohiwa Harbour in the Bay of Plenty (Figure 2.3) had a mean annual air

temperature of 13.6°C, and incidences of mean daily minimum temperatures below 10°C during 8 months of the year. Frosts, reported to occur here from May to October, were most prevalent during the period June – August. Mean daily minimum temperatures frequently dropped below 4°C during these months (Figure 4.2).

Latitudinally, Whitianga Harbour (Figure 2.5) lies roughly mid-way between Paihia and Ohiwa Harbour, and its climate (including extremes) also tended to be intermediate. Mean annual air temperature at Whitianga was 14.1°C. Incidences of mean daily minimum temperatures below 10°C and frosts occurred during six months of the year (May – October). Low temperatures occurred more frequently during June – August when mean daily minimum temperatures often dropped below 4°C (Figure 4.2).

Rainfall and sunshine hours were relatively similar at all three study sites with Paihia and Whitianga both receiving between 1500 and 2000 mm rain per annum and around 2000 – 2200 sunshine hours. Rainfall at Ohiwa harbour was slightly lower and sunshine hours were slightly higher than the other two study sites, (NIWA, 2003b).

4.3.4 Study-sites: microclimate characteristics

Sections 4.3.4.1 – 4.3.4.4 describe general microclimate characteristics of the three study sites, but do not include details of microclimate conditions during the actual study periods (these are described in section 4.5).

Study-site microclimate summaries including PFD, air and substrate temperatures, and relative humidity are given in tables 4.1 - 4.2. Each table represents the period encompassing both summer and winter sampling times

4.3.4.1 Air temperature (all study sites)

Concurrent measurements from all 3 sites (August – December 2001) showed that mean monthly on-site air temperatures decreased with increasing latitude (Tables 4.1 A-C). Mean air temperatures during this period were 15.7, 15.3 and 14.6°C at Paihia, Whitianga and Ohiwa harbours respectively. The coldest winter minima occurred at the Ohiwa harbour study site (Table 4.1-C). The highest summer air temperatures occurred at the Whitianga harbour study site (Table 4.1-B).

4.3.4.2 Photon flux density (all study sites)

Mean maxima of external-canopy PFD were consistent with season at all sites, with highest values occurring during summer and lowest during winter. Values ranged between 1107 and 2224 μmol m^{-2} s^{-1} with both extremes occurring at Ohiwa harbour in September and November respectively (Table 4.2-C). At Paihia, lowest mean maximal PFD occurred in September and highest in December (Table 4.2-A). At Whitianga harbour lowest and highest mean maximal PFD occurred in July and January respectively (Table 4.2-B).

4.3.4.3 Substrate Temperature (all study sites excluding Ohiwa Harbour)

Substrate temperatures varied according to whether the mud was exposed or covered with water. During winter nights at high tide, the water acted as a warming buffer, maintaining substrate temperatures much higher than on exposed mudflats. Mean substrate temperature at all sites was around 16°C.

4.3.4.4 Relative Humidity (all study sites)

Mean relative humidity was consistently higher at Paihia (87%) with values at Whitianga and Ohiwa harbours being similar to each other but lower (82 and 81% respectively, Tables 4.1 A-C, 4.2).

4.3.5 Study Period Microclimate

Site microclimate trends during the 3-4 day summer and winter measurement periods are presented in Figures 4.3 and 4.4. All parameters, including air and substrate temperature, relative humidity (%) and PFD, are depicted on the same daily time scale to allow immediate comparison; however, actual measurements were taken at different times of the year. Paihia plants were measured in December (summer) and August (winter); Whitianga plants in March (summer) and July (winter); Ohiwa plants in December (summer) and early September (winter).

Table 4.1 Microclimate at A: Paihia, Bay of Islands, B: Whitianga harbour, C: Ohiwa harbour: mean, extreme minima and extreme maxima for PFD outside and within the mangrove canopy (minima omitted, always zero); air and substrate temperature and relative humidity (maxima omitted, always close to 100%) during 2001 and 2002 study periods. "-" = missing data.

A	PFD outside-canopy ($\mu mol\ m^{-2}\ s^{-1}$)	PFD within-canopy ($\mu mol\ m^{-2}\ s^{-1}$)	Screened air temperature (°C)			Substrate temperature (°C)			Relative humidity (%)	
Month (2001)	Max.	Max.	Mean	Min.	Max.	Mean	Min.	Max.	Mean	Min.
Aug	1790	1404	12.6	4.5	22.2	13.8	8.0	18.9	90	56
Sept	1584	1563	14.2	5.8	25.0	15.3	10.6	25.8	83	41
Oct	1855	1114	15.9	7.1	24.0	16.8	10.4	27.2	87	43
Nov	1871	995	16.5	6.7	22.7	17.0	7.1	24.0	87	50
Dec	1984	942	19.2	9.7	25.7	19.3	10.3	25.4	88	45

B	PFD outside-canopy ($\mu mol\ m^{-2}\ s^{-1}$)	PFD within-canopy ($\mu mol\ m^{-2}\ s^{-1}$)	Screened air temperature (°C)			Substrate temperature (°C)			Relative humidity (%)	
Month 2001 - 2002	Max.	Max.	Mean	Min.	Max	Mean	Min.	Max.	Mean	Min.
July	1292	429	8.5	0.2	16.0	10.5	5.0	14.4	82	41
Aug	-	-	12.4	6.1	20.6	13.4	9.7	17.3	86	52
Sept	-	-	12.5	4.7	22.7	13.8	10.0	21.3	78	40
Oct	-	-	15.6	8.1	23.6	16.3	12.2	21.6	84	45
Nov	1518	1019	17.3	9.0	24.7	18.0	13.4	20.6	82	43
Dec	1675	1050	18.9	12.3	26.4	19.3	14.9	27.4	82	46
Jan	1733	1039	19.2	10.3	30.0	20.0	15.2	26.3	80	37
Feb	1615	1199	18.9	10.4	27.6	20.3	16.1	24.5	80	42
Mar	1450	938	18.5	10.6	26.2	19.7	16.3	24.2	81	43

C	PFD outside canopy ($\mu mol\ m^{-2}\ s^{-1}$)	Screened air Temperature (°C)			RH %	
Month (2001)	Max.	Mean	Min.	Max	Mean	Min.
Aug	-	10.2	3.0	16.8	86.8	67.0
Sep	1107	12.0	2.3	21.6	80.7	66.0
Oct	2088	15.7	3.5	24.0	83.4	45.0
Nov	2224	16.0	4.8	24.9	83.8	47.2
Dec	2149	19.3	16.9	23.4	92.3	75.4

Table 4.2 Microclimate at Ohiwa, Bay of Plenty (data recorded at the Whakatane airport AWS): mean daily maxima and minima air temperature, mean daily global radiation and relative humidity during April to December 2002.

Month (2002)	Mean daily maximum air temp (WH) (°C)	Mean daily minimum air temp (WH) (°C)	Mean daily global radiation (WH) (MJ m^{-2}),	RH%
Apr	20.2	9.6	12.5	78.4
May	17.9	7.2	9.0	85.1
Jun	16.1	6.2	6.9	86.4
Jul	13.8	2.5	8.3	85.5
Aug	15.4	4.8	10.5	85.1
Sep	17.2	8.5	13.6	79.4
Oct	17.6	8.5	18.5	74.1
Nov	14.5	8.7	22.2	69.1
Dec	22.9	12.3	23.9	73.1

4.3.5.1 Air Temperature during study periods

Although Paihia generally has a warmer climate than Whitianga or Ohiwa (see section 4.3.2), the timing of the sampling periods in this study was such that the warmest summer sampling period occurred at Whitianga Harbour, with maximum/minimum of 26.2/12.3°C (blue line, Figure 4.3-A). The corresponding study-period summer maxima/minima for air temperatures at Paihia and Ohiwa were 22.8/ 9.8°C (green line, Figure 4.3-A) and 27.2/6.0°C (red line, Figure 4.3-A) respectively. Paihia and Ohiwa harbour air temperatures were similar during the winter study periods with maxima/minima of 20.2/5.7°C and 19.2/6.3°C respectively (green and red lines, Figure 4.4-A). In contrast, air temperatures at Whitianga were much lower than the other two sites (blue line, Figure 4.4-A) because several very cold nights occurred there during the measurements with the lowest minimum reaching 0.2°C. Highest daytime temperature recorded at Whitianga was 14.9 °C.

4.3.5.2 Photon Flux Density during study periods

PFD was variable during the summer sampling days at all sites (Figure 4.3-D). At Paihia the sampling period was characterised by patchy cloud with occasional light rain on the first day. Maximal PFD during the study period was 1909 μmol m^{-2} s^{-1} (daily mean maximum = 1374 μmol m^{-2} s^{-1}). At Whitianga the sampling days were mainly clear and sunny, with maximal PFD during the study period reaching 1320 μmol m^{-2} s^{-1} (daily mean maximum = 1284 μmol m^{-2} s^{-1}). At Ohiwa harbour, the sampling days were mainly fine with some patchy cloud on

the second day, and the highest maximum was 1233 μmol m^{-2} s^{-1} (daily mean maximum = 1188 μmol m^{-2} s^{-1}). .

PFD was more variable during the winter sampling days at all sites (Figure 4.4-D). Paihia sampling days were characterised by patchy cloud cover and variable PFD up to a maximum of 1790 μmol m^{-2} s^{-1} (mean daily maximum = 1437 μmol m^{-2} s^{-1}). At Whitianga the sampling days were all heavily overcast and highest maximal PFD outside the canopy reached only 463 μmol m^{-2} s^{-1} (daily mean maximum = 322 μmol m^{-2} s^{-1}) whilst, at Ohiwa harbour the days were fine with patchy cloud and the highest PFD maximum was 1107 μmol m^{-2} s^{-1} (mean daily maximum = 1079 μmol m^{-2} s^{-1}). With the exception of Whitianga, there was little difference between summer and winter in the maximal PFD.

The average internal-canopy PFD during summer sampling was around 15% that of external PFD at Paihia and 22% at Whitianga. During the winter sampling periods, the equivalent values were approximately 30% at Paihia and 35% at Whitianga. No comparisons between internal and external PFD were possible for Ohiwa during either period due to a non-functional inner-canopy PFD sensor.

4.3.5.3 Substrate temperature during study periods

Substrate temperature probes were inserted to a depth of approximately 50 mm into the mud and temperatures were strongly influenced by the tide. The buffering effect of the water meant that minimum temperatures were not so low if there was a high tide during the night (Figures 4.3-B and 4.4-B).

During summer sampling, Paihia substrate temperatures ranged from 10.3 – 23.5°C compared to 17.0 – 23.0°C at Whitianga with the higher night-time temperatures coinciding with high tides ((Figure 4.3-B). No substrate data were collected at Ohiwa harbour. During winter sampling, Paihia substrate temperatures ranged from 7.9 – 16.9°C and were similar at Whitianga and Ohiwa at 5.0– 12.8°C and 4.5 – 17.8°C respectively (Figure 4.4-B). Warmest night-time temperatures were again associated with high tide occurrence.

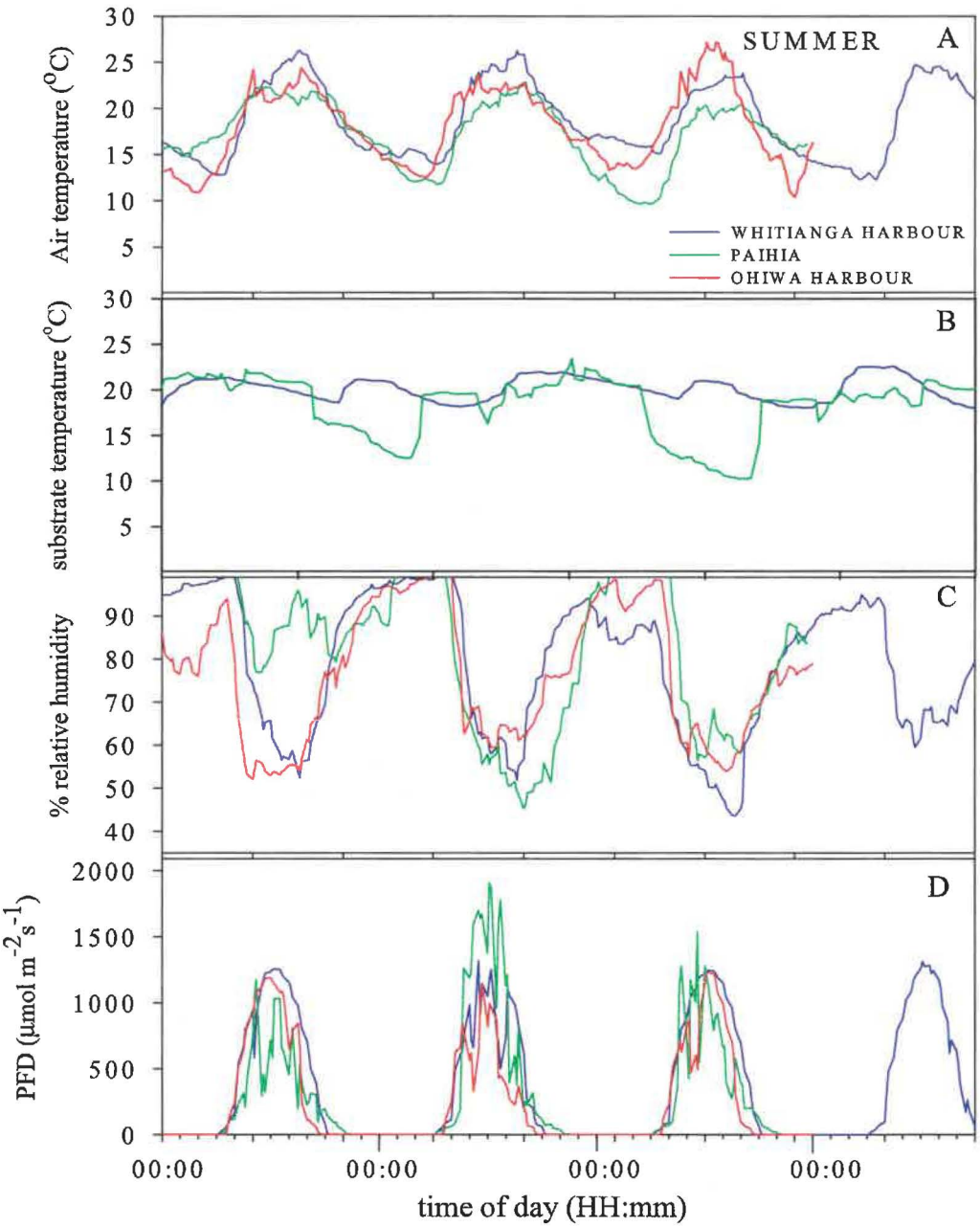

Figure 4.3 Microclimate during the summer study periods at Paihia (green line, sampled December), Whitianga harbour (blue line, sampled March) and Ohiwa harbour (red line, sampled December). Panel A: screened ambient air temperature (°C); Panel B: substrate temperature at 50 mm depth (°C); Panel C: % relative humidity; Panel D: Photon flux density (µmol m^{-2} s^{-1}).

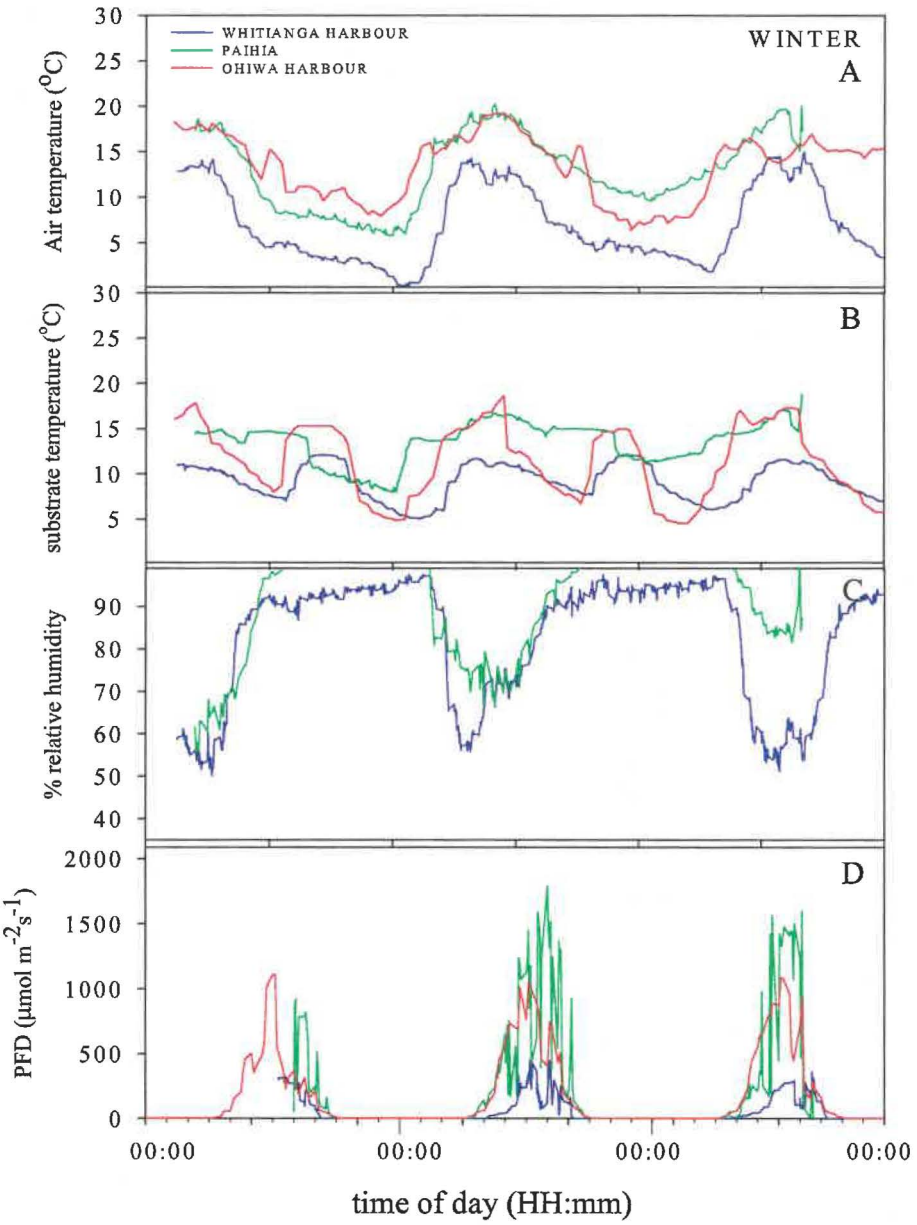

Figure 4.4 Microclimate during the winter study periods at Paihia (green line, sampled August), Whitianga harbour (blue line, sampled July) and Ohiwa harbour (red line, sampled September). Panel A: screened ambient air temperature (°C); Panel B: substrate temperature at 50 mm depth (°C); Panel C: % relative humidity; Panel D: Photon flux density (µmol m^{-2} s^{-1}).

4.3.5.4 Relative Humidity during study periods

Relative humidity was similar at all sites during the summer sampling periods (Figure 4.3-C). Mean RH at Ohiwa harbour was 76.7%, with the highest minimum of 52.2% with the equivalent values being 79 / 43.6% and 82 / 45% RH at Whitianga harbour and Paihia, respectively. The RH peak evident on the afternoon of the first day at Paihia (green line, Figure 4.3-C) was attributed to rain showers.

During the winter sampling periods (Figure 4.4-C), relative humidity at Paihia was again higher than at Whitianga, with a mean of 91.8% and minimum of 55.8%. In contrast, mean RH% at Whitianga was 83.1% with a minimum 49.9% whilst no records are available for Ohiwa.

Relative humidity at all sites peaked at around 100% at night during the summer measurement periods, except for two low-humidity nights at Whitianga where maxima only reached 88.9 and 94.2% (blue line, Figure 4.3-C). During winter sampling, night-time RH% values at Whitianga were also noticeably reduced with maximal values remaining below 97%.

4.3.6 Study Site Salinity

Substrate salinity was similar at all three sites, ranging from 31.2 mg g^{-1} at Whitianga to 34.7 mg g^{-1} at Paihia (Table 4.3).

Table 4.3 Latitude (°S) and substrate salinity (mg g^{-1}) at the three study sites of Paihia (Bay of Islands), Whitianga harbour and Ohiwa harbour, North Island, New Zealand

Sampling Site	Latitude (°S)	Salinity (mg g^{-1})
Paihia	35°17'	34.7±0.7
Whitianga	36°50'	31.2±0.8
Ohiwa	38°00'	34.1±0.7

4.3.7 Diurnal patterns of net photosynthesis

4.3.7.1 Paihia in summer: diurnal leaf performance

A typical single-day example of the diurnal patterns of leaf CO_2 assimilation rates (A), stomatal conductance (g_s), and F_v/F_m at Paihia in summer (December) is illustrated in Figure 4.5. On this particular day in December, ambient on-site air temperature reached a maximum of 22.8°C in late afternoon, after a previous-night minimum of 11.8°C. Average leaf temperatures, measured simultaneously with gas exchange or chlorophyll *a* fluorescence, ranged between 13.4 and 24.9 °C, with maxima occurring between 1200 and 1300 hr (Figure 4.5-A and -C). PFD levels reached a maximum of 1909 µmol m^{-2} s^{-1}, and remained ≥ 500 µmol m^{-2} s^{-1} for approximately 40% of the photoperiod (Figure 4.3-D). Percent relative humidity ranged between 45 and 100% with a minimum in mid-afternoon. In this example, leaves on two of the three sampled trees showed

typical photosynthetic behaviour of mangrove at the Paihia site in summer, in that A peaked both during the morning and in the afternoon (mean A_{max} = 9.1 μmol CO_2 m^{-2} s^{-1}), but was depressed throughout the middle of the photoperiod (Figure 4.5-D). Mean maximal g_s peaked at 93 mmol m^{-2} s^{-1} around the same time as CO_2 uptake, but remained low (between 7 – 44 mmol m^{-2} s^{-1}) for most of the photoperiod (Figure 4.5-E).

At the beginning of the day, leaf F_v/F_m were around 0.75 - 0.80. There was little variation throughout the day except for a slight decline in some leaves during mid-afternoon (Figure 4.5-B). Minimal values (lowest mean minimum = 0.67) coincided with the period of highest light and lowest relative humidity.

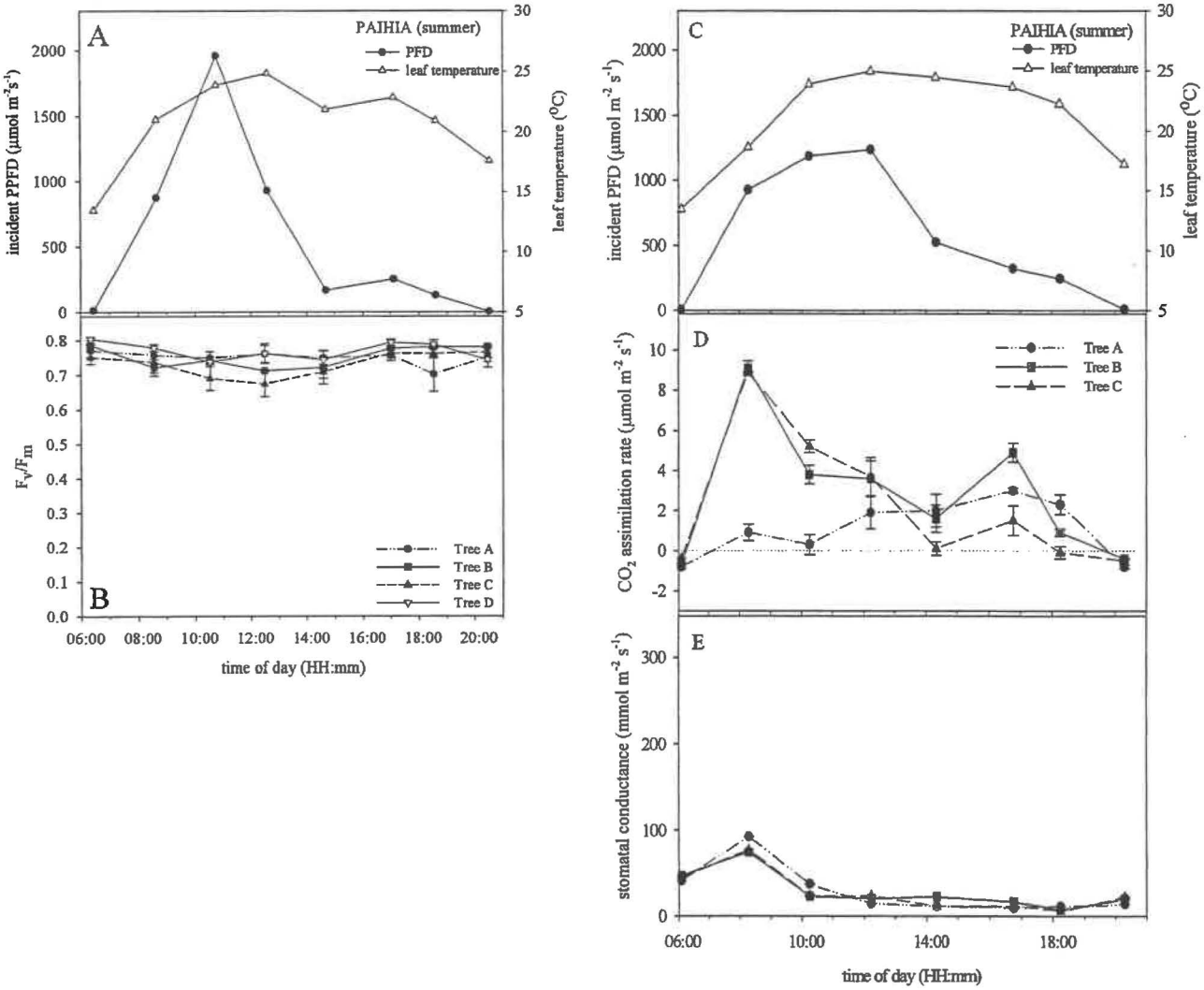

Figure 4.5 Paihia, Bay of Islands; An example of single-day diurnal patterns of net photosynthesis and associated parameters during **December (summer).** Mean leaf temperature (°C) and ambient PFD (μmol m^{-2} s^{-1}) measured simultaneously with either chlorophyll *a* fluorescence (Panel A) or gas exchange (Panel C); Panel B: maximal quantum efficiency of PSII primary photochemistry, (F_v/F_m); Panel D: rate of net photosynthesis, A (μmol m^{-2} s^{-1}); Panel E: stomatal conductance (mmol m^{-2} s^{-1}). Data points are the mean ± SE (n = 6 leaves on each tree). PFD and leaf temperature data are the mean of n = 18 leaves.

4.3.7.2 Paihia in winter: diurnal leaf performance

A typical single-day example of diurnal variation in leaf A, g_s and F_v/F_m at Paihia in winter (August) is illustrated in Figure 4.6. On this particular day in August, the weather conditions were fine with intermittent cloud cover. Maximum PFD of 1790 μmol m^{-2} s^{-1} and the lowest relative humidity of 66.8% occurred around mid-afternoon (Figure 4.4-D -C).

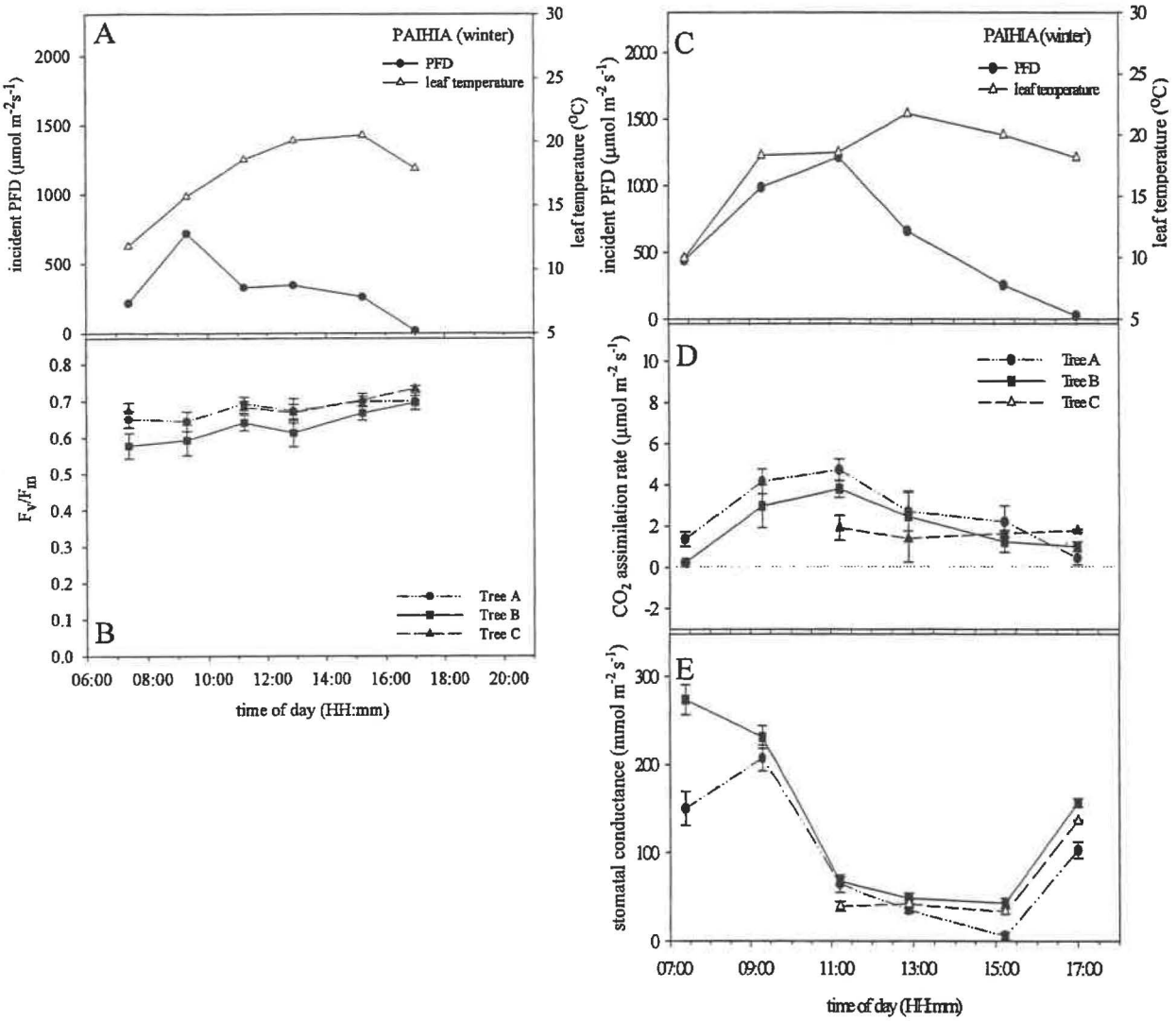

Figure 4.6 Paihia, Bay of Islands; An example of single-day diurnal patterns of net photosynthesis and associated parameters during **August (winter).** Mean leaf temperature (°C) and ambient PFD (μmol m^{-2} s^{-1}) measured simultaneously with either chlorophyll *a* fluorescence (Panel A) or gas exchange (Panel C); Panel B: maximal quantum efficiency of PSII primary photochemistry, (F_v/F_m); Panel D: rate of net photosynthesis, A (μmol m^{-2} s^{-1}); Panel E: stomatal conductance (mmol m^{-2} s^{-1}). Data points are the mean ± SE (n = 6 leaves on each tree). PFD and leaf temperature data are the mean of n = 18 leaves.

Air temperature reached a maximum of 20.2°C after a dry and slightly chilly night (minimum air temperature 5.7°C). Sampled leaves were exposed to light levels ≥ 500 μmol m^{-2} s^{-1} for approximately 43 % of the photoperiod. Leaf temperatures during measurement ranged from 9.5 °C to 23.7°C, peaking in mid afternoon (Figure 4.6-A -C).

A_{max} (mean = 4.7 μmol m^{-2} s^{-1}) occurred around 1100 hr and this was the only peak during the day (Figure 4.6-D). Stomatal conductance values were above 200 mmol m^{-2} s^{-1} at the beginning of the photoperiod, dropped to around 50 mmol m^{-2} s^{-1} for most of the day and then showed strong recovery to reach 100 mmol m^{-2} s^{-1} at sunset (Figure 4.6-E). The very high evening values, in comparison to other sites and times, probably indicate measurement anomalies due to the presence of dew on the leaf surfaces in early morning and evening.

Pre-dawn leaf F_v/F_m were low and variable (0.59 to 0.73), and then showed a steady rise through the remainder of the day (Figure 4.6-B).

4.3.7.3 Whitianga in summer: diurnal leaf performance

An example of diurnal variation in A, g_s and F_v/F_m for a typical day in summer at Whitianga (March) is illustrated in Figure 4.7. Weather conditions during this particular photoperiod were fine and cloud cover slight. Light levels were ≥ 500 μmol m^{-2} s^{-1} for approximately 66% of the photoperiod. PFD reached a maximum of 1257 μmol m^{-2} s^{-1} around early afternoon, slightly preceding the lowest relative humidity (minimum 52.5%). The highest ambient air temperature of 26.2°C occurred late afternoon following an overnight low of 12.8°C (Figure 4.3-A). Leaf temperatures, measured during sampling, ranged from 14.4°C to 27.0°C, reaching a maximum in early afternoon (Figure 4.7-A and -C).

CO_2 assimilation rates on this day varied between trees, and maximal values occurred at different times within a period of 4 hours in the afternoon (Figure 4.7-D). Highest A_{max} for any one leaf was 9.4 μmol m^{-2} s^{-1}. Maxima for stomatal conductance were 74 and 124 mmol m^{-2} s^{-1} and occurred between 0900 hr and 1000 hr (Figure 4.7-E).

Leaf F_v/F_m remained between 0.75 and 0.82 from early morning until mid-afternoon when all leaves showed a slight decline. However, recovery was evident in all leaves by the end of the day (Figure 4.8-B).

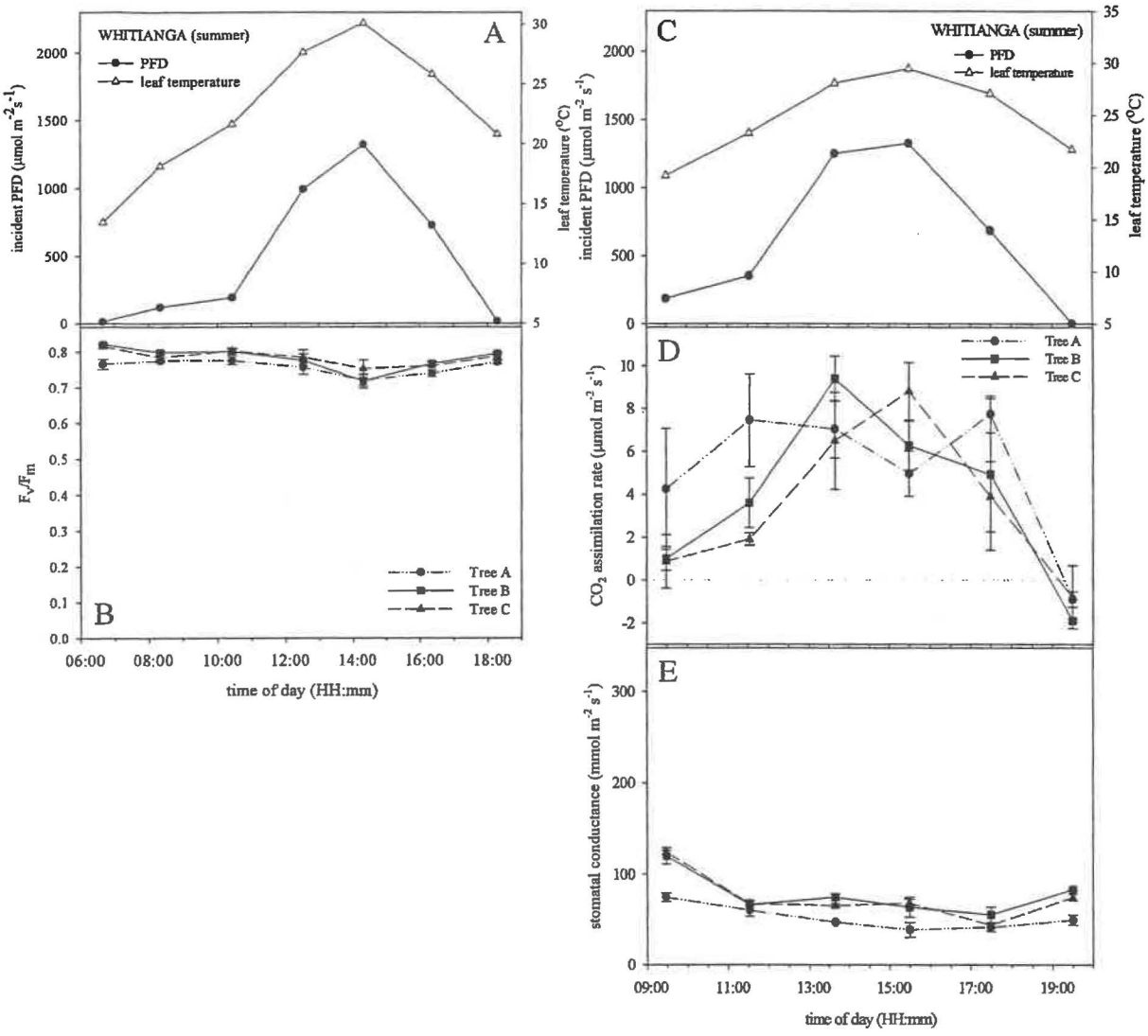

Figure 4.7 Whitianga Harbour; An example of single-day diurnal patterns of net photosynthesis and associated parameters during **March (summer).** Mean leaf temperature (°C) and ambient PFD (µmol m^{-2} s^{-1}) measured simultaneously with either chlorophyll *a* fluorescence (Panel A) or gas exchange (Panel C); Panel B: maximal quantum efficiency of PSII primary photochemistry, (F_v/F_m); Panel D: rate of net photosynthesis, *A* (µmol $m^{-2}s^{-1}$); Panel E: stomatal conductance (mmol m^{-2} s^{-1}). Data points are the mean ± SE (n = 6 leaves on each tree). PFD and leaf temperature data are the mean of n = 18 leaves.

4.3.7.4 Whitianga in winter: An example of diurnal leaf performance

A typical single-day example of diurnal variation in leaf A, g_s and F_v/F_m at Whitianga in winter (July) is illustrated in Figure 4.8. The weather conditions on this day were dry, with dense continuous cloud cover and low PFD values throughout the entire photoperiod. Maximal incident PFD (454.5 μmol m^{-2} s^{-1}) occurred around late morning. Ambient air temperature reached an afternoon maximum of 14.3°C after a low of 0.2°C in the preceeding night. Leaf

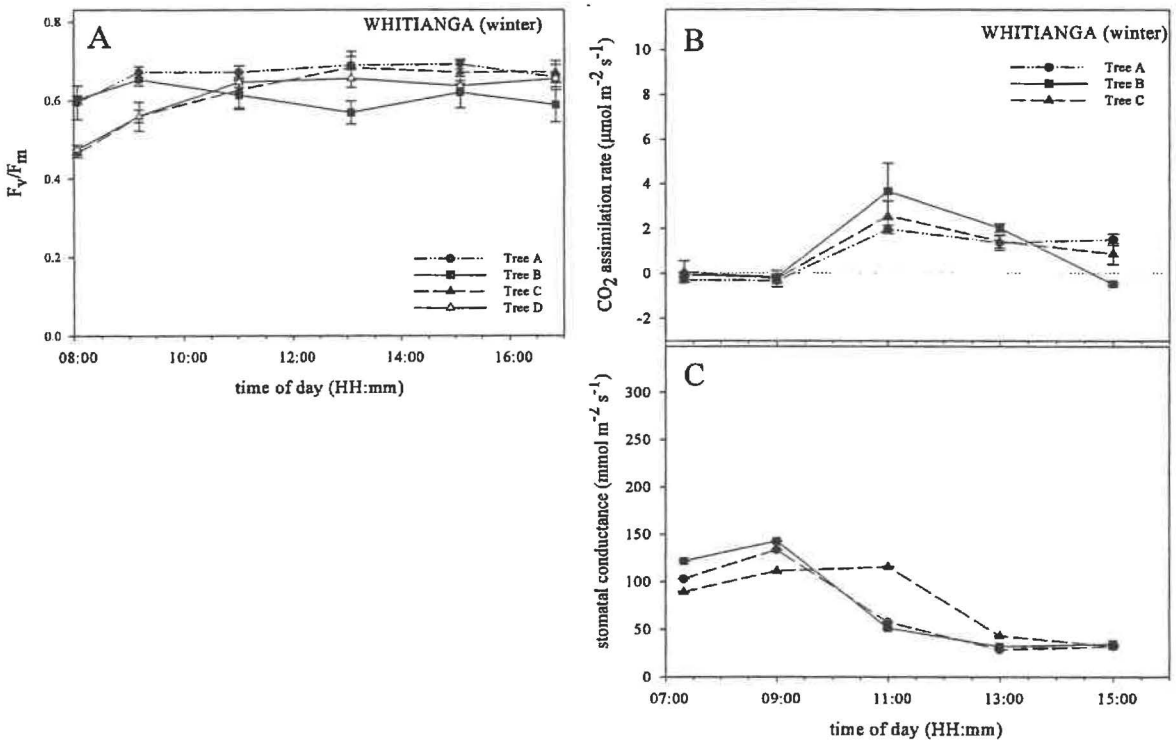

Figure 4.8 Whitianga Harbour; An example of single-day diurnal patterns of net photosynthesis and associated parameters during July (winter). Panel A: maximal quantum efficiency of PSII primary photochemistry, (F_v/F_m); Panel B: net photosynthesis rate, A (μmol m^{-2} s^{-1}); Panel C: stomatal conductance (mmol m^{-2} s^{-1}). Data for leaf temperature and PFD data at time of measurements were lost. Data points are mean ± SE (n = 6 leaves on each tree). PFD and leaf temperature data are the mean of n = 18 leaves.

A_{max} occurred between 1100 hr and 1300 hr after several hours of low or zero net photosynthesis by most leaves at the beginning of the photoperiod (Figure 4.8-B). The highest A_{max} was 5.9 μmol m^{-2} s^{-1} (mean = 3.7 μmol m^{-2} s^{-1}).

Mean g_s was generally high (> 100 mmol m^{-2} s^{-1}) at the beginning of the photoperiod, declining steadily after early morning to reach a minimum of around 32 mmol m^{-2} s^{-1} at the end of the measurement period (Figure 4.8-C). F_v/F_m were low (< 0.60) at the beginning of the day and then improved slightly to a be fairly constant but still variable through the day. At less than 0.70, values in all leaves were low relative to those typical of healthy leaves. The largest decline in any one leaf occurred in the early afternoon (Figure 4.8-A). In all cases F_v/F_m were at, or exceeded, pre-dawn levels by the end of the day.

4.3.7.5 Ohiwa in summer: single leaf performance

Diurnal changes in leaf A, g_s and F_v/F_m at Ohiwa harbour for a selected day in summer (December) are illustrated in Figure 4.9. Weather conditions for this day were fine with some scattered cloud. PFD was ≥ 500 μmol m^{-2} s^{-1} for approximately 37.5% of the photoperiod and reached a maximum of 1188 μmol m^{-2} s^{-1} around midday. Ambient air temperature ranged from an overnight minimum of 11.2°C to an early afternoon maximum of 22.1°C that coincided with lowest relative humidity (54.0%). During measurement, leaf temperatures varied from 13.1°C to 27.4°C (Figure 4.9-A and -C).

Most leaves had only one daily peak in A that occurred between 1100 and 1500 hr, however, Tree C showed a clear midday depression by all leaves (Figure 4.9-D). Mean A_{max} was 5.8 μmol m^{-2} s^{-1}.

Stomatal conductance values were highest in the early morning (in this case averaging between 95 and 100 mmol m^{-2} s^{-1}) then progressively decreased to <50 mmol m^{-2} s^{-1} at 1300 hr and the latter part of the sampling period (Figure 4.9-E).

Leaf F_v/F_m values were high at 0.76 - 0.80 until after midday when, in conjunction with high light and increased temperature, there was a decrease in F_v/F_m to between 0.60 and 0.78 as well as an increase in variability between leaves. Recovery to early-morning values occurred in all leaves by the end of the day (Figure 4.9-B).

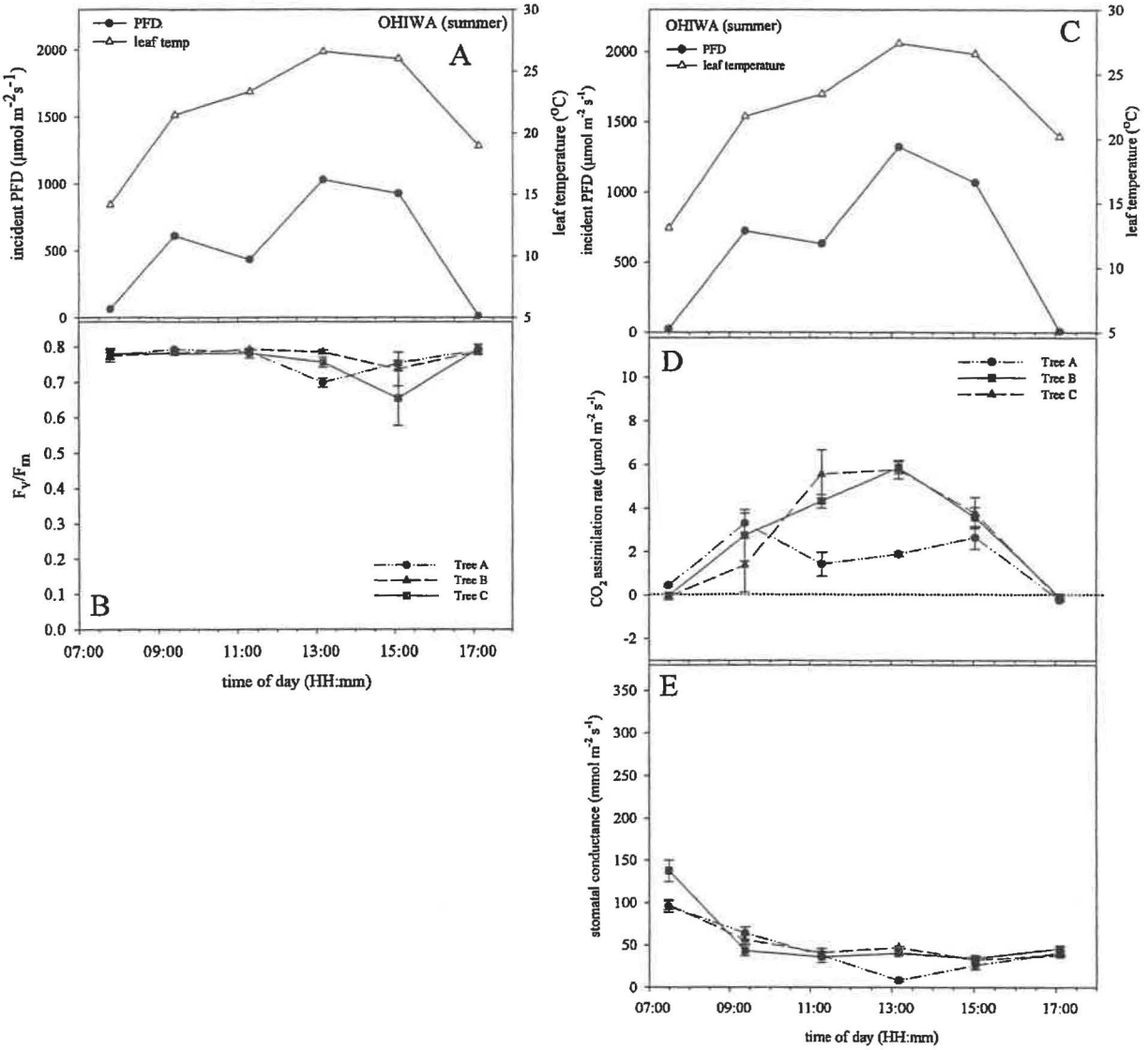

Figure 4.9 Ohiwa harbour; An example of diurnal patterns of net photosynthesis and associated parameters for one day in early **December (summer).** Mean leaf temperature (°C) and ambient PFD (µmol m^{-2} s^{-1}) measured simultaneously with either chlorophyll *a* fluorescence (Panel A) or gas exchange (Panel C); Panel B: maximal quantum efficiency of PSII primary photochemistry, (F_v/F_m); Panel D: rate of net photosynthesis, *A* (µmol m^{-2} s^{-1}); Panel E: stomatal conductance (mmol m^{-2} s^{-1}). Data points are mean ± SE (n = 6 leaves on each tree). PFD and leaf temperature data are the mean of n = 18 leaves.

4.3.7.6 Ohiwa in winter: single leaf performance

Diurnal changes in leaf *A*, g_s and F_v/F_m for a single leaf at Ohiwa harbour in winter (early September) are illustrated in Figure 4.10. Weather conditions on this sampling day were fine with scattered cloud. Prior to sampling, overnight air temperatures reached a minimum of 2.7°C and were followed by a maximum

daytime air temperature of 15.5°C and a mean relative humidity of 78%. PFD was maximal at 1046 μmol m^{-2} s^{-1} (Figure 4.10-A and -C) and was ≥ 500 μmol m^{-2} s^{-1} for approximately 37.8% of the photoperiod. It should be noted that the low levels of incident PFD (<500 μmol m^{-2} s^{-1}) shown in Figure 4.10-A are due to cloud cover present at the actual measurement times.

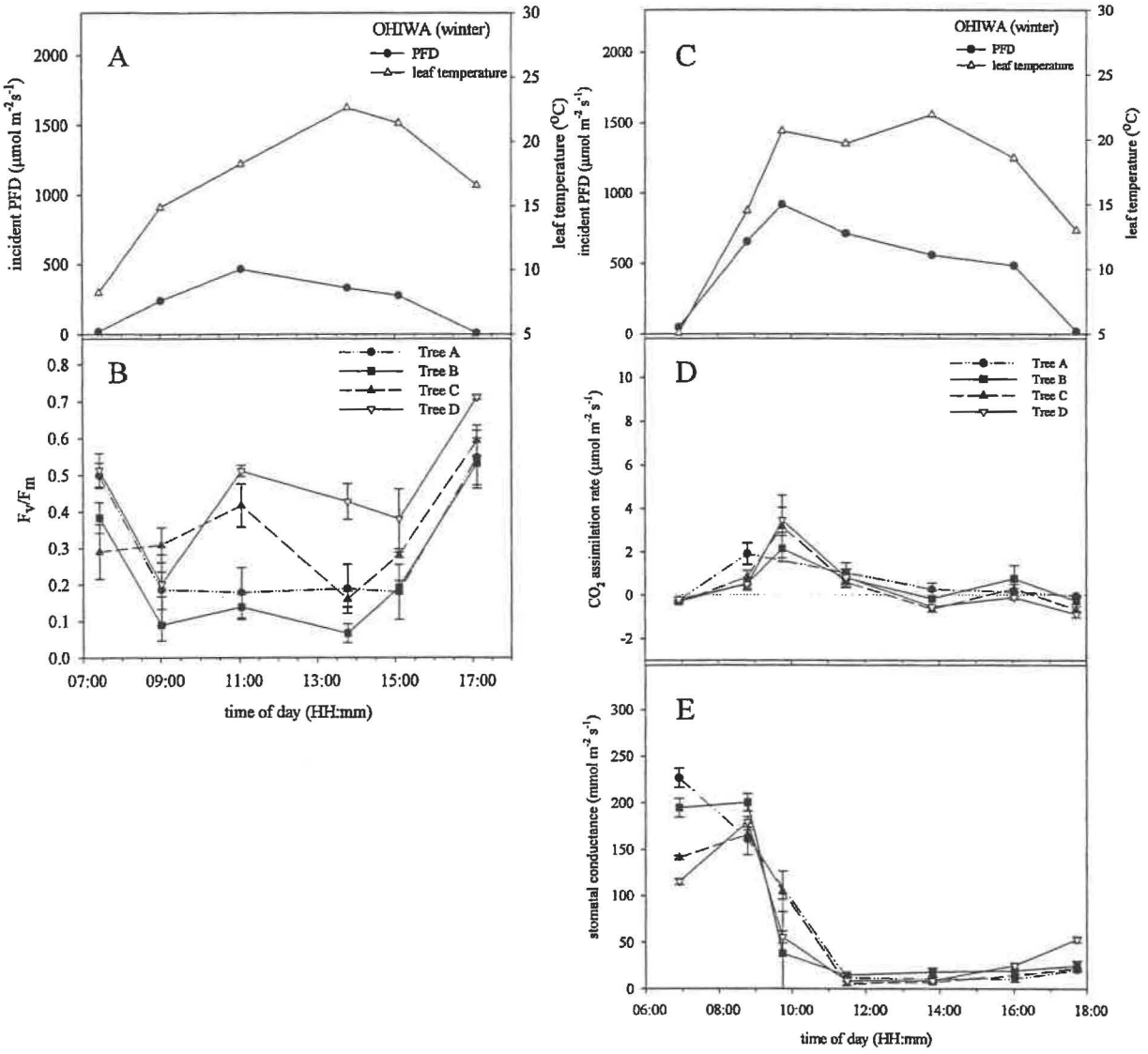

Figure 4.10 Ohiwa harbour; An example of single-day diurnal patterns of photosynthesis and associated parameters during **early September (winter).** Mean leaf temperature (°C) and ambient PFD (μmol m^{-2} s^{-1}) measured simultaneously with either chlorophyll *a* fluorescence (Panel A) or gas exchange (Panel C); Panel B: maximal quantum efficiency of PSII primary photochemistry, (F_v/F_m); Panel D: net photosynthesis rate, *A* (μmol m^{-2} s^{-1}); Panel E: stomatal conductance (mmol m^{-2} s^{-1}). Data points are mean ± SE (n = 6 leaves on each tree). PFD and leaf temperature data are the mean of n = 18 leaves.

The pattern of daily changes in A and g_s was similar for all sampled leaves. Net CO_2 uptake reached a maximum around 1000 hr and the highest rates were measured for plant D with A_{max} = 3.4 μmol m^{-2} s^{-1} but, by mid-afternoon, most leaves no longer showed positive net photosynthesis (Figure 4.10-D). Maximal g_s occurred during early morning, although it is possible that the high values were measurement anomalies caused by morning dew on the leaf surfaces. Conductance values declined progressively during the morning so that, by midday, stomata were almost closed in all leaves (g_s < 10 mmol m^{-2} s^{-1}) and remained so until some slight increase (possibly again dew fall) at sunset (Figure 4.10-E).

Early morning leaf F_v/F_m values were low (< 0.60) and decreased even further as the morning progressed. By 0900 hr F_v/F_m had fallen to between 0.05 and 0.20 in several leaves and remained low until 1500 hr. Recovery was then evident in all leaves so that, by the end of the day F_v/F_m had climbed to between 0.54 and 0.70, higher values than at dawn. The variability between leaves was much higher throughout the day than found in studies at other times and sites (Figure 4.10-B).

4.3.8 Water Relations – leaf water potential

The diurnal progression of leaf water potential (Ψ) in *Avicennia* followed a similar pattern at all three field sites during all sampling periods (Figure 4.11, row C). On every sampled day the highest Ψ levels were pre-dawn and then declined steadily until around midday followed by a slower recovery towards evening. In all cases equilibrium re-established overnight and Ψ returned to normal predawn levels by the time of the first measurement each day. The lowest pre-dawn Ψ values (-1.9 and -1.8 MPa) were at Ohiwa harbour in both summer and winter. The lowest day-time Ψ occurred in winter were at Ohiwa (-4.0 MPa), and at Paihia in summer (-4.8 MPa).

Seasonal differences were evident at all three sites, with Ψ always being higher (less negative) in the winter by approximately 0.4 MPa than in summer. The daily range at Paihia (i.e., the difference between pre-dawn and daily minimum Ψ) was larger in summer than in winter, but at Whitianga and Ohiwa the range in values was similar for both seasons (Figure). Ψ values for all three sites are tabled in Appendix IV.

Lower summer values are almost certainly due to increased evaporation because of higher temperatures and increased radiation. Predawn values were always lower in the summer and there are several possible explanations that are not exclusive. Low overnight humidity may have led to sustained water loss, and this explanation is supported by the fact that pre-dawn Ψ were usually much lower when dew did not form on the leaves. Also, the seawater (typically Ψ = c. –2.5 MPa) that inundated the plants may change in character with the season. The particularly high winter pre-dawn Ψ of around –1.0 MPa may reflect conditions of lower salinity than sea-water possibly due to higher winter rainfall and, therefore, a greater freshwater input to the estuarine waters. Alternatively, but not thought to be likely because of care taken during the measurements, the higher pre-dawn Ψ could represent determination errors. After cold nights, large amounts of free water were present in the leaf tissues, making the balance pressure of the xylem vessels difficult to read. The excess water was probably indicative of chilling damage to the cell membranes resulting in leakage of the cell contents into surrounding tissues.

4.3.9 General seasonal trends in leaf performance

4.3.9.1 Paihia: General trends in leaf performance over three consecutive days in summer

During the summer (December) sampling at Paihia, the highest A_{max} of any one leaf was 13.8 μmol m^{-2} s^{-1} (mean A_{max} = 5.5 μmol m^{-2} s^{-1}, see Figure 4.11). Rates typically peaked twice during a single photoperiod; near the beginning of the day (0800 hr – 0900 hr) and during the afternoon (1400 hr - 1600 hr). In all cases, a decline, associated with highest light and temperature, occurred around the middle of the photoperiod (Figure 4.11, row A, column Paihia). Stomatal conductance was generally highest at the beginning of the day, declining around mid-morning and remaining low (< 50 mmol m^{-2} s^{-1}) throughout the remainder of each photoperiod (Figure 4.11, row B, column Paihia).

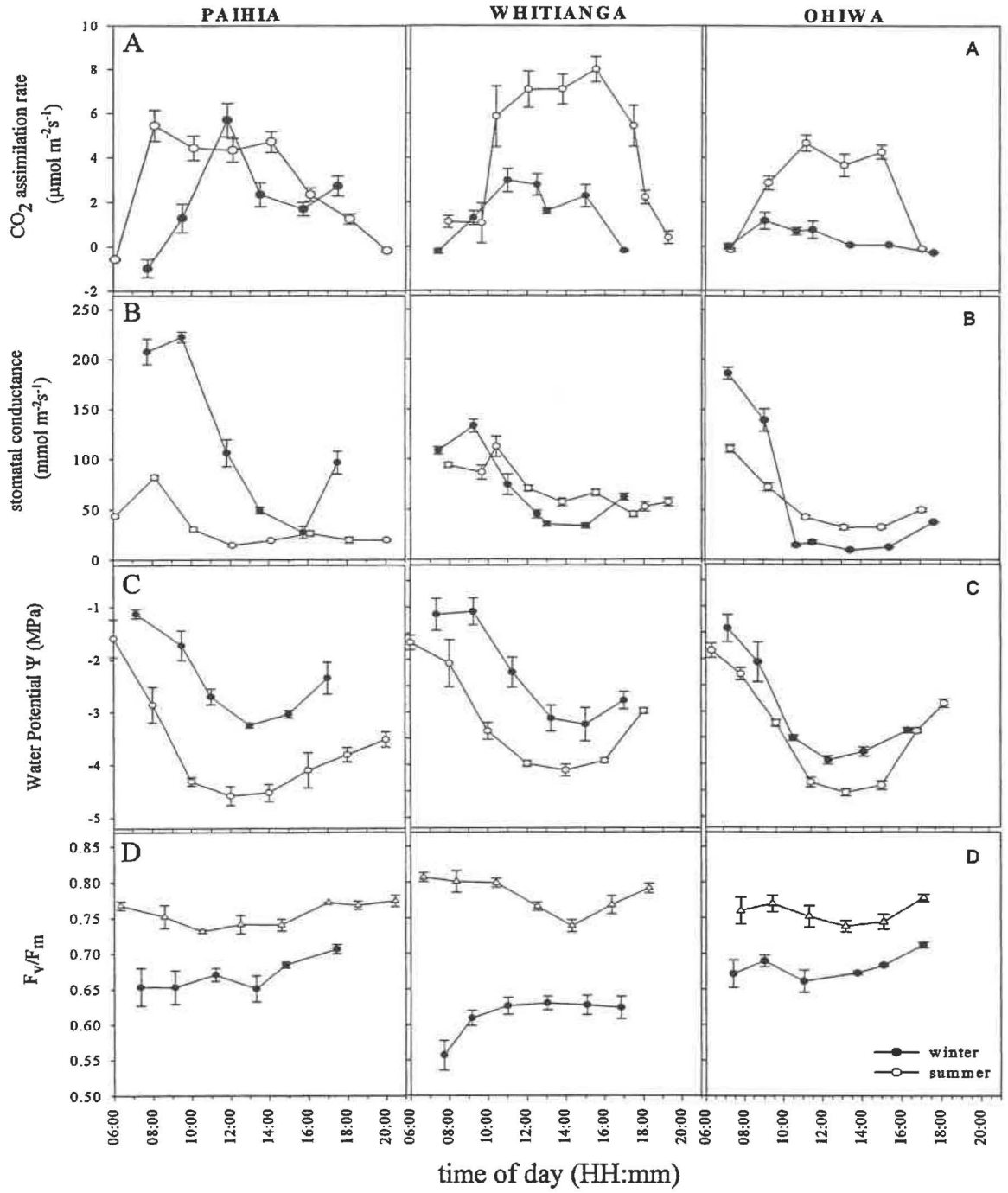

Figure 4.11 Seasonal differences in diurnal patterns of photosynthesis and associated parameters) at (left to right) Paihia, Whitianga and Ohiwa Harbours. Row A: rates of net photosynthesis, *A* (μmol m^{-2} s^{-1}); Row B: stomatal conductance (mmol m^{-2} s^{-1}); Row C: water potential, Ψ (MPa); Row D: maximal quantum efficiency of PSII primary photochemistry, F_v/F_m; Data points are mean ± SE (n = 12 for rows A, B, D), for row C (n = 6).

Diurnal variation in F_v/F_m during summer sampling at Paihia was relatively small, with values averaging around 0.75 (Figure 4.11 row D, column Paihia). Highest values (ranging from 0.76 to 0.80), generally occurred in the early morning, after which they declined until sometime between mid-morning and early afternoon. Recovery occurred during late afternoon and evening, during which time F_v/F_m returned to approximate early-morning levels. In all cases the observed decline in F_v/F_m occurred in association with the highest light levels.

4.3.9.2 Paihia: General trends in leaf performance over three consecutive days in winter

During the winter sampling period (August) at Paihia, highest A_{max} in any one leaf was 9.9 $\mu mol^{-2}\ s^{-1}$ (mean A_{max} = 5.7 $\mu mol^{-2}\ s^{-1}$, see Figure 4.11, row A, column Paihia). Maximal rates were usually reached around the middle of each photoperiod and, in contrast with the summer diurnal trends, only one daily peak was typical. Stomatal conductance values were generally very high at the beginning of the day (in any one leaf between 100 – 250 mmol $m^{-2}\ s^{-1}$), declined markedly between 1100 and 1500 hr and increased again at the end of the day to approximately 100 mmol $m^{-2}\ s^{-1}$ (Figure 4.11, row B, column Paihia).

F_v/F_m during winter sampling was lower than in summer at a mean value of approximately 0.67. Lowest values were in the early morning and and F_v/F_m rose gradually throughout the day to reach a maximum in the evening (Figure 4.11, row D, column Paihia).

4.3.9.3 Whitianga: General trends in leaf performance over four consecutive days in summer

During the summer measurement period (March) at Whitianga harbour the highest A_{max} of any one leaf was 14.6 $\mu mol\ m^{-2}\ s^{-1}$ (mean A_{max} = 8.0 $\mu mol\ m^{-2}\ s^{-1}$) and maximal rates generally occurred between 1500 hr and 1600 hr each day (Figure 4.11, row A, column Whitianga). Stomatal conductance values were highest early in the day (around 112 mmol $m^{-2}\ s^{-1}$) and declined to around 45 mmol $m^{-2}\ s^{-1}$ by late morning and then remained steady until a slight rise at the end of the day (Figure 4.11, row B, column Whitianga).

Early-morning F_v/F_m values ranged from 0.78 to 0.83 and subsequent variation throughout the photoperiod was small (Figure 4.11, row D, column

Whitianga). In general, maximal F_v/F_m occurred at the beginning of each day and remained fairly stable until a slight decline occurred until mid- to late afternoon when minimal values (mean 0.70) were reached. The decline usually coincided with the highest light levels incident on the leaf at the time of measurement. By evening F_v/F_m had recovered to values similar to the beginning of the day.

4.3.9.4 Whitianga: General trends in leaf performance over four consecutive days in winter

Photosynthesis at Whitianga harbour in winter (July) was depressed as a consequence of low ambient PFD and low overnight air temperatures. The highest A_{max} of any leaf was 7.4 μmol m^{-2} s^{-1}; approximately half of that attained during the summer measurement period. Mean A_{max} was 2.9 μmol m^{-2} s^{-1} again much lower than in summer (Figure 4.12). Stomatal conductance values were also lower; although typically starting high in the mornings (between 108 and 133 mmol m^{-2} s^{-1}) they dropped to lowest levels (mean minimum 33.5 mmol m^{-2} s^{-1}) around the middle of each photoperiod. Slight increases usually occurred again towards evening (Figure 4.11, row B, column Whitianga).

Leaf F_v/F_m were also much lower than in summer with a daily winter average of around 0.62 (Figure 4.11, row D, column Whitianga). Mean F_v/F_m peaked at 0.70 and the minimum was 0.37. Lowest values, between 0.43 and 0.67, occurred during early morning, then increased and remained relatively steady for the rest of the day, a pattern that indicated a negative effect from night-time chilling temperatures.

4.3.9.5 Ohiwa: General trends in leaf performance over three consecutive days in summer

The highest A_{max} of any one leaf during the summer measurement period at Ohiwa harbour (December) was 8.7 mol m^{-2} s^{-1} (mean = 4.6 μmol m^{-2} s^{-1}). Typically, two peaks; one around 1100 hr and one around 1500 hr, occurred during a single photoperiod (Figure 4.11, row A, column Ohiwa). Stomatal conductance values were high at around 110 mmol m^{-2} s^{-1} in the early mornings, and then declined gradually to minimal values around 32 mmol m^{-2} s^{-1} during the middle of each photoperiod, followed by a slight increase (mean = 37 mmol m^{-2} s^{-1}) by the end of each day (Figure 4.11, row B, column Ohiwa).

Daily leaf F_v/F_m values were relatively steady and high, averaging around 0.75 for most of each photoperiod. At first-light, values were around 0.76, and by mid- to late-afternoon had declined to minimal values of approximately 0.73. A final rise to values around 0.77 occurred in the evenings. Lowest F_v/F_m values coincided with the highest PFD and leaf temperatures (Figure 4.11, row D, column Ohiwa).

4.3.9.6 Ohiwa: General trends in leaf performance over three consecutive days in winter

Net photosynthesis was markedly depressed in the Ohiwa harbour plants during the winter measurement period in early September. Although the highest A_{max} in any one leaf, at 7.1 μmol m^{-2} s^{-1} was similar to that measured in summer, the mean maximal rate was much lower at 1.2 μmol m^{-2} s^{-1}. Peak rates generally occurred around 0900 hr each day and declined to near zero or below in the afternoon (Figure 4.11, row A, column Ohiwa). Stomatal conductance values were highest in the early mornings (> 150 mmol m^{-2} s^{-1}) but dropped to below 18 mmol m^{-2} s^{-1} around 1100 hr and remained low for the rest of the photoperiod (Figure 4.11, row B, column Ohiwa).

Early-morning leaf F_v/F_m values were also low (between 0.53 and 0.72), dropping to very low values (< 0.10) during the mornings with considerable variation between individual leaves throughout the course of each day. However, F_v/F_m in all leaves recovered in the evenings to give maximal values of around 0.76, (mean 0.67). The low values and high variability amongst individual leaves appeared to be consequences of exposure to low overnight temperatures.

4.3.10 Comparisons of maximal CO_2 assimilation and stomatal conductance

Clear seasonal differences in A_{max} were evident at all the field sites, with summer mean rates approximately double those obtained from the same trees during winter. All maximal rates, with the exception of the winter measurements at Whitianga, were measured under saturating PFD.

At Paihia (the northernmost site), mean A_{max} was 10.3 μmol m^{-2} s^{-1} in summer and 6.4 μmol m^{-2} s^{-1} in winter. The corresponding values were 12.2 μmol m^{-2} s^{-1} in summer and 4.8 μmol m^{-2} s^{-1} in winter at Whitianga harbour and 5.2 μmol m^{-2} s^{-1} and 1.8 μmol m^{-2} s^{-1} at Ohiwa harbour (the southernmost site) (Figure 4.12, left panel).

Mean stomatal conductance at A_{max} varied from around 50 mmol m^{-2} s^{-1} at Ohiwa to around 90 mmol m^{-2} s^{-1} at Paihia in both summer and winter (Figure 4.12, right panel). The occurrence of similar g_s in both summer and winter at all sites suggests that the depressed NP in winter was not a result of changes in g_s.

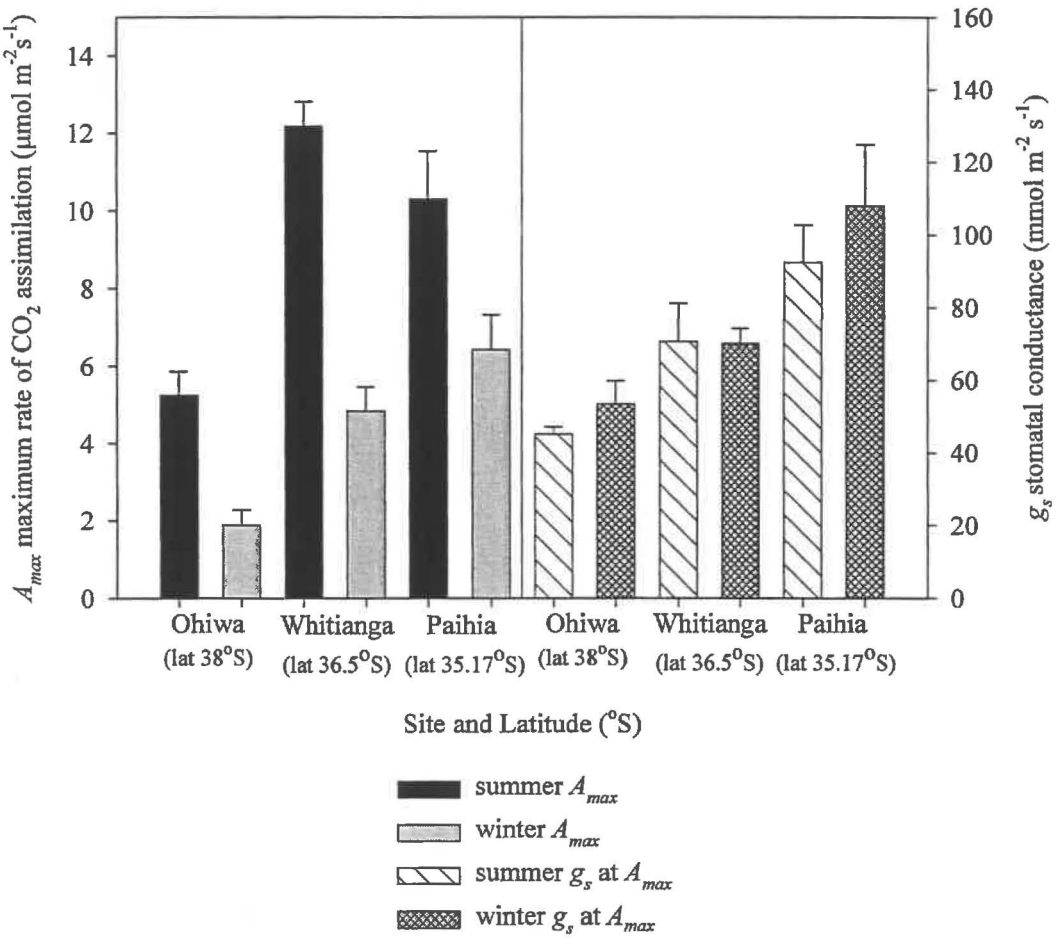

Figure 4.12 Mean daily maximal CO_2 assimilation rate, A_{max} (μmol m^{-2} s^{-1}) and stomatal conductance (g_S) at A_{max} (mmol m^{-2} s^{-1}) in the mangrove *Avicennia marina* subsp. *australasica*. Maximal rates were recorded between 0600 hr and 1800hr over 2-4 consecutive days during summer and winter at the three named field sites under natural conditions and saturating PFD (with exception of Whitianga winter; see text for explanation). Columns are mean values for 9 – 12 leaves at each site. Error bars represent + 1 SE of the mean.

4.3.11 Net daily photosynthetic income

Obvious differences in mean daily net PS income were evident between sites and between seasons at each site. During summer sampling the highest totals occurred at Whitianga harbour and the lowest at Ohiwa harbour. During winter plants at Ohiwa harbour again had the lowest daily net PS income, but the highest occurred at Paihia.

Winter income levels were lower than summer at all sites. At Paihia, the mean winter value of 96.4 mmol m^{-2} d^{-1} was about 74% of that calculated for the summer period and at Whitianga harbour the winter value of 75.6 mmol m^{-2} d^{-1} was approximately 32% of the summer mean. The difference between summer and winter values was greater at Ohiwa harbour than at the other two sites, with the winter mean of 17.4 mmol m^{-2} d^{-1} being only 14% that of the mean daily net PS income during summer sampling (Figure 4.13)

Net daily photosynthetic income was analysed using multiple regression analysis with previous-night minimum temperature and percentage of the photoperiod where PFD was greater or equal to 500 μmol m^{-2} s^{-1} used as predictors. Overall the regression relationship was significant ($F_{2, 208} = 61.4$, $p < 0.00005$), but a relatively poor fit, with the independent variables explaining slightly more than one third of the observed variation in daily net PS ($R^2_{adj} = 0.37$ However, on an individual basis (taking into account the effect of the other variables), both were significant predictors of daily net PS (PFD≥500 $t = 3.12$, $p = 0.002$, Min Temp $t = 7.04$, $p = 0.00001$,) (Table 4.5).

Table 4.4 Microclimate and mean net daily PS calculated from field measurements of leaf CO_2 gas exchange in *Avicennia marina* subsp. *australasica* in summer and winter at Paihia, Whitianga (Whit) and Ohiwa Harbours, New Zealand. % PFD is the percentage of the total photoperiod when PFD ≥ 500 μmol m^{-2} s^{-1}; Min Temp is the coldest air temperature (degrees Celsius) recorded during the night previous to measurement; Mean net PS is the mean net daily photosynthesis ± standard error (mmol m^{-2} d^{-1}) calculated for 3 or 6 leaves (n) per tree (A - D).

Site & month of sampling	% PFD > 500	Min. temp (°C)	net PS Tree A	Tree B	Tree C	Tree D	n
PAIHIA, Aug 01							
Day 1 (winter)	40.0	5.8	121.8 ± 28.1	88.9 ± 21.5	70.4 ± 9.6	-	3
Day 2	42.8	5.7	120.2 ± 6.7	96.6 ± 22.7	79.9 ± 7.5	-	3
PAIHIA, Dec 01							
Day 1 (summer)	26.7	14.8	135.7 ± 44.4	178.8 ± 14.2	104.5 ± 31.9	142.4 ± 9.0	3
Day 2	40.0	11.8	98.9 ± 24.6	169.2 ± 22.5	88.3 ± 45.7	122.9 ± 8.0	3
WHIT, Jul 01							
Day 1 (winter)	0.0	1.1	102.8 ± 19.5	74.8 ± 35.1	88.2 ± 14.6	155.3 ± 10.4	3
Day 2	0.0	0.2	62.3 ± 16.0	49.9 ± 4.5	87.9 ± 5.5	126.3 ± 6.1	3
Day 3	0.0	1.7	40.6 ± 3.9	41.8 ± 11.0	39.3 ± 4.5	37.8 ± 0.0	3
WHIT, Mar 02							
Day 1 (summer)	65.8	12.8	227.6 ± 50.3	193.1 ± 25.5	161.2 ± 5.2	-	3
Day 2	58.3	14.1	213.9 ± 43.9	254.6 ± 52.9	291.7 ± 33.1	-	3
Day 3	63.9	15.8	288.5 ± 9.0	235.2 ± 49.8	273.0 ± 71.7	-	3
OHIWA, Sep 01							
Day 1 (winter)	13.5	8.7	21.4 ± 2.7	31.4 ± 11.2	15.2 ± 3.2	15.1 ± 6.9	3
Day 2	37.8	2.7	29.3 ± 3.1	30.1 ± 5.9	23.0 ± 6.6	22.1 ± 15.2	3
Day 3	35.1	2.8	11.8 ± 3.6	17.9 ± 11.8	0.3 ± 0.2	1.1 ± 1.0	3
OHIWA, Dec 01							
Day 1 (summer)	37.5	11.5	51.2 ± 3.9	117.8 ± 11.4	125.2 ± 10.5	-	6
Day 2	59.4	11.2	95.6 ± 2.3	147.4 ± 8.6	168.5 ± 8.1	-	6

Table 4.5 Regression summary statistics for net daily PS (mmol m^{-2} d^{-1}). The independent variables are: %PFD ≥ 500 (the percentage proportion of the photoperiod when ambient PFD was equal or above 500 μmol m^{-2} s^{-1}) and minimum ambient air temperature reached during the night previous to the measurement of photosynthesis.

	Beta (standardised regression coefficient)	Partial Correlation	B (raw regression coefficient)	t (208)	p-level
N = 211					
Intercept			23.662	2.615	0.009
% PFD≥ 500	0.203	0.211	0.242	3.118	0.002
Min Temp	0.475	0.450	7.042	7.277	0.00001

Chapter Five

Chapter Five

Photosynthetic performance in *Avicennia marina* subsp. *australasica* during winter at Ohiwa Harbour, Bay of Plenty, New Zealand.

5.1 Introduction

The photosynthetic behaviour of mangroves has been widely studied in relation to a number of environmental stresses including (for the genus *Avicennia*); salinity (Ball & Farquhar, 1984b, Clough, 1984, Downton, 1982), light (Ball & Critchley, 1982, Björkman *et al.*, 1988, Kitao *et al.*, 2003) waterlogging (Naidoo *et al.*, 1997), pollution (Naidoo & Chirkoot, 2004) and nutrients (Naidoo, 1987). However, as yet there has been little focus on the physiological consequences of low temperature stress in mangrove apart from assessments of tissue death or damage by freezing (Chapman & Ronaldson, 1958, Sakai & Wardle, 1978) or chilling (Markley *et al.*, 1982, Maxwell, 2001). Not surprisingly, in view of the fact that the majority of mangrove species are tropical or subtropical in origin, the few existing studies of mangrove photosynthesis in relation to low temperatures focus on the effects of chilling, rather than freezing temperatures, e.g., Kao *et al.* (2004).

In sensitive species, low temperatures can disrupt all the major components of photosynthesis, including thykaloid electron transport, the carbon reduction cycle and the control of stomatal conductance (Allen & Ort, 2001). In severe cases these effects may be compounded by cell injuries sustained following freezing of the cell contents, leading to tissue death (necrosis) and ultimately to the partial or total loss of photosynthetic function (Levitt, 1980b, McKersie, 2003, Steponkus, 1984). In less extreme cases, a light dependent decrease and slowly reversible retardation of photosynthetic rates and photosynthetic efficiency, otherwise known as cold-induced photoinhibition, may occur following low temperature exposure (Powles, 1984). If the photoinhibited state is prolonged by ongoing stress exposure, then chronic and irreversible damage such as photo-bleaching (chlorosis) may subsequently develop (Close *et al.*, 1999, Powles, 1984). Such negative impacts compromise plant function, reducing ability to maintain an adequate carbon balance for successful growth and reproduction.

A. marina subsp. *australasica* shows inhibition of photosynthesis following overnight chilling or freezing (see Chapters 3, 4) in a manner similar to many cold-sensitive woody trees such as mango (Nir *et al.*, 1997) and *Eucalyptus* (Davidson *et al.*, 2004, King & Ball, 1998). The present work supports not only findings of previous studies indicating that it is a cold-sensitive species with a low tolerance to frost (Chapman & Ronaldson, 1958), but also suggestions that low winter temperatures may play an important role in determining the latitudinal range of this species (de Lange & de Lange, 1994).

In laboratory- or field-based experiments it is difficult to artificially reproduce the multifarious combinations of, or the diurnal and seasonal variations in, the wide range of stresses that affect plants in the natural environment. Therefore, the present study aimed to track changes in *Avicennia* leaf chlorophyll and photosynthesis under natural conditions in the field before, during and after winter. Ohiwa harbour in the Eastern Bay of Plenty of New Zealand was considered an ideal site for such a study, given that frost- and chilling-nights occur frequently here from late autumn through to early spring, and that the cold winter nights are typically followed by bright, sunny days.

Non-invasive techniques, including *in situ* measurements of leaf chlorophyll *a* fluorescence and gas-exchange and leaf chlorophyll content were used to assess changes in leaves for seven months from early autumn through winter into early spring. Measurements were carried out on two groups of leaves chosen according to their position in the canopy (i.e., exposed outer canopy leaves and protected inner-canopy leaves). It was expected that low-temperature injuries in the exposed leaves would be exacerbated by the high-light environment of the outer canopy and that the observed leaf yellowing was a symptom of photo-oxidative damage.

5.1.1 Chilling and Freezing Defined

Reference is made to both chilling and freezing air temperatures in this chapter. Freezing in this context is very simply defined as any temperature below 0°C, although this may be insufficient to cause freezing of the plant tissue. A "severe" freeze in this study was considered to be one that caused visible tissue injury in any part of the mangrove canopy; in this instance when air temperatures dropped to levels close to the measured frost tolerance limit for *Avicennia* at Ohiwa harbour; i.e., between –3.0 and –4.0°C; (see Chapter 3).

In contrast, a chilling temperature may be defined as "any temperature that is cool enough to produce injury but not cool enough to freeze the plant" (Levitt, 1980a). The point at which chilling injury occurs varies according to the temperature history of the plant, and also differs among plant species, therefore no one temperature can be regarded as a standard where chilling begins. In many chilling-sensitive species such as peanut, mango and coffee, temperatures between 0°C and 10°C are known to cause injury and compromise plant productivity, yet other more sensitive species e.g., sugar cane, incur injuries at temperatures below 15°C (Allen & Ort, 2001, Bell *et al.*, 1994, Guo & Cao, 2004, Levitt, 1980a). New Zealand *Avicennia* can also be classified as a chill-sensitive species as photosynthesis is compromised when the plants experience air temperatures below 4°C (see Chapter 6). It was therefore this temperature that was used as an arbitrary standard for the onset of "chilling" in *Avicennia* in the present study.

5.1.2 Characteristics of exposed and protected leaves in an *Avicennia* canopy

Two distinct leaf types are immediately obvious on *Avicennia* plants in many locations, but more so amongst the Ohiwa harbour and other eastern Bay of Plenty mangrove populations. Exposed leaves, occupying terminal and fully sunlit positions on the shoots, are oriented at steep angles relative to the main branch axes. They show typical sun-leaf morphology, being relatively small (between 25 – 50 mm x 10-30 mm) and thicker in cross-section than the protected leaves. Protected leaves are positioned within the canopy where incident PFD is much reduced or highly variable (e.g., sun-fleck.). They have larger dimensions (50 - 75 mm x 18-36 mm) than exposed leaves, are thinner in cross-section, and are oriented at wider angles to the main branch axes (Plate 5.1).

The steep-angled orientation typical of leaves in high-light environments diminishes the risk of photoinhibition by reducing the amount of surface area available to incoming light (Tupfers *et al.*, 1999). In addition, the near vertical position of the outer leaves allows greater light penetration through to the lower leaves, subsequently maximizing whole-canopy photosynthesis (Terashima & Hikosaka, 1995).

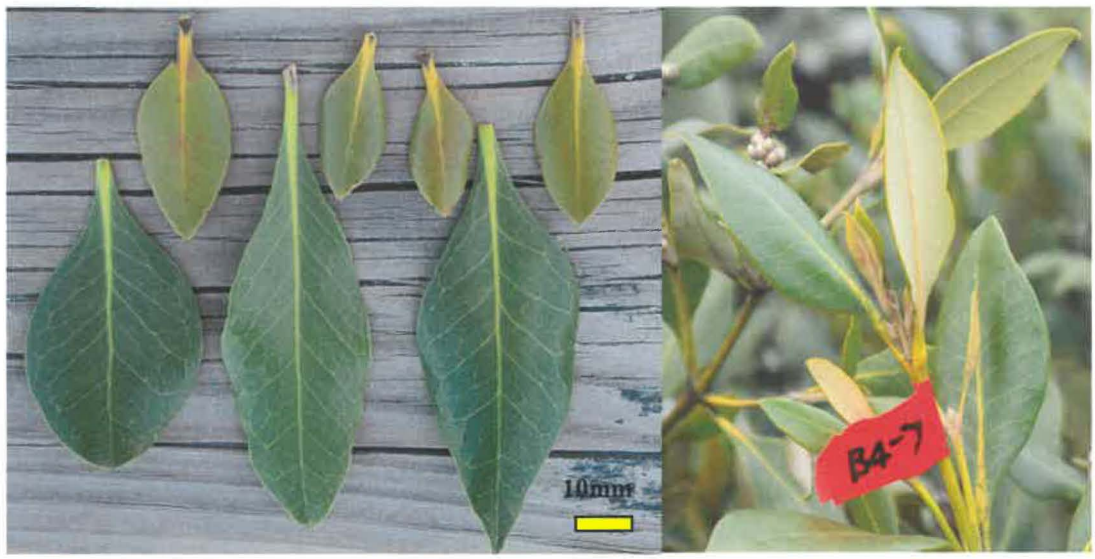

Plate 5.1 Left: Extreme forms of exposed (top) and protected (bottom) leaf forms in *Avicennia marina* subsp. *australasica*. Right: Steep-angled orientation of the exposed leaves relative to the branch axis. Photo: C. Beard (Ohiwa Harbour, December 2003).

5.1.3 Photoinhibition, Photoprotection and Photo-oxidative damage

Light, while necessary for photosynthesis, can cause damage if the absorbed light energy exceeds the ability of the light harvesting system to dissipate the energy that is not used in photosynthetic processes, or if the capacity of the carbon cycle is exceeded (Carpentier, 1997, Powles, 1984). Light damage is always a possibility in plants, because for the most part they are unable to regulate light input to their tissues. The extent of injury and the susceptibility of the organism to damage is dependent on a number of factors, both environmental (e.g., stress effects such as low temperature) and genotypic (e.g., sun or shade adaptations) in nature.

Plants however, are not entirely without protection. In some cases, structural alterations (e.g., leaf angle) may reduce the amount of light energy incident upon the photosynthetic surface and thus minimize potential for injury (Tupfers *et al.*, 1999, Werner *et al.*, 2001b). In addition, the photosynthetic apparatus itself is equipped with photo-protection mechanisms. Initially, processes such as the non-photochemical dissipation of excess energy in the form of heat (Demmig-Adams & Adams, 1992, Shang & Feierabend, 1998), or the diversion of excitation energy away from PSII by way of phosphorylation of the LHCII complex (Aro *et al.*, 1993) may protect the photosynthetic machinery. However, a problem arises when the capacity of these protective mechanisms is exceeded.

Photoinhibition occurs when the energy absorbed by the photosynthetic reaction centres exceeds the ability to use that energy in metabolic activity. It manifests in the form of photochemical inactivation (i.e., decreased photochemical activity) of photosystems II and I (PSII and PSI), and results in an overall net decrease of photosynthetic efficiency. By definition it is a broad term, encompassing both a protective (reversible) down-regulation process of the PSII reaction centres (Aro *et al.*, 1993) and a damaging (irreversible) impairment of the photosystems. If prolonged, the excess excitation energy may result in the formation of a highly reactive oxygen species that can directly damage the photosynthetic apparatus, resulting in photo-oxidative damage such as pigment loss (chlorophyll bleaching) and tissue death (Niyogi, 2000).

Exposure to high irradiances is not necessarily a prerequisite to photoinhibition. It is widely recognised that the potential for photoinhibitory damage is great even under moderate levels of PFD when present in combination with any environmental stress factor that decreases capacity to process light excitation energy (Kudoh & Sonoike, 2002, Loomis & Amthor, 1999). For instance, if the CO_2 supply is limited by stomatal closure (e.g., drought stress) or perhaps if low temperatures decrease the capacity for CO_2 reduction by suppressing the dark reactions of photosynthesis, then it is increasingly likely that PFD input will exceed the rate of use.

Ultimately, photoinhibition and photo-oxidative damage play a major role in restricting the geographic range of species (Ball *et al.*, 1991, Close *et al.*, 2000). Both influence how much solar radiation can be used by plant tissues and the efficiency with which this light energy is converted to stored chemical energy. Although the effects of photoinhibition on carbon balance and productivity have not been widely studied, they have been shown to impact potential carbon gain. Ögren and Sjostrom (1990) estimated a 10% loss to mild photoinhibition in leaves of a willow canopy and Werner *et al.* (2001a) estimated a slightly smaller loss in overall daily carbon gain of 6.1% in the canopy of the Mediterranean evergreen oak *Quercus coccifera*. Any losses in potential productivity will be exacerbated if there is a need to rebuild damaged tissues or organs.

5.2 Materials and Experimental Procedures

Two specimens of *A. marina* subsp. *australasica* were the focus of the study detailed in this chapter. The trees were both c. 1.5 m tall and occupied

similar positions on the northern edge of a one hectare mangrove forest on the harbour side of a causeway, Wainui Road, Ohiwa Harbour (Figure 2.3, Plate 2.8). A series of *in-situ* measurements of foliar chlorophyll content, net CO_2 assimilation rate, stomatal conductance and the ratio of maximum to variable fluorescence after dark adaptation (F_v/F_m) were made on a selected set of twenty leaves. Sample sets, on each of the two trees, comprised 10 leaves; 5 fully exposed and positioned in the outer canopy and 5 leaves positioned within the inner canopy. All were labelled with waterproof tape around the leaf petioles, and were measured at each sampling. Measurements were started in April 2003 and were repeated at intervals of 5-6 weeks until October 2003.

All measurements were made during low water[1] at, or close to, the same time (between 11^{30} hr and 12^{30} hr) on each sampling day. The timing of sampling was based on results of an earlier study of diurnal photosynthetic activity at the same research site (Chapter 4), and was chosen in order to sample at a point during the normal diurnal cycle when photosynthetic activity was most likely to be in the upper range for the Ohiwa plants (Figure 5.1)

5.2.1 Climate

Two StowAway Hobo TidbiT temperature loggers (Onset Computer Corporation, USA; see section 2.7.2) were attached to one of the mangrove plants; one exposed to direct sunlight in the top of the canopy, the other shaded within the canopy, and both occupying positions roughly similar to the sample leaves. Ambient air temperature was logged at 15-minute intervals and was downloaded in the field to a Hobo data shuttle or directly to a Toshiba Satellite laptop computer. Diurnal temperature data were used merely as a rough indication of the daytime temperature environment because differences of up to 6°C had been observed during summer between maximum daytime air temperatures recorded by the Hobo data logger positioned on-site in the top of the mangrove and those recorded by screened sensor at the Whakatane weather station. These disparities were most probably due to the heating effect of direct sunlight on the unscreened resin-enclosed probe; the drawbacks of which are fully discussed in section 2.7.2. The main purpose of the on-site data-loggers was to track overnight minimum air temperatures, during which time they were unaffected by radiative heating.

Only ambient air temperature was monitored on-site during this part of the study. All other data in Table 5.1 were obtained from the Whakatane airport

[1] *"Low water" in this instance does not refer to true low tide, but to tidal waters having receded fully from the mangrove site.*

automatic weather station (NIWA, 2003a), a site approximately 15 km north-west of the study area that occupies a similar coastal aspect and altitude.

5.2.2 Light

Photon flux density (PFD, μmol m^{-2} s^{-1}), incident upon Hom-me or LI-190SA Li-Cor Quantum sensors positioned above and within the mangrove canopy was monitored at the research site using a Campbell CR10-X data logger (see section 2.7.1) from September through December 2001, and from March through May 2002. On-site PFD measurements were discontinued after the data-logger was destroyed by a storm surge and subsequent salt-water immersion. As a result, the light environment during the autumn - spring period in 2003 (i.e., the period during which the work in this chapter was undertaken) was extrapolated from pyranometer measurements of mean daily global solar radiation data (MJ m^{-2}) at the Whakatane weather station (NIWA, 2003a).

A pyranometer measures radiation over a spectral range of approximately 300 – 2800 nm whereas photosynthetically active radiation in defined as solar radiation in the 400-700 nm spectral band. Given that global solar radiation is also strongly influenced by changes in clouds and aerosols in the atmosphere (Grant & Slusser, 2004), a simple conversion to PFD (the amount of photosynthetically useful light that strikes a leaf surface) is not always accurate. However, a study by Blackburn and Proctor (1983) showed that there is a strong correlation between the two parameters, and PFD on a daily basis can be calculated at approximately 47% of total solar irradiance incident upon the earth's surface. On an hourly basis this percentage can vary from 45% to 54%, depending on the amount of cloud cover present. A similar relationship was observed between solar irradiance measured at the Whakatane weather station and PFD measured at the Wainui Road research site (Figure 5.2). Although weather station measurements were not ideal for the accurate estimation of light levels because the light sensor was not located on-site, it was still possible to estimate whether the plants were subject to high or low PFD levels on a day-to-day basis. Site differences may account for the less-than-expected percentage conversion (34.3%).

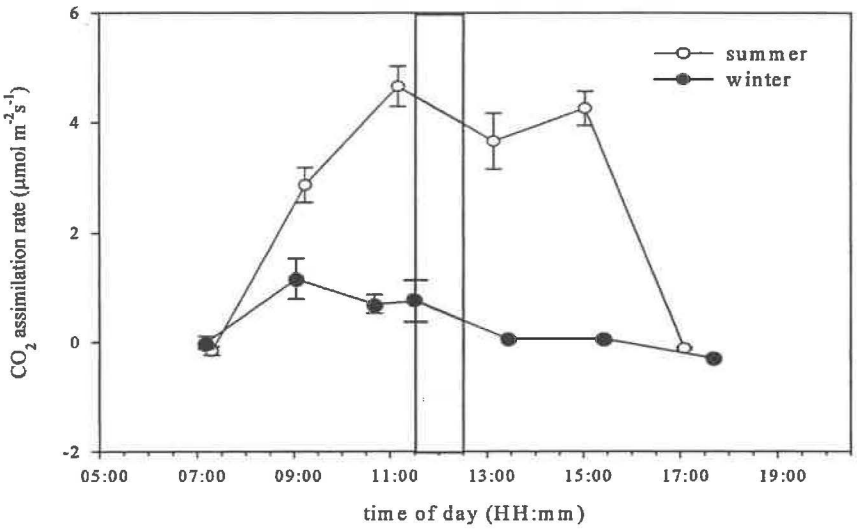

Figure 5.1 Typical diurnal patterns of the mean rate of CO_2 assimilation (± SE) in *Avicennia marina* subsp. *australasica* in summer and winter at the Wainui Road research site, Ohiwa harbour. Grey shading indicates the sampling period used for the study detailed in this chapter. N = 12 (summer), N = 9 (winter).

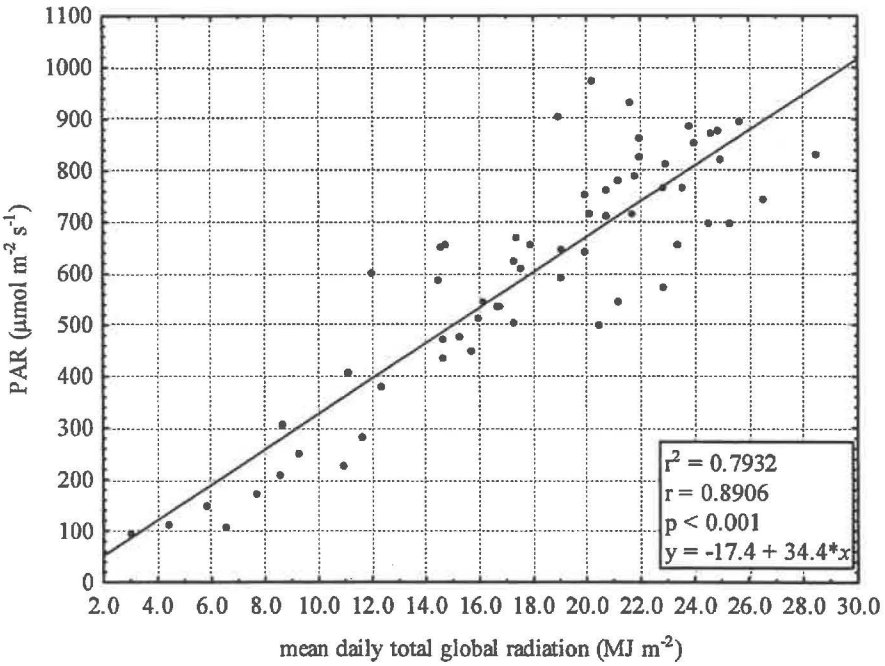

Figure 5.2 The relationship between mean daily solar radiation (MJ m^{-2}) measured at the Whakatane AWS and mean daily photosynthetically active radiation PFD (µmol m^{-2} s^{-1}) measured at the Wainui Road research site, Ohiwa harbour, October – November 2001.

5.2.3 Chlorophyll

Chlorophyll determinations were carried out *in-situ* using a SPAD-502 chlorophyll meter (Minolta Camera Co., Osaka, Japan), which allowed for a series of non-destructive measurements to be made using the same leaves (refer to

section 2.9.2 for methodology). An additional twenty leaves, comprising ten exposed and ten protected leaves, were removed from two of the study plants in August 2003 to calibrate the SPAD-502 unit values with actual chlorophyll a + b concentration as determined by absorbance of extracted pigments. These additional leaves were chosen on the basis that they were of similar size and occupied positions on the plants similar to those that remained *in-situ* for periodic measurements of chlorophyll content, fluorescence and gas exchange. The month of August was chosen as a useful sampling period to calibrate the two methods because the exposed and protected leaves were perceived to have the greatest differentiation in colour (yellow vs. green) at that time.

After removal from the tree, the leaves were placed into plastic bags with a small amount of water, and were kept cool (around 10°C) in complete darkness for approximately 12 hours until extraction. The leaves were then washed and a 10 mm diameter disc of healthy tissue was punched from the central portion of each blade, taking care to avoid main veins and damaged areas. Five SPAD-502 measurements were made on each disc and the mean values were calculated for use in subsequent analyses. Chlorophylls were then extracted following the protocol of Porra *et al.* (1989), as described in section 2.9.1).

At all other sampling times the SPAD-502 chlorophyll meter was used to make determinations of foliar chlorophyll content on the selected set of twenty attached leaves. Sampling comprised ten non-overlapping SPAD measurements on each leaf, ensuring that the sensor head was positioned over healthy tissue and avoided any major leaf veins. Mean SPAD-unit values were calculated for each leaf and were used in all subsequent statistical analyses.

5.2.3.1 Comparison of SPAD-units and extraction method

The correlation between measurements using the SPAD-502 chlorophyll meter and chlorophyll content determined by extraction did not compare well with other studies of broadleaf tree species in which leaf chlorophyll concentration had been measured with a hand-held absorbance meter (Cate & Perkins, 2003, Richardson *et al.*, 2002). These results suggest that a conversion factor should be calculated and applied to a single species rather than a broad range of species. The spread of data (Figure 5.3) also confirmed a problem highlighted by several researchers, in that the accuracy of chlorophyll estimation by chlorophyll meter decreased with increasing foliar chlorophyll content as determined by extraction.

Richardson *et al.* (2002) suggested that this effect might be due to non-uniform distribution of chlorophyll in the leaf, or to sensitivity limitations of the meter in relation to the small quantity of measurable light remaining after absorption in high-Chl leaves. On the strength of these results, the SPAD meter could not be recommended as a technique for obtaining precise estimations of foliar chlorophyll content in *A. marina* subsp *australasica*. However, given the advantages of its non-destructive measurement system, it is considered a useful method for tracking relative changes in chlorophyll content in the same leaves over longer periods of time.

The concentrations of total extracted chlorophyll and the SPAD chlorophyll meter values were found to be significantly and positively correlated (Figure 5.3: $P<0.0001$, $r^2 = 0.58$, $n = 20$).

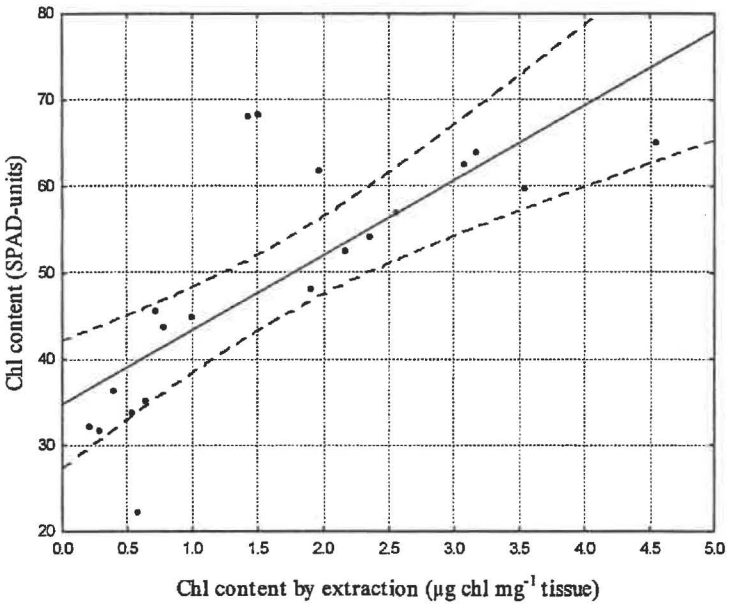

Figure 5.3 Relationship between chlorophyll content as measured by a Minolta SPAD-502 hand-held chlorophyll meter, and chlorophyll a + b content (µg Chl mg^{-1} tissue) as determined by absorbance of extracted pigments. August 2003, Ohiwa Harbour. ($P<0.0001$, $r = 0.76$, $n = 20$). Dotted lines represent the 95% confidence interval. The regression is SPAD = 34.74 + 8.65 * chl ug mg^{-1}.

5.2.4 Chlorophyll *a* Fluorescence:

Chlorophyll *a* fluorescence was measured with a portable fluorometer (Photosynthesis Yield Analyzer MiniPAM, Heinz Walz GmbH, Eiffeltrich, Germany; refer to section 2.11.6 for settings and protocols). The ratio of variable

to maximum fluorescence (F_v/F_m) in dark-adapted leaves was determined after 15 minutes acclimatisation within a dark leaf clip (Walz, DLC-8). Chlorophyll fluorescence parameters were calculated according to Schreiber *et al.* (1987).

5.2.5 Gas exchange

CO_2 assimilation rate (A) and stomatal conductance (g) were determined from a single measurement on each leaf using a CIRAS-1 portable photosynthesis system and Parkinson Leaf cuvette (PP-Systems, United Kingdom; refer to section 2.10 for methodology and protocols). During all measurements PFD inside the cuvette was maintained at 1200 μmol m^{-2} s^{-1} using a halogen light source powered by a 12V car battery. Data for May 2003 are missing due to the failure of equipment following a Supervisor's unexpected loss of equilibrium in muddy substrate.

5.3 Results:

5.3.1 General climate at Ohiwa Harbour April – October 2003

A summary of selected climate parameters at and near the study area over the seven month sampling period is given in Table 5.1.

5.3.1.1 Rainfall

Well below average winter rainfall was a feature of the Bay of Plenty region in 2003 (NIWA, 2003b). This was reflected in the rainfall figures for Whakatane where monthly totals reached a minimum in July with 3.98 mm and were at maximum in October with 20.42 mm (Table 5.1). The lowest number of rain-days per month occurred during April and July (8 and 9 days respectively), and the highest occurred in September (19 days).

5.3.1.2 Temperature

The warmest month was April with an average daily maximum air temperature of 20.2°C and average daily minimum of 9.6°C. The coldest month was July, with an average daily maximum air temperature of 13.8°C and a very low average daily minimum of 2.5°C.

A greater than average number of frosts occurred in many parts of the North Island of New Zealand during winter 2003 (NIWA, 2003b), and July in particular was unusually cold. At the research site there was a high incidence of

both chilling-nights (ambient air temperature between 0 and 4°C) and frost-nights (ambient air temperature below 0°C) followed by clear sunny days. In total, 17 frost nights and 52 chilling nights occurred there between April and October 2003, with the first chill occurring in April and the first frost in May. In July alone, on-site average air temperatures below 4°C were recorded on a total of 23 nights (Table 5.1). The overall lowest minimum air temperature in the mangrove stand (-3.38°C), also occurred during July.

Chill-night frequency was lowest at the study site in April and October with air temperatures dropping below 4°C for only 2 nights in both months. The highest number (13) occurred in August. Frost nights were less frequent, peaking in July with 11 and none occurring in April or September. One final frost occurred in early October (Table 5.1).

Table 5.1 Climate summary for the Wainui Road study area, Ohiwa Harbour (Latitude 37°59'S, Longitude 177°03'E) from April 2003 to October 2003. Lowest minimum air temperature (°C), number of frost nights (air temp <0°C), number of chill nights (air temp >0°C and <4°C) were recorded on-site (*data measured by external canopy sensor). Mean daily maximum and mean daily minimum temperatures (°C), percent relative humidity, total monthly rainfall (mm) and mean daily global radiation (MJ m^{-2}), were measured at Whakatane airport (WH) located at Latitude 37°56'S, Longitude 176°54'E.

Month (2003)	Lowest minimum air temp on-site (°C)*	Number of frost nights on-site <0°C*	Number of chill nights on-site 0<°C<4*	Mean daily maximum air temp (WH) (°C)	Mean daily minimum air temp (WH) (°C)	Total monthly rainfall (WH) (mm)	Mean daily global radiation (WH) (MJ m^{-2}),
APR	2.20	0	2	20.2	9.6	8.24	12.5
MAY	-0.74	1	9	17.9	7.2	9.36	9.0
JUN	-1.07	2	9	16.1	6.2	20.24	6.9
JUL	-3.38	11	12	13.8	2.5	3.98	8.3
AUG	-1.23	2	13	15.4	4.8	5.42	10.5
SEP	0.50	0	5	17.2	8.5	9.56	13.6
OCT	-1.56	1	2	17.6	8.5	20.42	18.5

5.3.1.3 Global solar radiation

Average daily global solar radiation measured at Whakatane was highest during the month of October at 18.5 MJ m^{-2}, and lowest in June at 6.9 MJ m^{-2}

Table 5.1). In July, the month when frosts were most frequent, the average daily value was 8.3 MJ m^{-2}, with the highest daily radiation levels that month (between 10.8 and 11.3 MJ m^{-2}) occurring on the days following some of the most severe night frosts (NIWA, 2003a).

5.3.2 Microclimate at the study site

5.3.2.1 Temperature

The temperature environments of the upper exposed part of the mangrove canopy and the inner protected parts were very different. Chilling and frost severity, duration and frequency were all noticeably greater in the exposed outer-canopy leaf environment (Figure 5.5). The lowest minimum temperatures consistently occurred in the exposed positions at the top of the mangrove canopy (approximately 1.5 m from substrate level) and, during a frost event, were between 0.6°C and 1.7°C lower than those recorded in the protected inner-canopy position. For example, on the night of 07 July 2003, minimum air temperature in the exposed position dropped to -3.38°C. However, the lowest inner-canopy air temperature measured over the same time period was slightly warmer at -2.28°C.

Plate 5.2 Frost damage in the top-tier of the short mangrove canopy at Ohiwa Harbour, July-August 2003. Left: general canopy damage (browned and wilting leaves) Right: leafless branchlets and shrivelled propagules after frost. (photo: C.Beard, August 2003)

Overall, frost duration was highly variable, with air temperatures during any one event remaining below 0°C for between 30 minutes and 11.6 hours (top canopy) and from 70 minutes up to 9.8 hours (inner canopy). Although warming

was typically slower in the protected canopy position, air temperatures in the exposed position generally remained lower for longer. In the example above, sub-zero conditions persisted for 2 hours and 3.5 minutes longer in the exposed position than they did inside the canopy. Frosts with the longest duration coincided with the lowest minimum air temperatures (Figure 5.5). Sub-zero conditions were also less commonplace in the protected inner-canopy position. Of the 17 frost nights recorded by the exposed sensor at the top of the canopy, only 8 occurred inside the shelter of the canopy (Figure 5.5).

Temperature disparities between exposed and inner canopy positions may partly explain the patterns of visible frost damage observed on the plants. After a week of recurrent severe night frosts at the research site in July 2003, a large proportion of the leaves, branchlets and developing propagules positioned in the top 100 to 250 mm of the mangrove crowns displayed chronic tissue damage and wilting (Plate 5.2). Within several days the tissues had dried out and shrivelled considerably, and by October, most of these damaged parts had dropped off the plants. In contrast, the leaves within the canopy remained visibly undamaged and attached to the plant.

5.3.2.2 Photon Flux Density

Outer-canopy exposed leaves were subject to very different light regimes than the inner protected leaves. During an earlier study (see Chapter 4), the mean difference in incident daily PFD between the exposed light sensor, positioned outside the canopy, and the inner-canopy light sensor, was approximately 582 μmol m^{-2} s^{-1}.

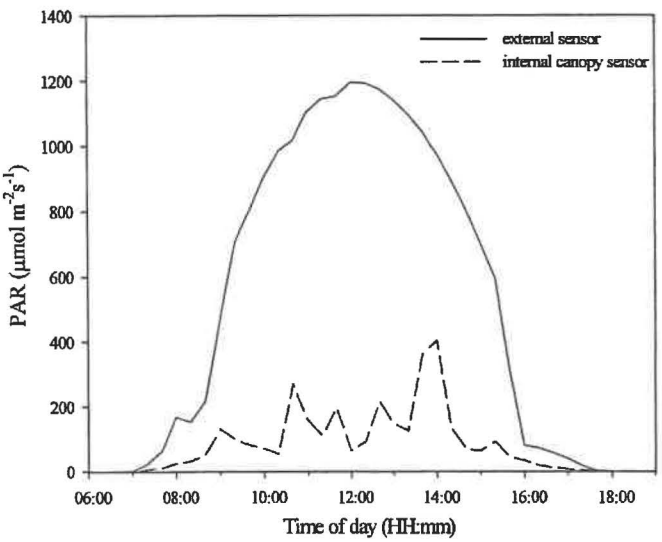

Figure 5.4 Example of diurnal variation in PFD in an *Avicennia* stand on a clear day at Ohiwa Harbour, May 2002. Lines are PFD (μmol m^{-2} s^{-1}) at the exposed top of the canopy (1.5 m above substrate) and within the canopy (600 mm above substrate). LAI = 3.0. Data are mean PFD, calculated every 20 minutes from measurements taken at 10 second intervals.

PFD reaching the inner canopy sensor was also highly variable due to leaf shading and sun-fleck. Figure 5.4 illustrates the typical diurnal variation in PFD received by the two sensors during the course of a clear autumn day at the study site.

Table 5.2 Ambient air temperatures (°C) and global radiation (MJ m^{-2}) during April – October 2003 at the Wainui Road research site, Ohiwa Harbour and the Whakatane weather station. Overnight minima were measured on-site amongst *A. marina* subsp. *australasica* leaves (exposed position only), during the 3 days preceding, and the day of, measurement** of chlorophyll content, fluorescence and gas exchange. *Data recorded at the Whakatane weather station (daytime ambient air temperature (°C) data are measured by screened sensor).

Month/date (2003)	Daytime Maximum* (°C)	Overnight Minimum (°C)	Overnight maximum (°C)	Global radiation* (MJ m^{-2})
APRIL '03				
09	20.1	8.2	11.9	14.5
10	21.5	8.6	11.4	14.3
11	19.9	7.0	23.6	17.0
12**	19.9			16.2
MAY '03				
21	19.5	17.2	17.9	2.8
22	19.9	8.2	12.7	6.9
23	18.2	8.1	11.8	10.5
24**	17.4			6.8
JUNE '03				
08	16.9	7.7	12.7	8.6
09	17.5	7.9	13.8	8.2
10	15.8	5.3	10.7	8.9
11**	14.5			8.2
JULY '03				
20	12.8	5.0	3.7	10.8
21	13.4	-2.4	1.5	10.8
22	14.0	-2.7	1.3	10.9
23**	14.8			10.0
AUGUST '03				
26	14.9	4.8	7.7	14.4
27	15.2	7.1	10.8	7.1
28	15.8	4.5	7.7	14.0
29**	16.8			11.6
OCTOBER '03				
05	16.0	-1.6	6.0	18.1
06	13.9	0.1	4.3	23.9
07	14.6	4.6	8.4	23.6
08**	15.6			20.3

5.3.3 Chilling and Freezing in the light

The plants were, for the most part, exposed to chilling- and sub-zero temperatures during darkness. However, because most cold nights were followed by clear mornings and because low air temperatures often persisted for up to two hours after sunrise, many plants were subjected to the additional stress of moderate to high PFD levels while their tissue temperatures remained chilled or frozen.

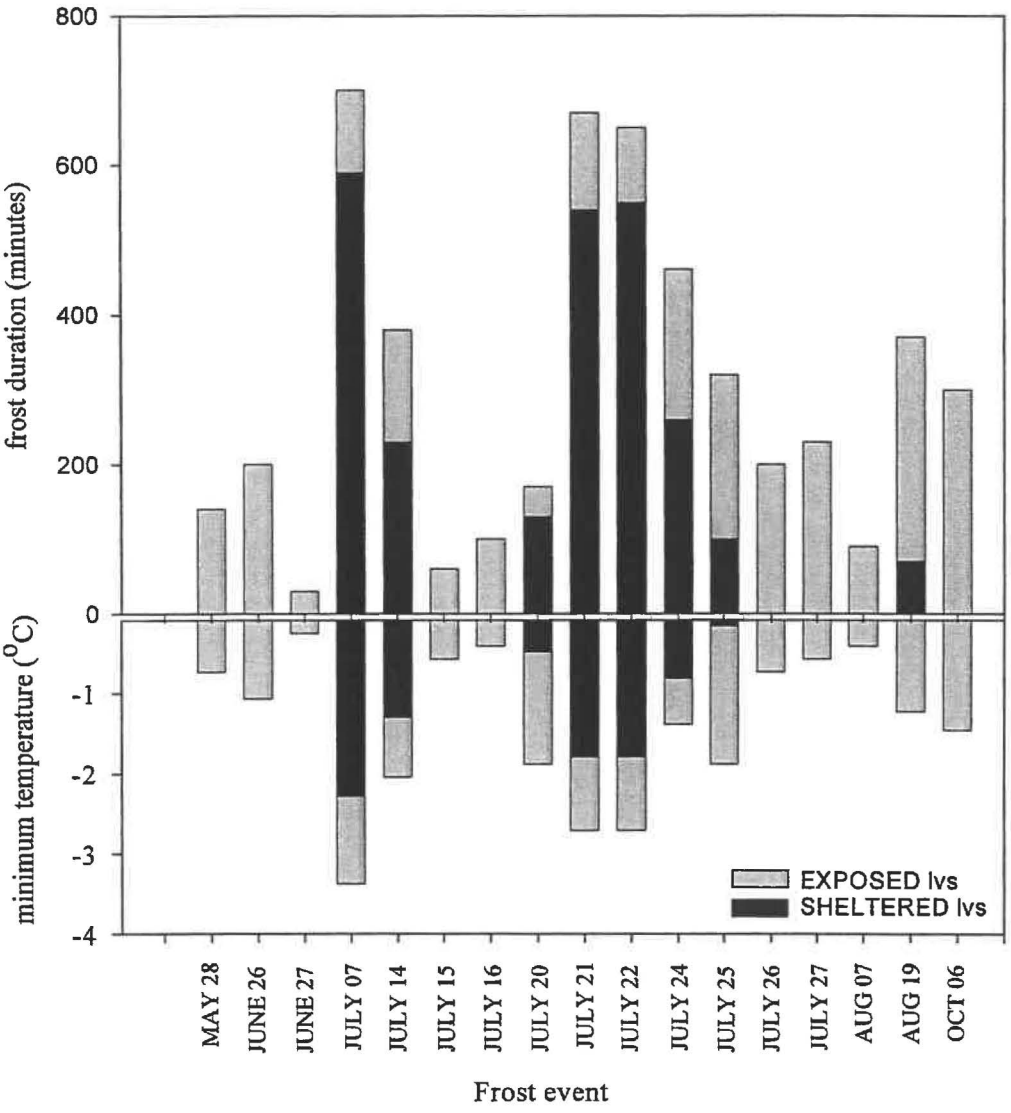

Figure 5.5 The frequency and duration of frost, and the lowest recorded minimum air temperatures during each frost event in the positions of exposed leaf (light grey bars on graph) and protected leaf (black bars on graph) at the Wainui Road site, Ohiwa Harbour, May – October, 2003. Data were obtained on-site using Hobo StowAway TidbiT temperature loggers (Onset Computer Corporation, U.S.A.).

Using standard New Zealand sunrise times (RASNZ, 2005) as a rough guide, the average time that the air temperature remained below 0°C after sunrise (following a frost-night) during this study was about 15 minutes. Air temperatures between 0 and 4°C prevailed for an average duration of 23 minutes after sunrise. Although the average duration of light-exposure at low temperature was relatively brief, in extreme cases these conditions persisted for several hours. The estimated maximum time of light exposure upon parts of the outer canopy (from sunrise, excluding pre-sunrise daylight) during this study was around 100 minutes in sub-zero air temperatures, up to 120 minutes below 4°C and up to 4 hours at temperatures below 10°C.

The combined stresses of light and low temperature had a greater impact on the outer canopy leaves because the inner canopy received very low incident light over much of a daily cycle, as shown by the example in Figure 5.4.

5.3.4 Variation in leaf chlorophyll content over a 7-month period

Over the course of the seven-month sampling period, chlorophyll content in the exposed leaves was consistently lower relative to that in protected leaves. The values were most similar in the two leaf types at the beginning of sampling in April when the mean chlorophyll content of the exposed-leaves was 48.96 SPAD-units and the mean for protected-leaves at 56.70 SPAD-units. According to the correlation realised in Figure 5.3 these values correspond respectively to 1.64 mg chl mg^{-1} and 2.5 mg chl mg^{-1} of leaf tissue.

In the exposed leaves chlorophyll values remained relatively constant from April to June, and then decreased noticeably in July and August following a period of frequent night frosts and sunny days. At the onset of spring in October, chlorophyll content again increased slightly. Maximum chlorophyll was present in the exposed leaves in June with a mean (± standard error) of 49.65 ± 1.36 SPAD-units and was lowest in August with a mean of 37.28 ± 2.42 SPAD-units; equivalent to 1.72 mg chl mg^{-1} and 0.29 mg chl mg^{-1} of leaf tissue respectively (Figure 5.6). Over the total study period, mean chlorophyll content of the exposed leaves varied by approximately 12 SPAD-units.

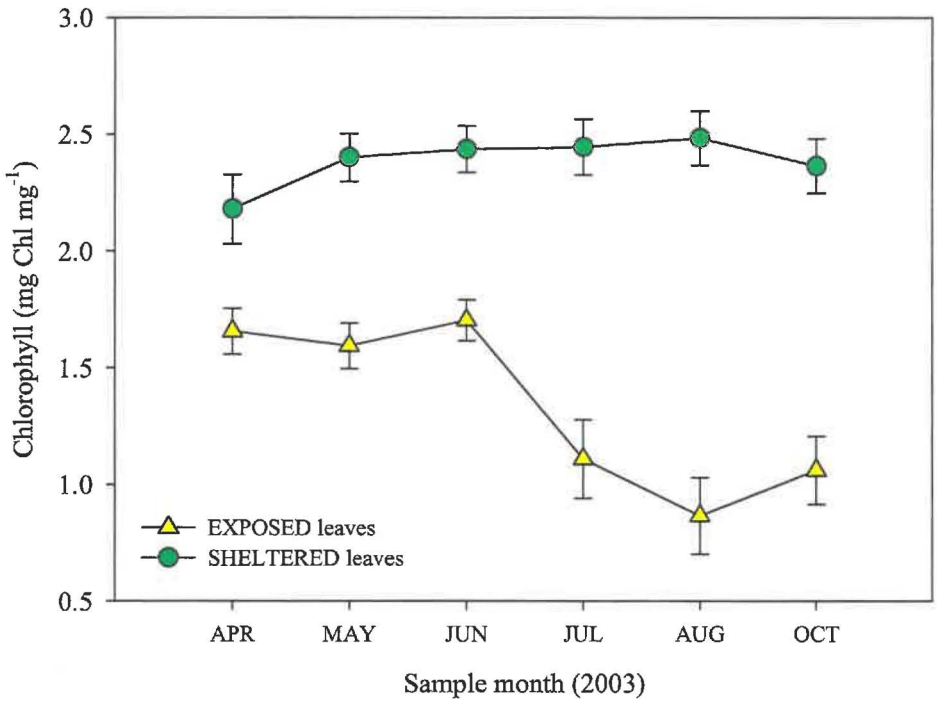

Figure 5.6 Variations in the foliar chlorophyll content of exposed and protected leaves of *Avicennia marina* subsp. *australasica* at Wainui Road research site, Ohiwa Harbour. April 2003 to October 2003. Data points are mean values ± standard error. N = 50. Measurements were made between April 2003 and October 2003 at approximately 5 – 6 week intervals.

In comparison, chlorophyll content in the protected leaves was relatively stable over the entire sampling period, varying by only 3 SPAD-units. The maximum was reached in July with a mean of 60.64 ± 1.76 SPAD-units. The lowest content occurred in April with a mean of 56.70 ± 2.02 SPAD-units; SPAD values equated to 2.99 mg chl mg^{-1} and 2.54 mg chl mg^{-1} of leaf tissue respectively (Figure 5.6).

5.3.5 Chlorophyll Fluorescence of PSII

Maximal quantum yield following dark incubation (F_v/F_m) was not only different between exposed and protected leaves throughout this study, but it also varied considerably in the individual leaf types during this time. In April, the mean (± standard error) protected-leaf F_v/F_m was 0.796 ± 0.006 and the mean

exposed-leaf F_v/F_m was 0.719 ± 0.015 (Figure 5.7). Given that values between 0.80 and 0.83 in protected-leaves and around 0.80 in exposed-leaves are regarded as normal for healthy tissues (Critchley, 2000), and that values similar to these had previously been measured on leaves of the same plants in an earlier study (see chapter 4), it appears that some PSII stress was already evident in these leaves at the beginning of the study period.

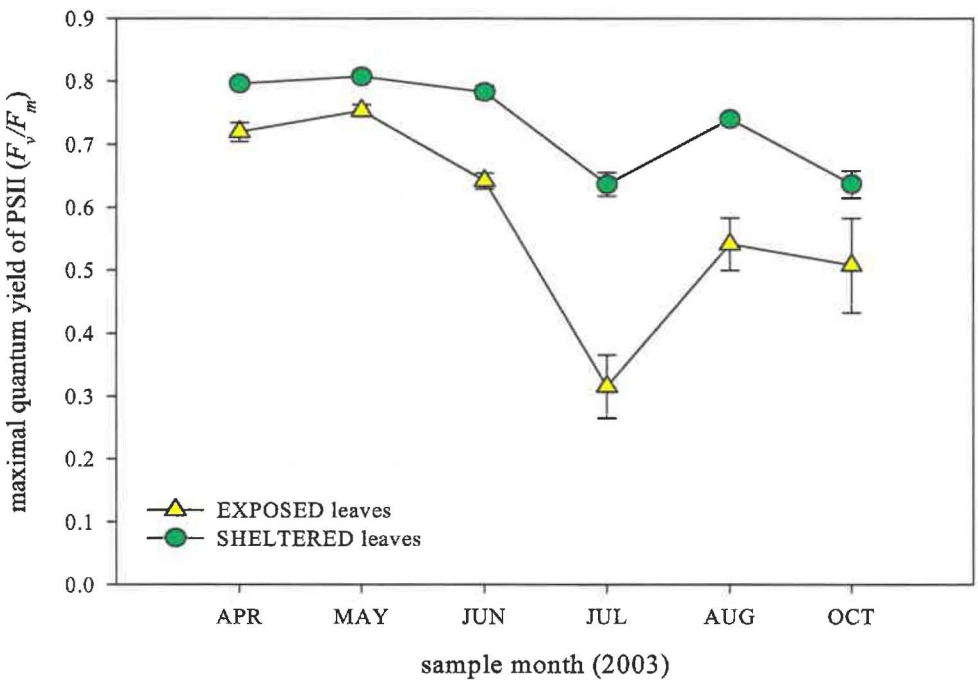

Figure 5.7 Variation in mean maximal quantum efficiency of PSII (the ratio of variable to maximal chlorophyll fluorescence, *Fv/Fm*), in exposed and protected leaves of *Avicennia marina* subsp *australasica* after 15 minutes dark adaptation. Measurements were made the Wainui Road research site, Ohiwa Harbour between April 2003 and October 2003 at approximately 5 – 6 week intervals. Values are the mean of 10 samples ± SE.

By May, F_v/F_m had increased slightly in both leaf types, but these values decreased in June and again in July when they dropped to the lowest values measured during this study. F_v/F_m values in exposed- and protected-leaves at this time were respectively 0.315 ± 0.050 and 0.636 ± 0.019. A partial recovery was evident in August and October, when F_v/F_m increased to 0.508 ± 0.075 in the exposed-leaves and 0.637 ± 0.022 in the protected-leaves. Over the entire 7

months, F_v/F_m values for the exposed-leaves remained consistently lower than those measured in protected-leaves.

5.3.6 Gas exchange and stomatal conductance

Gas exchange was measured under saturating light (approximately 1200 µmol m^{-2} s^{-1}) in order to define a mean of maximal net photosynthetic capacity. Although net rates of photosynthetic CO_2 uptake in both leaf types were very similar over the seven-month sampling period, overall variation was large; with mean maximal rates ranging from around 8.0 µmol m^{-2} s^{-1} in April to zero net CO_2 uptake in August (Figure 5.8).

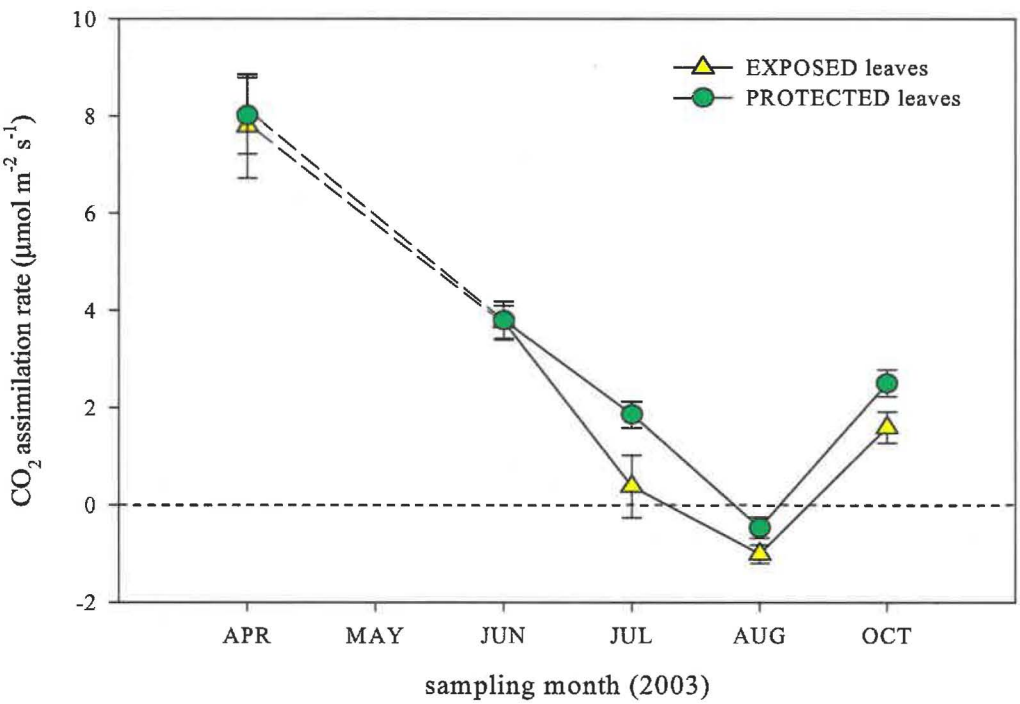

Figure 5.8 Variation in the mean CO_2 assimilation rate (µmol m^{-2} s^{-1}) in exposed and protected leaves of *Avicennia marina* subsp *australasica* at the Wainui Road research site, Ohiwa Harbour. Measurements were made between April 2003 and October 2003 at approximately 5 – 6 week intervals (with the exception of a 60 day interval between April and June 2003 due to equipment failure). Values are the mean of 10 samples ± SE.

Net photosynthesis and stomatal conductance were both at maxima in April, with values respectively (± standard error of the mean), for exposed leaves at 7.79 ± 1.07 µmol m^{-2} s^{-1} and 111.3 ± 7.9 mmol m^{-2} s^{-1} and for protected leaves at

8.01 ± 0.79 μmol m^{-2} s^{-1} and 113.2 ± 7.3 mmol m^{-2} s^{-1}. Decreasing values were then observed each month until the August sampling. In August, all leaves both exposed and protected, showed negative net photosynthesis, i.e., they were respiring. Exposed leaves had a mean net CO_2 assimilation rate at this time of -1.01 ± 0.19 μmol m^{-2} s^{-1} and stomatal conductance was 21.2 ± 0.8 mmol m^{-2} s^{-1}. Corresponding values in protected-leaves were -0.47 ± 0.22 μmol m^{-2} s^{-1} and 29.3 ± 1.7 mmol m^{-2} s^{-1}. In October, the mean net rates of photosynthesis in both leaf types had increased, but only to approximately half the levels recorded in April. Stomatal conductance values for both leaf types remained low (< 40 mmol m^{-2} s^{-1}) for the remainder of the study period (Figure 5.9).

Ambient carbon dioxide concentration (C*a*) may change between measurements therefore the ratio of internal and ambient carbon dioxide concentration (C*i*/C*a*) was used to indicate carboxylation inside the leaf. If carboxylation function had been damaged by low temperature stress, internal CO_2 concentration (C*i*) should rise and the ratio increase. Conversely, if stomatal function was affected such that closure occurred but carboxylation was unaffected, then the C*i*/C*a* ratio should decrease.

C*i*/C*a* ratios were about normal (0.7) in April – May and October, but increased during winter (Figure 5.10). Highest ratios coincided with the coldest months of winter (July –August).

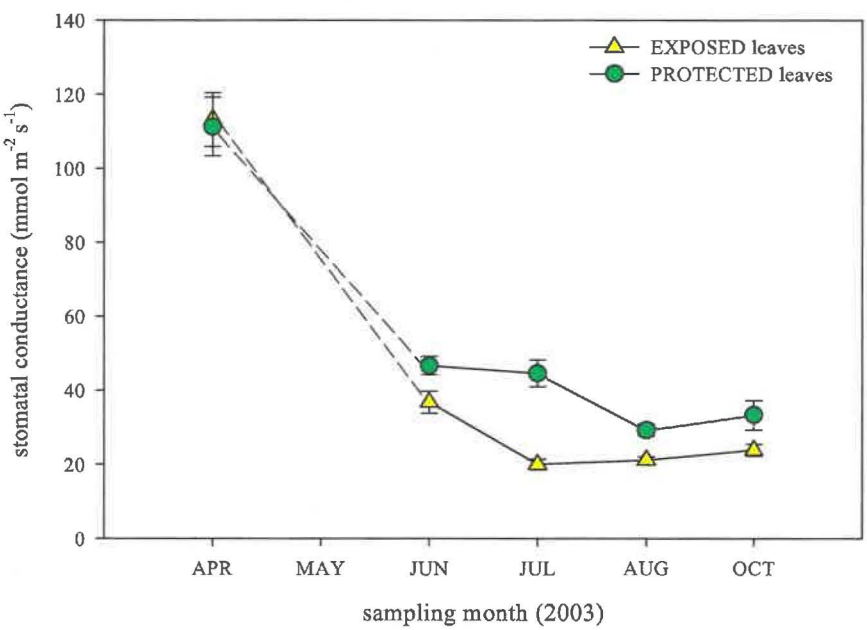

Figure 5.9 Variation in stomatal conductance (mmol m^{-2} s^{-1}) in exposed and protected leaves of *Avicennia marina* subsp. *australasica* at the Wainui Road research site, Ohiwa Harbour. Measurements were made between April 2003 and October 2003 at approximately 5 – 6 week intervals. Values are the mean of 10 samples ± SE

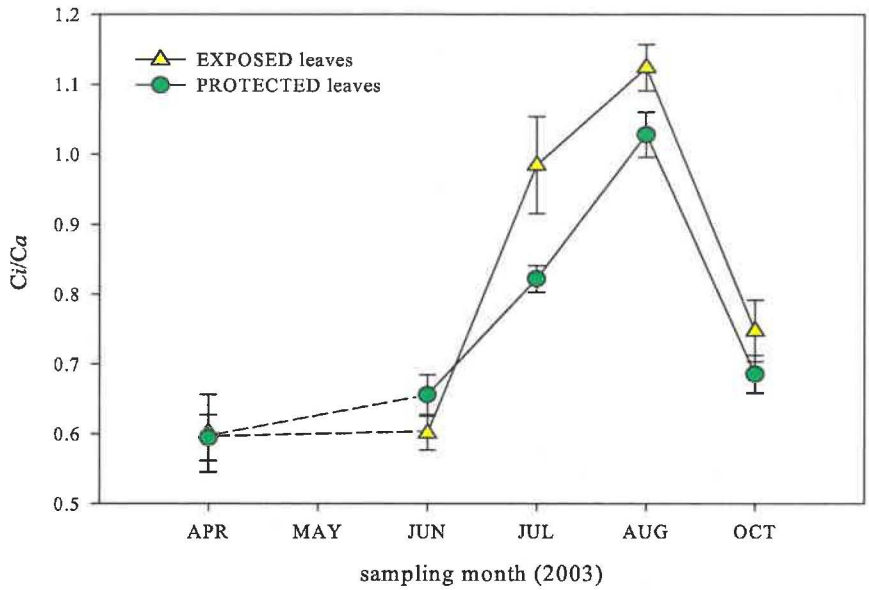

Figure 5.10 The ratio of internal CO_2 (*Ci*) to ambient CO_2 (*Ca*) concentrations (μmol mol^{-1}) in exposed and protected leaves of *Avicennia marina* subsp. *australasica* at the Wainui Road research site, Ohiwa Harbour. Sampling was carried out at intervals of approximately 5 – 6 weeks between April 2003 and October 2003. Values are the mean of 10 samples ± SE

5.4 Discussion

The main objectives of this study were to measure winter photosynthetic rates and damage extent in leaves of *Avicennia* growing near their southern geographical limit in New Zealand, and to also evaluate these results in relation to cold night temperatures and leaf canopy position (i.e., exposed vs. protected leaves). Winter 2003 at Ohiwa harbour proved to be the ideal time and location for addressing these objectives as a number of severe frosts and frequent chilling nights occurred there during the study period.

Many leaves showed visible structural injuries during the coldest months and, although the damage was worse in the leaves and organs exposed at the top of the mangrove plants, there was evidence of functional impairment in all leaves, regardless of their position in the canopy. Both exposed and protected leaves showed severe depressions of net photosynthesis and stomatal conductance after periods of chilling and frosts. However, the high-light and slightly colder temperature regime of the exposed-leaf environment resulted in prolonged photoinhibition, photo-oxidative damage and significant chlorophyll losses in these leaves over winter.

Visible structural injuries, such as wilting and development of necrotic tissue in leaves and other organs, were typical of those observed in chilling- or frost-sensitive species after exposure to critically low temperatures (e.g., during a severe[1] frost at Ohiwa harbour). Damage of this nature generally occurs when cell membrane structures are irreversibly altered during a freeze-thaw cycle (Levitt, 1980b), and usually follows several days after exposure. The result is the eventual loss of many of the damaged organs; including leaves, branchlets, flowers and developing propagules. Frost damage followed this sequence at Ohiwa harbour, but most of the structural damage was confined to the exposed parts. The question of why visible injuries were more prevalent amongst leaves that occupied exposed positions can be answered by closer examination of the temperature microclimate above and within the mangrove canopy. Sub-zero and chilling temperature conditions persisted for longer and critical low temperature minima occurred more frequently in exposed positions than they did inside the canopy. Not surprisingly, most of the serious damage was confined to terminal leaves and branches along the exposed edges and upper canopy of the mangrove stand. This pattern of frost damage was similar to that seen in other studies of woody trees; including mango in Bet-Dagan, Israel (Nir, 1997).

However, structural cell damage was not the only consequence of exposure to cold winter temperatures. Functional impairments were evident in all sampled leaves, including those that displayed little or no visible injuries. During the coldest months of the study (June – August), rates of CO_2 assimilation and stomatal conductance measured under saturating light were significantly depressed, and chlorophyll *a* fluorescence parameters indicated severe reductions in PSII efficiency. In the absence of a series of diurnal measurements, it is unclear whether the low values were a manifestation of cumulative damage sustained during the days or weeks prior to measurement, or, whether they were responses only to the environmental conditions prevalent at the time of measurement. The former is probably the case where lethal cold damage has not occurred, because several days under favourable conditions may be required before recovery of pre-stressed rates of CO_2 uptake can be achieved, e.g., photosynthetic recovery following chilling in coffee (Bauer *et al.*, 1985) and *Eucalyptus* (Davidson *et al.*, 2004).

Rates of net photosynthesis in exposed and protected leaves were significantly and equally depressed during the coldest months June – October,

[1] *The mangroves at Ohiwa harbour have a frost tolerance limit between -3.0 to -4.8°C (see chapter frost tolerance) therefore it is reasonable to assume that if overnight temperatures fell within this range the frost was 'severe']*

when all measurement days were immediately preceded by night-time air temperature minima below 8°C (Table 5.2). Marked increases in C*i*/C*a* ratios and low stomatal conductance values were measured during this period (Figures 5.9, 5.10). Although stomatal conductance also declined, the rise in *Ci* signals that photosynthesis was limited by carboxylation efficiency; a typical stress response of warm climate plants to chilling (Allen & Ort, 2001).

While leaf position in the canopy and therefore the light climate had little apparent influence in terms of leaf CO_2 uptake and stomatal behaviour, this was not the case in relation to PSII function. Exposed leaves exhibited significantly greater deterioration in optimal quantum efficiency of PSII during the study period than the protected leaves, suggesting that photoinhibition was more severe in the exposed leaves. This was not unexpected, given that the plants were growing in a high-light environment and that the exposed leaves were subject to consistently higher light doses than protected leaves (Figure 5.2), leaving the photosynthetic machinery particularly vulnerable to photoinhibition (Ball & Farquhar, 1984a, Björkman *et al.,* 1988, Clough & Sim, 1989, Kitao *et al.*, 2003). Moreover, when environmental conditions do not promote carbon fixation, the risk of photoinhibition and photodamage is exacerbated (Allen *et al.*, 2000). In sub-optimal conditions, leaf capacity to utilize incident PFD is reduced, so even moderate quantities of light may be enough to induce photoinhibitory damage, particularly if the stresses are prolonged (Govindachary *et al.*, 2004, Kudoh & Sonoike, 2002, Werner *et al.*, 2001a).

Low temperature stress resulted in impaired CO_2 uptake ability in both exposed and protected leaf types, but the exposed leaves were further stressed by up to four hours of moderate to high light exposure on mornings following frost-nights. Consequently the exposed leaves developed symptoms of chronic photoinhibition. Given that the occurrence and severity of photoinhibition are determined by light dosage (Werner *et al.*, 2001a) and also by the temperature of the preceding night (Allen & Ort, 2001, Nir *et al.*, 1997), F_v/F_m values for exposed leaves in this study can be directly related to the coincidence between frost occurrence and fluorescence measurement, the frequency of frost and chilling nights preceding measurement, and also whether the sampling day was fine or overcast.

All sampling days, except May (which was marked by continuous high cloud cover), were fine and sunny. In addition, night temperatures between 8.0

and 0.0°C preceded all of the sampling days except July when overnight temperatures dropped below 0°C on the two nights prior to sampling (Table 5.2). In response, the most notable decreases in F_v/F_m occurred in both the exposed and protected leaves in July (Figure 5.7). This was almost certainly influenced by frost severity and frequency during that part of the study period.

Repetitive cycles of chilly nights-sunny days, such as were characteristic of the June – August period at the Ohiwa mangrove site, enhance the possibility of chronic photoinhibition and photo-oxidative damage in the tissues because the stresses are not only prolonged under these conditions, but their effects are also gradually cumulative (Nir *et al.*, 1997). During the three weeks prior to the July measurement there were 7 frost-nights; the coldest on-site temperatures occurred during one of them, and two others (-2.7 °C and -2.4 °C) occurred on the two nights immediately prior to the July fluorescence measurements. Correspondingly, the weather during this time was colder, sunnier, drier, and frostier than average (NIWA, 2003), placing the plants under severe photoinhibitory stress.

Interestingly, F_v/F_m values for inner-canopy protected leaves did not show any serious decline until the July measurement period (Figure 5.7). On July 07, many of the exposed leaves and branchlets in the upper 150 mm of canopy were damaged by a severe frost (-3.38°C) and by the time the measurements were made on July 23 many of these had fallen off the plants. The resulting decline in protected-leaf F_v/F_m in July is probably indicative of increased light penetration into the canopy and increased photoinhibition of shade-acclimated leaves subsequent to leaf-drop. As Kitao *et al.* (2003) pointed out in reference to the mangrove *Xylocarpus granatum*; the outer leaves play a role in attenuating light intensity to the inner canopy, thereby protecting the inner leaves from photoinhibition. If this outer layer is removed, as it was in the Ohiwa plants, not only do light levels within the canopy increase, but loss of the protective buffer of outer branches and leaves also allows the temperature microclimate to be altered, thus increasing inner-leaf susceptibility to both light and temperature stress.

Deterioration of F_v/F_m was evident in both exposed and protected leaves at Ohiwa harbour over winter, however, only the exposed leaves developed symptoms consistent with photo-oxidative damage, i.e., the light and O_2-dependent degradation of photosynthetic pigments that typically develops after periods of prolonged photoinhibition (Wise & Naylor, 1987). This is not

surprising given that photo-oxidative damage is more severe in foliage exposed to direct sunlight (Treshow, 1970) and is enhanced by stress conditions such as exposure to chilling and freezing temperatures (Foyer *et al.*, 1994, Haldimann, 1998, Nicotra *et al.*, 2003, Wise & Naylor, 1987). In addition, high light levels are not necessarily a requirement for photo-oxidative damage to occur. Recent studies using chill-sensitive species such as cucumber, have shown that photoinhibition and subsequent photodamage can also develop under moderate light (Govindachary *et al.*, 2004, Kudoh & Sonoike, 2002).

Bearing in mind that F_v/F_m values (widely used as an indicator of photoinhibition (e.g., Lamontagne (2000) and Sonoike (1999)) of 0.8 or just below are considered typical for healthy sun-exposed leaves (Critchley, 2000), those around 0.72 obtained at the beginning of this study in April indicated that exposed leaves already showed some evidence of photoinhibition at this time. However a mildly photoinhibited state was not considered unusual for the *Avicennia* leaves at this site since earlier work there had revealed that exposed-leaves had consistently lower F_v/F_m values than protected leaves (Chapter 4). These differences are also consistent with depressions of F_v/F_m in sunlit leaves compared with shaded leaves in *A. marina* and *Aegiceras corniculatum* canopies. During the coldest months when frosts and chilling nights were frequent the severity of photoinhibitory effects increased (Björkman *et al.*, 1988).

By mid- to late-winter (July-August), after a period of severe frosts and frequent chilling nights, the total chlorophyll content of the sun-exposed leaves had reduced to 76% of the levels first measured in April, while the protected leaf chlorophyll remained relatively unchanged (Figure 5.6). This sequence is similar in other cold sensitive woody species where photoinhibition, driven by the combination of low temperature and high light, results in chlorosis of exposed leaves. For example, visible yellowing in sun-exposed leaves of unhardened *Eucalyptus* occurred at temperatures of 8°C in combination with high incident PAR (700-800 μmol m^{-2} s^{-1}) three days after an overnight frost (Close *et al.*, 1999). In mango, leaf chlorosis developed gradually and only in the sun-exposed leaves over the entire winter period (Nir *et al.*, 1997).

The exposed leaves at Ohiwa harbour already showed mild photo-oxidative damage (i.e., chlorosis, leaf yellowing) in April, but their condition worsened noticeably during the three months of winter when light and temperature stresses were at a peak. Chlorophyll loss was at its worst by July-August, coinciding with

the period when the exposed leaves were most affected by photoinhibition (Figures 5.6 and 5.7). It was not possible to estimate the exact period of chlorophyll decline because the measurements were undertaken at 5 or 6 week intervals. However, given that photoinhibition was severe at the time of the June measurement, and that chlorophyll losses did not decline radically until July, it is reasonable to assume that the onset of photo-oxidative damage followed a standard pattern of development where chlorosis was initiated after a time lag of days or several weeks following the onset of photoinhibition (Powles, 1984).

By October at Ohiwa harbour there was evidence of partial recovery in all leaves, due, in the most part, to slightly improved climatic conditions preceding measurement (i.e., temperatures were above 0°C on the night before the October measurement) and the fact that the plants were under a much reduced stress load by this time. Partial and often full recovery of photosynthetic function is relatively common if a return to favourable conditions occurs and if the photosynthetic tissues have escaped lethal injury, although this may require several days or weeks. For example, in the chilling-sensitive species *Coffea arabica* (coffee), net photosynthesis recovered within 2 - 6 days after single chilling treatments of between 2.5 and 8°C had reduced net photosynthesis to between 30 and 95% of the pre-stressed level.

The effects of photoinhibition are reversible (Powles 1984), as demonstrated in the recovery of leaves in this study. During the research period frost- and chill-night frequency declined from a maximum total of 23 nights in July to 5 in September and 3 at the beginning of October (Table 5.1). In October leaf *Fv/Fm* had returned to approximately 71% (exposed leaves) and 80% (protected leaves) and the rates of CO_2 assimilation improved to 20% and 31% of the values first measured in April. There was also a slight increase in exposed-leaf chlorophyll content.

Tissue damage and photosynthetic behaviour of *Avicennia* in response to New Zealand winter temperatures at Ohiwa harbour were comparable to those reported for other cold-sensitive mangrove species. Initial frost damage of tissues and subsequent leaf loss occurred in a similar manner to, and at much the same temperatures as for three species in a Florida mangrove forest after night frost temperatures between -2.7 and -5.5°C, indicating that all have some degree of frost hardiness (Lugo & Zucca, 1977). However, the post-freezing/chilling decline in *Avicennia* CO_2 assimilation rates, stomatal conductance and reductions

in quantum efficiency of PSII that occurred after chilling below 4°C or following frost exposure were typical of symptoms of chill injury observed in non-hardy woody evergreen species such as mango, papaya, citrus (Nir *et al.*, 1997) and *Eucalyptus* (Blennow *et al.*, 1998, Close *et al.*, 2000, Davidson *et al.*, 2004) after exposure to conditions beyond their low temperature thresholds. The corresponding decline in *Avicennia* leaf F_v/F_m with the progression of seasons from autumn to winter was similar to that reported for other evergreens (Blennow *et al.*, 1998, Ottander *et al.*, 1995) and culminated in photo-oxidative chlorophyll bleaching comparable to that reported for *Eucalyptus* after frost nights and high light exposure (Close *et al.*, 1999).

At less than 4.0 μmol m^{-2} s^{-1}, the maximal winter rates of CO_2 assimilation in *Avicennia* at Ohiwa harbour were very low in comparison to rates of 12.3 and 12.5 μmol m^{-2} s^{-1} measured in northern Queensland *Avicennia* (Ball & Critchley, 1982). They were also significantly lower than the maximal rate of 10.0 μmol m^{-2} s^{-1} measured in *Avicennia* at Paihia in northern New Zealand during winter (Chapter 4 and Walbert (2002)).

5.5 Summary

This study has shown that mangroves growing near their southern geographical limit on the east coast of New Zealand (i.e., Ohiwa harbour) encounter a number of detrimental impacts to photosynthesis that are directly related to low winter air temperatures. During winter, overnight frosts caused lethal tissue damage in a proportion of leaves and plant parts, and these were subsequently lost from the plants. In addition, those leaves that remained visibly undamaged were impaired at a functional level. Leaves exhibited progressively reduced rates of CO_2 assimilation and stomatal conductance as winter progressed, and in leaves exposed to high light, impairment of PSII function leading to cold-induced photoinhibition and photo-oxidative damage in the form of chlorophyll losses. When environmental conditions became more favourable towards the end of winter, some functional recovery was evident in all leaves.

The dead or damaged leaves and other organs represent several levels of losses to the plants. In the first instance, these leaves make little or no contribution to overall carbon gain. In the second instance, the energy cost of replacing lost or damaged parts (leaves, growing tips, developing propagules etc) is expensive; draining energy reserves and reducing the amount of carbon that can

be partitioned into additional growth or development (e.g., flower or seed production and propagule growth). In addition, evidence was produced confirming that many of the leaves positioned in both exposed and protected parts of the canopy are susceptible to photoinhibition and photo-oxidative damage, resulting in overall reduced photosynthetic efficiency and performance.

In the long-term reductions in photosynthetic performance diminish the success of a species in its environment. Factors impacting photosynthesis have a significant influence on plant productivity and carbon balance, ultimately determining whether a species can successfully grow and reproduce in its environment, or whether a negative carbon balance is maintained such that survival is not possible. The geographic limits of New Zealand mangrove may well be defined by factors such as these.

Chapter Six

Chapter six

Impacts of the frequency and severity of cold nights on photosynthesis in *Avicennia marina* subsp. *australasica*

6.1 Introduction

The frequency and /or severity of cold temperature events (e.g., frost), is a key factor governing the distribution and extent of a number of plant species, including mangroves (Chapman, 1976, Close *et al.*, 2000, Sherrod, 1986, Woodward, 1987). Frosts, in particular, introduce significant limitations to the growth and establishment of sensitive species by causing irreversible damage to plant parts and, if severe, this may ultimately lead to mortality of whole plants (Chapman & Ronaldson, 1958, Lugo & Zucca, 1977). Often, however, critical cell damage does not occur and the damage sustained during exposure is not visible, but manifests as a reversible, or irreversible, decrease in photosynthetic performance.

Low temperatures can affect all aspects of photosynthesis, including the carbon reduction cycle, stomatal control and thykaloid electron transport (Allen & Ort, 2001). When these processes are disrupted, the light energy captured by chlorophyll exceeds that which can be used in photochemistry or dissipated by other means, and photoinhibition of photosynthesis[1] may then result. Photoinhibition has a protective function (Aro *et al.*, 1993) but may also result in damage to the photosynthetic machinery (Close *et al.*, 1999). It is known to occur under high or low PFD, or under normal conditions, but is enhanced in situations where stresses (for example, low temperature or drought) limit photosynthesis and decrease the plants ability to use the absorbed light energy photochemically (Krause, 1994). In sensitive species (for example, mango), night chilling can cause reductions of both CO_2 fixation and stomatal conductance on the day following the chill and thus increase the plants susceptibility to photoinhibition (Nir *et al.*, 1997). However, this state may also induced by the combination of chilling or freezing in the light (Öquist *et al.*, 1987).

[1] *See Chapter 5 for further notes on photoinhibition of photosynthesis*

Prolonged or repeated exposure to stress conditions (e.g., several consecutive frost nights) has a cumulative but diminishing effect on photosynthetic function and also increases the amount of time needed for resumption of normal photosynthetic activity (Bell *et al.*, 1994, Davidson *et al.*, 2004). In such cases, the possibility of further, permanent damage arises. The reversible photoinhibited state, if prolonged by stress, may result in irreversible damage, such as chilling-, light-, and oxygen-dependent bleaching of chlorophylls

In New Zealand, frosts and chilling air temperatures are a regular occurrence from autumn through winter and spring in some estuarine areas that support growth of the mangrove *A. marina* subsp. *australasica.* Frost and chilling temperatures are more common in these areas at night, rather than during daylight hours, so it is likely that the primary low temperature impacts on *Avicennia* photosynthesis arise from dark-chilling impacts on carbon assimilation and stomatal control. However, after cold nights, temperatures often remain low for short periods of time during daylight hours, so the probability of chilling or freezing in the light and subsequent photoinhibition is also relatively high.

Previous aspects of this study confirmed that cold night temperatures were associated with significant decreases in photosynthetic function of New Zealand mangrove (see Chapters 4 and 5). This prompted further investigation into the photosynthetic consequences of frost/chilling intensity and frequency, and ability of the plants to recover from such exposure. An experiment was undertaken in which temperature conditions were manipulated in a natural field setting at Ohiwa Harbour using cooling chambers to imitate night-frost and chilling conditions. The effects of cold nights on light saturated photosynthesis (A_{max}) and ground, maximal and variable fluorescence (F_o, F_v, F_v/F_m) were then monitored to assess recovery time and to investigate the responses of leaf photosynthesis to the frequency and extent of overnight chilling and freezing.

6.2 Materials and Methods (General)

Ten sets of 5 leaves on several branches of a single *A. marina* subsp. *australasica* specimen were cooled in portable chambers over several nights at the Tuite research site Ohiwa harbour (section 2.6.1.2), in March 2003. One set of leaves was kept in ambient conditions (untreated control) for the duration of the experiment while the remaining sets were cooled according to the treatment combinations summarized in Table 6.1 and section 6.2.1. Leaf gas exchange and

variable fluorescence were then monitored after return to ambient day/night temperature conditions.

All leaves selected for the experiment were located in close proximity to each other on branches of the same tree; an individual approximately 1.5 m tall with a lateral spread of roughly 2 m, located in the estuary on the landward side of the mangrove fringe. All chosen leaves were fully expanded, undamaged, occupied the first- or second- pair position on the branch, and received full sunlight for most of the day. Each received a label around the petiole identifying sample number and treatment (i.e., overnight temperature and number of consecutive nights cooled) to ensure consistent measurement.

Table 6.1 Night-time cooling treatments on the leaves of *A. marina* subsp. *australasica* at Ohiwa harbour, March 2003. Overnight temperature (°C) = minimum air temperature inside the cooling chamber during treatment night; Number of nights treated = number of consecutive nights that leaves were exposed to that air temperature; Number of leaves in brackets are the totals for which dark-adapted fluorescence was measured (see text for explanation).

Treatment Designation (Tr)	Overnight Temperature (°C)	Number of nights treated	Number of leaves Per Tr
A	Ambient	5	5 (2)
B	4°C	1	5 (2)
C	4°C	2	5 (2)
D	4 °C	3	5 (2)
E	0 °C	1	5 (2)
F	0 °C	2	5 (2)
G	0 °C	3	5 (2)
H	-4 °C	1	5 (2)
I	-4 °C	2	5 (2)
J	-4 °C	3	5 (2)

6.2.1 Cooling treatments

Three cooling chambers of the design described in section 6.2.2 (Figure 6.1) were used to reduce overnight leaf temperatures to +4, 0, or -4 °C over a period of three nights. One or two branchlets bearing at least fifteen terminal leaves were cooled in each chamber; 5 leaves were cooled for one night, 5 for two consecutive nights and 5 for three consecutive nights. Five leaves were retained in ambient conditions outside the chambers as a control set.

Each cooling cycle was initiated at dusk and ended before sunrise the following day, after which the leaves/branches were moved (still *in situ*) to positions outside the cooling chambers. All leaves were then left to equilibrate in ambient conditions either for around three-quarters of an hour before the first fluorescence measurements were taken, or for around four hours before the first measurement of gas exchange (to allow the leaf surfaces to become dry enough for accurate CIRAS-1 readings). Chamber temperature profiles and ambient daytime air temperatures during this period, recorded by Campbell data logger with associated sensors, are shown in Figure 6.4.

This experiment was carried out under natural field conditions where daily changes in light levels; temperature, humidity, cloud-cover, and water availability (with regard to rainfall and tidal cycles) also contributed to the extent of daily variation in photosynthesis.

6.2.2 Portable cooling chambers

Artificial chill- and frost-nights were created using portable cooling chambers of a design based loosely upon that developed by Neuner and Bannister (1997) for *in situ* cooling of *Nothofagus*. In the present study, chambers were constructed from plastic polystyrene-insulated 33 litre Eskimo chilly-bins of internal dimensions 240 mm x 390 mm x 340 mm. A Tropicool XC3000 thermoelectric refrigeration unit (Tropicool Ltd, New Zealand), mounted on closed-cell foam through one end of the chilli-bin wall, cooled the air within the chamber. Internal chamber temperatures were maintained by a combination of the XC3000 refrigeration unit and a small thermostat-controlled heating coil, with fan, attached to the wall of the XC3000. Temperatures approximately 25°C below ambient were attainable with variations ± 0.6°C.

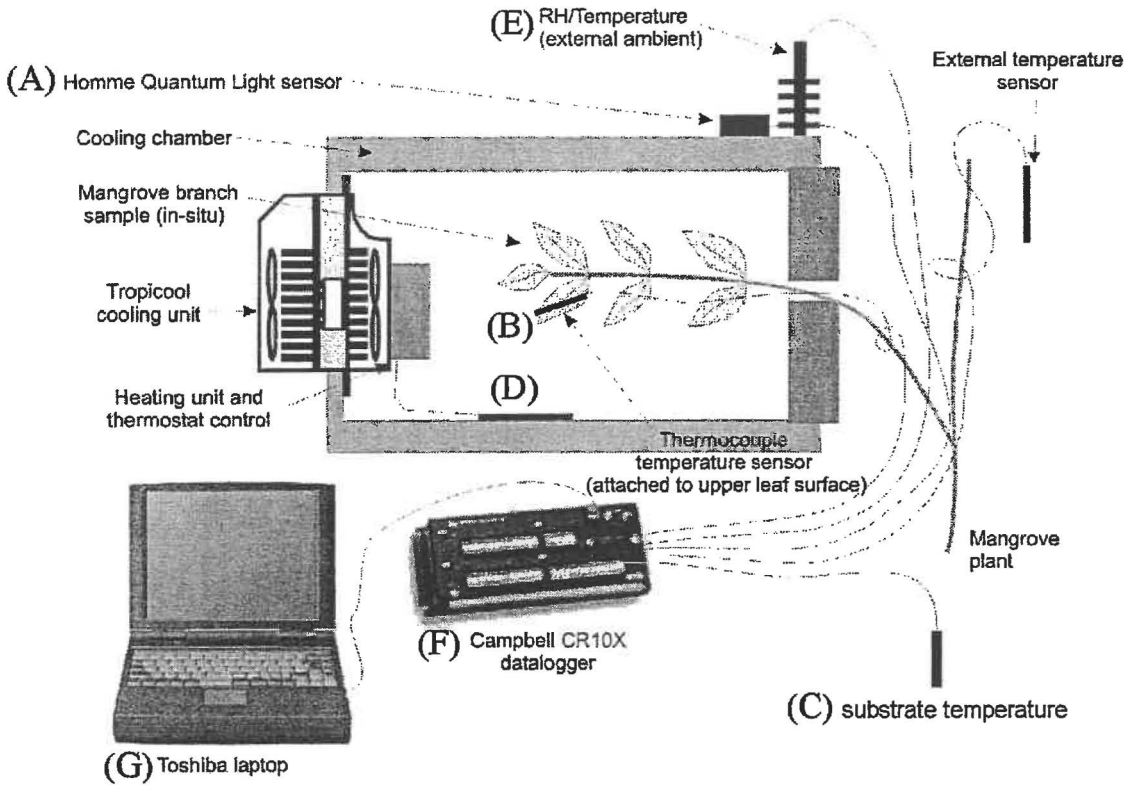

Figure 6.1 Portable cooling chamber and associated sensors. The chamber was a modified 33 L Eskimo chilly-bin with internal environment controlled by a Tropicool XC3000 refrigeration unit and heating coil. Sensors, including external light (A), temperature of the leaf (B), substrate (C); the internal chamber (D), and screened external ambient air and external relative humidity (E); were connected to a Campbell CR10X datalogger (F) and monitored via a Toshiba "Satellite" laptop computer (G).

The cooling system components (Figure 6.1) were supported in the field on plastic kitset shelving secured by webbing ratchet tie-down straps to metal stakes in the substrate. Electrical components, such as control-units and power plugs were contained within several large weather-proof boxes to prevent contact with seawater and overnight dew or rain. The entire setup was powered through a 50 m heavy-duty electrical cable by a 3KV petrol-driven generator situated on dry land.

Mangrove branches were positioned through a small opening between the two hinged and padded halves of the chamber lid. All gaps were plugged with plastic bubble-wrap and waterproof tape before the beginning of each cooling sequence to minimize exchange of air and heat with the external environment, and to improve temperature stability inside the chamber.

6.2.3 Sampling procedures

Measurements of chlorophyll a fluorescence and leaf gas exchange were carried out on "recovery" days, including those that immediately followed "treatment" days (i.e., the first day after final application of night-cooling), and the several days following. Measurements were made with a MiniPAM Fluorometer (Walz, Germany) and a CIRAS-1 portable photosynthesis system (PP-Systems, UK). Equipment and procedures are described below and in some detail in sections 2.9 -2.11.

6.2.3.1 Gas exchange and determination of A_{max}

All samples received a saturating irradiance of 1200 μmol m^{-2} s^{-1} during measurement of gas exchange from a halogen light source attached to the window of the leaf cuvette. At all other times of the day the leaves were exposed to natural levels of incident radiation.

A_{max} values were obtained between 11^{00} and 18^{00} hr as heavy overnight dew and humid conditions complicated use of the CIRAS-1 cuvette early and late in the day.

A_{max} values for cold-treated leaves during the recovery period (see section 6.3 for explanation) were converted to % A_{max}, calculated as a proportion of maximal A_{max} on the first day of untreated (ambient) leaves.

6.2.3.2 Chlorophyll *a* Fluorescence

All leaves were dark-adapted with WALZ DLC darkening-clips for 15 minutes prior to determination of the maximum quantum efficiency of PSII primary photochemistry (F_v/F_m).

Chlorophyll a fluorescence was measured 4 times each photoperiod, commencing around 07^{00} hr, and finishing after sunset each day. The limited number of leaf-darkening clips restricted F_v/F_m determinations to 2, rather than 5 leaves for each treatment.

Relative photoinhibition (%PI) was calculated as the percent decrease of F_v/F_m at mid-day relative to the mean maximal values on Day 1 for ambient leaves.

6.2.3.3 Foliar Chlorophyll Content

Foliar chlorophyll content was measured indirectly on all leaves *in situ* with a SPAD-502 chlorophyll meter at the conclusion of the experiments. Following SPAD measurement, the leaves were removed from the plant and chlorophyll content was determined in the laboratory by measuring the absorbance of extracted pigments (refer to section 2.10 for procedures).

6.2.4 Microclimate and Artificial Frost Measurements:

Temperature variations in the cooling-chambers were tracked during the cooling and warming cycles using two types of Campbell temperature sensors. Internal chamber temperatures were measured with a Campbell R107 sensor fixed to a branch amongst the treatment leaves. Actual leaf temperatures were measured simultaneously with a Campbell Type-T copper-constantan thermocouple attached with waterproof tape to the upper surface of a single leaf within the chamber (this leaf was designated not to be used for other measurements in case tissue damage occurred while securing the thermocouple wire). However, during the field trials, the fine thermocouple wires proved to be too delicate and after a number of breakages their use was discontinued in favour of the more robust R107 sensors. An offset correction value of 0.6°C was used to adjust leaf temperature measurements in the field because the R107 sensors returned consistently cooler values than those measured by thermocouple wire on the leaf surface. An example of a temperature trace during indoor trials is shown in Figure 6.2.

On-site microclimate data were recorded at two minute intervals during the treatment and measurement periods using a Campbell CR10-X data logger setup as described in section 2.7.1 (the CR10X operating programs are described in Appendix I). At the field site, sensors were positioned as illustrated in Figure 6.1 to measure ambient air, chamber, leaf and substrate temperatures, relative humidity, and ambient photon flux density (PFD). A HOMME quantum sensor, measuring PFD, was secured to the outside of a cooling chamber in close vicinity to the sample leaves, and a screened RH/Temperature sensor was positioned on top of the box containing the power controls. Additional R107 temperature sensors were also used to record chamber, leaf and substrate temperatures.

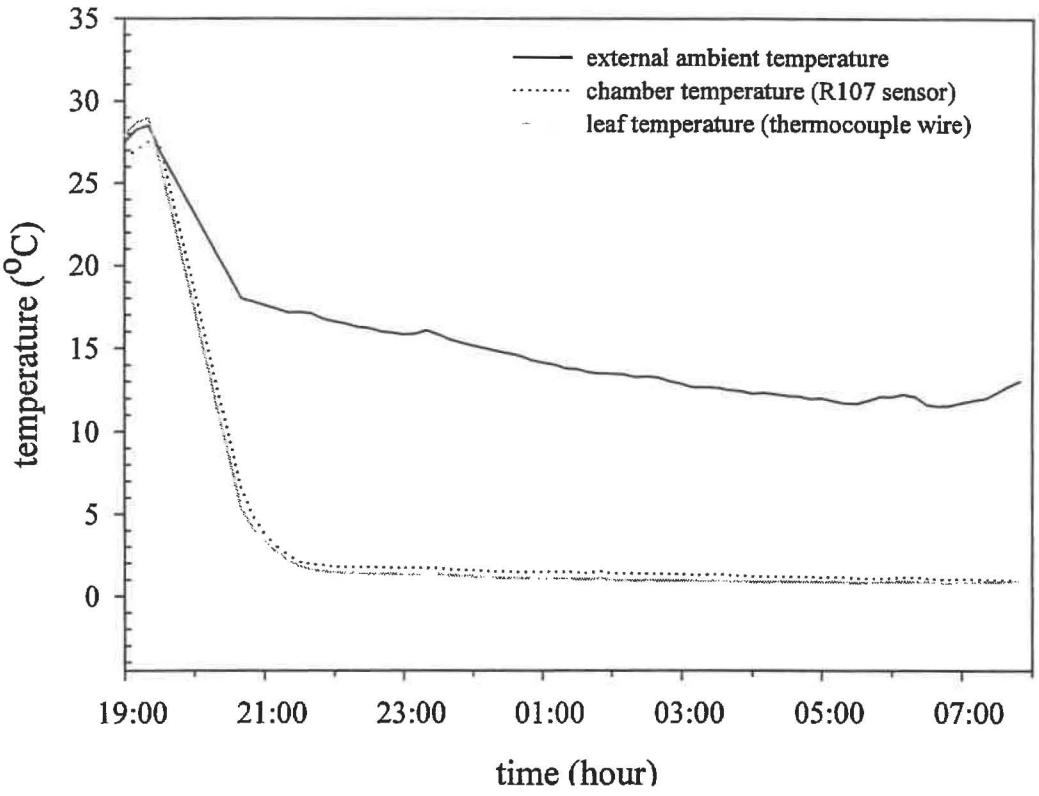

Figure 6.2 Example trace of temperature (°C) inside and outside a portable cooling chamber as measured by Campbell R107 sensors and a Campbell thermocouple wire attached to a leaf surface. Sample data are from equipment trials undertaken in the University glasshouse complex on potted *Avicennia* plants.

Regional climate data were obtained from the National Institute of Water and Atmospheric Research (NIWA) to supplement on-site climate measurements. Summaries of daily climatological records for Whakatane airport and Opotiki (NIWA, 2003a) were used to estimate rainfall at the research site and to compare air temperature, relative humidity and solar radiation. Additional temperature data were also recorded with Hobo StowAway TidbiT temperature data loggers (Onset Computer Corporation, U.S.A.) at a nearby site located in the estuary at Kutarere, approximately 2.5 km south of the research site (Section 2.6.1)

6.2.5 Statistical Analyses

Descriptive statistics, graphs and statistical analyses were produced with Sigmaplot vs. 8.0 (SPSS, 2002) and Statistica vs. 6.0 (StatSoft, 2003).

A_{max} values of all cold-treated leaves ("recovery" period only) were calculated as percentages relative to mean maximal A_{max} of untreated leaves on Day 1. Relative photoinhibition (% PI) was calculated to be the percent decrease

of F_v/F_m at midday relative to the mean value for ambient leaves on Day 1. A mixed-subject repeated-measures ANOVA was then performed on each dataset using % A_{max} or % PI as the dependent variable with two categorical predictor variables of minimum night-temperature (-4, 0, +4 °C) and number of consecutive nights (1, 2 or 3) that leaves were cold-treated prior to measurement. Significant differences were then assessed using a post-hoc Tukey HSD test.

6.3 Results: Field experiment

6.3.1 Local climate March 2003

The experiment was undertaken in March at the beginning of austral autumn when air temperatures were beginning to decrease from their summer maxima. Mean air temperatures recorded for Whakatane and Opotiki climate stations (both located within 20 kilometres distance from the study site), in March 2003 were 17.7 °C and 18.1 °C respectively, slightly cooler than their February means of 18.9 °C and 18.7 °C.

Daily minimum temperatures during March 2003 at Whakatane and Opotiki ranged from 6.5 °C to 19.2 °C, and 7.2 °C to 18.6 °C, respectively (NIWA, 2003a). Additional temperature data from unscreened sensors at the Wainui Road research site (section 2.6.1) indicated that the lowest minimum temperature occurring at amongst the mangroves there during the month of March 2003 was 6.7°C [1].

The Bay of Plenty area is recognised for relatively high sunshine hours, with an average of 2100 to 2200 hours per year. However, it also receives approximately 1000 mm of rain a year. For March 2003 rainfall was about average with 14 days totalling 6.74 mm at Whakatane and 6.37 mm for the same number of days at Opotiki. During the 30-day period preceding this experiment, rainfall totals of 10.2 mm and 10.7 mm were recorded at Whakatane and Opotiki stations respectively (NIWA, 2003a).

[1] *Maximal, and therefore average, temperatures were not included from this site because solar heating of the unscreened probe casing resulted in falsely high readings (see section 2.7.2). However, the less than 0.5 degree difference between minimum temperatures at all sites indicated that the climate station data from Whakatane and Opotiki were adequate estimators of temperatures occurring in the estuary.*

6.3.2 On-site climate during the study period (March 18 -23, 2003).

6.3.2.1 Air Temperature, Relative Humidity, Rainfall

Ambient climate on-site during the course of the field experiment was characterized by cool to mild night temperatures (lowest overnight minima ranging from 6.8°C to 16.1°C) followed by fine warm days (highest maxima from 24.7°C to 26.5°C) with very light winds and no rainfall. Increased cloud cover during the final two days of the study period was associated with slightly higher relative humidity during daylight hours and warmer nights relative to the first three days of the study period (Table 6.2).

Night-time air temperatures within the three cooling chambers were maintained at 4, 0 or -4°C with minor variations (Figure 6.4). The rate of cooling and warming in each chamber ranged between 0.1 and 0.07 degrees per minute.

6.3.2.2 Photon Flux Density

During the first two days of the experimental period, the complete absence, or low percentage, of cloud-cover resulted in exposure of the study plant to high light levels, with maximal PFD up to 1313 μmol m^{-2} s^{-1} (Figure 6.3). Maximal PFD was higher on the last two days of the study period as a result of reflected light from clouds which (Table 6.2) increased steadily in cover each day to approximately 100% on the final day.

Table 6.2 Microclimate at Ohiwa Harbour research site during the study period March 18th – March 23rd 2003. External PFD (maximum only) = photon flux density above canopy (μmol m^{-2} s^{-1}); external ambient temp, substrate temp, relative humidity = Minimum, maximum and average air temperature, substrate temperature (°C) and RH outside the cooling chambers.

Date (2003) and Max, min, average	External PFD (μmol m^{-2} s^{-1})	External ambient Temp (°C)	Relative Humidity (%)	Substrate temp (°C)
Night of March 18				
min		6.8	77.4	6.2
max		17.8	100.0	17.1
average		10.1	96.9	9.2
Day of March 19 min		10.2	40.7	9.5
max	1313	26.5	100.0	17.9
average		21.3	62.2	15.73
Night of March 19				
min		7.3	78.7	14.3
max		17.2	100.0	17.0
average		10.0	98.5	15.9
Day of March 20				
min		7.3	39.7	13.9
max	1237	26.1	100.0	16.9
average		19.9	71.0	15.5
Night of March 20				
min		8.5	90.0	14.5
max		15.6	100.0	16.9
average		11.0	99.5	16.0
Day of March 21				
min		10.2	52.4	14.4
max	1329	25.2	100.0	17.4
average		20.7	71.9	16.0
Night of March 21				
min		12.2	90.5	16.1
max		16.0	100.0	17.2
average		13.6	99.5	16.7
Day of March 22				
min		14.1	64.7	15.9
max	1505	24.7	100.0	18.5
average		20.8	78.2	17.4
Night of March 22				
min		16.1	94.1	17.7
max		18.0	100.0	18.3
average		17.1	99.6	18.0
Day of March 23				
min		16.2	58.7	17.5
max	1251	25.0	100.0	18.8
average		20.6	77.3	17.9

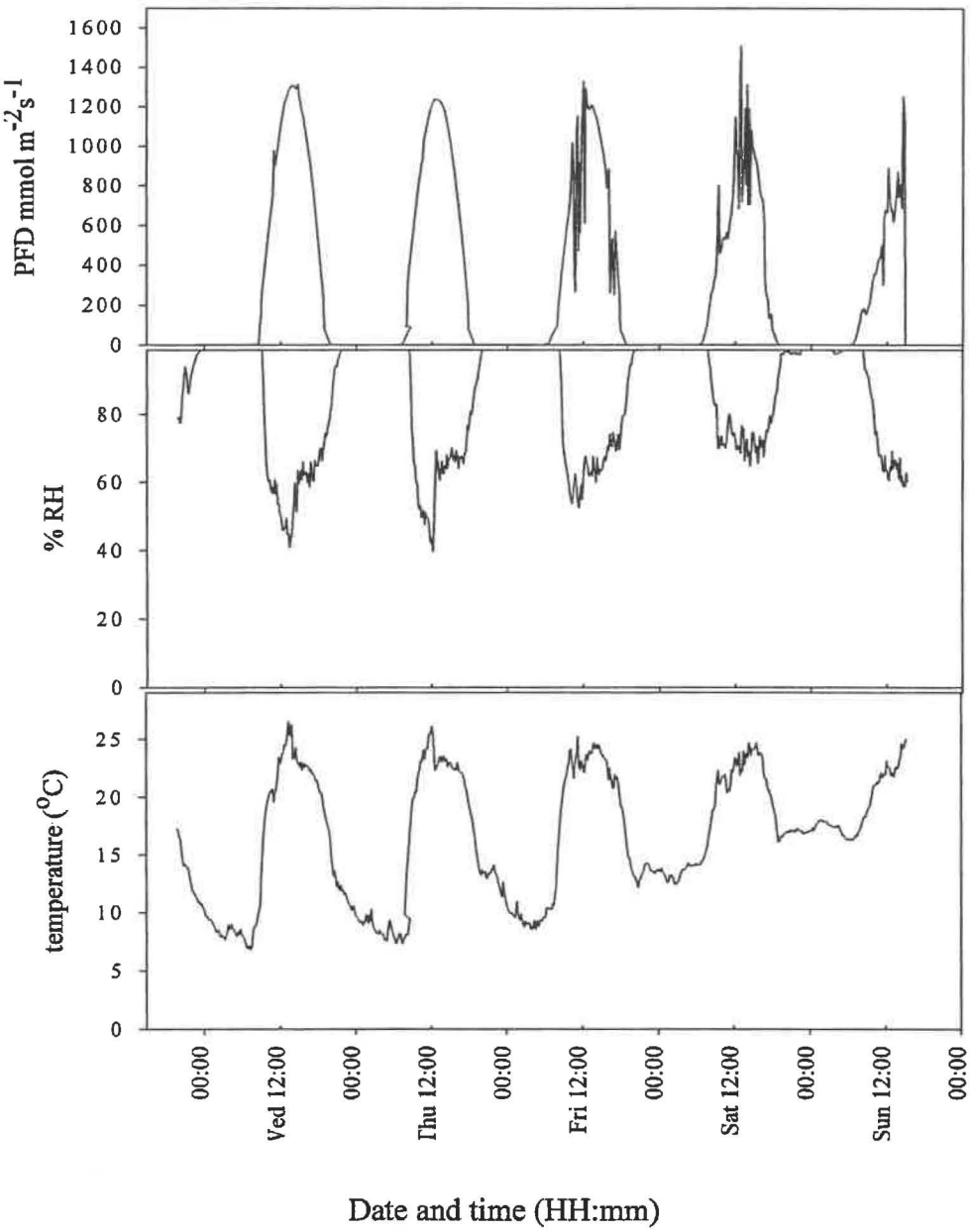

Figure 6.3 Ambient microclimate during the period of artificial frost experiments at the "Tuite" site, Ohiwa Harbour, March 2003. Top to bottom: Photon Flux Density, PFD (μmol m^{-2} s^{-1}, percent relative humidity (RH), ambient external air temperature (°C).

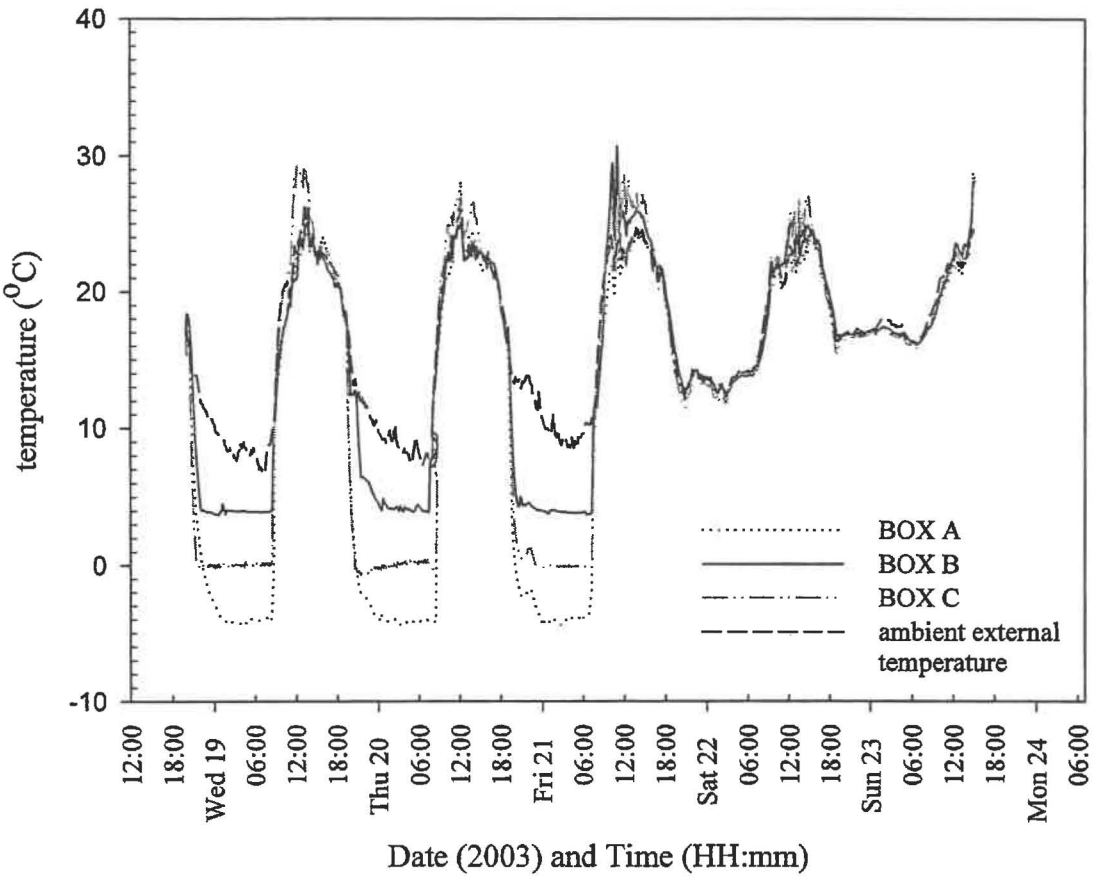

Figure 6.4 Air temperature within three cooling chambers (Box A - C) and of the ambient environment during an artificial frost experiment, March 19th – 24th, 2003 at the Tuite research site, Ohiwa harbour. BOX A, 3 treatments at -4°C; BOX B, 3 treatments at +4°C; BOX C, 3 treatments at 0°C.

6.3.4 Measurements of leaf gas exchange and chlorophyll *a* fluorescence

NOTE:

The experimental results are presented in three formats:

1. "Ambient" when the leaves had not received any chilling or freezing treatment and had remained exposed over night and through the day to ambient conditions (section 6.3.4.1, gas exchange and 6.3.4.7, chlorophyll fluorescence).

2. "Immediate" values are those measured on the first day following 1, 2 or 3 consecutive chilling/freezing night treatments. The data represented are a subset (day one) of those used in the

"Recovery" analysis and are presented in sections 6.3.4.2, gas exchange and 6.3.4.8, chlorophyll fluorescence.

3. "Recovery" values are those measured over a three day period after chilling/freezing treatment nights had been concluded. Recovery day one (or first day) refers to the photoperiod directly after the final chilling or freezing night. Recovery days two and three (or 2nd and 3rd days) refer to the following two consecutive photoperiods, which follow nights when leaves had remained in ambient conditions. The data are for the complete set as outlined in Table 6.1, and are presented in sections 6.3.4.3 - .6, gas exchange and 6.3.4.9 - .12, chlorophyll fluorescence.

6.3.4.1 Leaf gas exchange (ambient conditions)

Over the entire study period, mean A_{max} (CO_2 assimilation rates measured under saturating light) of individual untreated leaves (ambient night temperatures, 6.8 – 16.1°C) varied between 0.24 and 10.90 μmol m^{-2} s^{-1} and the highest rate measured in any one leaf was 12.9 μmol m^{-2} s^{-1}. The maximum for A_{max} was either reached in the morning with mean values around 10.9 μmol m^{-2} s^{-1} (particularly if preceded by warmer nights) or, more typically, it was reached around mid-afternoon and ranged between 5.7 and 7.6 μmol m^{-2} s^{-1}. Conductances were usually lowest at the start of daily sampling (between 11^{00} hr and 12^{00} hr) and increased until mid-afternoon after which a decline was generally observed before a slight increase towards the end of the day. Conductances ranged from 4.0 to 353.0 mmol m^{-2} s^{-1} (higher values, due to damp leaf surfaces, were omitted as erroneous data).

Maximal A_{max} occurred at conductances between 51.0 and 220.0 mmol m^{-2} s^{-1}. Leaf temperatures during sampling ranged from 22°C to 33°C, and were generally highest at the time of the first daily measurement.

6.3.4.2 Immediate A_{max} and g_s at A_{max} following 1 to 3-days of cold-night treatment

1. A_{max}

Mean "immediate" A_{max} values for 1 to 3 days night chilling or freezing are shown in Table 6.3. Immediate A_{max} of leaves dark-chilled to +4°C were between

4.3 and 9.5 μmol m^{-2} s^{-1}. A_{max} of leaves dark-chilled to 0°C were between -0.2 and 5.0 μmol m^{-2} s^{-1} and, at -4°C, A_{max} ranged from 0 to 4.0 μmol m^{-2} s^{-1}.

Relative to first day mean A_{max} of untreated leaves, A_{max} of the +4°C leaf (Figure 6.5, green line) was about 80% of the untreated leaves following 1 to 3 days treatment. In comparison, mean A_{max} of 0 and -4°C leaves were much lower, at around 20% for 1 and 2 days treatments and higher at 30 and 58% respectively, after three days (Figure 6.5, red and blue lines).

A significant correlation between A_{max} and previous night minimum temperature was evident, with lower temperatures being associated with lower A_{max} values ($r^2 = 0.70$, $p = 0.0001$).

Table 6.3 Immediate mean A_{max} of leaves following a 1, 2 or 3 day period of cold-night treatments. Values are the mean of 5 samples ± standard deviation. Trt night min temp = minimum air temperature on each of the three nights (+4, 0, and -4°C, ambient control). Day ONE = A_{max} after one cold night, Days TWO and THREE = A_{max} after two and three consecutive cold nights.

Trt-night min temp	N	Day ONE Mean A_{max} ± SD			Day TWO Mean A_{max} ± SD			Day THREE Mean A_{max} ± SD		
ambient	5	7.82	±	1.85	6.70	±	1.08	6.62	±	1.26
+4°C	5	6.20	±	0.93	6.82	±	2.10	6.28	±	0.62
0°C	5	1.46	±	0.39	1.56	±	1.25	4.34	±	0.95
-4°C	5	1.16	±	0.58	0.32	±	0.34	2.34	±	1.37

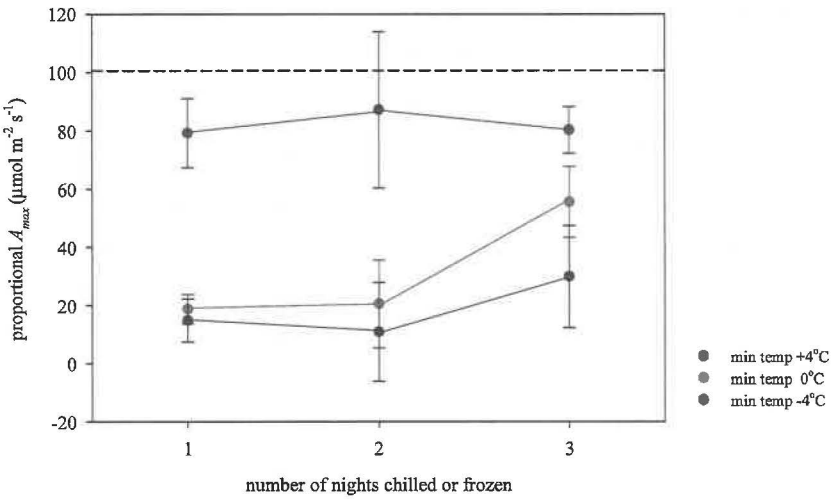

Figure 6.5 Comparison of %A_{max} (i.e., A_{max} relative to untreated leaves) after a 1, 2 or 3-day period of cold-night treatments. Treatments comprised night-chilling or freezing to minimum temperatures of -4, 0 and +4°C for 1, 2 or 3 consecutive nights. Dashed line at 100% represents untreated ambient controls (refer to Table 6.2 for overnight ambient minimum air temperatures). Values are mean ± standard deviation, n = 5.

2. "Immediate" stomatal conductance (g_s at A_{max}); (Data for A_{max} and g_s at A_{max} are tabled in Appendix VI)

Stomatal conductances below 150 mmol m^{-2} s^{-1} followed nights when air temperatures were under 8.5°C (this also includes ambient leaves) (Figure 6.6, blue, yellow, green data points, all panels). After a warm night (i.e., 12.2°C, as represented by red data points in Figure 6.6), g_s was higher in all treatments and reached between 174 – 260 mmol m^{-2} s^{-1} in +4°C leaves, 127 -256 mmol m^{-2} s^{-1} and 152 -210 mmol m^{-2} s^{-1} in -4°C leaves. Stomatal conductances during the cold night treatment period were associated with a range of A_{max} and depended on the previous night's temperature minimum. Although, in general, colder night temperatures were associated with larger reductions in A_{max} and lower g_s it is clear that g_s was not limiting photosynthesis. At similar g_s, A_{max} was significantly lower in leaves previously exposed to -4 and 0°C than in leaves exposed to +4 °C or at ambient conditions. This suggests that the primary effect of the chilling and freezing treatments was on the carbon fixation pathway and that low A_{max} led, rather than followed, lowered stomatal conductance.

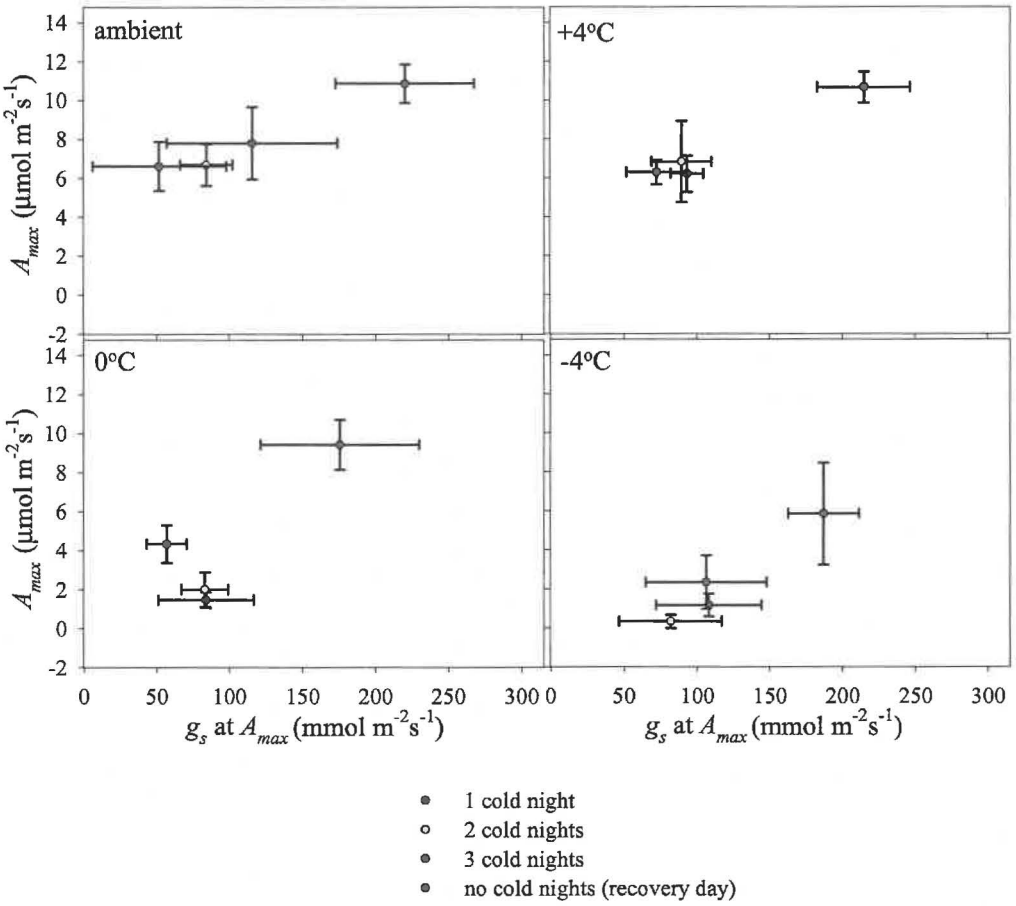

Figure 6.6 A_{max} vs. g_s at A_{max} in leaves either untreated (ambient) or chilled/frozen over 3 consecutive nights to -4, 0, and +4°C. Ambient night temperatures were in the order of 6.8, 7.3, 8.5, and 12.2°C. Values represented by the red data point (recovery day) in all panels were obtained after a frost- or chill-free night with ambient temperature = 12.2°C. Data points are mean ± standard deviation, n = 5.

6.3.4.3 Recovery: Leaf gas exchange in the three days following night-chilling at 4°C

Relative A_{max} of all leaves in the 4°C treatments (i.e., whether exposed to 1, 2 or 3 nights of 4°C) were similar on the first recovery day (Figure 6.7, first green data point in all panels). In addition, there was little evidence of any continuing damage and leaves even performed better than the original control at the end of the recovery (Figure 6.7, green lines). During the recovery period A_{max} varied between 2.4 and 9.3 µmol m^{-2} s^{-1} and were associated with conductance values between 40 and 305 mmol m^{-2} s^{-1}.

6.3.4.4 Recovery: Leaf gas exchange in the three days following night-chilling at 0°C

All leaves chilled to 0°C, whether for 1, 2 or 3 nights, showed significant depressions in photosynthetic activity following the final chilling night (Recovery Day 1). The most severe decline was in leaves chilled for a single night (treatment E), when mean A_{max} values were reduced to 1.3% those of original rate (Figure 6.7, panel I, red line). In contrast, leaves chilled for two and three consecutive nights (treatments F and G) appeared to be less affected at 34% and 60% (Figure 6.7, panels II and III, red line). All treatments showed rapid recovery and, by the end of the recovery period, A_{max} of leaves previously chilled for 2 and 3 successive nights exceeded the original control whilst 1 night treated leaves were at only 60%.

6.3.4.5 Recovery: Leaf gas exchange in the three days following night-chilling at -4°C

Leaves exposed to night temperatures of -4°C were severely affected and net photosynthesis was frequently negative for individual leaves, as also found in some leaves chilled at 0°C. The overall pattern was very similar to those treated at 0°C but with generally lower A_{max}. Leaves treated for 1 or 2 nights were most affected at first but showed strong recovery, although only the latter attained original values. Those treated for one night only reached 48.8% of untreated values (Figure 6.7, panel I, blue line). Leaves frozen for three consecutive nights reached a mean % A_{max} around 50.5% on day 2 but failed to recover further (45.7% on day 3, Figure 6.7, panel III, blue line).

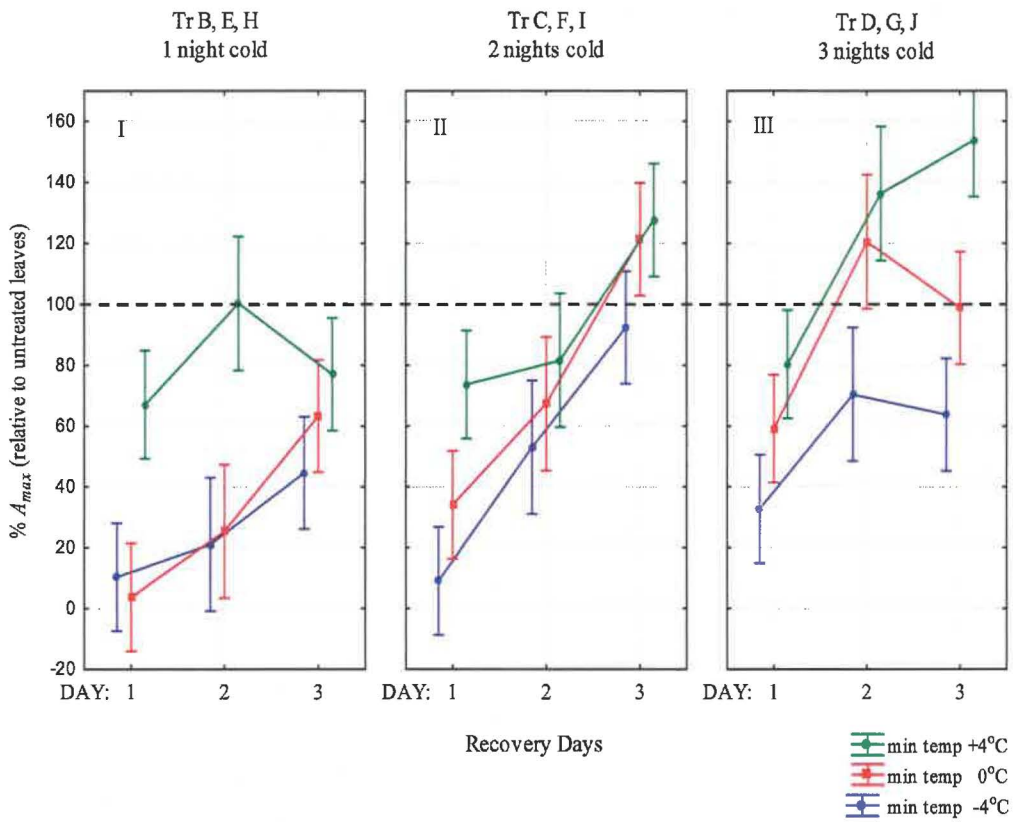

Figure 6.7 Recovery of A_{max} in leaves after a period of 1 (panel I), 2 (panel II) or 3 (panel III) consecutive nights chilled or frozen to -4 (blue lines), 0 (red lines) or 4°C (green lines). Values are percentages relative to untreated, original leaf A_{max} as represented by dashed line at 100%). Day 1 = first day after final night of cold treatment. Days 2 and 3 = subsequent days following cessation of cold night treatments. Data points are the mean of 5 samples ± 95% confidence intervals.

6.3.4.6 ANOVA results: recovery of A_{max}

Recovery of CO_2 uptake rates was highly significantly affected by both the number of cold nights and the temperature of the night treatment (both $p<0.0001$). The combination of treatment-night minimum temperature, the number of consecutive night exposures to the treatment temperature, and the number of recovery days was also highly significant [$F(8, 72) = 3.4126$, $p = 0.002$, Table 6.4]. This interaction reflects the different recovery patterns for 0 and especially -4°C when recovery was low after the third treatment. Also there was a large difference between the 4°C and other treatments after the single night treatment but between -4°C and the others after 3 treatment days. Overall the effect on A_{max} increased in the rank order 4, 0 and -4°C.

Table 6.4 Analysis of variance for A_{max} of artificially cold-treated leaves of *A.marina* subsp. *australasica* at Ohiwa Harbour. Significant effects (alpha level = 0.05) are in bold. Number of cold nights = number of consecutive nights that leaves were cooled (1, 2, or 3); Trt-night min temp = minimum air temperature during cold-night treatment (+4, 0 or -4°C); Recovery days = days following night-cooling treatment.

Source of variation	SS	DF	MS	F	p
Intercept	**659371.3**	**1**	**659371.3**	**1089.777**	**<0.0001**
Number of cold nights	**45966.9**	**2**	**22983.5**	**37.986**	**<0.0001**
Trt night min temp	**70746.6**	**2**	**35373.3**	**58.463**	**<0.0001**
Number of cold nights*Trt night min temp	6499.7	4	1624.9	2.686	0.046
Error	21781.9	36	605.1		
Within subjects					
Recovery days	**63782.7**	**2**	**31891.3**	**81.880**	**<0.0001**
Recovery days*treatment	**13181.3**	**4**	**3295.3**	**8.461**	**<0.0001**
Recovery days*min temp	1164.1	4	291.0	0.747	0.563
Recovery days*treatment*min temp	**10633.2**	**8**	**1329.2**	**3.413**	**0.002**
Error	**28043.2**	**72**	**389.5**		

6.3.4.7 F_v/F_m and relative photoinhibition (ambient conditions)

F_v/F_m in untreated leaves was typically between 0.77 and 0.81 at the first measurement of each day and changed relatively little over the course of each photoperiod. Relative Photoinhibition, (%PI) was expressed as the percent decrease of F_v/F_m in cold-night treated leaves at midday relative to the highest morning mean F_v/F_m of untreated ambient leaves)

6.3.4.8 F_v/F_m and relative photoinhibition immediately following a 1 to 3-day period of artificial cold night treatments

Cold nights resulted in an initial decrease of F_v/F_m in all cold-treated leaves, with early morning mean F_v/F_m between 0.76 - 0.79 in 4°C leaves, between 0.63 and 0.77 in 0°C leaves and between 0.65 and 0.80 in -4°C leaves. However, decreases in F_v/F_m became more pronounced once the plants had been exposed to several hours of sunlight. %PI ranged from 0 to 13.5% in leaves chilled to +4°C, (Figure 6.8, green line), 11.1 to 20.7% in leaves chilled to 0°C (red line) and between 16.0 and 27.2% for those frozen to -4°C (blue line) Leaves experiencing cold nights of -4°C had significantly greater %PI than leaves chilled to +4°C (Figure 6.8). The decline of % PI observed in +4°C leaves on the third day coincided with slightly overcast, warmer and more humid conditions than the previous two days (Table 6.2).

Overall, a significant trend was evident with lower previous night minimum temperatures associated with higher levels of relative photoinhibition ($r^2 = 0.70$, $p < 0.0001$).

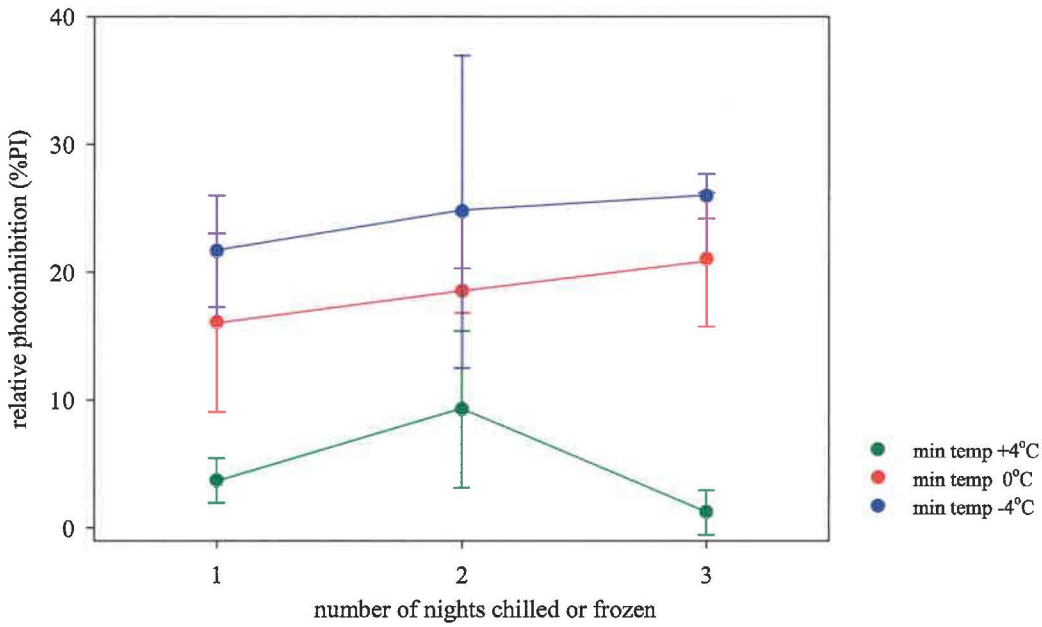

Figure 6.8 Comparison of relative photoinhibition in leaves chilled or frozen over 1, 2 or 3 consecutive nights. % PI was calculated as the percent decrease of F_v/F_m at midday relative to the highest mean on Day 1 in untreated leaves. Data points are mean ± standard deviation. Treatments comprised night-chilling or freezing to minimum temperatures of -4, 0 and +4°C with untreated (ambient) control (refer to Table 6.2 for night minima).

6.3.4.9 Recovery: relative photoinhibition in the three days following night-chilling at +4°C

There was an increase in %PI after one night treatment at 4°C to about 12% with a recovery to near-normal values after three days. In contrast the 2nd and 3rd day treatments had little immediate or long term effect (Figure 6.9, panels I and II). Overall there was little effect at this temperature.

6.3.4.10 Recovery: relative photoinhibition in the three days following night-chilling at 0°C

Percentage PI at 0°C increased to 18, 35 and 20% on the first day of the 1, 2 and 3 days of treatment, respectively. After 1 and 2 nights treatment there was a recovery to near normal values by the third recovery day (Figure 6.9, panels I and II) whereas recovery ceased after the second day for the 3 nights of chilling and

normal values were not reached with %PI remaining at about 10% (Figure 6.9, panel III).

6.3.4.11 Recovery: relative photoinhibition in the three days following night-chilling at -4°C

The response pattern after treatment at -4°C for 1 – 3 nights was almost identical to that found for 0°C and, for the 2 and 3-night treatments, the 0°C effect was actually stronger (Figure 6.9, Panels I to III).

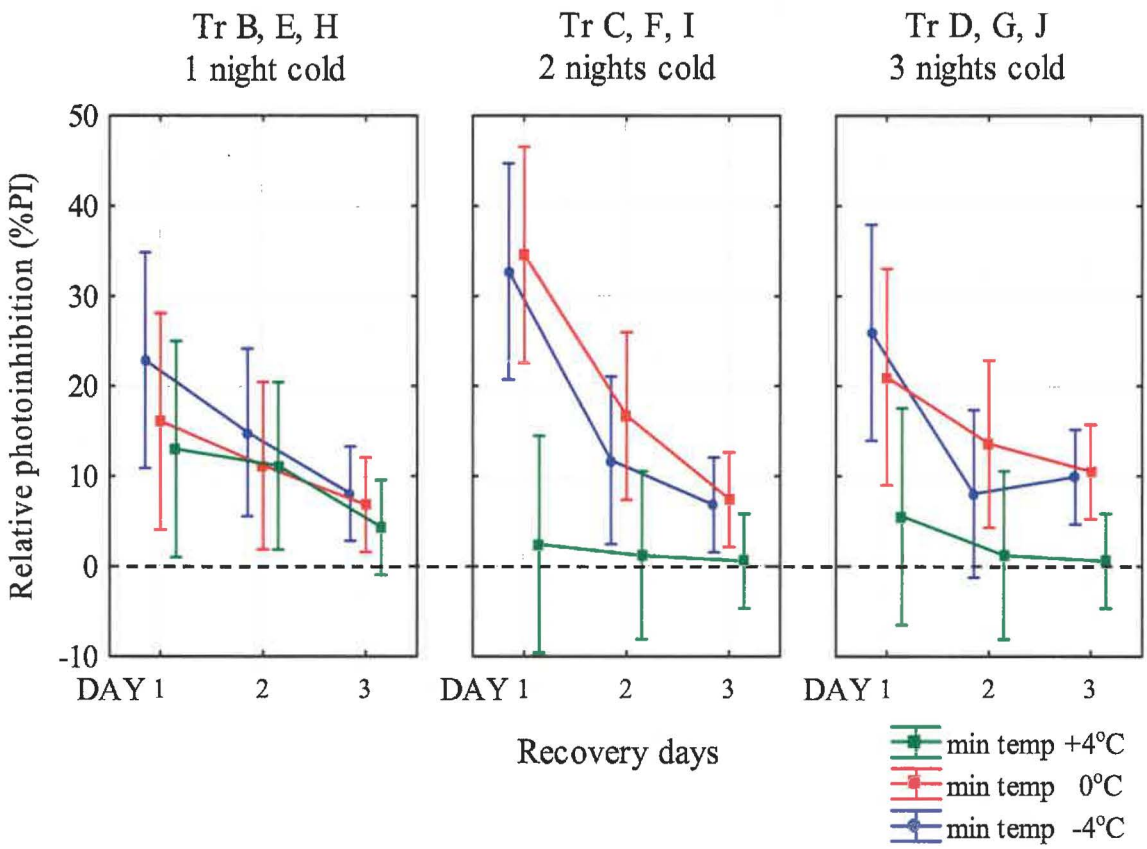

Figure 6.9 Differences in relative photoinhibition during recovery after 1 (panel I), 2 (panel II) or 3 (panel III) consecutive nights chilled or frozen to -4 (blue lines), 0 (red lines) or 4°C (green lines). Values are the %PI difference relative to %PI in untreated leaves (as represented by dashed line at 0%). Day 1 = first day after final night of cold treatment. Days 2 and 3 = subsequent days following cessation of cold night treatments. Data points are the mean of 5 samples ± 95% confidence intervals

Table 6.5 Analysis of variance for relative photoinhibition (%PI) of artificially cold-treated leaves of *A. marina* subsp. *australasica* at Ohiwa Harbour. Significant effects (alpha level < 0.05) are in bold. Number of cold nights = number of consecutive nights that leaves were cooled (1, 2, or 3); Trt-night min temp = minimum air temperature during cold-night treatment (+4, 0 or -4°C); Recovery days = days without night-cooling treatment.

Source of variation	SS	DF	MS	F	p
Between subjects					
Intercept	7515.1	1	7515.11	160.20	**0.00001**
Number of cold nights	36.74	2	18.37	0.39	**0.686**
Trt night min temp	**1455.23**	**2**	**727.61**	**15.51**	0.001
Number of cold nights*min temp	415.75	4	103.93	2.21	**0.147**
Error	422.19	9	46.91		
Within subjects					
Recovery days	**1669.63**	**2**	**834.81**	**31.00**	0.00001
Recovery days*number of cold nights	181.54	4	45.38	1.68	**0.197**
Recovery days*Trt night min temp	**391.37**	**4**	**97.84**	**3.63**	0.024
Recovery days*number of cold nights*Trt night min temp	203.22	8	25.40	0.94	**0.506**
Error	**484.68**	**18**	**26.92**		

6.3.4.12 Recovery period ANOVA results: relative photoinhibition

Minimum night temperature and length of time (days) that the leaves were in recovery (i.e., the number of days after cessation of cold-night treatment) both had a significant influence on leaf recovery from photoinhibition (i.e., reduction of %PI). This result indicates the strong recovery patterns, especially after 1 and 2 nights of treatment (Number of recovery days effect: $F(2, 18) = 31.0$, $p < 0.0001$) and also that the %PI was significantly greater in -4 and 0°C leaves than in +4°C leaves (Minimum temperature effect: $F(2, 9) = 15.51$, $p = 0.001$). (Table 6.5).

There was a significant interaction between minimum night temperature and the number of days in recovery [$F(4, 18) = 3.6336$, $p = 0.02438$ (Table 6.5)]; this is an indication of the different recovery patterns between the +4°C and the other temperatures, and the failure for recovery to continue after 2 nights of treatment at -4 and 0°C.

The number of consecutive cold nights that the leaves had been exposed to prior to the recovery period had no significant influence on recovery from photoinhibition.

6.4 Discussion

The results of this study confirm that cold nights have a negative impact on the photosynthetic performance of New Zealand *Avicennia*, but that, under the experimental conditions and the time of year, the extent of decline was due more to the severity of exposure rather than the frequency with which it occurs.

It is known that stressful conditions (e.g., temperature, salinity stress) can impair photosynthesis in mangrove via both stomatal and non-stomatal (carbon fixation pathways) processes (Ball & Farquhar, 1984a, 1984b, Kao *et al.*, 2004). The present study provides evidence that the major cause of decreased photosynthesis following chilling or freezing was a direct effect on the photosynthetic carbon fixation metabolism. There was an effect on stomatal opening, as found by previous reported studies (Guye & Wilson, 1987) so that was restricted to some extent after both chilling- and frost-nights. This stomatal effect was even evident in untreated (exposed to ambient temperature) leaves that experienced overnight temperatures between 6.8 and 8.5°C. (Figure 6.6). However, Figure 6.6 shows clearly that A_{max} was only slightly reduced in the untreated leaves whilst, in the treated leaves, particularly in -4 and 0°C leaves, it was substantially lower at the same stomatal conductances. Reduced A_{max} in this case could possibly be indicative of a decrease in RuBP regeneration capacity (Farquhar & Sharkey, 1982).

Recovery was rapid so that, as soon as the leaves experienced a day/night cycle free of night chilling or freezing, Amax and stomatal conductance increased to close to optimal values in ambient and +4 °C leaves.

Other studies have shown that successive frosts have a cumulative and negative effect on Amax. For example, it declines 17% and a further 9% in *Eucalyptus* after one and two frost nights of similar intensity (Davidson *et al.*, 2004), however there was little evidence of a similar effect in the present study. Night cooling regimes of 0 and -4°C resulted in reduced leaf A_{max} of around 85 and 81% after one cold-night; both significantly lower than the initial reductions of around 30% in leaves chilled at 4°C (Figure 6.5). However the only subsequent decrease following a second cold night occurred in -4°C leaves when Amax declined by a further 10%. No further major decrease was evident after the third successive exposures and Amax improved after a final third cold night by approximately 30% in 0 and -4°C leaves but declined by around 6% in +4°C

leaves. Therefore, whilst an overall decline in A_{max} (relative to untreated leaves) did occur during the cold-night treatments this was correlated with the level of the overnight temperature rather than with the number of consecutive exposures.

It is unclear what factors influenced A_{max} recovery during this period, and it appears somewhat curious that treatment for 3 nights seemed to have less affect than when treated for 1 or 2 nights, i.e., it was not accumulative. The most probable explanation for this is that the leaves were able to carry out substantial recovery during the days between treatments. Certainly these days were warm and would allow such recovery. In winter the shorter day length coupled with colder temperatures would probably prevent this recovery and cause the treatments to be additive. However, full recovery would be expected to return the leaf to its original condition and it should then behave like the leaves after the first night treatment. The fact that the leaves never reacted so strongly after the second and third treatments does suggest that some level of change has occurred which is allowing acclimation to the chilling conditions. This would make *A marina* similar to other sensitive species such as peanut (Bell *et al.*, 1994).

Recovery was influenced by both the level of overnight temperature and the number of nights on which low temperatures occurred (Figure 6.7). All leaves treated at 4°C whether for one or three nights had effectively fully recovered after one day. However, although recovery after both one and two nights treatment was substantial and rapid for the 0 and -4°C, there was little sign of its occurrence after three cold nights.

Chapter Seven

Chapter seven

Carbon isotopic composition of *Avicennia marina* subsp. *australasica* along gradients of latitude and salinity

7.1 Introduction

The sensitivity of a plant species to its environment may trigger stress responses that limit the uptake and assimilation of carbon. Stress effects on plant performance can be estimated by directly measuring the plant physiological responses, such as chlorophyll *a* fluorescence, stomatal conductance (g_s), or the rates of net CO_2 assimilation (A) and transpirational water loss (E). However, such measurements only provide a picture of how the plant is functioning at a specific point in time and interpretation of the data over any time-scale greater than the instant in which it is measured must be made with caution. Given that all plant processes are subject to variation according to a number of interacting factors, it is often more desirable to obtain an integrated measure of performance over a longer time-span. This approach can be particularly useful with regard to environmental stress factors (e.g., temperature, salinity) because the stress symptoms may only become visible after a long period of cumulative exposure and the constraints on carbon uptake can be very subtle, particularly in woody tree species (Panek & Waring, 1997).

In recent years the analysis of stable carbon isotopes has proven a useful tool for assessing long-term photosynthetic performance in plants. The carbon signature provides an integrated measure of isotopic discrimination over the entire period in which the carbon in that tissue was assimilated (O'Leary, 1988). It is directly linked to plant function in that the fractionation of carbon is associated with the diffusion of CO_2 and the chemical processes of photosynthesis, and is a function of both photosynthetic rate and stomatal conductance, i.e., WUE (Farquhar, 1980).

The main objective of the work presented in this chapter was to investigate long-term photosynthetic performance in *A. marina* subsp. *australasica* under field conditions by way of an analysis of stable carbon isotope abundance in leaf, stem and propagule tissue sampled from the entire natural range of this species in New Zealand. The findings were used to make an evaluation of the photosynthetic differences between the populations of mangrove, to establish

which, if any, were subject to greater levels of photosynthetic stress, and to ascertain what implications this might have regarding the current southern geographic limit of mangrove in New Zealand.

7.2 Theory of carbon isotope fractionation

Atmospheric CO_2 provides plants with the carbon that is essential to the construction and functioning of all plant tissue. It contains relatively constant proportions of the stable (non-radioactive) and unstable (radioactive) isotopic forms of carbon, of which the stable isotopes ^{12}C and ^{13}C, respectively make up approximately 98.9% and 1.1% of the total (Griffiths, 1993, O'Leary, 1988).

The accurate measurement of absolute isotope quantities is problematic, given the small natural abundance of ^{13}C and the difficulties inherent in maintaining precision of measurement during analysis. Instead, the isotope ratios (R) of a sample and a reference standard are normally measured, and the relative difference between them, delta (δ), is calculated as follows:

$$\delta^{13}C\ (^{o}/_{oo}) = (R_{Sample} - R_{Standard})/R_{Standard} \times 1000$$

$$\text{or} = [(R_{Sample} / R_{Standard}) - 1]\ 1000 \qquad (1)$$

where R_{Sample} and $R_{Standard}$ are the molar abundance ratios ($^{13}C/^{12}C$) of the sample and a defined standard respectively (Farquhar *et al.*, 1982). Carbon isotope values are typically expressed in the unit-less measure of parts per thousand, or per mille (‰). The accepted standard against which the sample carbon ratio is normally compared is CO_2 generated from belemnites in the Pee Dee limestone formation in South Carolina, with a $^{13}C/^{12}C$ ratio of 0.01124. Alternatively, a number of secondary standards that have been calibrated against the original PDB carbonate may be used for comparison (Griffiths, 1993). By definition, if a sample has a positive δ value it contains more of the heavier isotope (^{13}C) than the standard. Conversely, if a sample has a negative value, it contains less of the heavier isotope than the standard. For instance, if a leaf sample is found to have a $^{13}C/^{12}C$ ratio R less than the standard's by 10 parts per thousand, this value is reported as $\delta^{13}C = -10$ ‰.

$^{13}C/^{12}C$ carbon isotope ratios in plant tissue are generally smaller than that in the PDB carbonate standard, so the values for sample $\delta^{13}C$ are normally negative. If the carbon source is already ^{13}C-depleted (e.g., if the plants are making use of respired CO_2), or if discrimination against ^{13}C occurs to a greater degree, then according to equation (1), $\delta^{13}C$ values of the plant tissue will be increasingly negative. For aquatic plants the values are slightly different due to fractionation associated with the dissolution of atmospheric CO_2 into water and the dehydration of dissolved CO_2 into bicarbonate ions (Keely *et al.*, 1986).

7.3 Carbon isotope fractionation and photosynthesis

Typically, the ^{13}C /^{12}C ratio in plant tissue is smaller than that in the atmosphere due to the isotopic fractionation associated with the processes of photosynthesis. It occurs because the greater mass of ^{13}C and its ability to form stronger chemical bonds cause the reactions and processes involving the heavier isotope to proceed at a slower rate, thus allowing the lighter isotope, ^{12}C to be taken up more readily.

In terrestrial plants there are two primary causes of fractionation; namely diffusion of CO_2 into the cytoplasm, and the carboxylation step(s) of photosynthesis (Farquhar *et al.*, 1982, Park & Epstein, 1961). Ultimately, a smaller proportion of the heavier isotope is incorporated into the plant tissue relative to the carbon source (e.g., atmospheric CO_2) due to discrimination against ^{13}C by these processes; in other words, the tissue is depleted in ^{13}C relative to the source of CO_2.

Since the realisation that the $\delta^{13}C$ values of plant tissue are directly linked to discrimination against ^{13}C by the initial carboxylation reaction of photosynthesis (Craig, 1953 as reviewed by O'Leary, (1981)), carbon isotope analysis has become a widely used technique for determining pathways of CO_2 fixation in higher plants. Vascular plants fix atmospheric CO_2 by one of three main photosynthetic pathways; C_3 (Calvin-Benson cycle), C_4 (Hatch-Slack pathway) or by CAM (Crassulacean acid metabolism). Enzymatic and anatomical characters specific to each of these groups of plants determine the extent of isotopic fractionation, giving rise to a distinctive range of ^{13}C content in the tissues. $\delta^{13}C$ values in C_3 plants generally fall between -20 ‰ to -35 ‰. In C_4 plants $\delta^{13}C$ values fall between – 11 ‰ and -15 ‰ due to fractionations associated

with two carboxylation enzymes rather than one. For CAM plants, the range of $\delta^{13}C$ values sits in between those of C_3 and C_4 plants (Dawson *et al.*, 2002).

Mangroves possess the anatomical and physiological characters typical of plants employing C_3 photosynthetic biochemistry. As summarised by Ball (1986), mangrove leaves do not have bundle sheath cells characteristic of C_4 species; their photosynthetic rates are maximal at leaf temperatures less than 35°C; light saturation generally occurs at intensities 30–50% that of full sunlight, and foliar carbon isotope composition lie well within the reported range for C_3 plants.

Following advancements in the use of stable carbon isotopes to investigate the different photosynthetic pathways, several models describing the fractionation of carbon isotopes during C_3 photosynthesis were subsequently developed. Of these, the most widely utilised is that developed by Farquhar *et al.* (1982) relating the $\delta^{13}C$ value of C_3 plant tissue ($\delta^{13}C_p$), relative to the PDB limestone standard, to the ratio of intercellular and ambient partial pressures of CO_2 (p_i / p_a). The model defines the value of $\delta^{13}C_p$ as influenced by three factors:

- Discrimination associated with the diffusion of $^{13}CO_2$ relative to $^{12}CO_2$ through air (*a* in equation 2) and with carboxylation due to ribulose-1,5-biphosphate carboxylase-oxygenase (RuBisCO), the primary carbon-fixing enzyme in C_3 plants carboxylation (*b* in equation 2);
- The isotopic composition of atmospheric CO_2 ($\delta^{13}C_a$), relative to the defined standard PDB limestone.
- Stomatal factors affecting the ratio of intercellular to ambient partial pressures of CO_2 (p_i / p_a).

The Farquhar (1982) model is defined in terms of the following relationship:

$$\delta^{13}C_p = \delta^{13}C_a - a - (b - a)\, p_i / p_a \qquad (2)$$

where the ratio p_i / p_a is in turn determined by the balance between the net photosynthetic rate (A) and stomatal conductance to CO_2 (gS) according to the relationship[1]

$$p_i = p_a - \frac{A}{gS} \qquad (3)$$

[1] *[pressure units are calculated assuming a standard temperature of 20°C and atmospheric pressure of 0.1013 MPa]*

In C_3 vascular land plants the values of a and b in equation 2 are considered to be constant. Fractionation associated with the slower diffusion of $^{13}CO_2$ relative to $^{12}CO_2$ (i.e., a in equation 2) amounts to about 4.4‰ (Craig, 1953, O'Leary, 1993). The carboxylation step in C_3 plants, involving the enzyme ribulose-1,5-biphosphate carboxylase-oxygenase (RuBisCO), discriminates against $^{13}CO_2$ relative to $^{12}CO_2$ by about 29‰ (O'Leary, 1988, Roeske & O'Leary, 1984).

According to the above equations and assuming also a constant value for p_a, the carbon isotopic composition of plant biomass is determined by any factor that influences p_i through changes in stomatal conductance and the net rate of photosynthetic CO_2 assimilation. If stomatal conductance is low relative to the net rate of photosynthesis, then p_i is low, and isotopic discrimination ($\delta^{13}C_p$) approaches the value of a in equation 2 (4.4‰; the fractionation associated with the diffusion limitation imposed by stomatal conductance). Equally, if stomatal conductance is high relative to the net photosynthetic rate, the p_i is high and isotopic discrimination tends towards the value of b in equation 2 (29‰; the fractionation associated with carboxylation).

Over time, modifications to the basic model were developed that account for isotopic fractionations associated with additional cell processes such as dark and light respiration, and in C_4 plants, CO_2 leakage from the parenchyma sheath cells to the mesophyll cells (Vogel, 1993). More recently Ivlev (2004) compared two isotopically different models of carbon flow in plant cells where effects of environmental factors on the carbon isotope composition of plant biomass could either be defined by the variable contributions made by diffusion and carboxylation to discrimination of ^{13}C during CO_2 assimilation (Farquhar *et al.*, 1982), or alternatively by the counteracting effects of photoassimilation and photorespiration (Ivlev, 2004, Jillon & Griffiths, 1997). Unlike photoassimilation (as above) which results in discrimination against ^{13}C and depletion of the heavier isotope in the tissues relative to the source, photorespiration produces the opposite effect.

According to equation 2, the $\delta^{13}C$ value of plant biomass is determined to some extent by the $\delta^{13}C$ value of the source air. Since $\delta^{13}C$ of the source is a variable parameter e.g., soil respired CO_2 is generally more depleted of ^{13}C relative to atmospheric CO_2 (Schleser & Jayasekera, 1985), carbon isotope values in tissue are often defined in terms of discrimination (Δ), to account for this

variation. The use of Δ corrects for the effects of source CO_2, taking into account the difference in $\delta^{13}C$ between the source and the product, producing an estimate of discrimination that is directly proportional to the extent of fractionation for the biological process alone. Although $\delta^{13}C$ and Δ represent different parameters, their values are expressed using the same notation (‰), however, Δ values are generally positive. Δ is calculated according to the relationship (Farquhar & Lloyd, 1993) :

$$\Delta = \frac{\delta^{13}C_{air} - \delta^{13}C_{plant}}{1 + \delta^{13}C_{plant}/1000} \quad (4)$$

where the values for $\delta^{13}C_{air}$ and $\delta^{13}C_{plant}$ are derived respectively from R_a/R_s-1, and R_p/R_s-1. R_a represents the isotopic constituents of the source air, R_p the plant organic material and R_s the PDB standard. Since the year 1990, the accepted value for R_a is 0.01115, thus giving δ_{air} a value of 0.008 (or in terms of $\delta^{13}C$, -8.0 ‰) (Griffiths, 1993). δ_p, the isotope composition of the plant sample ranges between -8.9‰ and -30.1‰ (Farquhar & Lloyd, 1993). The second part to the denominator of equation 4 is fairly small and is often omitted in calculations (O'Leary, 1993).

7.4 Water use efficiency and foliage $\delta^{13}C$ in C_3 plants

Carbon isotope discrimination also provides a useful estimate of plant water-use efficiency; the ratio of CO_2 assimilation rate (*A*) to transpirational water loss (*E*) (Ehleringer *et al.*, 1992, Farqhuar *et al.*, 1989). Both $\delta^{13}C$ (or Δ) and A/E are a function of p_i / p_a, as illustrated by equations (5) – (7):

$$E = vg \quad (5)$$

and

$$A = (p_a - p_i)g/1.6 \quad (6)$$

where *v* is the water vapour pressure difference between the leaf intercellular spaces and the atmosphere, and *g* is the leaf conductance for water vapour. 1.6 is the ratio of gaseous diffusivities of CO_2 and water vapour in air (i.e., the binary diffusivity of water vapour and air is 1.6 times greater than that of CO_2 and air).

$$\frac{A}{E} = \frac{p_a\left(1 - \frac{p_i}{p_a}\right)}{1.6v} \quad (7)$$

Since the diffusion through the stomata is the same for A and E, instantaneous water-use efficiency can be determined without an estimate for g (Ehleringer *et al.*, 1992).

In C_3 plants there is a negative correlation between water use efficiency and carbon isotope discrimination (O'Leary, 1988). Water use efficiency increases either when stomatal closure occurs in association with unchanged carboxylation capacity, or if CO_2 assimilation increases at a fixed stomatal conductance. Both may ultimately be growth-limiting since the former results in a drop in p_i and reduced photosynthesis in response to increasingly limiting CO_2 levels, and the latter is energy and nutrient expensive.

The comparatively high WUE of mangrove species relative to other C_3 plants is assumed to be a consequence of growth in a saline environment. The high energy costs associated with the exclusion of salt during water uptake and the maintenance of tissue salt concentrations at physiologically acceptable levels promote conservative water use strategies (Ball, 1986, 1988a). Under escalating environmental stress, water use efficiency in mangrove increases (Clough & Sim, 1989) but it does so at the expense of CO_2 assimilation and ultimately growth, since any restriction in water efflux from the leaves also restricts the rate of CO_2 influx into the leaves.

7.5 Carbon isotope discrimination in *Avicennia marina* subsp. *australasica* over latitudinal and salinity gradients

7.5.1 Materials and Methods

Leaf, stem and propagule tissue was collected from fourteen mangrove sites within the natural range of *Avicennia* in New Zealand to investigate the variability in stable carbon isotopes over gradients of latitude and salinity. Ten sites of similar salinity were selected from latitudes between 34°55'S and 38°03'S.

Four additional sites located around latitude 35°36'S; one close to open ocean water and the remainder common to a single estuarine system, were selected on the basis of contrasting salinities (Figure 7.1). Salinity of these four sites ranged from brackish in the upper reaches of the Ngunguru river estuary

(approximately 8 km from the open coastline), to close to full-strength seawater at Matapouri where the mangroves grow within 500 m of open coastal waters (refer to Figure 7.2: Matapouri and Ngunguru River).

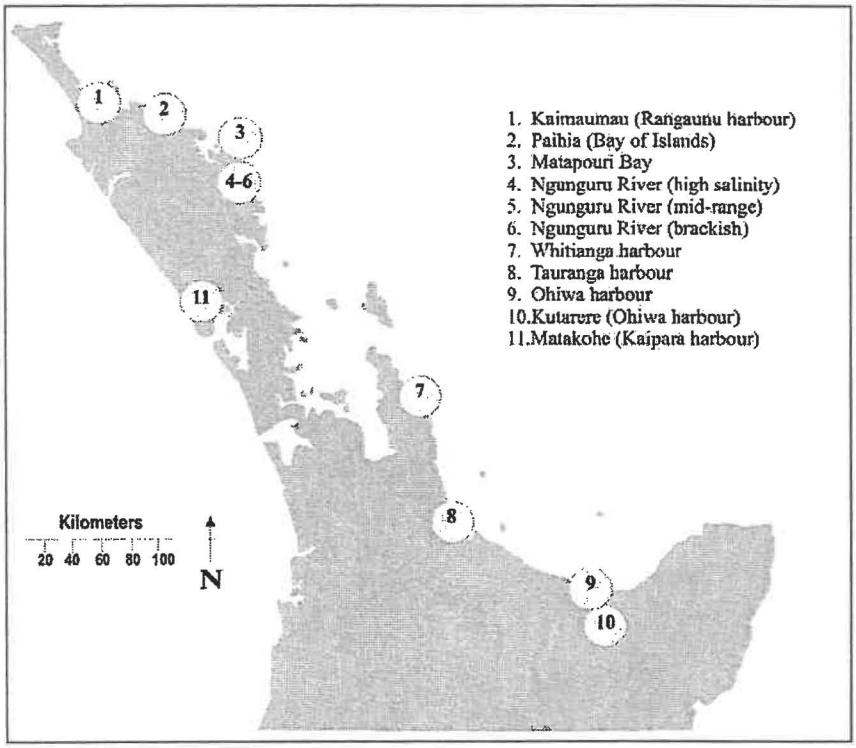

Figure 7.1 Schematic of the upper North Island of New Zealand showing locations of *Avicennia marina* subsp. *australasica* populations sampled for stable carbon isotope analysis.

7.5.1.1 Site salinity measurements

Substrate salinity was estimated from samples of interstitial water (pore water drained from between the soil particles), collected from a series of 20 cm-deep core holes around the base of the sampled trees. Five water samples were collected from at each site shortly after the low tide had occurred and when no significant depths of standing water were present round the mangroves. The conductivity and temperature of each sample were measured immediately after collection using a Series 3 RE 387 Tx conductivity meter and glass platinum-plate dip cell (range 100µS – 200mS) and a temperature probe attached to a DR 359 Tx ion concentration pH meter (EDT Instruments Ltd, United Kingdom) Conductivity values were converted to a salinity scale and adjusted for temperature using the 1978 Practical Salinity Scale Equations (1980).

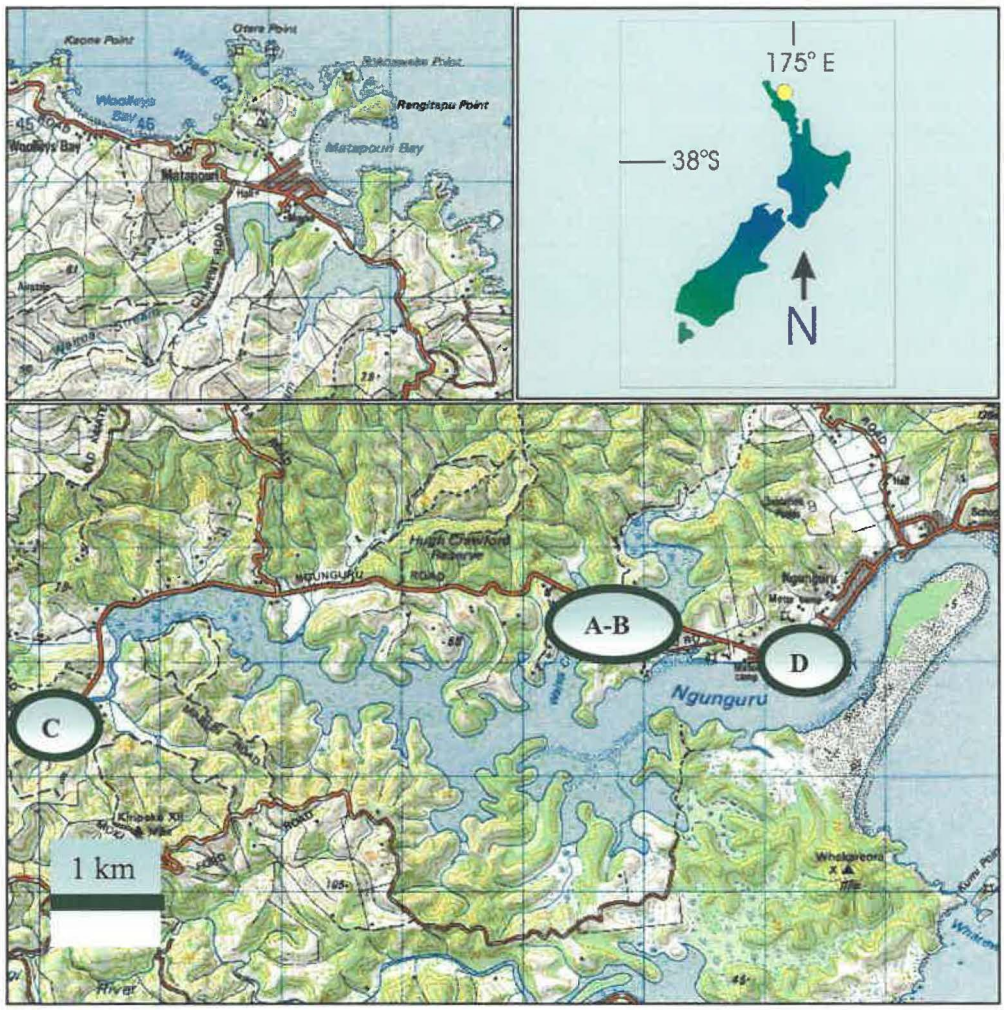

Figure 7.2 Site locations of *Avicennia marina* subsp. *australasica* populations sampled for stable carbon isotope analysis at Matapouri and in the Ngunguru River and estuary, Northland, North Island, New Zealand. Map: http://www.nztopoonline.co.nz

7.5.1.2 Tree selection and sample collection

Samples comprising single branchlets of approximately 30 cm in length were removed from up to five individuals at each of the selected mangrove populations (points 1-11 in Figure 7.1) in October 2002, July 2003 and November 2003. Given that leaf carbon isotope ratios are strongly correlated to the light environment (Ehleringer & Osmond, 1989), all samples were selected from north-facing, fully sunlit positions on the trees to ensure the closest match in light regime. Where possible, trees were chosen for their similarity in size, position in the mangrove fringe, and the presence of propagules. Following collection, the samples were transported in sealed plastic bags to the laboratory where they were prepared for drying.

7.5.1.3 Sample preparation

Leaf, stem and propagule samples, as detailed below, were removed from the detached branchlets within two days of collection.

Leaf samples comprised one entire leaf of the first fully expanded pair (i.e., one leaf of the penultimate pair) on a branchlet.

Stem samples consisted of a 1 cm length cross-section of the previous season's woody tissue removed from just above the third node of each branchlet. Before drying, bark was stripped from the sample sections with a sharp blade.

Cotyledon tissue was removed from fully-developed, but still-attached propagules

All the sampled tissue was dried to a constant weight at 80°C in a Contherm Series 5 (Contherm Scientific Ltd, New Zealand) laboratory oven after which it was ground to powder (fineness <10 μm) using a Retsch GmBH & Co. MM 200 (Germany) ball mill. The ground samples were transferred to storage in glass screw-top vials until analysis could be completed.

7.5.1.4 Laboratory analysis

Stable carbon isotope abundance in the mangrove tissue was measured at the University of Waikato Stable Isotope Unit using a Dumas elemental analyser (Europa Scientific ANCA-SL) interfaced to a stable isotope mass spectrometer (Europa Scientific Tracermass, Scientific Ltd, Crewe, United Kingdom). Up to five samples from each population were analysed to account for natural variability.

The analysis procedure involved introducing individual samples (comprising 3 – 4 mg of dried ground tissue encapsulated in tinfoil) into an oxygen-enriched combustion reactor maintained at a temperature of around 1020°C. After combustion, the gases were swept with helium carrier-gas through a reduction reactor and water filter onto a gas chromatograph column. CO_2, produced by combustion of carbon in the solid sample, was then separated from the other gases and a sub-sample was transferred into the mass spectrophotometer for the measurement of $\delta^{13}C$ abundance. Using this system, the precision of measurement for isotopic composition of duplicate samples was ± 0.14‰.

All samples were analysed against a laboratory sucrose reference with a delta value of -10.80‰. The reference was standardized against a CSIRO

(Canberra, Australia) certified sucrose standard (calibrated relative to Pee Dee Belemnite).

7.5.1.5 Calculations and statistical analyses

Datasets of leaf $\delta^{13}C$ values obtained at two different times of the year were subjected to a t-test to ascertain similarity of the mean values with a view to combining the data.

Discrimination Δ, was calculated according to Farquhar and Lloyd (1993), using the following equation and assuming the value for $\delta^{13}C$ of air = -8.0‰.

$$\Delta = \frac{\delta C_{air} - \delta C_{plant}}{1 + \delta C_{plant}}$$

The carbon isotope data were compared on the basis of latitude and salinity gradients. All sites where the average salinity of the standing water at low tide was between 26.7 and 36.2 ppt were compared over a range of latitude (i.e., they were treated in the analysis as "similar salinity sites" on the basis that salinity in the stated range contributed no significant variation to the observed $\delta^{13}C$ values, see section 7.6.3). The remaining sites encompassed a range of salinity and were compared on that basis (average salinity ranged between 6.7 and 36.2 ppt at these sites).

Correlation and regression analyses were undertaken to determine the associations between leaf, stem and propagule isotope data with latitude and salinity. A regression was also calculated for leaf $\delta^{13}C$ and mean monthly air temperature at the sample sites. The leaf sample set was used in these calculations because this had the largest sample numbers of the three tissue types.

All statistical analyses were performed with STATISTICA (data analysis software system), version 6. StatSoft, Inc. (2003). www.statsoft.com.

7.6 Results

The raw and mean primary mass-spectrophotometer values for $\delta^{13}C$ and mean Δ values calculated for foliage, stem and propagule tissue of *Avicennia marina* subsp. *australasica* over latitudinal (°S) and salinity (mg g^{-1}) gradients in New Zealand are tabled in Appendix VI.

All calculations, graphs and discussion relevant to the **leaf** samples are based on a combined dataset made up of two collections (August and December 2003) from the same sites. These data were pooled on the strength of t-test and

f-test results which revealed no significant differences between the means and variances of either group.

7.6.1 Tissue differences

The leaf samples were significantly more depleted in ^{13}C (leaf mean δ^{13} C = -25.60, *SD* = 0.84) relative to both stem and propagule samples; stem mean δ^{13} C = -24.58, *SD* = 1.42, t (71) = -3.77, p <0.001, and propagule mean δ^{13} C = -24.73, *SD* = 0.97, t (71) = -3.82, $p < 0.001$. However, ^{13}C-depletion in the stem and propagule samples did not differ significantly.

7.6.2 Carbon isotope discrimination over a gradient of latitude

The variation in raw values of Δ and $\delta^{13}C$ at mangrove sites of similar salinity, sampled over a range of approximately 3.5° latitude, amounted to 4.3 ‰ in leaves, 5.4 ‰ in stems and 4.2 ‰ in cotyledons. Mean $\delta^{13}C$ values (± standard deviation) were between -23.69 ± 0.49 ‰ and -26.36 ± 0.69 ‰ in leaves, -22.17 ± 1.10 ‰ to -26.05 ± 0.20 ‰ in stems and -23.97 ± 0.62 ‰ to -25.03 ± 0.36 ‰ in cotyledons. Corresponding mean Δ values (± standard deviation) were 16.6 ± 0.3 ‰ to 18.4 ± 0.7 ‰ in leaves, 14.2 ± 1.1 ‰ to 18.1 ± 0.2 ‰ in stems and between 15.9 ± 0.62 ‰ and 17.3 ± 0.36 ‰ in cotyledons (see Appendix VII for raw data).

Leaf samples from Paihia, at latitude 35°17'S (Figure 7.1) were the most depleted in ^{13}C relative to samples from all the other sites of similar salinity (i.e., Δ values were highest and $\delta^{13}C$ were the most negative at this site). In contrast, the stem and cotyledon samples with the most ^{13}C-depleted carbon signature were collected from the northern-most site at Kaimaumau (Figure 7.1). In all tissue types, the samples least depleted in ^{13}C were those from Ohiwa harbour at latitude 38°00'S (Figure 7.1), close to the southern geographical limit of mangrove in New Zealand.

A negative correlation was evident between latitude and the isotopic discrimination of ^{13}C in leaves, stems and propagules i.e., moving from north to south the plant tissues became less depleted in ^{13}C (signified by smaller Δ and less negative $\delta^{13}C$ values).

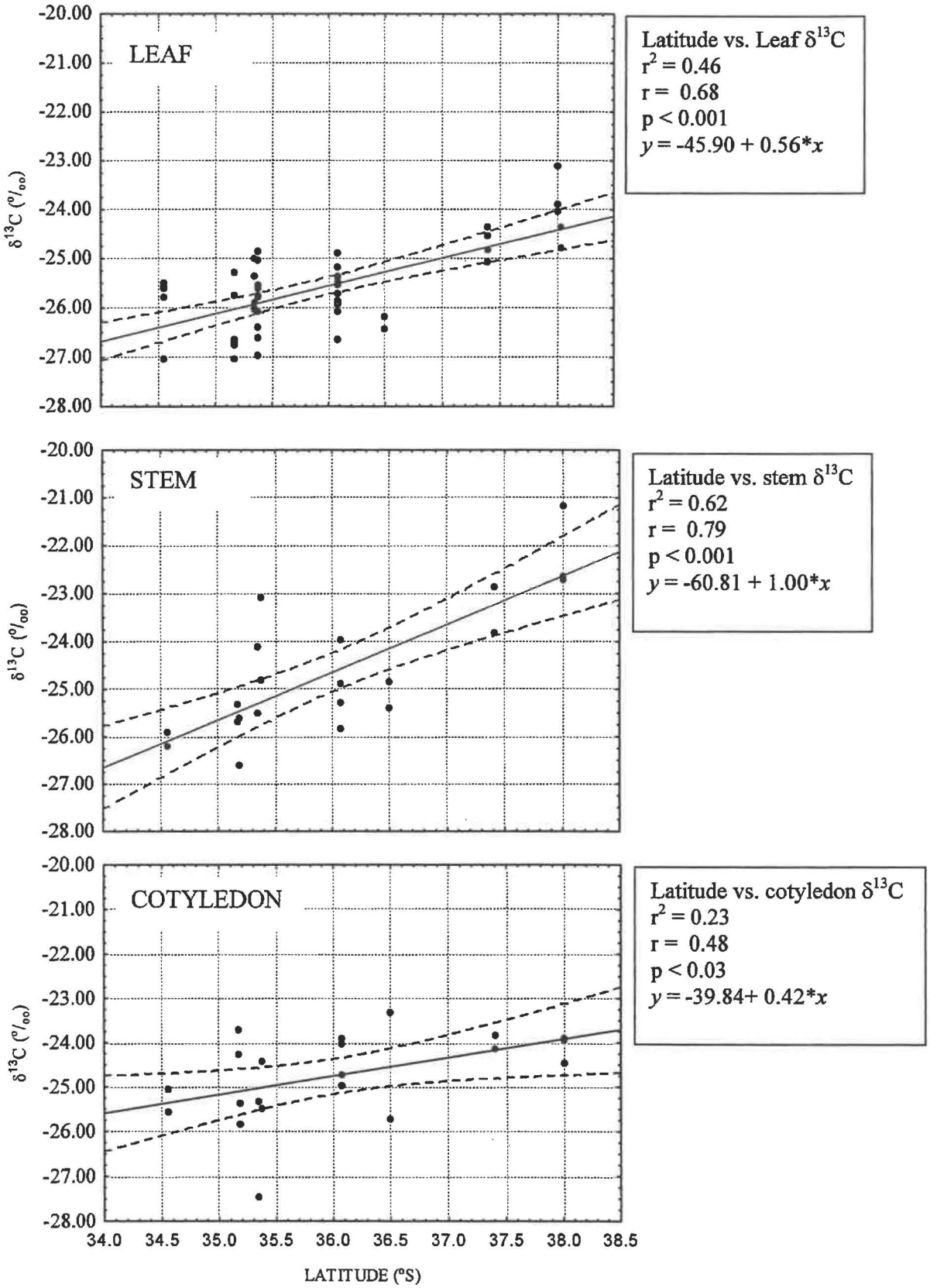

Figure 7.3 Latitudinal variation of $\delta^{13}C$ in leaf (top), stem (middle) and propagule cotyledon (bottom) tissue of *Avicennia marina* subsp. *australasica* from sites sampled over a range of latitude in New Zealand. Dotted lines indicate 95% confidence limits.

Carbon isotopic composition of stem tissue showed the closest association with site latitude (n = 21, r^2 = 0.62, p < 0.0000). However, significant associations with latitude were also observed with leaf tissue (n = 50, r^2 = 0.46, p < 0.0000) and with cotyledon tissue (n = 21, r^2 = 0.23, p < 0.027) (Figure 7.3). All correlations are summarized in table 7.2.

The relationship between sample site mean monthly temperature and $\delta^{13}C$ of leaf tissue was significant (r = -0.66, p<0.001). Furthermore, a temperature response of -1.3‰ $\delta^{13}C$ $°C^{-1}$ was established for *Avicennia* in New Zealand from a regression of these two variables (Figure 7.4).

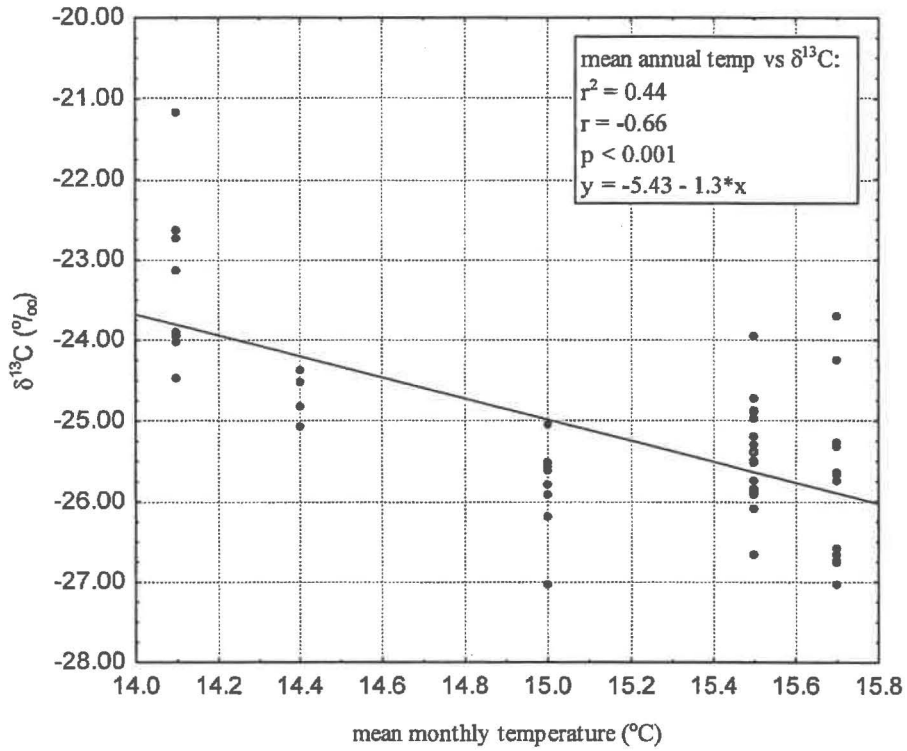

Figure 7.4 The relationship between mean monthly temperature (°C) of *Avicennia* locations in New Zealand and foliar $\delta^{13}C$ abundance (‰) in samples from those locations.

The $\delta^{13}C$ values reported in the literature for *Avicennia* spp. growing at low-latitude locations were significantly more ^{13}C-depleted relative to the New Zealand samples. In the temperate latitudes of New Zealand $\delta^{13}C$ values averaged around -26.4 ‰, whereas in tropical latitudes the average was between -27.0 ‰ and -29.0 ‰ (Figure 7.5).

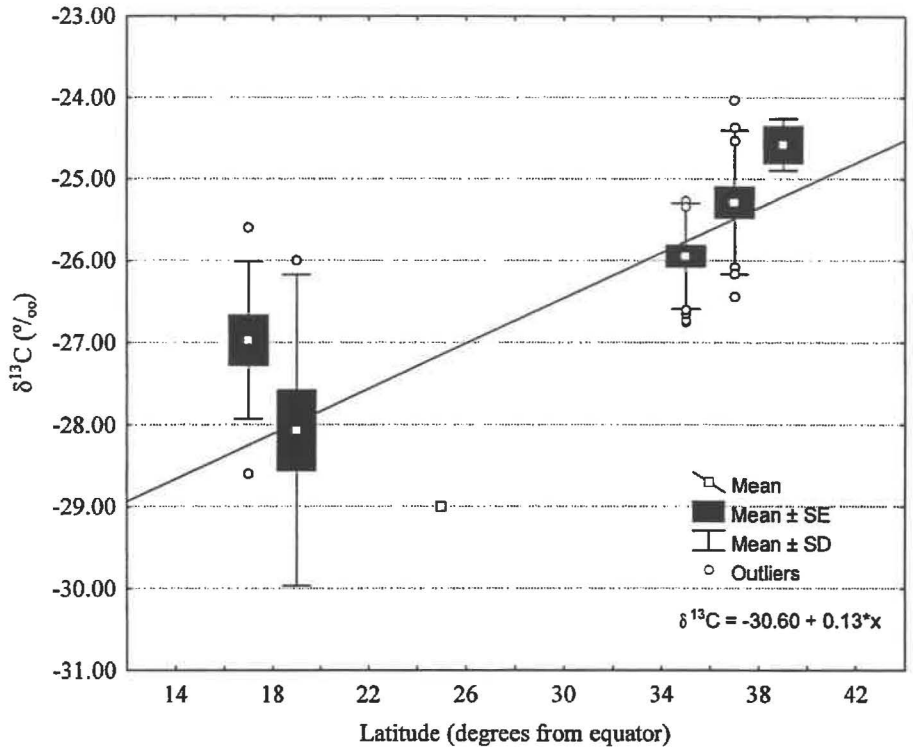

Figure 7.5 The relationship between foliar $\delta^{13}C$ (‰) and latitude of origin (in degrees from the equator). New Zealand means are derived from the foliar $\delta^{13}C$ values measured in the current study. Lower latitude means are derived from *Avicennia* $\delta^{13}C$ values reported in the literature.

7.6.3 Carbon isotope discrimination over a salinity gradient

Carbon discrimination was measured on plant tissues from sites along a salinity gradient within the Ngunguru estuary (Table 7.1, Figure 7.2, Appendix VII for raw data). Mean $\delta^{13}C$ values (± standard deviation) for leaves ranged from -27.15 ± 0.65 ‰ at the most brackish site (Ngunguru C) to -25.65 ± 0.46 ‰ at the site with the highest measured salinity (Ngunguru D). Mean $\delta^{13}C$ values in stems and cotyledons ranged from -25.65 ± 1.07 ‰ to -23.95 ± 1.07 ‰ and from -26.37 ± 1.50 ‰ to -24.19 ± 0.35 ‰. This gave total ranges of 3.3 ‰, 3.09 ‰ and 3.49 ‰ for leaves, stems and cotyledons, respectively. Corresponding Δ values at the same sites were 19.2 ± 0.7 ‰ and 17.7 ± 0.5 ‰, 17.7 ± 1.1 ‰ and 15.9 ± 1.2 ‰, and 16.2 ± 0.35 ‰ and 18.4 ± 1.50 ‰ for leaves, stems and cotyledons, respectively.

Table 7.1 Sampling sites with associated latitude (°S) (North Island, New Zealand) and salinity of substrate water (mg g^{-1})

Sampling Site	Latitude (°S)	Salinity (mg g^{-1})
Kaimaumau	34°55'	26.7±3.8
Paihia	35°17'	34.7±0.7
Matapouri	35°34'	36.2±1.0
Ngunguru (D)	35°38'	33.1±1.5
Ngunguru (A)	35°37'	21.4±0.7
Ngunguru (B)	35°37'	21.4±0.7
Ngunguru (C)	35°38'	6.7±0.4
Matakohe	36°08'	27.9±1.2
Mangawhai	36°08'	28.4±2.5
Whitianga	36°50'	31.2±0.8
Tauranga	37°40'	29.0±1.4
Ohiwa	38°00'	34.1±0.7
Kutarere	38°03'	30.3±1.3

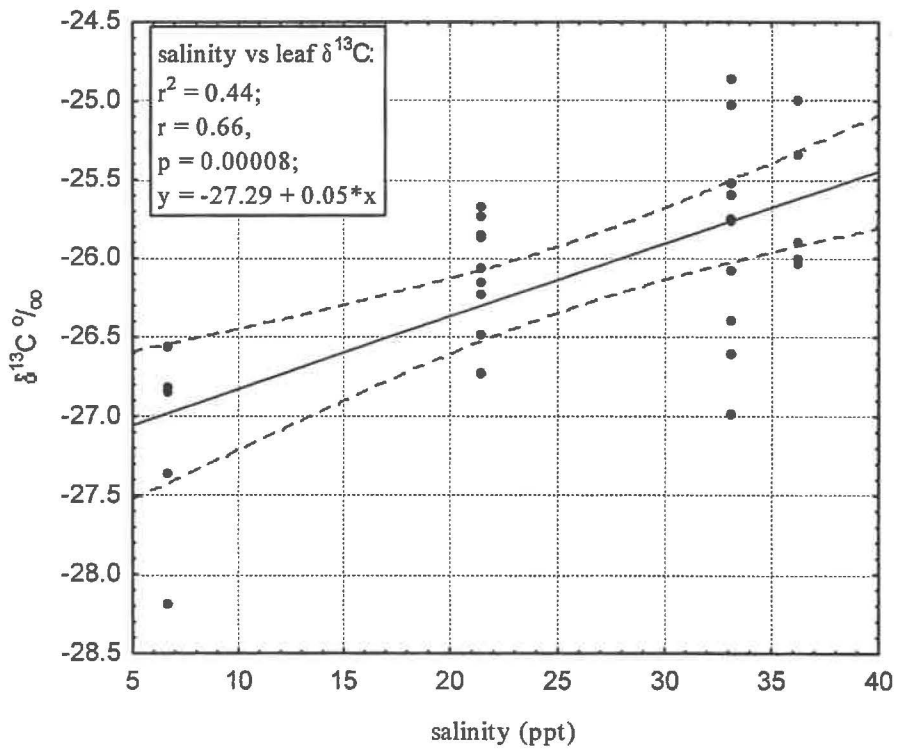

Figure 7.6 ^{13}C discrimination in leaf tissue of *Avicennia marina* subsp. *australasica* from sites ranging in salinity but common to a single estuarine system at approximate latitude 35°36'S in New Zealand (Ngunguru river estuary, refer to Figures 7.1 and 7.2). Solid line is a linear regression, dotted lines indicate 95% confidence limits

There was no significant difference in carbon isotopic discrimination between sites where salinity ranged between 15ppt to 36 ppt. However, on inclusion of the brackish site values (low salinity, around 6.7 ppt) in a linear regression analysis, a significant overall trend of decreasing ^{13}C discrimination ($\delta^{13}C$ values less negative) at sites of higher salinity was evident ($n = 29$, $r^2 = 0.44$. $p < 0.0000$, $y = -27.29 + 0.05 * x$) (Figure 7.6). Salinity had no significant effect on the variation of carbon isotopic discrimination in stem tissue ($n = 8$, $r^2 = 0.11$, $p = 0.42$) or in cotyledon tissue ($n = 8$, $r^2 = 0.41$, $p = 0.08$).

Table 7.2 Correlation and regression summary statistics for $\delta^{13}C$ in *Avicennia* leaf, stem and cotyledon tissue sampled over latitude and salinity gradients. The regression constants are only shown for significant correlations ($\delta^{13}C = a + b * \text{latitude}$ and $\delta^{13}C = a + b * \text{salinity}$).

Sampling gradient	n	r^2	p	Constant (a)	Slope (b)
Latitude (leaf tissue)	50	0.46	<0.0000	-45.90	0.56
Latitude (stem tissue)	21	0.62	<0.0000	-60.81	1.00
Latitude (cotyledon tissue)	21	0.23	0.0266	-39.84	0.42
Salinity (leaf tissue)	29	0.44	<0.0000	-27.29	0.05
Salinity (stem tissue)	8	0.11	0.42	_	_
Salinity (cotyledon tissue)	8	0.41	0.08	_	_

7.7 Discussion

A latitudinal decline in ^{13}C discrimination was clearly evident in all the *Avicennia* tissues sampled in this study, with a decrease in $\delta^{13}C$ values over 3° of latitude (north to south) of between 4.2 and 5.4 ‰. A similar latitude-specific response in carbon discrimination was reported by Körner *et al.* (1991) in sampling a number of terrestrial C_3 plant species from altitudinally similar sites over a latitudinal range of 80°. They reported mean Δ values around 19.1 ‰ in plants from sub-Antarctic and Arctic sites, while the mean Δ for tropical species was approximately 21.8 ‰ (Δ was used on this occasion to account for the variability in $\delta^{13}C$ of source air over time).

Interestingly, when $\delta^{13}C$ values for New Zealand *Avicennia* were also compared with those of *Avicennia* spp. examples in the literature, in this case from lower latitudes between latitude 16° and 18° N (Lin & Sternberg, 1992,

Medina & Francisco, 1997), a similar latitudinal cline was found. In the temperate latitudes of New Zealand, $\delta^{13}C$ values averaged around -26.4 ‰, whereas in more tropical latitudes they averaged around -29 ‰. The carbon isotope values obtained for *Avicennia* in the present study ($\delta^{13}C$ between 15.6 ‰ and 17.5 ‰), were slightly lower than those reported for woody plants from similar latitudes by Körner *et al.* (1991) and may be due to the higher water-use efficiencies that prevail amongst mangrove species (Ball, 1986) as compared with other C_3 plants.

In each case, the change in ^{13}C discrimination is consistent with a temperature response, since the effects of decreasing temperatures on C_3 photosynthesis are generally manifested in the form of plant tissue that is less-depleted in ^{13}C (i.e., less negative $\delta^{13}C$ values, lower Δ values). For example, $\delta^{13}C$ values were less negative by about 3 ‰ in tomato plants grown between 17°C and 32°C, a difference attributed to the effects of cooler growing temperatures (O'Leary, 1988). Another example is seen in work with juniper (*Juniperus monosperma*), where a temperature response of -0.27‰ $\delta^{13}C$ $^{\circ}C^{-1}$ was calculated from a regression of mean monthly temperatures and leaf-cellulose $\delta^{13}C$ (Leavitt & Long, 1982). In the present study, mean monthly temperatures over a geographical gradient were used to assess a temperature relationship for *Avicennia* in New Zealand. The resulting temperature response was significant ($r = 0.66$), but was larger in magnitude at -1.3 ‰ $\delta^{13}C$ $^{\circ}C^{-1}$.

The basis for these differences in ^{13}C lies in the relationship defined in equation 2 by Farquhar *et al.* (1982), in which the carbon isotopic composition of plant biomass is determined by any factor that influences p_i through changes in stomatal conductance and the net rate of photosynthetic CO_2 assimilation. Unfortunately other factors, for instance suboptimal light levels, can also influence the stable carbon isotope composition of the various plant tissues (O'Leary, 1981). Using carbon isotopic data alone it is not possible to distinguish which factor (stomatal or biochemical) has the greatest influence on CO_2 assimilation and p_i. However, separating the two can be attempted if the isotopic abundances of other elements are also considered. Recently Scheidegger *et al.* (2000) developed a model incorporating oxygen ($\delta^{18}O$) and carbon ($\delta^{13}C$) isotopes that allows distinction between stomatal responses and alterations in photosynthetic capacity in reaction to changes or stresses in the environment. Unfortunately this model was not tested in the present study because elements

other than carbon were not analysed; instead, interpretation of the results is augmented by comparison with gas exchange data collected at three field sites, all of which were included in the isotope study.

The carbon isotopic composition of plant biomass is influenced by a variety of environmental factors including growth temperature, CO_2 source, light, water and nutrient availability, osmotic stress and age of the photosynthesising tissue. However the means by which these factors impact the carbon isotope composition of plant tissue is open to different interpretations. In terms of a steady-state model based on Farquhar *et al.* (1982), changes in carbon isotope composition of plant biomass result from variable contributions of isotope effects by diffusion and RuBP carboxylation to ^{13}C discrimination. Environmental factors, through their impact on p_i (the partial pressure of CO_2 in the leaf), alter the relative contributions of both processes, and thereby influence the levels of ^{13}C-enrichment or depletion in the plant tissues. However, in terms of the discrete model of carbon isotope fractionation in photosynthesis, as discussed by Ivlev (2004), changes in isotope composition result from opposing isotope effects associated with photorespiration and photoassimilation. Ivlev's work showed that some environmental stress factors increase the isotopic contribution from the ^{13}C-enriched photorespiratory flow to plant biomass, thereby resulting in ^{13}C-enriched tissues.

In both models, environmental factors will also introduce some variability in ^{13}C discrimination; therefore, in the present study sampling was carefully planned such that variables other than those targeted would be minimized as much as possible. At each sample site, leaf, stem and propagule samples of similar age and stage of development were taken from positions of similar aspect and light regime from comparable trees occupying similar positions in the mangrove fringe

Significant differences in the $\delta^{13}C$ content occur not only between individuals, but also on a number of levels within a single plant. These differences arise through changes in p_i, which can be altered by structural characteristics that define the gas exchange properties of the leaves (e.g., branch morphology), or by the different photosynthetic properties of the various organs (e.g., photosynthetic twigs, pods, or leaves) (Behboudian *et al.*, 2000, Walcroft *et al.*, 1996). The observed variation in the carbon isotope composition of the different tissue types in *Avicennia* may also result from differences in their chemical composition (Hobbie & Werner, 2004). Carbon fractionations, beyond those coupled with the

initial processes of diffusion and carboxylation, are involved with the production of a diverse range of tissues, metabolites and structural compounds in plants (e.g., starch, lignin, cellulose, glucose and lipids). A range of organs or tissues may therefore be ^{13}C-enriched or depleted relative to the whole-plant biomass (O'Leary, 1981). For example; wood is generally about 2 ‰ less depleted in ^{13}C than leaf tissue due to further fractionation steps associated with the formation of wood-cellulose and translocation of assimilates from sites of fixation (leaves) to the growing tissue (Damesin & Lelarge, 2003, Panek & Waring, 1997).

Some of the isotopic variation evident between the tissue types may also be due to the origins of the assimilated carbon and the period of time over which the tissue was formed (Miller *et al.*, 2001, Panek & Waring, 1997). Wood for example, continues to form throughout the year and is derived from the photosynthate of many leaves. Its carbon signature therefore reflects the conditions and photosynthetic activity in various portions of the crown during different seasons and over longer time periods than the comparatively shorter period during which an individual leaf reaches full expansion. In such cases the ^{13}C signature of the wood is probably more indicative of optimal photosynthetic activity rather than whole-canopy, since the leaves in the crown that operate at greater rates of photosynthesis contribute a comparatively greater proportion of assimilates to the tissues.

Avicennia at higher salinity were less ^{13}C-depleted relative to those samples taken from low salinity sites. This trend can be explained by the limitations placed on CO_2 assimilation by diffusion (Ball, 1988b, Ball & Farquhar, 1984a, O'Leary, 1988). A positive shift in substrate salinity increases soil-water potential and causes the plant to close stomata, thus inhibiting water loss but at the same time reducing movement of CO_2.

The resulting decreases in p_i are reflected in less negative $\delta^{13}C$ values (i.e., reduced ^{13}C discrimination) (Arens *et al.*, 2000). This trend has been confirmed by a number of studies, including those by Guy *et al.* (1980) and Neales *et al.* (1983) where $\delta^{13}C$ values in halophytes were less depleted in ^{13}C by up to 10 ‰ in response to increasing salinity. Impaired photosynthetic performance may also occur at low salinity as a result of K+ and N deficiencies in the leaves (Tuffers *et al.*, 2001), but in the present study no obvious effects were observed. The role of photorespiration in the synthesis of key metabolites has also been suggested as an

important influence on the carbon isotopic composition of halophyte plant biomass. In this case ^{13}C-enrichment of the tissues is caused by the activation of photorespiration in response to stresses such as increased salinity, and the subsequent increased contribution of the ^{13}C-enriched photorespiratory flow to plant biomass (Ivlev, 2004).

Seasonal changes in $\delta^{13}C$ have been observed in a range of plants including woody, herbaceous, evergreen and deciduous species (Ehleringer *et al.*, 1992, Leavitt & Long, 1985, Walcroft, 1994). Gradual seasonal increases of up to 5‰ have been reported in the carbon isotope ratios of some species (i.e., a decrease in ^{13}C discrimination) (Ehleringer *et al.*, 1992). In others, the carbon isotope ratios decreased as the growing season progressed, and in some there was no significant change (Damesin *et al.*, 1998, Walcroft, 1994). No significant differences in leaf carbon isotope composition were observed between sampling times in the present study but the possibility cannot be discounted. Sampling was only undertaken twice over a short time period (during and after winter) and the largest average discrepancy reported between sampling times amounted to a statistically insignificant 1.1 ‰. It is possible that if additional sampling had been undertaken throughout the year, significant seasonal differences, as seen in many other plant species, may have become evident.

7.8 Summary

The analysis of $\delta^{13}C$ isotope abundance in leaf, stem and cotyledon tissue of New Zealand mangrove has revealed a significant trend in relation to the latitudinal origin of these plants. A decrease in tissue ^{13}C depletion along an increasing latitudinal gradient indicates that mangrove growing near their southern geographical limits are subject to greater photosynthetic stresses than those growing in more favourable northern environments. Contributing factors are likely to be increasingly lower growing temperatures, shorter growing seasons, cold-induced photoinhibition and greater frequencies of winter chilling, frosts and frost damage with increasing latitude. In addition, plant performance is decreased by high salinity. Even though plants generally possess the ability to assimilate more than enough carbon to counter these kinds of losses (Körner, 1999), the combination of factors discussed in this chapter may contribute to overall decreased performance at the geographic limits of *Avicennia* in New Zealand.

Chapter Eight

Chapter Eight

Final Discussion

8.1 The Project

Avicennia marina subsp. *australasica* is New Zealand's only representative of the taxonomically diverse group of woody intertidal plants known as mangroves. It is one of several plant species in New Zealand with a clearly defined southern distribution limit around latitude 38°S. (Wardle, 1991). Until fairly recently, two main theories had been proposed to account for this boundary: the southern spread of this species was thought to be constrained solely by the lethal effects of extreme, low winter temperatures (frosts) (Chapman & Ronaldson, 1958), or, it was suggested that it was due to poor dispersal potential and lack of suitable habitat (de Lange & de Lange, 1994). These hypotheses had merit, but both were based on very little actual experimental evidence about mangrove performance in New Zealand. Neither addressed the possibility that mangrove extent in New Zealand may be controlled by the physiological limitations of the species as is known for distribution patterns of a number of other species (Close *et al.*, 2000, Duke, 1998, Guo & Cao, 2004). The present study was undertaken to investigate physiological responses of *Avicennia* to frost and low winter temperatures, to evaluate the physical consequences of frost exposure, and to assess the importance of these factors in defining the southern limits of this species in New Zealand. In so doing the idea was to contribute to our understanding of another biogeographical problem – why is latitude 38°S so important?

8.2 *Avicennia* performance

Optimal photosynthetic performance in New Zealand mangrove occurs at around 25°C and light saturation at about 700 μmol m^{-2} s^{-1} (Walbert, 2002), and these conditions are approached during the summer period over most of its latitudinal range in New Zealand. Under favourable conditions, diurnal leaf CO_2 exchange in New Zealand *Avicennia* was shown to be similar to that previously reported for some tropical mangrove species. Maximal A_{max} under saturating PFD reached 12.2 μmol m^{-2} s^{-1} (Figure 4.12) which is similar to field-measured rates reported for *Avicennia marina* in Durban, South Africa at latitude 29°53' S (7.8 -

9.9 μmol m^{-2} s^{-1} (Naidoo *et al.*, 1997, 1998, Tuffers *et al.*, 2001)), and Queensland, Australia at latitude 19°16' S (6.4 – 11.6 μmol m^{-2} s^{-1}). Within New Zealand , and given appropriate microclimate conditions, field studies showed that mangrove leaves could achieve similar photosynthetic rates regardless of whether they were growing near their southern geographic limits at Ohiwa harbour (latitude 38°S) or in the warmer northern climate at Paihia (around latitude 35°S).

8.3 Actual performance

It was found that some New Zealand mangrove plants, did not achieve optimal performance levels, and photosynthesis was clearly limited in autumn, winter and spring. This study showed that New Zealand mangrove share affinities with tropical tree species such as mango and *Eucalyptus* in that they are chill- and frost-sensitive on a number of levels (Close *et al.*, 2000, Davidson *et al.*, 2004, Nir *et al.*, 1997). Colder temperatures typical of the temperate New Zealand climate can therefore be detrimental to both the physical structure and physiological functions of mangrove during cold periods of the year. Function may be lost as a result of tissue damage and partial or entire death of plants after rare, severe frosts, but importantly, less severe, and not necessarily freezing temperatures also result in significant functional limitations due to impacts on photosynthesis. In the natural environment and also during a series of artificially imposed cold-nights below 4°C *Avicennia* leaves exhibited greatly reduced rates of CO_2 assimilation and stomatal conductance. Several days under favourable conditions were required before recovery of pre-stressed rates of CO_2 uptake could be achieved, again similar to responses in tropical plants e.g., photosynthetic recovery following chilling in coffee (Bauer *et al.*, 1985) and *Eucalyptus* (Davidson *et al.*, 2004). Exposure to high light further intensified photosynthetic losses through cold-induced photoinhibition and PSII impairment by chilling and other stresses associated with exposure to low temperatures.

These problems were exacerbated with increasing latitude. Plants near the southern mangrove limit had much reduced daily net photosynthetic income during winter months, particularly on days preceded by cold nights. At latitude 38°S (Ohiwa harbour) daily net photosynthetic income calculated over several days in winter was approximately 14% of the equivalent value in summer. For plants growing in frost-free warmer northern climates this seasonal difference was considerably less, at around 75%.

Stable carbon isotope analyses also produced evidence that mangrove at higher latitudes were under greater photosynthetic stress. There was a decrease in ^{13}C depletion of tissue with increase of latitude indicating greater stomatal limitation of photosynthesis. Contributing factors are likely to be increasingly lower growing temperatures, shorter growing seasons, cold-induced photoinhibition and greater frequencies of winter chilling, frosts and frost damage with increasing latitude.

8.4 The Mechanism

It is well known that photosynthesis in chill-sensitive plants may be significantly reduced if air temperatures drop below a critical temperature (Allen & Ort, 2001). Photosynthesis can be limited via both stomatal and non-stomatal (carbon fixation) processes (Ball & Farquhar, 1984a, 1984b, Guye & Wilson, 1987). The present study provided evidence that the major cause of decreased photosynthesis following chilling or freezing was a direct effect on the photosynthetic carbon fixation metabolism and, in this case, the reduction was possibly indicative of a decrease in RuBP regeneration capacity (Farquhar & Sharkey, 1982). Stomatal opening, as found by previously reported studies (Kao *et al.*, 2004), was reduced after chilling and freezing but did not limit A_{max}.

When cold frosty nights are followed by clear sunny days (a frequent pattern of winter climate in New Zealand) leaves receive very high incident PFD while their photosynthetic rates remain low from the chilling damage. As a result of these reduced rates of carbon fixation, the chloroplast photocentres are unable to utilise the absorbed light or dissipate it quickly enough through protective processes and photoinhibition of PSII results (Powles, 1984). Initially photoinhibition may serve to protect (Aro *et al.*, 1993), and may be fully reversible but, if exposure to the factors that caused it (low temperature and high PFD) is repeated or prolonged, then further photodamage will result. This was the case at Ohiwa harbour, when chlorophyll content of exposed leaves in the mangrove canopy dropped by over half during winter.

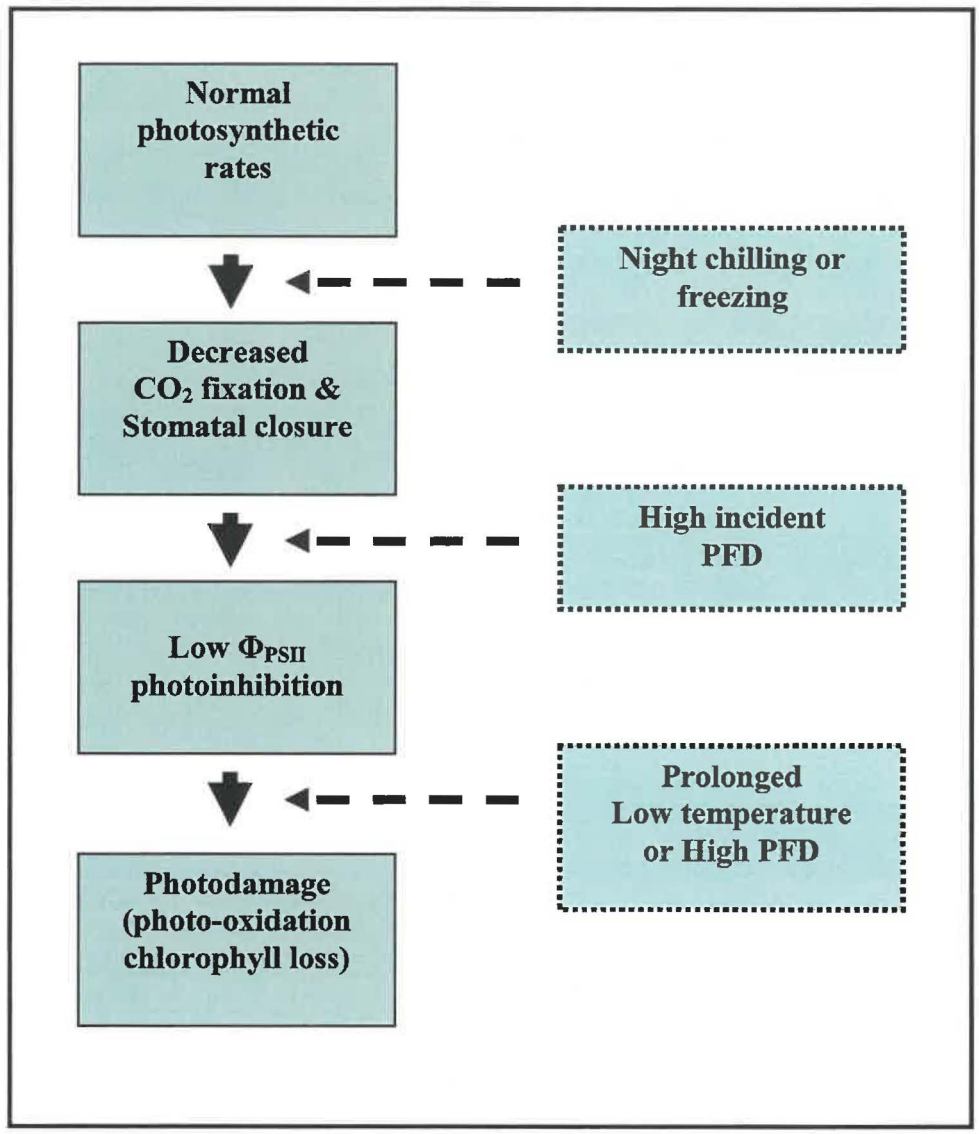

Figure 8.1 The sequence of events responsible for reduction of photosynthesis and photodamage following exposure to low night temperatures (chilling or freezing).

8.5 Consequences

Significant carbon costs to the mangrove are associated with physical damage and photosynthetic decline resulting from cold temperature exposure. The effects of frost and chilling have both short and long term effects on plant performance. Chronic impacts on existing leaves (e.g., full or partial tissue death) not only impose replacement costs on the plant, but delay the reinvestment of photosynthate into new leaves and plant parts (King & Ball, 1998). Decreased photosynthetic performance means that affected plants are at a disadvantage when it comes to assimilating enough carbon to counter these kinds of losses. At the geographical limits a less favourable climate (more chilling nights, colder days,

shorter growing season, less optimal temperatures) means that the likelihood of getting a sufficient number of days of conditions suitable for optimal photosynthesis is also reduced. Additional costs to the plants occur in the form of reduced reproductive success. The timing of severe frosts in relation to New Zealand *Avicennia* is such that developing propagules are often destroyed by freezing (Plate 5.2). Their position in the upper and outer parts of the canopy almost ensures their destruction in a severe freeze.

Species distributions may be constrained by lethal conditions (e.g., temperature) that need only occur occasionally (i.e., the rare, but severe, event) to prevent survival of individuals or reproductive success so the species cannot persist through generations. In the case of *Avicennia*, lethal conditions occur with the frosts that occur from autumn through winter and spring throughout approximately half the present latitudinal range of this species in New Zealand. *Avicennia* in New Zealand has a limited ability to tolerate frosts, and, like chilling tolerance in tropical mangrove, this increases with latitude (Markley *et al.*, 1982, McMillan, 1974). However, even ultimate tolerance levels of around -5°C put *Avicennia* in a similar class as subtropical species. Frosts severe enough to overcome the buffering effect of the warm water and sediments would certainly kill the plants.

8.6 Where are we?

Mangrove distribution appears to be defined by the effects of physiological stress. Comparative studies of water relations, gas exchange, stomatal conductance and chlorophyll fluorescence undertaken during this project revealed that physiological performance in *Avicennia* becomes increasingly depressed near its geographic limits. Importantly, when exposed to low overnight temperatures, *Avicennia* responses were found to be more consistent with those known for subtropical plant species. Major decreases in photosynthetic production following exposure to overnight temperatures of 4°C and lower indicated that critical stress limits were reached well above freezing. However, frosts probably still play an important, additional and episodic role in defining the range of mangrove in New Zealand. Physiological stress effects were compounded by freezing temperatures and productivity in frost-prone areas was significantly reduced by physical damage to leaves, branches and reproductive tissue. Freeze-injury of this form

also reduced the likelihood of successful seedling establishment and long-term survival of saplings

It appears, therefore, that the destructive effects of frost in combination with chronic depression in photosynthetic rate from chilling is sufficient to explain the inability of *Avicennia* to grow further south in New Zealand. The mechanisms of this depression in photosynthetic ability are clear and well known for other plants.

8.7 Do we need more?

Unfortunately the ecophysiological studies do not add to our understanding of the dispersal of this species. Some initial genetic studies of population relationships were carried out during this thesis. The overall result was that the level of genetic differentiation within the species in New Zealand was low. However, populations within each large estuary were more similar to each other than to plants in other estuaries. This is a possible indication of a founder effect with initial colonisation of each estuary by a small number of individuals followed by local spread with in the estuary. This suggests that longer distant dispersal is not common and that dispersal could limit the further expansion of the species.

However, although we cannot eliminate the limitation through dispersal, it appears that it is unnecessary to consider this possibility because the physiological limitations are strong enough to explain the boundary. It may be concluded from these findings that latitude 38° S represents a physiological barrier defined by stress and the performance of an essentially subtropical species in a cold climate. Long-term survival and reproduction of mangrove further south are unlikely unless favourable microclimates exist.

References

References

Allan H.H. (1961) *Flora of New Zealand* (vol. 1). P.D. Hasselberg, Government Printer, Wellington New Zealand.

Allan H.H. (1982) *Flora of New Zealand* (vol. 1). P.D. Hasselberg, Government Printer, Wellington New Zealand.

Allen D.J. & Ort D.R. (2001) Impacts of chilling temperatures on photosynthesis in warm-climate plants. *Trends in Plant Science*, 6, 36-42.

Allen D.J., Ratner K., Giller Y., Gussakovsky E., Shahak Y. & Ort D.R. (2000) An overnight chill induces a delayed inhibition of photosynthesis at midday in mango (*Mangifera indica* L.). *Journal of Experimental Botany*, 51, 1893-1902.

Andrews T.J., Clough B.F. & Muller G.J. (1984) Photosynthetic gas exchange properties and carbon isotope ratios of some mangroves in North Queensland. In: *Physiology and management of mangroves* (ed H.J. Teas), pp. 15-23. Dr W. Junk Publishers, The Hague.

Arens N.C., Jahren A.H. & Amundson R. (2000) Can C_3 plants faithfully record the carbon isotopic composition of atmospheric carbon dioxide? *Paleobiology*, 26, 137-164.

Aro E.-M., Virgin I. & Anderson B. (1993) Photoinhibition of Photosystem II. Inactivation, protein damage and turnover. *Biochimica et Biophysica Acta*, 1143, 113-134.

Ball M.C. (1986) Photosynthesis in mangroves. *Wetlands (Australia)*, 6, 12-22.

Ball M.C. (1988a) Ecophysiology of mangroves. *Trees*, 2, 129-142.

Ball M.C. (1988b) Salinity tolerance in the Mangroves *Aegiceras corniculatum* and *Avicennia marina*. I. Water Use in Relation to Growth, Carbon Partitioning and Salt Balance. *Australian Journal of Plant Physiology*, 15, 447-464.

Ball M.C. (1996) Comparative ecophysiology of mangrove forest and tropical lowland moist rainforest. In: *Tropical forest plant ecophysiology* (eds R. Mulkey & A. Smith), pp. 461-496. Chapman and Hall, New York.

Ball M.C., Cowan I.R. & Farquhar G.D. (1988) Maintenance of Leaf Temperature and the Optimisation of Carbon Gain in Relation to Water Loss in a Tropical Mangrove Forest. *Australian Journal of Plant Physiology*, 15, 263-276.

Ball M.C. & Critchley C. (1982) Photosynthetic responses to irradiance by the grey mangrove, *Avicennia marina*, grown under different light regimes. *Plant Physiology*, 70, 1101-1106.

Ball M.C. & Farquhar G.D. (1984a) Photosynthesis and stomatal responses of two mangrove species, *Aegiceras corniculatum* and *Avicennia marina*, to long term salinity and humidity conditions. *Plant Physiology*, 74, 1-6.

Ball M.C. & Farquhar G.D. (1984b) Photosynthesis and stomatal responses of the grey mangrove, *Avicennia marina*, to transient salinity conditions. *Plant Physiology*, 74, 7-11.

Ball M.C., Hodges V.S. & Laughlin G.P. (1991) Cold-induced photoinhibition limits regeneration of snow gum at the tree-line. *Functional Ecology*, 5, 663-668.

Ball M.C. & Passioura J.B. (1995) Carbon gain in relation to water use: Photosynthesis in Mangroves. In: *Ecophysiology of Photosynthesis* (eds E.D. Schulze & M.M. Caldwell), pp. 247-261. Springer Verlag, Berlin Heidelberg New York.

Ball M.C. & Sobrado M.A. (1999) Ecophysiology of mangroves: challenges in linking physiological processes with patterns in forest structure. In: *Physiological Plant Ecology; The 39th Symposium of the British Ecological Society* (eds M. Press, J. Scholes, & M. Barker), pp. 331-346. Blackwell Science, London.

Bannister P. (1976) *Introduction to Physiological Plant Ecology*. John Wiley and Sons, New York.

Bauer H., Wierer R., Hatheway W.H. & Larcher W. (1985) Photosynthesis of *Coffea arabica* after chilling. *Physiologia Plantarum*, 64, 449-454.

Beaglehole J.C. (1955) *The Journals of Captain James Cook: The Voyage of the Endeavour 1768-1771* (vol. 1). Cambridge (for the Hakluyt Society), Cambridge.

Beck E., Senser M., Scheibe R., Steiger H.-M. & Pongratz P. (1982) Frost avoidance and freezing tolerance in Afroalpine "giant rosette" plants. *Plant, Cell & Environment*, 5, 215-222.

Becker P., Azman A., Mohamad J.M., Moksin M. & Tyree M. (1997) Sap flow rates of mangrove trees are not unusually low. *Trees - Structure and Function*, 11, 432 - 435.

Behboudian M.H., A Q.M., Turner N.C. & Palta J.A. (2000) Discrimination against $^{13}CO_2$ in leaves, pod walls and seeds of water-stressed chickpea. *Photosynthetica*, 38, 155-157.

Bell M.J., Michaels T.E., McCullough D.E. & Tollenar M. (1994) Photosynthetic response to chilling in peanut. *Crop Science*, 34, 1014-1023.

Bhosale L.J. (1983) The significance of cryptovivipary in *Aegiceras corniculatum*. In: *The Biology and Ecology of Mangrove* (ed H.J. Teas), pp. Chapter 14.

Bilger H.-W., Schreiber U. & Lange O.L. (1984) Determination of leaf heat resistance: comparative investigation of chlorophyll fluorescence changes and tissue necrosis methods. *Oecologia*, 63, 256-262.

Bilger W., Schreiber U. & Bock M. (1995) Determination of the quantum efficiency of photosystem II and of non-photochemical quenching of chlorophyll fluorescence in the field. *Oecologia*, 102, 425-432.

Björkman O. (1987) Low temperature chlorophyll fluorescence in leaves and its relationship to photon yield of photosynthesis in photoinhibition. In: *Photoinhibition* (ed DJ Kyle), pp. 123-143. Elsevier Science Publishers B.V. (Biomedical Division).

Björkman O., Demming B. & Andrews T. (1988) Mangrove Photosynthesis: Response to high-irradiance stress. *Australian Journal of Plant Physiology*, 15, 43-61.

Blackburn W.J. & Proctor J.T.A. (1983) Estimating photosynthetically active radiation from measured solar irradiance. *Solar Energy*, 31, 233-234.

Blasco F. (1984) Climatic factors and the biology of mangrove plants. In: *Chapter 2: The Mangrove Ecosystem; Research Methods* (ed S.C. Snedaker).

Blennow K., Lang A.R.G., Dunne P. & Ball M.C. (1998) Cold-induced photoinhibition and growth of seedling snow gum (*Eucalyptus pauciflora*) under differing temperature and radiation regimes in fragmented forests. *Plant, Cell & Environment*, 21, 407-.

Boorse G.C., Bosma T.L., Meyer A.-C., Ewers F.W. & Davis S.D. (1998) Comparative methods of estimating freezing temperatures and freezing injury in leaves of chapparal shrubs. *International Journal of Plant Science*, 159, 513-521.

Burns B.R. (1982) *Population Biology of Avicennia marina var. resinifera.* Master of Science, Auckland University.

Carpentier R. (1997) Influence of high light intensity on photosynthesis: photoinhibition and energy dissipation. In: *Handbook of photosynthesis* (ed M. Pessarakli), pp. 443 - 450. Marcel Dekker Inc., New York.

Cate T.M. & Perkins T.D. (2003) Chlorophyll content monitoring in sugar maple (*Acer saccharum*). *Tree Physiology*, 23, 1077-1079.

Chapman V. (1976) *Mangrove Vegetation.* J. Cramer Verlag, Germany.

Chapman V. & Ronaldson J. (1958) *The Mangrove and Salt-marsh flats of the Auckland Isthmus* (Bulletin 125). New Zealand Department of Scientific and Industrial Research.

Chapman V.J. (1977) *Ecosystems of the World* (vol. I). Elsevier Scientific Publishing Company, Amsterdam.

Cheeseman J., Clough B., Carter D., Lovelock C., Eong O. & Sim R. (1991) The analysis of photosynthetic performance in leaves under field conditions: A case study using *Bruguiera* mangroves. *Photosynthesis Research*, 29, 11-22.

Cheeseman J.M. (1994) Depression of photosynthesis in mangrove canopies. In: *Photoinhibition of Photosynthesis - from molecular mechanisms to the field* (eds N.R. Baker & J.R. Bowjer), pp. 377-389. BIOS Scientific Publishers Ltd., Oxford.

Close D.C., Beadle C.L., Brown P.H. & Holz G.K. (2000) Cold-induced photoinhibition affects establishment of *Eucalyptus nitens* (Deane and Maiden) Maiden and *Eucalyptus globulus* Labill. *Trees*, 15, 32-41.

Close D.C., Beadle C.L., Holz G.K. & Ravenwood I.C. (1999) A photobleaching event at the North Forest Products' Somerset nursery reduces growth of *Eucalyptus globulus* seedlings. *Tasforests*, 11, 59-67.

Clough B., Andrews T. & Cowan I. (1979) *Mangrove ecosystems in Australia: structure, function and managment.* Paper presented at the Australian National Mangrove Workshop, Australian Institute of Marine Science, Cape Ferguson 19-20 April 1979.

Clough B., Andrews T. & Cowan I. (1982) *Physiological Processes in Mangroves.*

Clough B. & Sim R. (1989) Changes in gas exchange characteristics and water use efficiency of mangroves in response to salinity and vapour pressure deficit. *Oecologia*, 79, 38-44.

Clough B.F. (1984) Growth and salt balance of the mangroves *Avicennia marina* (Forsk.) Vierh. and *Rhizophora stylosa* Griff. in relation to salinity. *Australian Journal of Plant Physiology*, 11, 419-430.

Craig H. (1953) The geochemistry of the stable carbon isotopes. *Geochimica et Cosmochimica Acta*, 3, 53-92.

Crawford R.M.M. (1989) *Studies in Plant Survival: Ecological case histories of plant adaptation to adversity.* Blackwell Scientific Publications, Oxford.

Crisp P., Daniel L. & Tortell P. (1990) *Mangroves in New Zealand: Trees in the Tide.* GP Books, Wellington N.Z.

Critchley C. (2000) Photoinhibition. In: *Photosynthesis: A comprehensive treatise (Chapter 20)* (ed A.S. Raghavendra), pp. 264-272. Cambridge University Press.

Damesin C. & Lelarge C. (2003) Carbon isotope composition of current-year shoots from *Fagus sylvatica* in relation to growth, respiration and use of reserves. *Plant, Cell & Environment*, 26, 207-219.

Damesin C., Rambal S. & Joffre R. (1998) Seasonal and annual changes in leaf d13C in two co-occurring Mediterranean oaks: relations to leaf growth and drought progression. *Functional Ecology*, 12, 778-785.

Daniel L. (1986, 1986) New Plant Records: *Avicennia marina* var. *resinifera*, Tolaga Bay, Uawa estuary. *New Zealand Botanical Society Newsletter*, pp. 11-13.

Davidson N.J., Battaglia M. & Close D.C. (2004) Photosynthetic responses to overnight frost in *Eucalyptus nitens* and *E. globulus*. *Trees*, 18, 245-252.

Dawes C.J. (1998) *Marine Botany*. (2nd ed.). John Wiley & Sons Ltd.

Dawson T.E., Mambelli S., Plamboek A.H., Templer P.H. & Tu K.P. (2002) Stable Isotopes in Plant Ecology. *Annual Review of Ecological Systematics*, 33, 507-559.

de Lange W. & de Lange P. (1994) An Appraisal of Factors Controlling the Latitudinal Distribution of Mangrove (*Avicennia marina* var. *resinifera*) in New Zealand. *Journal of Coastal Research*, 10, 539-548.

Demmig-Adams B. & Adams W.W. (1992) Photoprotection and other responses of plants to high light stress. *Annual Review of Plant Physiology and Plant Molecular Biology*, 43, 599-626.

Dexter S., Tottingham W.E. & Graber L.F. (1932) Investigations of the hardiness of plants by measurement of electrical conductivity. *Plant Physiology*, 7, 63-78.

Dingwall P. (1984) Overcoming problems in the management of New Zealand mangrove forests. In: *Physiology and Management of Mangroves (Chapter 13)* (ed H.J.Teas), pp. 97-106. Dr W. Junk Publishers.

Dodd R.S., Afsal-Rafii Z., Kashani N. & Budrick J. (2002) Land barriers and open oceans: effects on gene diversity and population structure in *Avicennia germinans* L. (Avicenniaceae). *Molecular Ecology*, 11, 1327-1338.

Downton W.J.S. (1982) Growth and Osmotic Relations of the Mangrove *Avicennia marina*, as Influenced by Salinity. *Australian Journal of Plant Physiology*, 9, 519-528.

Duke N. (1990) Phenological trends with latitude in the mangrove tree *Avicennia marina*. *Journal of Ecology*, 78, 113--133.

Duke N. (1991) A Systematic Revision of the Mangrove Genus *Avicennia* (Avicenniaceae) in Australasia. *Austr. Syst. Bot.*, 4, 299-324.

Duke N.C. (1992) Mangrove floristics and biogeography. In: *Tropical Mangrove Ecosystems* (eds A.I. Robertson & D.M. Alongi), pp. 63 -100. American Geophysical Union, Washington DC.

Duke N.C. (1995) Genetic diversity, distributional barriers and rafting continents - more thoughts on the evolution of mangroves. *Hydrobiologia*, 295, 167-181.

Duke N.C., Marilyn C. Ball and Joanna C. Ellison (1998) Factors influencing biodiversity and distributional gradients in mangroves. *Global Ecology and Biogeography letters*, 7, 27-47.

Eggert A., Hasselt P. & Breeman A. (2003) Chilling-induced photoinhibition in nine isolates of Valonia utricularis (Chlorophyta) from different climate regions. *Journal of Plant Physiology*, 160, 881-891.

Ehleringer J., Phillips S.L. & Comstock J.P. (1992) Seasonal variation in the carbon isotopic composition of desert plants. *Functional Ecology*, 6, 396-404.

Ehleringer J.R. & Osmond C.B. (1989) Stable Isotopes (Chapter 13). In: *Plant Physiological Ecology; Field Methods and Instrumentation* (eds R.W. Pearcy, J. Ehleringer, H.A. Mooney, & P. Rundel). Chapman and Hall, London.

Ellison A.M. (2002) Macroecology of mangroves: large-scale patterns and processes in tropical coastal forests. *Trees*, 16, 181-194.

Farnsworth E. (2000) The ecology and physiology of viviparous and recalcitrant seeds. *Annual Review of Ecology and Systematics*, 31, 107-138.

Farqhuar G.D., Ehleringer J. & Hubick K.T. (1989) Carbon isotope discrimination and photosynthesis. *Annual Review of Plant Physiology and Molecular Biology*, 40, 503-537.

Farquhar G. & Sharkey T. (1982) Stomatal conductance and photosynthesis. *Annual review on Plant Physiology*, 33, 317-345.

Farquhar G.D. (1980) Carbon dioxide discrimination by plants: effects of carbon dioxide concentration and temperature via the ratio of inter-cellular and atmospheric CO_2 concentrations. In: *Carbon Dioxide and Climate* (ed G.I. Pearman), pp. 105-110. Australian Academy of Science, Canberra, Australia.

Farquhar G.D. & Lloyd J. (1993) Carbon and Oxygen Isotope Effects in the Exchange of Carbon Dioxide between Terrestrial Plants and the Atmosphere. In: *Stable Isotopes and Plant Carbon-Water Relations* (eds J. Ehleringer, G.D. Farquhar, & A. Hall, E), pp. 47-70. Academic Press Ltd.

Farquhar G.D., O'Leary M.H. & Berry J.A. (1982) On the relationship between carbon isotope discrimination and the intercellular carbon dioxide concentration in leaves. *Australian Journal of Plant Physiology*, 9, 121-137.

Flexas J., Escalona J.M., Evain S., Gulias J., Moya I., Osmond C.B. & Medrano H. (2002) Steady-state chlorophyll fluorescence (Fs) measurements as a tool to follow variations of net CO2 assimilation and stomatal conductance during water-stress in C3 plants. *Physiologia Plantarum*, 114, 231-240.

Flint H.L.B., B R; Beattie, D J (1967) Index of Injury - a useful expression of freezing injury to plant tissues as determined by the electrolytic method. *Canadian Journal of Plant Science*, 47, 229-230.

Foyer C.H., Lelandais M. & Kunert K.J. (1994) Photooxidative stress in plants. *Physiologia Plantarum*, 92.

Francey R.J., Gifford R.M., Sharkey T.D. & Weir B. (1985) Physiological influences on isotope discrimination in huon pine (*Lagarostrobos franklinii*). *Oecologia*, 66, 211-218.

Fryer M., Andrews J., Ocborrough K., Blowers D. & NR B. (1998) Relationship between CO_2 assimilation, photosynthetic electron transport, and active O_2 metabolism in leaves of maize in the field during periods of low temperature. *Plant Physiology*, 116, 571-580.

Genty B., Briantais J.-M. & Baker N.R. (1989) The relationship between the quantum yield of photosynthetic electron transport and quenching of chlorophyll fluorescence. *Biochimica et Biophysica Acta*, 990, 87 - 92.

Govindachary S., Bukhov N., Joly D. & Carpentier R. (2004) Photosystem II inhibition by moderate light under low temperature in intact leaves of chilling-sensitive and -tolerant plants. *Physiologia Plantarum*, 121, 322-333.

Grant R.H. & Slusser J.R. (2004) Estimation of Photosynthetic Photon Flux Density from 368-nm Spectral Irradiance. *Journal of Atmospheric and Oceanic Technology*, 21, 481-487.

Green P.S., ed (1994) *Flora of Australia Volume 49, Oceanic Islands 1* (Vol. 49). Australian Government Printing Service, Canberra.

Griffiths H. (1993) Carbon Isotope Discrimination. In: *Photosynthesis and Production in a Changing Environment: A Field and Laboratory Manual* (eds D.O. Hall, J.M.O. Scurlock, & H. Bolhar-Nordenkampf). Chapman and Hall, London.

Guo Y.-H. & Cao K.-F. (2004) Effect of night chilling on photosynthesis of two coffee species grown under different irradiances. *Journal of Horticultural Science and Biotechnology*, 713-716.

Guy R., Reid D. & Krouse H.R. (1980) Shifts in carbon isotope ratios of two C3 halophytes under natural and artificial conditions. *Oecologia*, 44, 241-247.

Guye M.G. & Wilson J.M. (1987) The effects of chilling and chill-hardening temperatures on stomatal behaviour in a range of chill sensitive species and cultivars. *Plant Physiology and Biochemistry*, 25, 717-721.

Haldimann P. (1998) Low growth temperature-induced changes to pigment composition and photosynthesis in *Zea mays* genotypes differing in chilling sensitivity. *Plant, Cell & Environment*, 21, 200-208.

Healy T.R. (2002) Muddy coasts of mid-latitude oceanic islands on an active plate margin - New Zealand. In: *Muddy Coasts of the World: Processes, Deposits and Function* (eds T.R. Healy, Y. Wang, & J.-A. Healy), pp. 347-373. Elsevier Science.

Healy T.R. & Kirk R.M. (1982) Coasts. In: *Landforms of New Zealand* (eds J.M. Soons & M.J. Selby), pp. 81-104. Longman Paul, Auckland.

Hobbie E.A. & Werner R.A. (2004) Intramolecular, compound-specific, and bulk carbon isotope patterns in C3 and C4 plants: a review and synthesis. *New Phytologist*, 161, 371-385.

Hutchings P. & Saenger P. (1987) *The ecology of mangroves*. University of Queensland Press, Brisbane.

Inouye D. (2000) The ecological and evolutionary significance of frost in the context of climate change. *Ecology Letters*, 3, 457-463.

Ivlev A.A. (2004) Contribution of photorespiration to changes of carbon isotope characteristics in plants affected by stress factors. *Russian Journal of Plant Physiology*, 51, 271-280.

Iyengar E. & Reddy M. (1996) Photosynthesis in highly salt-tolerant plants. In: *Handbook of Photosynthesis* (ed P. M.). Marcel Dekker, Inc., New York.

Jensen R. (1980) Biochemistry of the chloroplast. In: *The Biochemistry of Plants* (ed N. Tolbert). Academic Press, New York.

Jillon J.S. & Griffiths H. (1997) The influence of (photo)respiration on carbon isotope discrimination in plants. *Plant, Cell & Environment*, 20, 1217-1230.

Kao W.-Y., Kao W.-Y., Shih C.-N. & Tsai T.-T. (2004) Sensitivity to chilling temperatures and distribution differ in the mangrove species *Kandelia candel* and *Avicennia marina*. *Tree Physiology*, 24, 859-864.

Keely J., Sternberg L. & DeNiro M. (1986) The use of stable isotopes in the study of photosynthesis in freshwater plants. *Aquatic Botany*, 26, 213-223.

King D.A. & Ball M.C. (1998) A model of frost impacts on seasonal photosynthesis of *Eucalyptus pauciflora*. *Australian Journal of Plant Physiology*, 25, 27-37.

Kitao M., Utsugi H., Kuramoto S., Tabuchi R., Fujimoto K. & Lihpai S. (2003) Light-dependant photosynthetic characteristics indicated by chlorophyll fluorescence in five mangrove species native to Pohnpei Island, Micronesia. *Physiologia Plantarum*, 117, 376-382.

Körner C. (1999) *Alpine Plant Life: Functional Plant Ecology of High Mountain Ecosystems*. Springer-Verlag, Berlin Heidelberg.

Krause G.H. (1994) Photoinhibition induced by low temperatures. *Photoinhibition of Photosynthesis: From Molecular Mechanisms to the Field*, 331-348.

Krause G.H. & Weis E. (1991) Chlorophyll fluorescence and photosynthesis: the basics. *Annual Review of Plant Physiology and Plant Molecular Biology*, 42, 313-349.

Kudoh H. & Sonoike K. (2002) Irreversible damage to photosystem I by chilling in the light: cause of the degradation of chlorophyll after returning to normal growth temperature. *Planta*, 215, 541-548.

Laisk A. & Oja V. (1998) *Dynamics of Leaf Photosynthesis, Rapid Response Measurements and their Interpretations*. CSIRO Australia.

Lamontagne M., Bigras F.J. & Margolis H.A. (2000) Chlorophyll fluorescence and CO2 assimilation of black spruce seedlings following frost in different temperature and light conditions. *Tree Physiology*, 20, 249-255.

Lear R. & Turner T. (1977) *Mangroves of Australia*. University of Queensland Press, St Lucia:.

Leavitt S.W. & Long A. (1982) Evidence for $^{13}C/^{12}C$ fractionation between tree leaves and wood. *Nature*, 298, 742-744.

Leavitt S.W. & Long A. (1985) Stable isotope composition of maple sap and foliage. *Plant Physiology*, 78.

Levitt J. (1980a) Chapter 3. Chilling Injury and Resistance. In: *Responses of Plants to Environmental Stresses. Vol 1: Chilling, Freezing and High Temperatures.*

Levitt J. (1980b) Chapter 7: Freezing Resistance - Types, Measurement, and Changes. In: *Responses of Plants to Environmental Stresses. Vol 1: Chilling, Freezing and High Temperatures.*

Lichtenthaler H. & Burkart S. (1999) Photosynthesis and High Light Stress. *Bulg. Journal of Plant Physiology*, 25, 3-16.

Lin G. & Sternberg S.L. (1992) Differences in morphology, carbon isotope ratios and photosynthesis between scrub and fringe mangroves in Florida, USA. *Aquatic Botany*, 42, 303-313.

Loomis R.S. & Amthor J.S. (1999) Yield potential, plant assimilatory capacity, and metabolic efficiencies. *Crop Science*, 39, 1584-1596.

Lugo A.E. & Zucca C.P. (1977) The impact of low temperature stress on mangrove structure and growth. *Tropical Ecology*, 18, 149-161.

Markley J., McMillan C. & Thompson G.J. (1982) Latitudinal differentiation in response to chilling temperatures among populations of three mangroves, *Avicennia germinans, Laguncularia racemosa* and *Rhizophora mangle,* from the western tropical Atlantic and Pacific Panama. *Canadian Journal of Botany*, 60, 2704-2715.

Maxwell G. (2001) Chill shock tolerance differentiates local and Thai ecotypes of *Avicennia marina. Memoirs of the Hong Kong Natural History Society*, 24, 205-206.

Maxwell K. & Johnson G. (2000) Chlorophyll fluorescence - a practical guide. *Journal of experimental Botany*, 51, 659-668.

McKensie D.W. (1995) *Reed New Zealand Atlas.* Reed Publishing (NZ) Ltd, Auckland.

McKersie B.D. (2003) Plant environment interactions and stress physiology, Module 2: Freezing Stress, Chilling Stress,
http://www.agronomy.psu.edu/Courses/AGRO518/contents.htm.

McMillan C. (1974) *Adaptive differatiation to chilling in mangrove populations.* Paper presented at the Proceedings of the International Symposium on Biologu and Management of Mangroves, East-West Center, Honolulu, Hawaii.

McNae W. (1966) Mangroves in Eastern and Southern Australia. *Australian Journal of Botany*, 14, 67-104.

McNae W. (1968) A general account of the fauna and flora of mangrove swamps and forests in the indo-west-pacific region. *Advances in marine biology*, 6, 73-230.

Medina E. & Francisco M. (1997) Osmolality and d13C of leaf tissues of mangrove species from environments of contrasting rainfall and salinity. *Estuarine, Coastal and Shelf Science*, 45, 337-344.

Melcher P.J., Meinzer F.C., Yount D.E., Goldstein G. & Zimmerman U. (1998) Comparative measurements of xylem pressure in transpiring and non-transpiring leaves by means of the pressure chamber and the xylem pressure probe. *Journal of Experimental Botany*, 49, 1757-1760.

Mildenhall D. & Brown L. (1987) An early Holocene occurrence of the mangrove *Avicennia marina* in Poverty Bay, North Island, New Zealand: Its climatic and geological implications. *New Zealand Journal of Botany*, 25, 281-294.

Mildenhall D.C. (1994) Early to Mid Holocene pollen samples containing mangrove pollen from Sponge Bay, East Coast, North Island, New Zealand. *Journal of the Royal Society of New Zealand*, 24, 219-230.

Mildenhall D.C. (2001) Middle Holocene mangroves in Hawke's Bay, New Zealand. *New Zealand Journal of Botany*, 39, 517-521.

Miller J.M., Williams R.J. & Farquar G.D. (2001) Carbon isotope discrimination by a sequence of *Eucalyptus* species along a subcontinental rainfall gradient in Australia. *Ecology*, 15, 222-232.

Miyawaki A. (1980) Vegetation of Japan. (ed A. Miyawaki), pp. 118-120. Shibundo Publishers, Tokyo.

Monte L., Nesbitt R.C., Ebel D.F., Wilkins B., Woods F. & Himelrick D. (2002) Assays to Assess Freeze Injury of Satsuma Mandarin. *HortScience 2002*, 37.

Moore R., Miller P., Albright D. & Tieszen L. (1972) Comparative gas exchange characteristics of three mangrove species during the winter. *Photosynthetica*, 6, 387-393.

Mueller P., Xiao-Ping L. & Niyogi K. (2001) Non-Photochemical Quenching. A Response to Excess Light Energy. *Plant Physiology*, 125, 1558-1566.

Mwangi Theuri M., Kinyamario J.I. & van Speybroeck D. (1999) Photosynthesis and related physiological processes in two mangrove species, *Rhizophora mucronata* and *Ceriops tagal*, at Gazi Bay, Kenya. *African Journal of Ecology*, 37, 180-193.

Naidoo G. (1987) Effects of salinity and nitrogen on growth and water relations in the mangrove, *Avicennia marina* (Forssk.) Vierh. *New Phyotologist*, 107, 317-325.

Naidoo G. & Chirkoot D. (2004) The effects of coal dust on photosynthetic performance of the mangrove, *Avicennia marina* in Richards Bay, South Africa. *Environmental Pollution*, 127, 359-366.

Naidoo G., Rogalla H. & von Willert D. (1997) Gas exchange response of a mangrove species, *Avicennia marina*, to waterlogged and drained conditions. *Hydrobiologia*, 352, 39-47.

Naidoo G., Rogalla H. & von Willert D. (1998) Field measurements of gas exchange in *Avicennia marina* and *Bruguiera gymnorrhiza*. *Mangroves and Salt Marshes*, 2, 99-107.

Neales T.F., Fraser M.S. & Roksandic Z. (1983) Carbon isotope composition of the halophyte *Disphyma clavellatum* (Haw.) Chinnock (Aizoaceae), as affected by salinity. *Australian Journal of Plant Physiology*, 10, 437-444.

Neuner G.B., P. (1997) Ice formation and foliar frost resistance in attached and excised shoots from seedlings and adult trees of *Nothofagus menziesii*. *New Zealand Journal of Botany*, 35, 221-227.

Nicotra A.B., Hofmann M., Siebke K. & Ball M.C. (2003) Spatial patterning of pigmentation in evergreen leaves in response to freezing stress. *Plant, Cell & Environment*, 26, 1893-1904.

Nir G., Ratner K., Gussakovsky E. & Shahak Y. (1997) *Photoinhibition of Photosynthesis in Mango Leaves: Effect of Chilly Nights*. Paper presented at the ISHS Acta Horticulturae V International Mango Symposium.

NIWA (2003a) Daily Climatological Record at 0900 Local (F301) for stations B76995 (Whakatane Airport), and B87023 (Opotiki). http://www.niwa.cri.nz National Institute of Water and Atmospheric Research, accessed: December 2003.

NIWA (2003b) National Climate Summaries. http://www.niwa.cri.nz National Institute of Water and Atmospheric Research, accessed: December 2003.

Niyogi K. (2000) Safety Valves for Photosynthesis. *Current Opinion in Plant Biology*, 3, 455-460.

Oceanic Engineering (1980) 1978 Practical Salinity Scale Equations. *IEEE Journal of Oceanic Engineering*, OE-5, 14.

O'Leary M.H. (1981) Carbon isotope fractionation in plants. *Phytochemistry*, 20, 553-567.

O'Leary M.H. (1988) Carbon Isotopes in Photosynthesis. *Bioscience*, 38, 328-336.

O'Leary M.H. (1993) Biochemical Basis of Carbon Isotope Fractionation. In: *Stable Isotopes and Plant Carbon Water Relations* (eds J. Ehleringer, A. Hall, E, & G.D. Farquar), pp. 19-28. Academic Press Inc.

Onset Computer Corporation (2004) Onset StowAway Tidbit temperature logger. Onset Computer Corporation.

Öquist G., Greer D.H. & Ögren E. (1987) Light stress at low temperature (chapter 3). In: *Photoinhibition* (eds D.J. Kyle, C.B. Osmond, & C.J. Arntzen), pp. 67-87. Elsevier Scientific Publishers.

Ottander C., Campbell D. & Öquist G. (1995) Seasonal-changes in photosystem-II organization and pigment composition in *Pinus sylvestris*. *Planta*, 197, 176-183.

Panek J.A. & Waring R.H. (1997) Stable carbon isotopes as indicators of limitations to forest growth imposed by climate stress. *Ecological Applications*, 7, 854-863.

Park R. & Epstein S. (1961) Metabolic fractionation of ^{13}C and ^{12}C in plants. *Plant Physiology*, 36, 133-138.

Parkhill J.-P., Maillet G. & Cullen J.J. (2001) Fluorescence-based maximal quantum yield for PSII as a diagnostic of nutrient stress. *Journal of Phycology*, 37, 517.

Passioura J., Ball M. & Knight J. (1992) Mangroves may salinize the soil and in so doing limit their transpiration rate. *Functional Ecology*, 6, 476-481.

Pocknall D.T. (1989) Late Eocene to early Miocene vegetation and climate history of New Zealand. *Journal of the Royal Society of New Zealand*, 19, 1-18.

Porra R., Thompson W. & Kriedmann P. (1989) Determination of accurate extinction coefficients and simultaneous equations for assaying chlorophylls a and b extracted with four different solvents: verification of the concentration of chlorophyll standards by atomic absorption spectroscopy. *Biochimica et Biophysica Acta*, 975, 384-394.

Pospisil P., Skotnica J. & Naus J. (1998) Low and high temperature dependence of minimum F_0 and maximum F_m chlorophyll fluorescence in vivo. *Biochimica et Biophysica Acta*, 1363, 95-99.

Powles S.B. (1984) Photoinhibition of photosynthesis induced by visible light. *Annual Review of Plant Physiology*, 35, 15-44.

RASNZ (2005) Sun rise and set times for New Zealand. Royal Astronomical Society of New Zealand http://www.rasnz.org.nz/SRSStimes.htm accessed February 2005.

Read J.A.H., Geoffrey S. (1989) Foliar frost resistance of some evergreen tropical and extratropical Australasian *Nothofagus* species. *Australian Journal of Botany*, 37, 361-373.

Richardson A., Duigan S. & GP B. (2002) An evaluation of noninvasive methods to estimate foliar chlorophyll content. *New Phytologist*, 153, 185-194.

Roeske C. & O'Leary M.H. (1984) Carbon isotope effects on the enzyme-catalyzed carboxylation of ribulose biphosphate. *Biochemistry*, 23, 6275-6284.

Sakai A., Paton D. & Wardle P. (1981) Freezing resistance of trees of the south temperate zone, especially subalpine species of Australasia. *Ecology*, 62, 563-570.

Sakai A. & Wardle P. (1978) Freezing resistance of New Zealand Trees and shrubs. *New Zealand Journal of Ecology*, 1, 51-61.

Salmon J.T. (1980) *The Native Trees of New Zealand*. Reed, Wellington.

Scheidegger Y., Saurer M., Bahn M. & Siegwolf R. (2000) Linking stable oxygen and carbon isotopes with stomatal conductance and photosynthetic capacity: a conceptual model. *Oecologia*, 125, 350-357.

Schleser G. & Jayasekera R. (1985) $d^{13}C$ variations of leaves in forests as an indication of reassimilated CO_2 from the soil. *Oecologia*, 65, 536-542.

Scholander P.F., Hammel H.T., Bradsteet E.D. & Hemmingsen E.A. (1965) Sap pressure in vascular plants. *Science*, 148, 339-346.

Schreiber U. (1997) Chlorophyll fluorescence and photosynthetic energy conversion: Simple introductory experiments with the TEACHING-PAM Chlorophyll Fluorometer. Heinz Walz GmbH.

Schreiber U. & Berry J.A. (1977) Heat induced changes of chlorophyll fluorescence in intact leaves, correlated with damage of the photosynthetic apparatus. *Planta*, 136, 233-238.

Schreiber U., Bilger W. & Neubauer C. (1987) Chlorophyll fluorescence as a non-intrusive indicator for rapid assessment of in vivo photosynthesis. In: *Ecophysiology of Photosynthesis (Ecological Studies)* (eds E. Schulze & M. Caldwell), pp. 49-70. Springer-Verlag, Berlin.

Schwarzbach A.E. & McDade L.A. (2002) Phylogenetic relationships of the mangrove family Avicenniaceae based on chloroplast and nuclear ribosomal DNA sequences. *Systematic Botany*, 27, 84-98.

Seymour R.S. & Schultze-Motel P. (1997) Heat-producing flowers. *Endeavour*, 21, 125-129.

Shang W. & Feierabend J. (1998) Slow turnover of the D1 reaction center protein of photosystem II in leaves of high mountain plants. *FEBS Letters*, 425, 97-100.

Sherrod C.L., Hockaday, Donald L., and McMillan, Calvin (1986) Survival of red mangrove, *Rhizophora mangle*, on the Gulf of Mexico coast of Texas. *Contributions to Marine Science*, 27-36.

Silva E.A., DaMatta F.M., Ducatti C., Regazzi A.J. & Barros R.S. (2004) Seasonal changes in vegetative growth and photosynthesis of Arabica coffee trees. *Field Crops Research*, 89, 349-357.

Slavik B. (1974) *Methods of Studying Plant Water Relations*. Springer-Verlag, Berlin, Heidelberg, New York.

Smillie R. & Nott R. (1979) Heat injury in leaves of alpine, temperate and tropical plants. *Australian Journal of Plant Physiology*, 6, 135-141.

Smith J.A.C., Popp M., Lüttge U., Cram J.M., Diaz M., Griffiths H., Lee H.J.S., Medina E., Schäfer C.S., Stimmel K.-H. & Thonke B. (1989) Ecophysiology of xerophytic and halophytic vegetation of a coastal alluvial plain in northern Venezuela. *New Phytologist*, 111, 293-307.

Sobrado M.A. (1999) Leaf photosynthesis of the mangrove *Avicennia germinans* as affected by NaCl. *Photosynthetica*, 36, 547-555.

Sobrado M.A. (2000) Relation of water transport to leaf gas exchange properties in three mangrove species. *Trees*, 14, 258-262.

Sonoike K. (1999) The different roles of chilling temperatures in the photoinhibition of photosystem I and photosystem II. *Journal of Photochemistry and Photobiology B: Biology*, 48, 136-141.

Spectrum (2002) Chlorophyll Meter SPAD-502 Instruction Manual. Spectrum Technologies Inc, Available at: http://www.geneq.com/catalog/en/spad-502.html (October 2003).

SPSS (2002) Sigmaplot for Windows version 8.0.

StatSoft (2003) STATISTICA (data analysis software system) version 6. *www.statsoft.com*.

Steponkus P.L. (1984) Role of the Plasma Membrane In Freezing Injury and Cold Acclimation. *Annual Review of Plant Physiology*, 35, 543-584.

Sun M., Wonga K. & Leea J. (1998) Reproductive biology and population genetic structure of Kandelia candel (Rhizophoraceae), a viviparous mangrove species. *American Journal of Botany*, 85, 1631-1637.

Sutcliffe J.F. (1977) *Plants and Temperature*. Edward Arnold Publishers, London.

Terashima I. & Hikosaka K. (1995) Comparative ecophysiology of leaf and canopy photosynthesis. *Plant, Cell & Environment*, 18, 1111-1128.

Tomlinson P.B. (1986) *The botany of mangroves*. Cambridge University Press.

Treshow M. (1970) *Environment and Plant Response*. McGraw-Hill Book Company, New York.

Tuffers A., Naidoo G. & von Willert D. (2001) Low salinities adversely affect photosynthesis performance of the mangrove *Avicennia marina*. *Wetlands Ecology & Managment*, 9, 225-232.

Tupfers A., Von Willert D. & Naidoo G. (1999) The contribution of leaf angle to photoprotection in the mangroves *Avicennia marina* (Forssk.) Vierh. and *Bruguiera gymnorrhiza* (L.) Lam. under field conditions in South Africa. *Flora*, 267-275.

Tyree M.T. (1997) The Cohesion-Tension theory of sap-ascent: current controversies. *Journal of Experimental Botany*, 48, 1753-1765.

Vogel J.C. (1993) Variability of carbon isotope fractionation. In: *Stable isotopes and plant carbon-water relations* (eds J. Ehleringer, A. Hall, E, & G.D. Farquar), pp. 29-45. Academic Press Inc, San Diego.

Walbert K. (2002) Investigations in the New Zealand mangrove, *Avicennia marina* var. *australasica*. Master of Science, Waikato University.

Walcroft A.S. (1994) Aspects of stable carbon isotope variation in tree foliage and wood. Master of Science, University of Waikato.

Walcroft A.S., Silvester W.B., Grace J.C., Carson S.D. & Waring R.H. (1996) Effects of branch length on carbon isotope discrimination in *Pinus radiata*. *Tree Physiology*, 16, 281-286.

Walsby J. (1992) Forests in the Sea. *New Zealand Geographic*, 15, 45-64.

Wardle P. (1985) Environmental influences on the vegetation of New Zealand. *New Zealand Journal of Botany*, 23, 773-788.

Wardle P. (1991) *Vegetation of New Zealand.* University Press Cambridge, Cambridge.

Wei C., Tyree M.T. & Bennink J.P. (2000) The transmission of gas pressure to xylem fluid pressure when plants are inside a pressure bomb. *Journal of Experimental Botany*, 51, 309-316.

Welander N.T., Gemmell P., Hellgren O. & Ottosson B. (1994) The consequences of freezing temperatures followed by high irradiance on in vivo chlorophyll fluorescence and growth in *Picea abies*. *Physiologia Plantarum*, 91, 121-127.

Werner C., Ryel R.J., Correia O. & Beyschlag W. (2001a) Effects of photoinhibition on whole-plant carbon gain assessed with a photosynthesis model. *Plant, Cell & Environment*, 24, 27-40.

Werner C., Ryelb R., Correiac O. & Beyschlaga W. (2001b) Structural and functional variability within the canopyand its relevance for carbon gain and stress avoidance. *Acta Oecologica*, 22, 129-138.

Wise R.R. & Naylor A.W. (1987) Chilling Enhanced Photooxidation: Evidence for the role of singlet oxygen and superoxide in the breakdown of pigments and endogenous antioxidants. *Plant Physiology*, 83, 277-282.

Woodward F.I. (1987) *Climate and Plant Distribution.* Cambridge University Press.

Zhang M.I.N. & Willison J.H.M. (1987) An improved conductivity method for the measurement of frost hardiness. *Canadian Journal of Botany*, 65, 710-715.

Zhang Q.-M., Sui S.-Z., Zhang Y.-C., Yu H.-B., Sun Z.-X. & X-S W. (2001) Marine environmental indexes related to mangrove growth. *Acta Ecologia Sinica*, 21, 1427-1437.

Appendices

Appendix I

Campbell CR10X data-logger programmes (Chapters 2, 4, 5, 6)

1. Microclimate Station: example for Ohiwa Harbour

Measures external PFD, internal canopy PFD, substrate temperature (°C), external RH (%) and air temperature (°C)

```
;{CR10X}
;

*Table 1 Program
        01:   10   Execution Interval (seconds)

;measure external light
1: Volt (SE) (P1)
 1: 1       Reps
 2: 23      25 mV 60 Hz Rejection Range
 3: 01      SE Channel
 4: 1       Loc [ LightEX   ]
 5: 263.6   Mult
 6: 0.0     Offset

;measure internal canopy light
2: Volt (SE) (P1)
 1: 1       Reps
 2: 23      25 mV 60 Hz Rejection Range
 3: 02      SE Channel
 4: 2       Loc [ LightIN   ]
 5: 268.3   Mult
 6: 0.0     Offset

;measure substrate temperature
3: Temp (107) (P11)
 1: 1       Reps
 2: 03      SE Channel
 3: 01      Excite all reps w/E1
 4: 3       Loc [ tempMUD   ]
 5: 1.0     Mult
 6: 0.0     Offset

;measure relative humidity (external canopy)
4: Volt (SE) (P1)
 1: 1       Reps
 2: 15      2500 mV Fast Range
 3: 11      SE Channel
 4: 4       Loc [ RH        ]
 5: 0.1     Mult
 6: 0.0     Offset

;measure external ambient air temperature
5: Volt (SE) (P1)
 1: 1       Reps
 2: 35      2500 mV 50 Hz Rejection Range
 3: 12      SE Channel
 4: 5       Loc [ tempAIR   ]
 5: 0.1     Mult
 6: 0.0     Offset
```

```
;measure battery voltage
6:  Batt Voltage (P10)
 1: 7       Loc [ BattV     ]


7:  If time is (P92)
 1: 0000    Minutes (Seconds --) into a
 2: 2       Interval (same units as above)
 3: 10      Set Output Flag High (Flag 0)


8:  Real Time (P77)
 1: 120     (Same as 220) D,Hr/Mn

9:  Sample (P70)
 1: 6       Reps
 2: 1       Loc [ LightEX   ]

End Program
```

Appendix II

Campbell CR10X data-logger programmes

Artificial Frost Experiment (Chapter 6)

Measures battery supply voltage, reference temperature, external ambient temperature (°C), coldbox temperatures (2 treatments, °C), coldbox leaf temperatures (2 treatments, °C) and calculates the difference between box and leaf temperature.

```
;Measure battery voltage
1: Batt Voltage (P10)
 1: 1       Loc [ BattV    ]

;Measure CR10X reference junction temperature
2: Internal Temperature (P17)
 1: 2       Loc [ REFTEMC  ]

;Measure external ambient temperature
3: Temp (107) (P11)
 1: 1       Reps
 2: 3       SE Channel
 3: 1       Excite all reps w/E1
 4: 3       Loc [ EXTEMP   ]
 5: 1.0     Mult
 6: 0.0     Offset

;Measure 107 temperature sensor box A
4: Temp (107) (P11)
 1: 1       Reps
 2: 1       SE Channel
 3: 1       Excite all reps w/E1
 4: 4       Loc [ TEMPA    ]
 5: 1.0     Mult
 6: 0.0     Offset

;measure 107 temperature sensor box B
5: Temp (107) (P11)
 1: 1       Reps
 2: 2       SE Channel
 3: 1       Excite all reps w/E1
 4: 6       Loc [ TEMPB    ]
 5: 1.0     Mult
 6: 0.0     Offset

;measure leaf temperature in box A
6: Thermocouple Temp (DIFF) (P14)
 1: 1       Reps
 2: 2       7.5 mV Slow Range
 3: 5       DIFF Channel
 4: 2       Type E (Chromel-Constantan)
 5: 2       Ref Temp (Deg. C) Loc [ REFTEMC  ]
 6: 5       Loc [ LEAFA    ]
 7: 1.0     Mult
 8: 0.0     Offset

;measure leaf temperature in box B
7: Thermocouple Temp (DIFF) (P14)
 1: 1       Reps
 2: 2       7.5 mV Slow Range
 3: 6       DIFF Channel
```

```
 4: 2      Type E (Chromel-Constantan)
 5: 2      Ref Temp (Deg. C) Loc [ REFTEMC   ]
 6: 7      Loc [ LEAFB     ]
 7: 1.0    Mult
 8: 0.0    Offset


;Calculate difference between leaf A temp and box temp A
8:  Z=X-Y (P35)
 1: 4      X Loc [ TEMPA     ]
 2: 5      Y Loc [ LEAFA     ]
 3: 8      Z Loc [ TEMPDIFFA ]

;Calculate difference between leaf B temp and box B temp

9:  Z=X-Y (P35)
 1: 6      X Loc [ TEMPB     ]
 2: 7      Y Loc [ LEAFB     ]
 3: 9      Z Loc [ TEMPDIFFB ]


10:  If time is (P92)
 1: 0      Minutes (Seconds --) into a
 2: 10     Interval (same units as above)
 3: 10     Set Output Flag High (Flag 0)

11:  Set Active Storage Area (P80)
 1: 1      Final Storage Area 1
 2: 100    Array ID


12:  Real Time (P77)
 1: 120    (Same as 220) D,Hr/Mn

End Program
```

Appendix III

Frost Tolerance data (Chapter 3)

Table 1. Data matrix for the frost tolerance study (Chapter Three) in the New Zealand mangrove *Avicennia marina* subsp. *australasica*. Site = location; Coast = East (E) or West (W) of the North Island, New Zealand; Life Stage = Adult (A) or Seedling (S); LT_{50} = frost tolerance (°C) as calculated by the electrical conductivity method.

SITE	LATITUDE (°S)	COAST	LIFE STAGE	MONTH	LT_{50}
TPO	34.26	E	A	may	-2.98
TPO	34.26	E	A	may	-2.94
TPO	34.26	E	A	may	-2.94
TPO	34.26	E	A	may	-2.86
TPO	34.26	E	A	may	-2.79
TPO	34.26	E	A	may	-2.68
TPO	34.26	E	A	may	-2.58
TPO	34.26	E	A	may	-2.55
TPO	34.26	E	A	may	-2.53
TPO	34.26	E	A	may	-2.50
PAI	35.12	E	A	may	-3.93
PAI	35.12	E	A	may	-3.68
PAI	35.12	E	A	may	-3.59
PAI	35.12	E	A	may	-3.26
PAI	35.12	E	A	may	-3.18
PAI	35.12	E	A	may	-3.08
PAI	35.12	E	A	may	-3.06
PAI	35.12	E	A	may	-2.92
PAI	35.12	E	A	may	-2.60
PAI	35.12	E	A	may	-2.48
MAN	36.07	E	A	may	-3.93
MAN	36.07	E	A	may	-4.36
MAN	36.07	E	A	may	-4.28
MAN	36.07	E	A	may	-4.15
MAN	36.07	E	A	may	-4.13
MAN	36.07	E	A	may	-4.03
MAN	36.07	E	A	may	-3.95
MAN	36.07	E	A	may	-3.91
MAN	36.07	E	A	may	-3.78
MAN	36.07	E	A	may	-3.77
TGA	37.40	E	A	may	-4.84
TGA	37.40	E	A	may	-4.79
TGA	37.40	E	A	may	-4.78
TGA	37.40	E	A	may	-4.77
TGA	37.40	E	A	may	-4.76
TGA	37.40	E	A	may	-4.76
TGA	37.40	E	A	may	-4.75
TGA	37.40	E	A	may	-4.73
TGA	37.40	E	A	may	-4.53
TGA	37.40	E	A	may	-4.15
OHI	38.03	E	A	may	-5.99
OHI	38.03	E	A	may	-5.54
OHI	38.03	E	A	may	-4.77

OHI	38.03	E	A	may	-4.68
OHI	38.03	E	A	may	-4.55
OHI	38.03	E	A	may	-4.53
OHI	38.03	E	A	may	-4.48
OHI	38.03	E	A	may	-4.45
OHI	38.03	E	A	may	-4.33
OHI	38.03	E	A	may	-4.26
HER	35.15	W	A	may	-4.30
HER	35.15	W	A	may	-4.17
HER	35.15	W	A	may	-4.09
HER	35.15	W	A	may	-4.09
HER	35.15	W	A	may	-4.03
HER	35.15	W	A	may	-4.01
HER	35.15	W	A	may	-3.93
HER	35.15	W	A	may	-3.87
HER	35.15	W	A	may	-3.81
HER	35.15	W	A	may	-3.48
RAG	37.48	W	A	may	-4.76
RAG	37.48	W	A	may	-4.73
RAG	37.48	W	A	may	-4.73
RAG	37.48	W	A	may	-4.71
RAG	37.48	W	A	may	-4.71
RAG	37.48	W	A	may	-4.61
RAG	37.48	W	A	may	-4.58
RAG	37.48	W	A	may	-4.56
RAG	37.48	W	A	may	-4.55
RAG	37.48	W	A	may	-4.63
KAI	36.07	W	A	may	-3.53
KAI	36.07	W	A	may	-3.45
KAI	36.07	W	A	may	-3.45
KAI	36.07	W	A	may	-3.44
KAI	36.07	W	A	may	-3.43
KAI	36.07	W	A	may	-3.34
KAI	36.07	W	A	may	-3.32
KAI	36.07	W	A	may	-3.30
KAI	36.07	W	A	may	-3.16
KAI	36.07	W	A	may	-3.33
TPO	34.26	E	A	nov	-4.23
TPO	34.26	E	A	nov	-4.16
TPO	34.26	E	A	nov	-3.95
TPO	34.26	E	A	nov	-3.92
TPO	34.26	E	A	nov	-3.89
TPO	34.26	E	A	nov	-3.41
TPO	34.26	E	A	nov	-2.94
TPO	34.26	E	A	nov	-2.91
TPO	34.26	E	A	nov	-2.89
TPO	34.26	E	A	nov	-2.76
PAI	35.12	E	A	nov	-4.56
PAI	35.12	E	A	nov	-4.22
PAI	35.12	E	A	nov	-3.92
PAI	35.12	E	A	nov	-3.78
PAI	35.12	E	A	nov	-3.78
PAI	35.12	E	A	nov	-3.48
PAI	35.12	E	A	nov	-3.46
PAI	35.12	E	A	nov	-3.31
PAI	35.12	E	A	nov	-3.08
PAI	35.12	E	A	nov	-3.92

MAN	36.07	E	A	nov	-4.84
MAN	36.07	E	A	nov	-5.21
MAN	36.07	E	A	nov	-4.74
MAN	36.07	E	A	nov	-4.67
MAN	36.07	E	A	nov	-4.67
MAN	36.07	E	A	nov	-4.58
MAN	36.07	E	A	nov	-4.74
MAN	36.07	E	A	nov	-4.51
MAN	36.07	E	A	nov	-4.82
MAN	36.07	E	A	nov	-4.58
TGA	37.40	E	A	nov	-5.14
TGA	37.40	E	A	nov	-5.14
TGA	37.40	E	A	nov	-5.12
TGA	37.40	E	A	nov	-5.11
TGA	37.40	E	A	nov	-5.07
TGA	37.40	E	A	nov	-5.04
TGA	37.40	E	A	nov	-5.03
TGA	37.40	E	A	nov	-4.98
TGA	37.40	E	A	nov	-4.75
TGA	37.40	E	A	nov	-4.58
HER	35.15	W	A	nov	-5.08
HER	35.15	W	A	nov	-4.88
HER	35.15	W	A	nov	-4.82
HER	35.15	W	A	nov	-4.80
HER	35.15	W	A	nov	-4.48
HER	35.15	W	A	nov	-4.44
HER	35.15	W	A	nov	-4.41
HER	35.15	W	A	nov	-4.09
HER	35.15	W	A	nov	-3.62
HER	35.15	W	A	nov	-4.58
RAG	37.48	W	A	nov	-4.96
RAG	37.48	W	A	nov	-4.89
RAG	37.48	W	A	nov	-4.88
RAG	37.48	W	A	nov	-4.85
RAG	37.48	W	A	nov	-4.70
RAG	37.48	W	A	nov	-4.64
RAG	37.48	W	A	nov	-4.53
RAG	37.48	W	A	nov	-4.53
RAG	37.48	W	A	nov	-4.42
RAG	37.48	W	A	nov	-4.37
TPO	34.26	E	S	may	-5.06
TPO	34.26	E	S	may	-4.58
TPO	34.26	E	S	may	-3.77
TPO	34.26	E	S	may	-3.68
TPO	34.26	E	S	may	-3.62
PAI	35.12	E	S	may	-4.17
PAI	35.12	E	S	may	-4.02
PAI	35.12	E	S	may	-3.99
PAI	35.12	E	S	may	-3.74
PAI	35.12	E	S	may	-3.30
MAN	36.07	E	S	may	-4.38
MAN	36.07	E	S	may	-4.35
MAN	36.07	E	S	may	-4.09
MAN	36.07	E	S	may	-4.03
MAN	36.07	E	S	may	-3.96
TGA	37.40	E	S	may	-4.39
TGA	37.40	E	S	may	-4.32

TGA	37.40	E	S	may	-4.31
TGA	37.40	E	S	may	-4.25
TGA	37.40	E	S	may	-4.19
OHI	38.03	E	S	may	-3.16
OHI	38.03	E	S	may	-3.13
OHI	38.03	E	S	may	-3.00
OHI	38.03	E	S	may	-2.89
OHI	38.03	E	S	may	-2.92
HER	35.15	W	S	may	-4.92
HER	35.15	W	S	may	-4.80
HER	35.15	W	S	may	-4.57
HER	35.15	W	S	may	-4.55
HER	35.15	W	S	may	-4.49
RAG	37.48	W	S	may	-4.44
RAG	37.48	W	S	may	-4.34
RAG	37.48	W	S	may	-4.28
RAG	37.48	W	S	may	-4.16
RAG	37.48	W	S	may	-4.07
KAI	36.07	W	S	may	-5.00
KAI	36.07	W	S	may	-4.96
KAI	36.07	W	S	may	-4.83
KAI	36.07	W	S	may	-4.78
KAI	36.07	W	S	may	-4.75
TPO	34.26	E	S	nov	-4.94
TPO	34.26	E	S	nov	-4.87
TPO	34.26	E	S	nov	-4.78
TPO	34.26	E	S	nov	-4.56
TPO	34.26	E	S	nov	-4.42
PAI	35.12	E	S	nov	-5.05
PAI	35.12	E	S	nov	-5.00
PAI	35.12	E	S	nov	-4.86
PAI	35.12	E	S	nov	-4.57
PAI	35.12	E	S	nov	-2.90
MAN	36.07	E	S	nov	-5.20
MAN	36.07	E	S	nov	-5.00
MAN	36.07	E	S	nov	-4.96
MAN	36.07	E	S	nov	-4.78
MAN	36.07	E	S	nov	-4.71
TGA	37.40	E	S	nov	-5.14
TGA	37.40	E	S	nov	-4.94
TGA	37.40	E	S	nov	-4.88
TGA	37.40	E	S	nov	-4.79
TGA	37.40	E	S	nov	-4.74
HER	35.15	W	S	nov	-5.01
HER	35.15	W	S	nov	-4.95
HER	35.15	W	S	nov	-4.82
HER	35.15	W	S	nov	-4.73
HER	35.15	W	S	nov	-4.59
RAG	37.48	W	S	nov	-4.87
RAG	37.48	W	S	nov	-4.69
RAG	37.48	W	S	nov	-4.56
RAG	37.48	W	S	nov	-4.57
RAG	37.48	W	S	nov	-4.24

Appendix IV

Diurnal Study summary data (Chapter 4)

Tables 1 – 6:
Leaf water potential Ψ (MPa) as measured by Scholander-type Pressure Bomb. Data are mean values ± SE of 2 leaves on each of four trees at each of three study sites (Paihia, Whitianga and Ohiwa Harbours).

Table 1: OHIWA HARBOUR (summer)

Time	21st Dec	22nd Dec
06:20	-1.95 ± 0.21	-1.57 ± 0.19
08:00	-1.36 ± 0.37	-1.88 ± 0.53
10:00	-2.40 ± 0.69	-2.25 ± 0.62
12:00	-2.92 ± 0.82	-3.28 ± 0.90
14:00	-3.26 ± 0.91	-3.17 ± 0.86
16:00	-2.97 ± 0.81	-3.20 ± 0.88
18:00	-2.36 ± 0.66	-2.47 ± 0.68
19:30	-2.69 ± 0.09	-2.95 ± 0.11

Table 2: OHIWA HARBOUR (winter)

Time	8th Sept	9th Sept	10th Sept
07:15	-1.51 ± 0.06	-0.93 ± 0.22	-1.82 ± 0.08
09:00	-2.80 ± 0.06	-1.86 ± 0.04	-1.52 ± 0.20
11:00	-3.40 ± 0.12	-3.57 ± 0.22	-3.55 ± 0.24
13:00	-4.06 ± 0.08	-3.93 ± 0.13	-3.79 ± 0.21
15:00	-3.59 ± 0.12	-3.83 ± 0.12	-3.88 ± 0.13
17:30	-3.29 ± 0.07	-3.46 ± 0.04	-3.34 ± 0.07

Table 3: WHITIANGA HARBOUR (winter)

Time	10th Jul	25th Jul	26th Jul
07:20	-1.62 ± 0.08	-0.57 ± 0.23	-1.23 ± 0.17
09:15	-1.59 ± 0.08	-0.90 ± 0.15	-0.77 ± 0.22
11:15	-2.67 ± 0.23	-2.35 ± 0.42	-1.70 ± 0.22
13:15	-3.48 ± 0.14	-3.24 ± 0.50	-2.64 ± 0.27
15:00	-3.52 ± 0.09	-3.59 ± 0.16	-2.60 ± 0.16
17:00	-2.84 ± 0.10	-3.03 ± 0.09	-2.47 ± 0.21
20:00	-2.15 0.07	-3.63 ± 0.16	-3.53 0.07

Table 4: WHITIANGA HARBOUR (summer)

Time	21st Mar	22nd Mar	23rd Mar
06:00	-1.58 ± 0.07	-1.50 ± 0.01	-1.95 ± 0.22
08:00	-1.57 ± 0.00	-1.68 ± 0.03	-2.97 ± 0.26
10:00	-3.20 ± 0.04	-3.53 ± 0.27	-4.10 ± 0.23
12:00	-3.93 ± 0.11	-3.92 ± 0.01	-4.12 ± 0.12
14:00	-3.91 ± 0.04	-4.30 ± 0.23	-3.96 ± 0.20
16:00	-3.99 ± 0.03	-3.83 ± 0.02	-3.06 ± 0.07
18:00	-2.99 0.04	-2.88 ± 0.01	-3.53 0.22

Table 5: PAIHIA, Bay of Islands (winter)

Time	21st Aug	22nd Aug	23rd Aug
07:10	-1.28 ± 0.08	-1.00 ± 0.05	-1.09 ± 0.18
09:30	-2.17 ± 0.23	-1.80 ± 0.06	-1.20 ± 0.15
11:00	-2.88 ± 0.21	-2.82 ± 0.11	-2.40 ± 0.24
13:00	-3.33 ± 0.25	-3.16 ± 0.12	-3.26 ± 0.02
15:00	-3.12 ± 0.07	-2.94 ± 0.14	-1.76 ± 0.28
17:00	-2.78 ± 0.18	-2.50 ± 0.08	

Table 6: PAIHIA, Bay of Islands (summer)

Time	12th Dec	13th Dec	14th Dec
06:00		-1.94 ± 0.13	-1.23 ± 0.21
08:00	-2.53 ± 0.14	-3.53 ± 0.30	-2.50 ± 0.33
10:00	-4.43 ± 0.06	-4.36 ± 0.07	-4.16 ± 0.26
12:00	-4.24 ± 0.14	-4.82 ± 0.22	-4.70 ± 0.07
14:00	-4.21 ± 0.21	-4.73 ± 0.24	-4.63 ± 0.16
16:00	-3.77 ± 0.15	-4.44 ± 0.10	
18:00	-3.67 0.13	-3.94 ± 0.10	
20:00	-3.38 0.08	-3.66 ± 0.09	

Table 7. CO_2 assimilation rate (A) and stomatal conductance (*gs*) in leaves of *Avicennia* at Ohiwa Harbour during summer and winter (values are mean ± std error)

Summer time	A (μmol m^{-2} s^{-1})	se	*gs* (mmol m^{-2} s^{-1})	se
07:18:00	-0.15	0.08	110.80	3.67
09:14:00	2.86	0.31	72.62	3.88
11:10:00	4.65	0.36	42.75	1.77
13:08:00	3.66	0.50	32.52	2.22
15:02:00	4.25	0.31	32.63	1.43
17:05:00	-0.11	0.02	50.02	1.88
Winter time				
07:11:00	-0.03	0.11	186.30	6.08
09:03:00	1.15	0.37	139.53	11.22
10:41:00	0.69	0.16	14.89	1.64
11:31:00	0.75	0.38	17.83	1.99
13:27:00	0.06	0.002	9.86	0.35
15:25:00	0.06	0.0001	12.75	0.20
17:40:00	-0.28	0.0001	37.70	0.17

Table 8. CO_2 assimilation rate (A) and stomatal conductance (*gs*) in leaves of *Avicennia* at Paihia during summer and winter (values are mean ± std error)

Summer Time	A (μmol m^{-2} s^{-1})	se	*gs* (mmol m^{-2} s^{-1})	se
06:06:00	-0.57	0.03	43.66	1.29
08:07:00	5.45	0.69	82.12	2.29
10:07:00	4.43	0.54	30.36	1.90
12:07:00	4.34	0.52	14.55	1.07
14:07:00	4.71	0.47	19.23	1.07
16:07:00	2.34	0.29	26.29	2.71
18:07:00	1.24	0.22	19.83	2.98
20:03:00	-0.18	0.06	19.70	1.24
Winter time				
07:45:00	-0.98	0.41	207.73	12.78
09:32:00	1.27	0.64	222.35	5.11
11:50:00	5.70	0.75	106.44	13.46
13:33:00	2.34	0.54	49.33	3.33
15:45:00	1.68	0.30	27.33	5.91
17:31:00	2.73	0.44	96.80	11.33

Table 9. CO_2 assimilation rate (A) and stomatal conductance (*gs*) in leaves of *Avicennia* Whitianga Harbour during summer and winter (values are mean ± std error)

Summer time	A (μmol m^{-2} s^{-1})	se	*gs* (mmol m^{-2} s^{-1})	se
07:56:00	1.11	0.26	93.88	2.26
09:41:00	1.05	0.90	86.72	7.09
10:25:00	5.8667	1.3797	112.44	10.22
12:03:00	7.0926	0.8262	70.66	2.84
13:48:00	7.1000	0.6842	57.22	3.83
15:31:00	8.0000	0.5748	66.37	3.30
17:28:00	5.4294	0.9244	45.00	2.82
18:04:00	2.2111	0.3025	52.55	4.69
19:16:00	0.3960	0.2790	57.11	4.04
Winter time				

07:25:00	-0.2208	0.5379	108.37	18.09
09:15:00	1.2792	1.5391	133.25	31.38
11:00:00	2.9750	1.8241	74.50	35.57
12:30:00	2.7833	1.6629	45.16	13.46
13:00:00	1.5917	0.4852	35.33	8.57
15:00:00	2.2818	2.4632	33.59	12.16
17:00:00	-0.1917	0.1505	62.33	11.46

Table 10. *Fv/Fm* in leaves of *Avicennia* at Ohiwa Harbour during summer and winter (values are mean ± std error)

Summer time	Fv/Fm	se
07:47:00	0.7600	0.01
09:24:00	0.7702	0.01
11:18:00	0.7520	0.01
13:10:00	0.7381	0.007-3
15:05:00	0.7443	0.0103
17:07:00	0.7780	0.005
Winter time		
07:25:00	0.6715	0.01
09:01:00	0.6894	0.008
11:03:00	0.6610	0.01
13:47:00	0.6725	0.002
15:06:00	0.6833	0.001
17:06:00	0.7115	0.003

Table 11. *Fv/Fm* in leaves of *Avicennia* at Whitianga Harbour during summer and winter (values are mean ± std error)

Summer time	Fv/Fm	se
06:40:00	0.8070	0.006
08:21:00	0.8008	0.015
10:26:00	0.7991	0.006
12:32:00	0.7661	0.005
14:19:00	0.7387	0.008
16:22:00	0.7681	0.0126
18:17:00	0.7914	0.006
Winter time		
07:43:00	0.5565	0.021
09:11:00	0.6089	0.010
11:01:00	0.6261	0.011
13:03:00	0.6303	0.009
15:05:00	0.6274	0.013
16:51:00	0.6238	0.015

Tables 12- 14

Net daily photosynthesis calculated from field measurements of leaf CO_2 gas exchange in *Avicennia marina* subsp. *australasica* in summer and winter at Paihia (table 1), Whitianga (table 2) and Ohiwa Harbours (table 3), New Zealand. % PFD is the percentage of the total photoperiod with PFD $\geq$ 500 μmol m^{-2} s^{-1}; Min Temp is the coldest air temperature (degrees Celsius) recorded during the night previous to measurement; Net PS is the net daily photosynthesis (mmol m^{-2} day^{-1}) calculated for each leaf.

Table 12

LEAF	Net PS	% PFD	Min Temp	Sample month
P2108A1	66.9	40.0	5.9	AUG
P2108A2	138.9	40.0	5.9	AUG
P2108A3	159.7	40.0	5.9	AUG
P2108B1	131.3	40.0	5.9	AUG
P2108B2	74.1	40.0	5.9	AUG
P2108B3	61.3	40.0	5.9	AUG
P2108C1	71.7	40.0	5.9	AUG
P2108C2	86.6	40.0	5.9	AUG
P2108C3	53.4	40.0	5.9	AUG
P2208A1	106.9	42.8	9.7	AUG
P2208A2	129.4	42.8	9.7	AUG
P2208A3	124.4	42.8	9.7	AUG
P2208B1	135.3	42.8	9.7	AUG
P2208B2	56.6	42.8	9.7	AUG
P2208B3	98.0	42.8	9.7	AUG
P2208C1	93.5	42.8	9.7	AUG
P2208C2	78.5	42.8	9.7	AUG
P2208C3	67.8	42.8	9.7	AUG
P1212A1	223.0	26.7	14.8	DEC
P1212A2	78.2	26.7	14.8	DEC
P1212A3	105.7	26.7	14.8	DEC
P1212B1	201.6	26.7	14.8	DEC
P1212B2	181.9	26.7	14.8	DEC
P1212B3	152.8	26.7	14.8	DEC
P1212C1	66.7	26.7	14.8	DEC
P1212C2	78.9	26.7	14.8	DEC
P1212C3	168.0	26.7	14.8	DEC
P1212D1	142.3	26.7	14.8	DEC
P1212D2	158.0	26.7	14.8	DEC
P1212D3	126.7	26.7	14.8	DEC
P1312A1	148.2	40.0	11.8	DEC

P1312A2	76.5	40.0	11.8	DEC
P1312A3	72.1	40.0	11.8	DEC
P1312B1	145.1	40.0	11.8	DEC
P1312B2	214.3	40.0	11.8	DEC
P1312B3	148.3	40.0	11.8	DEC
P1312C1	48.4	40.0	11.8	DEC
P1312C2	37.1	40.0	11.8	DEC
P1312C3	179.4	40.0	11.8	DEC
P1312D1	137.9	40.0	11.8	DEC
P1312D2	110.4	40.0	11.8	DEC
P1312D3	120.4	40.0	11.8	DEC

Table 13

LEAF	Net PS	% PFD	Min Temp	Sample month
W1007A1	139.9	0.0	3.1	JUL
W1007A2	73.9	0.0	3.1	JUL
W1007A3	94.4	0.0	3.1	JUL
W1007B1	111.1	0.0	3.1	JUL
W1007B2	4.6	0.0	3.1	JUL
W1007B3	108.7	0.0	3.1	JUL
W1007C1	98.3	0.0	3.1	JUL
W1007C2	106.8	0.0	3.1	JUL
W1007C3	59.5	0.0	3.1	JUL
W1007D1	159.2	0.0	3.1	JUL
W1007D2	171.0	0.0	3.1	JUL
W1007D3	135.7	0.0	3.1	JUL
W1107A1	78.1	0.0	-1.0	JUL
W1107A2	30.6	0.0	-1.0	JUL
W1107A3	79.3	0.0	-1.0	JUL
W1107B1	47.3	0.0	-1.0	JUL
W1107B2	43.8	0.0	-1.0	JUL
W1107B3	58.6	0.0	-1.0	JUL
W1107C1	83.4	0.0	-1.0	JUL
W1107C2	97.4	0.0	-1.0	JUL
W1107C3	78.2	0.0	-1.0	JUL
W1107D1	120.1	0.0	-1.0	JUL
W1107D2	138.5	0.0	-1.0	JUL
W1107D3	120.4	0.0	-1.0	JUL
W1207A1	42.1	0.0	-2.0	JUL

W1207A2	46.7	0.0	-2.0	JUL
W1207A3	33.1	0.0	-2.0	JUL
W1207B1	39.9	0.0	-2.0	JUL
W1207B2	23.8	0.0	-2.0	JUL
W1207B3	61.7	0.0	-2.0	JUL
W1207C1	31.1	0.0	-2.0	JUL
W1207C2	46.7	0.0	-2.0	JUL
W1207C3	39.9	0.0	-2.0	JUL
W1207D1	37.8	0.0	-2.0	JUL
W2103A1	156.0	65.8	12.8	MAR
W2103A2	325.0	65.8	12.8	MAR
W2103A3	210.0	65.8	12.8	MAR
W2103B1	167.4	65.8	12.8	MAR
W2103B2	167.8	65.8	12.8	MAR
W2103B3	244.2	65.8	12.8	MAR
W2103C1	152.6	65.8	12.8	MAR
W2103C2	160.3	65.8	12.8	MAR
W2103C3	170.5	65.8	12.8	MAR
W2203A1	126.6	58.3	14.1	MAR
W2203A2	266.8	58.3	14.1	MAR
W2203A3	248.2	58.3	14.1	MAR
W2203B1	354.1	58.3	14.1	MAR
W2203B2	173.4	58.3	14.1	MAR
W2203B3	236.2	58.3	14.1	MAR
W2203C1	258.9	58.3	14.1	MAR
W2203C2	357.9	58.3	14.1	MAR
W2203C3	258.3	58.3	14.1	MAR
W2303A1	306.2	63.9	15.8	MAR
W2303A2	276.7	63.9	15.8	MAR
W2303A3	282.6	63.9	15.8	MAR
W2303B1	333.6	63.9	15.8	MAR
W2303B2	172.9	63.9	15.8	MAR
W2303B3	199.2	63.9	15.8	MAR
W2303C1	379.2	63.9	15.8	MAR
W2303C2	305.5	63.9	15.8	MAR
W2303C3	136.4	63.9	15.8	MAR

Table 14

LEAF	Net PS	% PFD	Min Temp	Sample month
O0809A1	23.3	13.5	8.7	SEP
O0809A2	24.8	13.5	8.7	SEP
O0809A3	16.2	13.5	8.7	SEP
O0809B1	42.2	13.5	8.7	SEP
O0809B2	13.3	13.5	8.7	SEP
O0809B3	8.9	13.5	8.7	SEP
O0809C1	13.8	13.5	8.7	SEP
O0809C2	21.	13.5	8.7	SEP
O0809C3	10.5	13.5	8.7	SEP
O0809D1	6.1	13.5	8.7	SEP
O0809D2	28.6	13.5	8.7	SEP
O0809D3	10.6	13.5	8.7	SEP
O0909A1	23.1	37.8	2.7	SEP
O0909A2	31.9	37.8	2.7	SEP
O0909A3	32.9	37.8	2.7	SEP
O0909B1	33.5	37.8	2.7	SEP
O0909B2	18.7	37.8	2.7	SEP
O0909B3	38.1	37.8	2.7	SEP
O0909C1	10.3	37.8	2.7	SEP
O0909C2	32.3	37.8	2.7	SEP
O0909C3	26.5	37.8	2.7	SEP
O0909D1	19.7	37.8	2.7	SEP
O0909D2	21.7	37.8	2.7	SEP
O0909D3	24.9	37.8	2.7	SEP
O1009A1	10.7	35.1	2.8	SEP
O1009A2	18.5	35.1	2.8	SEP
O1009A3	6.0	35.1	2.8	SEP
O1009B1	4.1	35.1	2.8	SEP
O1009B2	8.1	35.1	2.8	SEP
O1009B3	41.4	35.1	2.8	SEP
O1009C1	0.0	35.1	2.8	SEP
O1009C2	0.0	35.1	2.8	SEP
O1009C3	0.8	35.1	2.8	SEP
O1009D1	3.2	35.1	2.8	SEP
O1009D2	0.0	35.1	2.8	SEP
O1009D3	0.0	35.10	2.8	SEP
O0405A1	42.3	37.50	11.5	DEC

O0405A2	59.3	37.5	11.5	DEC
O0405A3	54.5	37.5	11.5	DEC
O0405A4	59.8	37.5	11.5	DEC
O0405A5	54.7	37.5	11.5	DEC
O0405A6	36.9	37.5	11.5	DEC
O0405B1	166.5	37.5	11.5	DEC
O0405B2	92.7	37.5	11.5	DEC
O0405B3	108.5	37.5	11.5	DEC
O0405B4	93.3	37.5	11.5	DEC
O0405B5	132.3	37.5	11.5	DEC
O0405B6	113.3	37.5	11.5	DEC
O0405C1	95.7	37.5	11.5	DEC
O0405C2	148.7	37.5	11.5	DEC
O0405C3	150.3	37.5	11.5	DEC
O0405C4	92.9	37.5	11.5	DEC
O0405C5	123.2	37.5	11.5	DEC
O0405C6	140.4	37.5	11.5	DEC
O0505A1	94.9	59.4	11.2	DEC
O0505A2	87.2	59.4	11.2	DEC
O0505A3	101.1	59.4	11.2	DEC
O0505A4	91.8	59.4	11.2	DEC
O0505A5	101.8	59.4	11.2	DEC
O0505A6	96.7	59.4	11.2	DEC
O0505B1	138.9	59.4	11.2	DEC
O0505B2	159.9	59.4	11.2	DEC
O0505B3	174.6	59.4	11.2	DEC
O0505B4	155.9	59.4	11.2	DEC
O0505B5	113.	59.4	11.2	DEC
O0505B6	140.9	59.4	11.2	DEC
O0505C1	199.4	59.4	11.2	DEC
O0505C2	172.0	59.4	11.2	DEC
O0505C3	180.5	59.4	11.2	DEC
O0505C4	152.8	59.4	11.2	DEC
O0505C5	145.2	59.4	11.2	DEC
O0505C6	160.9	59.4	11.2	DEC

Appendix V

Seasonal study summary data (Chapter Five)

All measurements were made between April 2003 and October 2003 at approximately 5 to 6 week intervals (with the exception of a 60 day interval between April and June 2003 for CO_2 assimilation rates and stomatal conductance, due to equipment failure). Data are the mean values ± standard error of 10 samples, except where otherwise indicated.

Table 1. Foliar chlorophyll content of exposed and protected leaves of *Avicennia marina* subsp. *australasica* as measured *in-situ* with a Minolta SPAD-502 Chlorophyll Meter. Data points are mean values (SPAD-units) ± standard error. N = 50.

Sampling month (2003)	Mean chlorophyll content (EXPOSED leaves)	Mean chlorophyll Content (PROTECTED leaves)	N
April	48.96 ± 1.52	56.70 ± 2.20	50
May	48.03 ± 1.52	59.97 ± 1.51	50
June	49.65 ± 1.36	60.49 ± 1.47	50
July	40.86 ± 2.62	60.64 ± 1.76	50
August	37.28 ± 2.42	60.27 ± 1.36	50
October	39.99 ± 2.16	59.35 ± 1.62	50

Table 2. Maximum quantum efficiency of PSII or the ratio of variable to maximum chlorophyll fluorescence, (F_v/F_m, unitless values), in exposed and protected leaves of *Avicennia marina* subsp *australasica* after 15 minutes dark adaptation.

Sampling month (2003)	EXPOSED leaves Maximum quantum efficiency of PSII (Fv/Fm)	PROTECTED leaves Maximum quantum efficiency of PSII (Fv/Fm)	N
April	0.7194 ± 0.0150	0.7961 ± 0.0061	10
June	0.6417 ± 0.0126	0.7826 ± 0.0102	10
July	0.3151 ± 0.0501	0.6363 ± 0.0186	10
August	0.5414 ± 0.0416	0.7399 ± 0.0068	10
October	0.5076 ± 0.0751	0.6367 ± 0.0215	10

Table 3. Stomatal conductance (m mol $m^{-2}s^{-1}$) in exposed and protected leaves of *Avicennia marina* subsp *australasica*.

Sampling month (2003)	EXPOSED leaves stomatal conductance (μ mol $m^{-2}s^{-1}$)	PROTECTED leaves stomatal conductance (μ mol $m^{-2}s^{-1}$)	N
April	113.2 ± 7.27	111.3 ± 7.92	10
June	36.8 ± 2.97	46.7 ± 2.45	10
July	20.0 ± 1.40	44.6 ± 3.63	10
August	21.2 ± 0.80	29.3 ± 1.69	10
October	23.9 ± 1.60	33.4 ± 3.96	10

Table 4. CO_2 assimilation rates (μ mol $m^{-2}s^{-1}$) in exposed and protected leaves of *Avicennia marina* subsp *australasica*.

Sampling month (2003)	EXPOSED leaves CO_2 assimilation rate (μ mol $m^{-2}s^{-1}$)	PROTECTED leaves CO_2 assimilation rate (μ mol $m^{-2}s^{-1}$)	N
April	7.79 ± 1.07	8.01 ± 0.79	10
June	3.76 ± 0.34	3.79 ± 0.40	10
July	0.38 ± 0.64	1.86 ± 0.27	10
August	-1.01 ± 0.19	-0.47 ± 0.22	10
October	1.59 ± 0.32	2.50 ± 0.28	10

Appendix VI

Artificial Frost Study (Chapter 6)

Table 1. Relative photoinhibition (% PI) during three treatment days, each preceded by a cold night at +4, 0 and -4°C. Values are the percent decreaae in F_v/F_m at midday in treated leaves relative to first morning F_v/F_m in untreated leaves.

Leaf	Day number	%PI	min temp
B1a	day one	24.69	-4
B1b	day one	18.52	-4
B2a	day two	16.05	-4
B2b	day two	33.33	-4
B3a	day three	24.69	-4
B3b	day three	27.16	-4
C1a	day one	4.94	4
C1b	day one	2.47	4
C2a	day two	13.58	4
C2b	day two	4.94	4
C3a	day three	2.47	4
C3b	day three	0.00	4
A1a	day one	20.99	0
A1b	day one	11.11	0
A2a	day two	19.75	0
A2b	day two	17.28	0
A3a	day three	17.28	0
A3b	day three	24.69	0

Table 2. Relative photoinhibition (% PI) during three recovery days following cold-night treatment at +4, 0 and -4°C. Values are the percent decreaae in F_v/F_m at midday in treated leaves relative to first morning F_v/F_m in untreated leaves.

Leaf	Number of cold nights	Min Temp (°C)	%PI 1st recovery day	%PI 2nd recovery day	%PI 3rd recovery day
B1a	1night	4	6.17	8.64	-1.23
B1b	1night	4	19.75	13.58	9.88
B2a	2nights	4	2.47	0.00	1.23
B2b	2nights	4	2.47	2.47	0.00
B3a	3nights	4	6.17	2.47	2.47
B3b	3nights	4	4.94	0.00	-1.23
C1a	1night	0	22.22	12.35	6.17
C1b	1night	0	9.88	9.88	7.41
C2a	2nights	0	29.63	16.05	6.17
C2b	2nights	0	39.51	17.28	8.64
C3a	3nights	0	17.28	24.69	13.58
C3b	3nights	0	24.69	2.47	7.41
A1a	1night	-4	33.33	18.52	7.41
A1b	1night	-4	12.35	11.11	8.64
A2a	2nights	-4	28.40	13.58	7.41
A2b	2nights	-4	37.04	9.88	6.17
A3a	3nights	-4	24.69	7.41	8.64
A3b	3nights	-4	27.16	8.64	11.11

Table 3. A_{max}, gs at A_{max} and Relative A_{max} (%) during three treatment days, each preceded by a cold night at +4, 0 and -4°C. % Amax values are Amax of treated leaves relative to first A_{max} of untreated leaves.

Day number	A_{max} -4oC	g_s -4oC	% A_{max} -4oC	A_{max} +4oC	g_s +4oC	% A_{max} +4oC	A_{max} 0oC	g_s 0oC	% A_{max} 0oC
1	1.9	115	24.2	4.9	103	62.6	2.1	120	26.8
1	1.6	61	20.4	7.2	88	92.0	1.2	74	15.3
1	0.8	149	10.2	5.9	82	75.4	1.1	104	14.0
1	0.5	134	6.3	6	85	76.7	1.5	88	19.1
1	1	82	12.7	7	107	89.5	1.4	34	17.9
2	0.8	48	10.2	8.4	115	107.4			
2	0	98	0	9.5	87	121.4	3.3	97	42.1
2	0	55	0	5.8	59	74.1	1.7	93	21.7
2	0.3	134	3.8	4.3	85	54.9	1.3	61	16.6
2	0.5	74	6.3	6.1	100	78.0	1.7	82	21.7
3	3.5	102	44.7	5.7	40	72.8	3.2	65	40.9
3	4	127	51.1	5.8	85	74.1	5	63	63.9
3	1.9	129	24.2	6.6	76	84.3	4	34	51.1
3	1.6	138	20.4	6.1	66	78.0	3.9	55	49.8
3	0.7	36	8.9	7.2	94	92.0	5.6	68	71.6

Table 4. Relative Amax (%) during three treatment days, each preceded by a cold night at +4, 0 and -4°C. % Amax values are Amax of treated leaves relative to first A_{max} of untreated leaves.

leaf	treatment	min temp	A_{max} day one	%A_{max} day one	A_{max} day two	% A_{max} day two	A_{max} day three	% A_{max} day three
B1a	1night	4	6.6	84.4	9.5	121.5	4.9	62.7
B1b	1night	4	9.3	118.9	9.7	124.0	8.3	106.1
B1c	1night	4	2.4	30.7	7	89.5	5.8	74.2
B1d	1night	4	4.1	52.4	6.3	80.6	5.2	66.5
B1e	1night	4	3.8	48.6	6.7	85.7	5.9	75.4
B2a	2nights	4	6.8	87.0	4.5	57.5	9	115.1
B2b	2nights	4	7.9	101.0	6.7	85.7	8.5	108.7
B2c	2nights	4	5.6	71.6	5.4	69.1	10.4	133.0
B2d	2nights	4	3.4	43.5	8.4	107.4	9.7	124.0
B2e	2nights	4	5.1	65.2	6.9	88.2	12.3	157.3
B3a	3nights	4	5.7	72.9	10.8	138.1	12.7	162.4
B3b	3nights	4	5.8	74.2	11.9	152.2	11	140.7
B3c	3nights	4	6.6	84.4	9.9	126.6	12.7	162.4
B3d	3nights	4	6.1	78.0	10.7	136.8	12.6	161.1
B3e	3nights	4	7.2	92.1	10	127.9	11.1	141.9
C1a	1night	0	0.1	1.3	5.2	66.5	5.9	75.4
C1b	1night	0	0	0.0	2.2	28.1	2.8	35.8
C1c	1night	0	0	0.0	-0.9	-11.5	8.9	113.8
C1d	1night	0	0.6	7.7	0.5	6.4	2.8	35.8
C1e	1night	0	0.7	9.0	2.9	37.1	4.3	55.0
C2a	2nights	0	3.5	44.8	8.7	111.3	10.6	135.5
C2b	2nights	0	5.8	74.2	5.1	65.2	9.3	118.9
C2c	2nights	0	1.5	19.2	4.2	53.7	10.4	133.0
C2d	2nights	0	0.3	3.8	4.8	61.4	8.5	108.7
C2e	2nights	0	2.2	28.1	3.5	44.8	8.6	110.0

C3a	3nights	0	3.2	40.9	10.7	136.8	9.6	122.8
C3b	3nights	0	5	63.9	10.7	136.8	5.7	72.9
C3c	3nights	0	4	51.2	8.2	104.9	9.1	116.4
C3d	3nights	0	3.9	49.9	9.4	120.2	8.9	113.8
C3e	3nights	0	7	89.5	8.1	103.6	5.3	67.8
A1a	1night	-4	0.7	9.0	1.7	21.7	3.3	42.2
A1b	1night	-4	2.8	35.8	5.1	65.2	5.1	65.2
A1c	1night	-4	0.3	3.8	1.2	15.3	3.5	44.8
A1d	1night	-4	0	0.0	0.2	2.6	2.3	29.4
A1e	1night	-4	0.2	2.6	0	0.0	3.2	40.9
A2a	2nights	-4	1.7	21.7	4.5	57.5	7.5	95.9
A2b	2nights	-4	0.2	2.6	3	38.4	6.9	88.2
A2c	2nights	-4	0.6	7.7	4.3	55.0	7.7	98.5
A2d	2nights	-4	0.1	1.3	3.5	44.8	6.4	81.8
A2e	2nights	-4	0.9	11.5	5.4	69.1	7.6	97.2
A3a	3nights	-4	3.5	44.8	3.8	48.6	6.3	80.6
A3b	3nights	-4	4	51.2	8.3	106.1	2.6	33.2
A3c	3nights	-4	1.6	20.5	0.7	9.0	2.5	32.0
A3d	3nights	-4	0.7	9.0	6.5	83.1	6.5	83.1
A3e	3nights	-4	3	38.4	8.2	104.9	7	89.5

Appendix VII

Stable Isotope study (Chapter 7)

Table 1. Primary mass-spectrometer values for δ^{13} C and Δ values calculated for foliage, stem and cotyledon (propagule) tissue of *Avicennia marina* subsp. *australasica* over a latitudinal gradient (°S) [Table 1] and a salinity gradient [Table 2] in the North Island of New Zealand. All figures are the mean ± standard deviation (n for tissue type varies between 2 and 10 at each site). Salinity data (ppt) have been calculated according to the 1978 Practical Salinity Scale Equations (1980) using conductivity values (mS). Δ is calculated assuming δ^{13}C for source air of -8.0 ‰ (Griffiths, 1993).

Site	Latitude (°S)	Salinity (mg g^{-1})	Leaf δ^{13}C (‰)	Leaf Δ (‰)
Kaimaumau	34°55'	26.7±3.8	-25.90±0.64	17.9±0.6.
Paihia	35°17'	34.7±0.7	-26.36±0.69	18.4±0.7
Matapouri	35°34'	36.2±1.0	-25.65±0.46	17.7±0.5
Ngunguru (D)	35°38'	33.1±1.5	-25.86±0.67	17.9±0.7
Matakohe	36°08'	27.9±1.2	-25.58±0.46	17.6±0.5
Mangawhai	36°08'	28.4±2.5	-25.77±0.45	17.8±0.5
Whitianga	36°50'	31.2±0.8	-26.30±0.91	18.3±0.9
Tauranga	37°40'	29.0±1.4	-24.70±0.31	16.7±0.3
Ohiwa	38°00'	34.1±0.7	-23.69±0.49	15.7±0.5
Kutarere	38°03'	30.3±1.3	-24.58±0.32	16.6±0.3

Site	Latitude (°S)	Salinity (mg g^{-1})	Stem δ^{13}C (‰)	Stem Δ (‰)
Kaimaumau	34°55'	26.7±3.8	-26.05±0.20	18.1±0.2
Paihia	35°17'	34.7±0.7	-25.80±0.56	17.8±0.6
Matapouri	35°34'	36.2±1.0	-24.80±0.98	16.8±1.0
Ngunguru (D)	35°38'	33.1±1.5	-23.95±1.22	15.9±1.2
Matakohe	36°08'	27.9±1.2	-24.41±0.65	16.4±0.7
Mangawhai	36°08'	28.4±2.5	-25.57±0.39	17.6±0.4
Whitianga	36°50'	31.2±0.8	-25.13±0.37	17.1±0.4
Tauranga	37°40'	29.0±1.4	-23.34±0.66	15.3±0.7
Ohiwa	38°00'	34.1±0.7	-22.17±1.10	14.2±1.1
Kutarere	38°03'	30.3±1.3	Not sampled	Not sampled

Site	Latitude (°S)	Salinity (mg g^{-1})	Cotyledon δ^{13}C (‰)	Cotyledon Δ (‰)
Kaimaumau	34°55'	26.7±3.8	-25.03±0.36	17.3±0.36
Paihia	35°17'	34.7±0.7	-25.60±0.35	17.6±0.35
Matapouri	35°34'	36.2±1.0	-26.37±1.50	18.4±1.50
Ngunguru (D)	35°38'	33.1±1.5	-24.94±0.74	16.9±0.74
Matakohe	36°08'	27.9±1.2	-23.97±0.62	15.9±0.62
Mangawhai	36°08'	28.4±2.5	-24.84±0.18	16.8±0.18
Whitianga	36°50'	31.2±0.8	-24.50±1.71	16.5±1.71
Tauranga	37°40'	29.0±1.4	-23.99±0.22	15.9±0.22
Ohiwa	38°00'	34.1±0.7	-24.11±0.31	16.1±0.31
Kutarere	38°03'	30.3±1.3	Not sampled	Not sampled

Table 2

Site	Latitude (°S)	Salinity (mg g^{-1})	Leaf $\delta^{13}C$ (‰)	Leaf Δ (‰)
Matapouri	35°34'	36.2±1.0	-25.65±0.46	17.7±0.5
Ngunguru (D)	35°38'	33.1±1.5	-25.86±0.67	17.9±0.7
Ngunguru (A)	35°37'	21.4±0.7	-26.04±0.33	18.0±0.3
Ngunguru (B)	35°37'	21.4±0.7	-26.13±0.40	18.1±0.4
Ngunguru (C)	35°38'	6.7±0.4	-27.15±0.65	19.2±0.7

Site	Latitude (°S)	Salinity (mg g^{-1})	Stem $\delta^{13}C$ (‰)	Stem Δ (‰)
Matapouri	35°34'	36.2±1.0	-24.80±0.98	16.8±1.0
Ngunguru (D)	35°38'	33.1±1.5	-23.95±1.22	15.9±1.2
Ngunguru (A)	35°37'	21.4±0.7	-25.65±1.07	17.7±1.1
Ngunguru (B)	35°37'	21.4±0.7	Not sampled	Not sampled
Ngunguru (C)	35°38'	6.7±0.4	-25.16±1.44	17.2±1.4

Site	Latitude (°S)	Salinity (mg g^{-1})	Cotyledon $\delta^{13}C$ (‰)	Cotyledon Δ (‰)
Matapouri	35°34'	36.2±1.0	-26.37±1.50	18.4±1.50
Ngunguru (D)	35°38'	33.1±1.5	-24.94±0.74	16.9±0.74
Ngunguru (A)	35°37'	21.4±0.7	-24.59±0.62	16.6±0.62
Ngunguru (B)	35°37'	21.4±0.7	Not sampled	Not sampled
Ngunguru (C)	35°38'	6.7±0.4	-24.19±0.35	16.2±0.35

Ngunguru (A) = tall plants, (B) = dwarf plants, (C) = brackish site, (D) = 1st bridge

Stable Isotope study (Chapter 7))

Table 1

Raw data values for **foliar** $\delta^{13}C$ and Δ (sampled over a **latitudinal** gradient)

Sample Site	LATITUDE (°S)	$\delta^{13}C$ (‰)	Δ (‰)
KAIMAUMAU	34.55	-25.56	17.56
	34.55	-25.62	17.62
	34.55	-25.51	17.51
	34.55	-25.80	17.80
	34.55	-27.03	19.03
PAIHIA	35.17	-26.75	18.75
	35.17	-25.27	17.27
	35.17	-26.73	18.73
	35.17	-26.65	18.65
	35.17	-25.74	17.74
	35.17	-27.04	19.04
MATAPOURI	35.34	-25.34	17.34
	35.34	-25.00	17.00
	35.34	-25.9	17.90
	35.34	-26.00	18.00
	35.34	-26.03	18.03
NGUNGURU (D)	35.38	-25.03	17.03
	35.38	-24.86	16.86
	35.38	-25.77	17.77
	35.38	-25.59	17.59
	35.38	-26.39	18.39
	35.38	-25.52	17.52
	35.38	-26.60	18.60
	35.38	-25.75	17.75
	35.38	-26.98	18.98
	35.38	-26.08	18.08
MATAKOHE	36.08	-25.52	17.52
	36.08	-25.88	17.88
	36.08	-26.08	18.08
	36.08	-25.91	17.91
	36.08	-25.19	17.19
	36.08	-24.90	16.90
MANGAWHAI	36.08	-25.90	17.90
	36.08	-25.73	17.73
	36.08	-26.65	18.65
	36.08	-25.85	17.85
	36.08	-25.39	17.39
	36.08	-25.48	17.48
	36.08	-25.36	17.36
WHITIANGA	36.50	-26.44	19.44
	36.50	-26.16	18.16
TAURANGA	37.40	-24.37	16.37
	37.40	-24.53	16.53
	37.40	-24.82	16.82
	37.40	-25.06	17.06
OHIWA	38.00	-23.91	15.91
	38.00	-24.03	16.03
	38.00	-23.12	15.12
KUTARERE	38.03	-24.80	16.80
	38.03	-24.35	16.35

Table 2

Raw data values for **foliar** $\delta^{13}C$ and Δ (sampled over a **salinity** gradient)

Sample Site	LATITUDE (°S)	$\delta^{13}C$ (‰)	Δ (‰)
MATAPOURI	35.34	-25.34	17.34
	35.34	-25.00	17.00
	35.34	-25.90	17.90
	35.34	-26.00	18.00
	35.34	-25.52	17.52
	35.34	-26.78	18.78
	35.34	-26.57	18.57
	35.34	-24.31	16.31
	35.34	-24.76	16.76
	35.34	-24.98	16.98
	35.34	-26.56	18.56
	35.34	-26.03	18.03
NGUNGURU TALL	35.37	-25.87	17.87
	35.37	-25.73	17.73
	35.37	-26.07	18.07
	35.37	-25.54	17.54
	35.37	-25.68	17.68
	35.37	-26.48	18.48
NGUNGURA DWF	35.37	-25.86	17.86
	35.37	-25.68	17.68
	35.37	-26.72	18.72
	35.37	-26.23	18.23
	35.37	-26.16	18.16
NGUNGURU 1st Br	35.38	-25.03	17.03
	35.38	-24.86	16.86
	35.38	-25.77	17.77
	35.38	-25.59	17.59
	35.38	-26.39	18.39
	35.38	-25.52	17.52
	35.38	-26.6	18.60
	35.38	-25.75	17.75
	35.38	-26.98	18.98
	35.38	-26.08	18.08
	35.38	-25.81	17.81
	35.38	-25.95	17.95
	35.38	-26.73	18.73
	35.38	-25.48	17.48
NGUNGURU BRACKISH	35.38	-26.85	18.85
	35.38	-26.81	18.81
	35.38	-26.56	18.56
	35.38	-27.36	19.36
	35.38	-28.19	20.19
	35.38	-26.85	18.85
	35.38	-26.28	18.28